PUBLISCIENCE

A RESEARCH JOURNAL OF HIGH SCHOOL RESEARCH

VOLUME 3 ISSUE 1
JUNE 2020

ISSN: 2619-7359

EDITORIAL BOARD

DISCLAIMER

Publiscience (ISSN: 2619-7359) is published annually by the Research Unit of Philippine Science High School – Western Visayas Campus, Brgy. Bito-on, Jaro, Iloilo City spearheaded by the Editorial Board composed of Batch 2020 students.

Please address all matters regarding exchange of publications to the Editors-in-Chief of the Publiscience Editorial Board of Philippine Science High School – Western Visayas Campus, Brgy. Bito-on, Jaro, Iloilo City, Philippines.

Mail: The Editors-in-Chief
Publiscience
Philippine Science High School
Western Visayas Campus
Brgy Bito-on, Jaro, Iloilo City
5000 Philippines

Trunklines: *Director's Office Direct Line*
+63-33-3295644

Registrar's Office Direct Line
+63-33-3290501

+63-33-5014335
+63-33-5014133

E-mail: publiscience@wvc.pshs.edu.ph

You may visit the website for the softcopy of the journal and previous issue via the QR code or by visiting: http://publiscience.org/

ABOUT THE COVER

The cover features the ethanolic plant extract of *Euphorbia hirta* (tawa-tawa) in a rotating flask of the rotary evaporator. The rotary evaporator is used to separate the crude sample extracts from the solvents. It rotates the rotating flask continuously until the process is done. Indeed, while research seems to just be rotating and going around a single circle, like the rotary evaporator, the result at the end is worthwhile. It teaches us to never give up and keep on trying and waiting because it will all be worth it in the end. All our hardships will pay off and our efforts will be realized.

About PSHS

MISSION

The Philippine Science High School, operating under one System of Governance and Management, provides scholarship to students with high aptitude in science and mathematics.

The PSHS System offers an education that is humanistic in spirit, global in perspective, and patriotic in orientation. It is based on a curriculum that emphasizes science and mathematics and the development of well-rounded individuals.

The PSHS System prepares its students for careers in Science and Technology and contributes to nation building by helping the country attain a critical mass of professionals and leaders in Science and Technology.

VISION

We are the leading science high school in the Asia Pacific Region preparing our scholars to become globally competitive Filipino scientists equipped with 21st century skills and imbued with the core values of truth, excellence, and service to nation.

MANDATE

The Philippine Science High School System is a service institute of the Department of Science and Technology (DOST) whose mandate is to offer scholarship in secondary education with special emphasis on subjects pertaining to the sciences to prepare its students for a science career (R.A. 3661). Its primary function is to administer the country's scholarship program in special science secondary education.

Be a PSHS Scholar today!

Requirements for Eligibility

grades of at least

85

in S&T subjects

certified Filipino citizen

w/ no pending app.

must not be younger than

EXACTLY 12 Y.O.

at August 1 of the incoming school year

have a satisfactory rating

or its equivalent in SY 2019-2020 report card

and most importantly,

HAVE NOT YET TAKEN THE NCE PREVIOUSLY

Application Requirements

Two (2) filled out application forms

Two (2) identical 1x1 ID photos

non-refundable test fee
public - free
private - P100

certified true copy of report card

Perks of Being a PSHS Scholar

free tuition

free books

monthly allowance
up to PHP 4000

dorm lodging

uniform
transpo
living
allowance
for low income families

more info at: **www.pshs.edu.ph**

FOREWORD

The Philippine Science High School - Western Visayas Campus (PSHS - WVC) takes pride for this third Issue of Publiscience. PSHS - WVC is the very first and still is the only PSHS Campus that has successfully published all the Science and Technology Research works of its graduating scholars. Moreso, the publication just gets better every year. This is made possible by the efforts and desire of the students and whole Research Unit to embrace the value of "*Pagpasanyog*", a Hiligaynon word which means to improve or become better. This is a testament of such positive spirit for continued growth and learning, and testimony of the hard work and perseverance of the students to pursue the untarnished truth using their knowledge and skills in science and technology; thereby contributing to the body of knowledge providing solutions to real-life problems. Kudos to Batch 2020!

SHENA FAITH M. GANELA
Campus Director III

* * *

Congratulations on this monumental triumph, Batch 2020! You have reached the ultimate desire of researchers that is to publish their own investigation.

For a high school researcher like you, this is an awe-inspiring phenomenon to many who wish to level-up with your achievement. This is a strong manifestation of your dedication, tenacity, and willingness to learn and unlearn ways of doing things as you embrace the process of research.

I know you went through a lot before reaching this very end. I feel proud of you for letting go of some of your joys to accommodate your research data gathering schedule. I appreciate you for managing your hurt in the midst of emotionally driven, chaotic schedules. And above all, I feel so proud of you for not giving up.

My heart brims with bliss and excitement to see and take hold of the fruit of your labor. Again, my warmest congratulations.

ROLANDO S. LIBUTAQUE
Curriculum Instruction Division Chief

* * *

The COVID-19 pandemic, together with other global challenges we are facing, has highlighted the importance of science research. From understanding the problem and finding the possible solutions, research is the essential tool. PSHS - WVC has envisioned its alumni to be at the forefront of professionals who uses science and technology to address global problems. Thus, scholars are trained to acquire skills vital for them to be valuable researchers. This Publiscience is the manifestation of their research potentials.

HAROLD P. MEDIODIA
Research Academic Unit Head

REVIEW PROCESS

THE RESEARCH PROGRAM

The research program is a three-year undertaking that aims to inculcate the scholars with the quality and skills becoming of a world-class Filipino scientist. Each year starting from Grade 10 focuses on an aspect of research paramount to the growth of scholars in becoming leading figures in their respective fields.

RESEARCH 1

Research as a subject is introduced in Grade 10. It is the formative year for the budding researcher with in-depth discussions on the Scientific Method, and the Research Process. Particularly, it introduces scholars in topic selection, literature search, research design, and paper presentation. Scholars were also taught the basics of writing a proposal, and a research paper – both in instruction, and in practice. Each group or work unit is composed of at most five members with general topics provided by the Research 1 teachers. Research 1 culminates with the paper presentation of the Grade 10 scholars in *Pagsuguidadon.*

RESEARCH 2

Research 2 is the reinforcement year in Grade 11. The writing of the proposal, and the research paper are further scrutinized in this year. Each section of a standard research paper: abstract, introduction, method, results, discussion, and conclusion are more pronounced in the syllabus. Research 2 is performed in work units of, at most, three. Scholars are allowed to select any topic in alignment with their science options and/or elective under the supervision of their advisers, propose and defend their proposal to a panel, develop and/or enhance skills related to the study, perform the method outlined in their proposal, and report their findings in a full-fledged research paper. Research 2 concludes with the presentation of the results in the final defense.

RESEARCH 3

Research 3 is the culminating year of the research curriculum. It is reserved for Grade 12 scholars who organize activities and events that share their respective study's findings, including but not limited to: research presentation (*Pagbantala*), poster presentation (*Pagbalandra*), seminar-workshop (*Pahisayod*), and community science conference (*Pagwaragwag*) with more events described at the end of this journal. This very journal is a fruit of the previous two batches' research experience. Research 3 focuses on finalizing the study and networking the results. It focuses on community-oriented approach in making science more accessible. This is evident in the oral and poster presentations for students and professionals, workshops and seminars for high school students, and gamification of each study for elementary students during the aforementioned events. Each study is given the opportunity to be published in this journal, provided that they have accomplished the review process outlined at the left.

THE RESEARCH COMMITTEE

The Research Committee is tasked with ensuring the quality of all research projects produced by the Batch 2020 scholars, performed from the 10th to the 12th grade. It is headed by the Research Unit Head who oversees and approves all research work, and composed of the research teachers who handle the Research class for a specific school year and grade level and the research advisers who provide guidance, insight, and assistance in a consulting capacity in their fields of expertise. The Science Research Assistants (SRA) manage the different labs, apparatuses, equipment, and reagents for the use of the scholars in the conduct of their respective studies.

* * *

RESEARCH UNIT HEAD

Harold P. Mediodia

RESEARCH 3 TEACHERS SY 2019-2020

Aris C. Larroder
Catherine Joy A. Mediodia
Ramon Angelo N. Sinco

RESEARCH 2 TEACHERS SY 2018-2019

Athenes Joy Presno-Aban
Maria Milagrosa A. Nulla
Zennifer L. Oberio

RESEARCH 1 TEACHERS SY 2017-2018

Athenes Joy Presno-Aban
Julnafe B. Libo-on
Harold P. Mediodia

RESEARCH ADVISERS

BIOLOGICAL SCIENCES & MICROBIOLOGY

Andrea Lucyle M. Bela-ong
Oliver J. Fuentespina
Fernando Christian G. Jolito III
Catherine Joy A. Mediodia
Harold P. Mediodia
Virna Jane M. Navarro
Zennifer L. Oberio
Angelo P. Olvido

CHEMISTRY & INTEGRATED SCIENCE

Athenes Joy Presno-Aban
Mialo L. Bautista
Michael Patrick M. Padernal
Ramon Angelo N. Sinco

PHYSICS & ENGINEERING

Aris C. Larroder
Raphael Eric C. Yturralde

COMPUTER SCIENCE &TECHNOLOGY

Eisen Ed C. Briones
Maria Milagrosa A. Nulla
Gerald U. Salazar

STATISTICS TEACHERS

Charmaigne D. Aguirre
Ma. Romy Alexis C. Consulta
Myrna B. Libutaque

SCIENCE RESEARCH ASSISTANT (SRA)

CHEMISTRY	INSTRUMENTATION	MICROBIOLOGY	PHYSICS
Leilani C. Estilo	Mark V. Rosales Amafe B. Gavile Michael Patrick M. Padernal	Rusty A. Balcoba Cherry Rose D. Haro	Gabriel Z. Bermejo Rusty A. Balcoba

REVIEWERS AND PANELISTS

The research curriculum of PSHS - WVC is predominantly composed of highly immersive activities that develop the scholars' skills as researchers and scientific communicators. From Grade 10, the scholars experience the rigors of having to defend their proposals and, ultimately, their final paper.

PAGSUGUIDADON

PAGSUGUIDADON, from the Hiligaynon word *suguid* or "to report", is the culminating event for the Grade 10 Research curriculum. Scholars present and defend their paper to a three-person panel, composed of two invited panelists and a faculty member of PSHS-WVC. The papers are presented in five clusters, namely: Water Studies, Marine Science, Biology, Plant science, and Development, with each studies' overarching theme as the basis of grouping.

INVITED PANELISTS

Maria Robelyn Insik
JB FASTEST WATER TEST CO.

Catherine Erazo
OTON NATIONAL HIGH SCHOOL

Rowena Cadiz
UNIVERSITY OF THE PHILIPPINES - VISAYAS

Kenneth Anabo
LO-ONG NATIONAL HIGH SCHOOL

Fernando Christian Jolito III
UNIVERSITY OF SAN AGUSTIN

Andrea Libo-on
BACOLOD NATIONAL HIGH SCHOOL

Justin Brian Chiongson
UNIVERSITY OF SAN AGUSTIN

Louinne Grace Insular
LEGANES CENTRAL ELEMENTARY SCHOOL

Zenith Montel
PHARMA GALENX INNOVATIONS, INC.

Joven Llabore
ASSUMPTION ILOILO

PSHS-WV FACULTY

Erika Eunice Salvador
WATER STUDIES

Lovie Grace Aguaras
MARINE SCIENCE

Joseph Simon Madriñan
BIOLOGY

Ramon Angelo Sinco
PLANT SCIENCE

Xavier Romy Braña
DEVELOPMENT

PAGBANTALA

PAGBANTALA, from the Hiligaynon word *bantala* or "to inform", is the oral presentation of the scholars' studies to a panel of experts composed of an invited panelist, an alumni, and a faculty member of PSHS - WVC. For SY 2019-2020, the studies were presented in 8 clusters namely: Wastewater Remediation, Antibacterial Studies, Health and Toxicity, Agriculture, Aquatic and Natural Resources, Industry, Energy, and Emerging Technology, Material Science, and Computer Science (ordered below left to right, top to bottom).

INVITED PANELISTS

Felix Ojario
CENTRAL PHILIPPINE UNIVERSITY

Leopoldo Ayukil III
UP HIGH SCHOOL ILOILO

Matthew Tubola
UNIVERSITY OF SAN AGUSTIN

Rhoda Erdao
OTON NATIONAL HIGH SCHOOL

Stephen Sabinay
WESTERN VISAYAS STATE UNIVERSITY – ILS

Sharon Nuñal
UNIVERSITY OF THE PHILIPPINES - VISAYAS

Raul Sampani
INTERNATIONAL BUILDERS CORPORATION

Mark Joseph Solidarios
WESTERN VISAYAS STATE UNIVERSITY

PSHS-WV ALUMNI

Lurylee Olarte
GLOBAL BUSINESS POWER CORPORATION

Ardee Caro
JOSE MONFORT NATIONAL SCIENCE HIGH SCHOOL

Jeriel Rose Solis
PAVIA NATIONAL HIGH SCHOOL

Excalibur Seterra
ILOILO PROVINCIAL AGRICULTURE OFFICE

Mary Camille Samson
PSHS-WV BATCH 2012

Jonalyn Peconcillo Mateo
UNIVERSITY OF THE PHILIPPINES - VISAYAS

Ian John Galupar
PAVIA NATIONAL HIGH SCHOOL

Rommel Jun Payba
CENTRAL PHILIPPINE UNIVERSITY

PSHS-WVC FACULTY

Erika Eunice Salvador
WASTEWATER REMEDIATION

Era delos Reyes
ANTIBACTERIAL STUDIES

Cherry Rose Haro
HEALTH AND TOXICITY

Oliver Fuentespina
AGRICULTURE

Julnafe Libo-on
AQUATIC AND NATURAL RESOURCES

David Bryan Lao
INDUSTRY, ENERGY, AND EMERGING TECHNOLOGY

Mark Rosales
MATERIAL SCIENCE

Rubie Anne Bito-on
COMPUTER SCIENCE

THE FINAL DEFENSE

THE FINAL DEFENSE is the final step towards the end of the research curriculum. The scholars invite one external expert and two PSHS - WVC faculty to compose a three-person panel to assess the merits and validity of their findings. The final defense panel recommends revisions to the study's manuscript as well as continually review the same until approval.

INVITED PANELISTS

Cathrina Bagarinao **Angel Queenee Dequito** **Arnold Gaje** **Jean Pierre Montecillo**
UNIVERSITY OF THE PHILIPPINES - VISAYAS

Eric Justin Blancaflor **Socorro Leong-on** **Ramon Salanio**
UNIVERSITY OF SAN AGUSTIN

Virginia Agreda **Arla Arenga** **Julius De Luna Limjoco**
DEPARTMENT OF AGRICULTURE – WESTERN VISAYAS AGRICULTURAL RESEARCH CENTER

Joeben Gubatanga **Roxzien Sesbreño**
DEPARTMENT OF SCIENCE AND TECHNOLOGY – REGION VI

Arjun Marven Calvo **Raul Lorilla**
DEPARTMENT OF ENVIRONMENT AND NATURAL RESOURCES

Queenie Carbaquel
BUREAU OF PLANT INDUSTRY – NSQCS VI

Excalibur Seterra
ILOILO PROVINCIAL AGRICULTURE OFFICE

Jaya Lavalle Sitjar
NATIONAL CHENG KUNG UNIVERSITY, TAIWAN

Carlo Nolan Carado
PHILIPPINE RED CROSS –ILOILO CHAPTER

Annie Franco
SOUTHEAST ASIAN FISHERIES DEVELOPMENT CENTER

Eldy Barrientos
ST. ANTHONY COLLEGE HOSPITAL

Ma. Beth Concepcion
WESTERN VISAYAS STATE UNIVERSITY

PSHS-WVC FACULTY

Fernando Christian Jolito III **Ma. Deanna Jolito** **Julnafe Libo-on**
Catherine Joy Mediodia **Virna Jane Navarro** **Angelo Olvido**
BIOLOGICAL SCIENCES UNIT

Athenes Joy Presno-Aban **Mark Rosales**
Erika Eunice Salvador **Michael Patrick Padernal** **Ramon Angelo Sinco**
CHEMISTRY AND INTEGRATED SCIENCES UNIT

Ranel Abellar **Xavier Romy Braña** **Oliver Fuentespina**
PHYSICAL SCIENCES UNIT

Rubie Anne Bito-on **Eisen Ed Briones**
COMPUTER SCIENCE AND TECHNOLOGY UNIT

David Bryan Lao **Zennifer Oberio**
MATHEMATICS UNIT

THE EXTERNAL REVIEWERS

THE EXTERNAL REVIEWERS are PSHS - WVC alumni recommended by the Research Unit and invited by the Editorial Board to assess the merit and substance of each of the published papers. These individuals serve as the final reviewers prior to an article's publication. Before the publication of this section, their identities are anonymous to the authors.

Bee Gee Belle Agustin
INSTRUCTOR
AKLAN STATE UNIVERSITY, PH

Aldrean Paul Alogon
PROSPECTIVE ECONOMICS MAJOR IN PHYSICS
WESLEYAN UNIVERSITY, USA

John Rafael Ambag
BS MOLECULAR BIOLOGY AND BIOTECHNOLOGY
UNIVERSITY OF THE PHILIPPINES - DILIMAN, PH

Kate Mariene Baldonado
BS COMPUTER ENGINEERING
UNIVERSITY OF THE PHILIPPINES - DILIMAN, PH

Justin Enrique Banusing
BS INFORMATICS AND ENTREPRENEURSHIP
UNIVERSITY OF WASHINGTON, USA

Juan Paolo Lorenzo Gerardo Barrios
BS PHYSICS
DURHAM UNIVERSITY, UK

Regine Bastareche
INTARMED
UNIVERSITY OF THE PHILIPPINES - MANILA, PH

Jared Billena
CHAIRPERSON OF DEP'T OF LABORATORY
AND DEP'T OF PATHOLOGY
THE MEDICAL CITY ILOILO AND
ILOILO DOCTORS' COLLEGE OF MEDICINE, PH

Cris Jericho Cruz
BS CHEMICAL ENGINEERING
KOREA ADVANCED INSTITUTE OF SCIENCE, SK

Christian Deo Deguit
RESEARCHER
UNIVERSITY OF THE PHILIPPINES –
NATIONAL INSTITUTE OF HEALTH, PH

John Jewish Dominguez
RESEARCHER
AUSTRALIAN NATIONAL CENTRE, AUS

Yevgeny Aster Dulla
RESEARCHER
INTRALINK JAPAN, JAPAN

Emil Emmanuel Estilo
STUDENT RESEARCHER
HIROSHIMA UNIVERSITY, JAPAN

Philip Caesar Flores
STUDENT RESEARCHER
UNIVERSITY OF THE PHILIPPINES –
NATIONAL INSTITUTE OF PHYSICS, PH

Ina de la Fuente
GRADUATE TEACHING ASST. AND INSTRUCTOR
UNIVERSITY OF CONNECTICUT, USA AND
UNIVERSITY OF THE PHILIPPINES - DILIMAN, PH

Riel Carlo Ingeniero
STUDENT RESEARCHER
GEOMER HELHOLTZ CENTRE FOR OCEAN
RESEARCH, GER

Angelo Jamerlan
MOLECULAR NEUROBIOLOGIST
GACHON UNIVERSITY, SK

Ma. Christina Jamerlan
LEAD AI ENGINEER
ABS-CBN CORPORATION, PH

Marmelou Popes
RESEARCHER
UNIVERSITY OF THE PHILIPPINES –
MARINE SCIENCE INSTITUTE, PH

Leo Albert Sala
RESEARCHER
CZECH ACADEMY OF SCIENCES, CZR

Alexandria Marie Sombiro
BS INDUSTRIAL ENGINEERING
UNIVERSITY OF THE PHILIPPINES -
DILIMAN, PH

Liezel Tamon
RESEARCHER
MRC WETHERALL INSTITUTE
OF MOLECULAR MEDICINE, UK

John Noel Viana
RESEARCHER
AUSTRALIAN NATIONAL CENTRE, AUS

Dominic Yap
BS MOLECULAR BIOLOGY AND
BIOTECHNOLOGY
UNIVERSITY OF THE PHILIPPINES - DILIMAN, PH

TABLE OF CONTENTS

PREFACE

We are honored to present the third volume of Publiscience, the homegrown journal of PSHS-WVC scholars. Publiscience contains the studies of first-time researchers, culminating their three-year research journey. Keeping true to the spirit of *Pagpasanyog* – a Hiligaynon word for 'innovate' - each batch continues to improve the journal in every volume from the establishment of the journal in 2018, to publication by a student-led Editorial Board in 2019. This year's *pagpasanyog* focuses in improving reader experience. This includes the introduction of the external reviewer in the review process, linking of the published journal to its online counterpart via QR coding, citations in College of Science Editor (CSE) and American Psychological Association (APA), and the integration of cluster representatives.

This volume is a compilation of 25 Science and Technology (S&T) studies spanning different fields in Biology, Chemistry, Physics, and Engineering. The studies were grouped in eight (8) clusters, each of which are in cognizance with the Harmonized National Research and Development Agenda (HNRDA) of the Department of Science and Technology: under Agenda 1, National Integrated Basic Research Agenda (NIBRA), is wastewater remediation; Agenda 2, Health, is further subdivided into Antibacterial Studies, and Health and Toxicity; Agenda 3, Agriculture, Aquatic, and Natural Resources (AANR), is split into studies in Agriculture, and Aquatic and Natural Resources; and Agenda 4, Industry, Energy, and Emerging Technology (IEET), houses a section with the same name, Material Science, and Computer Science studies. The authors, the Editorial Board, and the Research Unit recognize the role of research in nation building, and so have organized the studies proximal to each agenda. With the HRNDA at the central framework of this journal, we hope that aside from affording scientific knowledge, the studies may also yield tangible social and economic benefits.

To emphasize the community-oriented stance of the journal, each cluster is represented by characters deeply ingrained in the Visayan culture. This is a reminder that research should begin in the community. To pursue national prosperity means uplifting its most basic foundations.

This volume is published during times of great uncertainty. In times like these, it becomes increasingly imperative to perform research, listen to its findings, and above all, scrutinize its merits. Pursuing the untarnished truth, after all, is a lifelong calling to ask. We hope that through these articles, we may be able to inspire the next generation of critical thinkers, global innovators, and world-class Filipino leaders in S&T.

THE EDITORIAL BOARD

* * *

DEDICATION

This journal is dedicated to every researcher in the field and the laboratory,
to every front liner that has battled the COVID-19 pandemic,
and to all those who continue to serve with passion and integrity.

MUROPURO

WASTEWATER REMEDIATION

MUROPURO is a figure in the pantheon of Visayan deities responsible for the springs, rivers, and lakes – bodies of water which grow increasingly polluted with rapid industrialization and population growth as they serve as dumping sites for industrial, commercial, and residential effluents. This section contains studies that explore various materials to treat a particular type of waste – wastewater – that are among the principal effluents polluting these bodies. The material of interest in each study are used to remediate different pollutants such as heavy metals – usually from manufacturing waste, and phosphates and nitrates – run-offs from agricultural activity.

These studies fall under the National Integrated Basic Research Agenda (NIBRA). Particularly, these address research for sustainable communities on understanding and, if applicable, addressing environmental and anthropogenic activities.

BASED ON: Harmonized National Research and Development Agenda (HNRDA)

Organo-mineral composites from the shells of *Crassostrea iredalei* (slipper cupped oyster), *Perna viridis* (green shell), and *Telescopium telescopium* (horned snail) in the removal of chromium (VI) from water

CHLOE ELLESSE S. FACIOLAN, FRANCIS HARRY SHONE V. LEONORA, LEONARD VINCENT A. MAJADUCON, and RAMON ANGELO N. SINCO

Philippine Science High School - Western Visayas Campus, Brgy. Bito-on, Jaro, Iloilo City 5000, Department of Science and Technology, Philippines

Abstract

This paper presents and compares organo-mineral composites from *Crassostrea iredalei* (slipper cupped oyster), *Perna viridis* (green shell), and *Telescopium telescopium* (horned snail) in the removal of hexavalent chromium from water. Shells were oven-dried, ground, and sieved to fine powder size. Replicates of 10 ppm dichromate solution were individually treated with 1 mg of shell powder for 20 minutes. Following conversion of absorbance to concentration and % Cr^{6+} removed, *T. telescopium* was found to be most efficient in Cr^{6+} remediation with 9.632% removal, followed by *P. viridis* at 8.444%, and *C. iredalei* at 3.431%. Chromium removal is attributed to electronegativity differences between the metal and structural organic components of the shell composites, as well as the capacity of $CaCO_3$ to facilitate surface adsorption. Differences in the concentrations of Cr^{6+} removed result from variances in biomineralization among mollusk species, which dictate the characterization and concentration of $CaCO_3$ in their shell layers.

Keywords: *bioremediation, heavy metal removal, chromium (VI), mollusk shells, calcium carbonate*

Introduction. Heavy metals are increasingly emergent pollutants in bodies of water as a by-product of anthropogenic industrialization, and they continue to rise in concentration in recent years [1, 2]. These metals enter the aquatic ecosystem through waste disposed by industrial, commercial, and urban residential areas near bodies of water [3], as well as through direct contact or abrasion with road-deposited sediments usually displaced by storm run-off [2]. In trace amounts, these metals are essential to natural biogeochemical cycles [4]. Beyond safe concentrations, however, they disrupt the normal functions of the ecosystem, and are potentially hazardous to its organic components [5, 6].

Lead, cadmium, and chromium are among the most prevalent heavy metals in bodies of water, already exceeding safe limits in aquatic food products as demarcated by the United States Environmental Protection Agency (US-EPA), World Health Organization (WHO), Food and Agriculture Organization of the United Nations (FAO), and the Food and Drugs Administration (FDA) [4, 6]. Of these, chromium—a key material in the production of stainless steel, metal plating, and the manufacturing of industrial dyes and paints—has become alarmingly prevalent in water systems. Effluents containing chromium contribute to the existing heavy metal pollution in water, primarily hailing from chemical plants, tobacco smoke, and contaminated landfills [1, 7, 8].

Generally, heavy metals have cytotoxic, mutagenic, and carcinogenic effects to the health of organisms upon prolonged exposure [6]. In its hexavalent oxidation state, Cr (VI), chromium posits similar harmful effects: it is toxic to vital tissues of biotic organisms near contaminated water, a strong irritant, and a potential human carcinogen [1]. Moreover, the bioaccumulation of Cr^{6+} in humans can cause fatal complications in metabolism and regular bodily functions, resulting in acute organ failure and even death [8]. As a result, hexavalent chromium compounds are categorized by the Department of Environmental and Natural Resources (DENR) under its Priority Chemical List (PCL), for strict regulation and monitoring in the environment. Despite this, Cr^{6+} in the ecosystem continues to exceed the 0.1 ppm Philippine safe standard, reaching concentrations of up to 16 ppm [9].

Numerous technologies and treatments, which make use of various physical and chemical interactions in the environment, are currently employed to address heavy metal pollution in water. Among these strategies, the most favorable method of remediation is adsorption, a process involving the deposit of atoms and ions onto the surface of a highly porous, solid material [8]. Biological by-products are considered more novel, potential sources of good adsorbents, a facet of the method's cost-effectiveness, low energy demand, feasibility, accessibility, and sustainability [11].

Organic waste from agricultural activity were tested and proven efficacious as low-cost heavy metal adsorbents [11]. While land-based waste products are prevalently sourced and studied in adsorptive remediation research, the potential of

How to cite this article:
CSE: Faciolan CE, Leonora FHS, Majaducon LV, Sinco RA. 2020. Organo-mineral composites from the shells of *Crassostrea iredalei* (slipper cupped oyster), *Perna viridis* (green shell), and *Telescopium telescopium* (horned snail) in the removal of chromium (VI) from water. Publiscience. 3(1): 2-5.
APA: Faciolan, C.E., Leonora, F.H.S., Majaducon, L.V., & Sinco, R.A. (2020). Organo-mineral composites from the shells of *Crassostrea iredalei* (slipper cupped oyster), *Perna viridis* (green shell), and *Telescopium telescopium* (horned snail) in the removal of chromium (VI) from water. *Publiscience. 3*(1): 2-5.

waste products derived from aquatic resources are, in comparison, yet to be maximized. Nonetheless, the effective heavy metal removal of calcium carbonate ($CaCO_3$)—a mineral potently occurring in limestone, lime mud, eggshells, and mollusk shells—is well-established [12, 13, 14, 15].

Of these calcium reservoirs, mollusk shells—considered by-products of global shellfish consumption and big contributors to solid waste management problems in the country [17]—emerge as a more renewable and novel, albeit less explored $CaCO_3$-rich bioadsorbent [14, 16]. Generally, these shells are composites of several superimposed calcified layers structured by organic functional groups [15, 18]. A large percentage of the shell's chemical makeup is composed of either one of two naturally-occurring polymorphs of $CaCO_3$ [19]; however, the identity of the polymorph produced, as well as its percent composition, varies across mollusk species as a result of interspecies variations in shell formation [18, 20, 21, 22]. Thus, the capacities of shells derived from different mollusk species are expected to differ with respect to the identity and amount of heavy metal contaminant that the composites can remove [18].

However, there is a current lack of batch studies that consider differences in the remediation efficiencies of different speciated mollusk shells. To address this gap, this study investigated the short-term Cr^{6+} removal efficiencies of three of the most commonly consumed and produced mollusks in the Philippines [23]: *Crassostrea iredalei* (slipper cupped oyster), *Perna viridis* (green shell), and *Telescopium telescopium* (horned snail).

Specifically, the study aimed to:

(i) measure the initial and final absorbance of the Cr^{6+} solution before and after treatment of *C. iredalei*, *P. viridis*, and *T. telescopium* using UV-Visible spectrophotometry;

(ii) obtain the concentration of Cr^{6+} removed by *C. iredalei*, *P. viridis* and *T. telescopium* using a Cr^{6+} calibration curve; and

(iii) compare the concentration of Cr^{6+} removed by *C. iredalei*, *P. viridis* and *T. telescopium* using One-way ANOVA.

Methods. Prior to treatment, *C. iredalei*, *P. viridis*, and *T. telescopium* shell composites were oven-dried and processed to fine powder size. These treatments were then incorporated in 1 mg doses to three replicates of a 10 ppm Cr^{6+} solution per shell species. Treatments were incorporated to the solution for a contact time of 20 minutes. The absorbances of the solutions before and after treatment were measured using UV-Visible Spectrophotometry, from which Cr^{6+} concentration values were derived. One-way analysis of variance (ANOVA) was conducted to test for significant differences among and between treatments.

Preparation of shell samples. Samples were purchased from a local wet market, segregated by species, and boiled at 100°C for 10 minutes to remove unnecessary organic matter. Shell meat and flesh were removed prior to fragmentation, and the shells were shattered before rinsing with distilled water. Samples were subsequently oven dried at 105°C for a total of 24 hours, crushed to fine powder, and sieved to a particle size range of ≤ 63µm.

Treatment. Prior to testing, a 10 ppm Cr^{6+} solution was freshly prepared from the dilution of potassium dichromate ($K_2Cr_2O_7$) in distilled water. The initial absorbance of the stock solution was measured using a Shimadzu UV-Visible (UV-Vis) Spectrophotometer. The initial pH value was also recorded using a pH meter, and the solution was adjusted to a value below 3 through the addition of 1 M hydrochloric acid (HCl). Acidic conditions were maintained to prevent the reduction of Cr^{6+} ions to Cr^{3+} in solution, which occurs upon basification or with the incorporation of the organo-$CaCO_3$ treatment [24]. Setups corresponding to each of the three shell species were prepared, with three 100-mL replicates of the 10 ppm Cr^{6+} solution prepared per setup. A milligram of the corresponding treatment was incorporated to each replicate, and all set-ups were agitated for 20 minutes at 100 rpm, using a laboratory shaker. Shell powders were filtered out of the replicates using Whatman No. 40 filter papers. The absorbance of each replicate was measured, and final pH values per setup were recorded.

Data analysis. The concentration of Cr^{6+} removed, expressed in ppm, was obtained from the difference between the initial and final concentrations of the solution, while the adsorption efficiency (Q) of the three treatments was calculated from the formula:

$$Q = 100 \times \frac{(C_0 - C_1)}{C_0},$$

where C_0 and C_1 represent the initial and final concentrations of the Cr^{6+} solution, respectively. Tests for significant differences among the Cr^{6+} concentrations removed by each treatment using one-way Analysis of Variance (ANOVA) was conducted after data gathering, and post-Hoc Least Significant Difference (LSD) test was used in the further determination of significant differences between treatments. All statistical tests were run using the R statistical tool.

Safety Procedure. At all times, personal protective equipment (PPE) were used in the handling of laboratory reagents, apparatus, and equipment. Organic matter in samples were treated immediately to prevent unwanted interference in treatment and analysis. All used chemicals were collected in empty plastic bottles for collection and disposal.

Results and Discussion. *T. telescopium* removed 0.784 ppm chromium (VI) from a starting concentration of 10 ppm (9.632%), the highest amount among the three treatments, as seen in Table 1.

Table 1. A summary of adsorption efficiencies (Q), concentration (in ppm) of Cr^{6+} removed (C_o-C_l), initial, and final pH values for all treatments.

Treatment	C_o-C_l (ppm)	Q (%)	pH	
			initial	final
C. iredalei	0.279	3.431	2.12	2.14
P. viridis	0.687	8.444	2.12	2.16
T. telescopium	0.784	9.632	2.12	2.17

A significant difference was found among groups at the 95% confidence interval. Furthermore, following a post-Hoc test for least significant difference (LSD), significant differences were found to exist between *C. iredalei* and *T. telescopium,* and *C. iredalei* and *P. viridis.* However, no significant difference exists between *T. telescopium* and *P. viridis,* implying that the two treatments are not significantly different in effectivity and efficiency.

Increments in the final pH were observed for all treatments, given a starting value of 2.12 (Table 1), signifying that CO_3^{2-} ions in the shell powders were released and incorporated into the solution during the 20-minute contact period [10]. While these values have not exceeded the threshold of pH 3 to report significant basification, it was ensured that acidic conditions were maintained to prevent Cr^{6+} reduction [24].

These findings support the idea that differences in shell formation per species contribute to variances, if any, in the efficiency of organo-mineral composites in terms of chromium removal [18]. Localizations in the biomineralization process for each mollusk species result to variations in the dominant $CaCO_3$ polymorph formed and the quality of the compound expressed [25]. Moreover, differences in the percent composition of $CaCO_3$ and organic matter among mollusk shells have an apparent effect in the concentration of heavy metal removed by the material, as the former may not be the sole compound involved in surface adsorption [15].

Although *Crassostrea sp.* and *P. viridis* are reported to contain more $CaCO_3$ than *T. telescopium* [19, 21, 22], the latter surpassed the two in chromium removal and adsorption efficiency. This can be attributed to the larger percentage of structural biomolecules, which have larger electronegativity differences with Cr^{6+} than $CaCO_3$ and are responsible for the adsorption of carbonate salts formed by displacement reactions involving the species [15, 20, 26].

While no other batch study comparing the heavy metal removal efficiencies of *C. iredalei, P. viridis,* and *T. telescopium* exists, previous studies have established their individual capacities for other heavy metals. *Telescopium spp.* shells have a maximum adsorption capacity of 4.6 ppt for copper [20], *Perna spp.* shells can adsorb up to 89.23 ppm of zinc [27], and *Crassostrea spp.* shells are 96.2% efficient in removing cadmium from water [28].

Limitations. The results of this study support the claim rooted in literature that variances in chromium adsorption efficiency are largely accounted to differences in the organic and mineral composition of unique mollusk species. However, the researchers were not able to determine the specific functional groups active in the adsorption mechanism, as well as the amount and the identity of the $CaCO_3$ polymorph present in the samples used, as they required additional characterizations via scanning electron microscope with electron dispersive spectroscopy (SEM-EDS) and infrared (IR) spectroscopy. Apart from this, treatment periods were limited to 20 minutes per replicate; thus, the data presented by this study are only short-term removal efficiencies of these shell composites. Information on whether the *T. telescopium* treatment remains the most efficient among the three species at extended contact times cannot be provided or justified by this study. Lastly, while a concentration of 1 mg per replicate was used for all three treatments, this value serves exclusively as a baseline for comparison; optimizing the concentration of adsorbent used is beyond the scope of this study.

Conclusion. The shells of *Crassostrea iredalei, Perna viridis,* and *Telescopium telescopium* are all capable of removing Cr^{6+} from water, with the latter of the three reporting the highest amount of the metal removed and, subsequently, the highest removal efficiency. These findings are caused by both the chemical properties of the organo-mineral components of the shells and differences in the formation of each shell contribute to their variances in removed Cr^{6+}.

Recommendations. The study serves as a baseline for future comparative analyses of different mollusk shells in the removal of certain heavy metals from water. It is highly recommended that similar batch studies be undertaken to address the dearth of knowledge in this sector of water remediation. Future studies are advised to simulate real-time conditions of heavy metal pollution as a practical application of this line of research. Additionally, the researchers recommend that the amount of adsorbent added per unit volume of replicates be considered in determining the optimal removal efficiencies of the treatments used. Lastly, for a more accurate reflection of the shells' removal capacities, the effects of contact time to the concentrations of metal removed should be considered in the future, and that batch adsorption kinetics and equilibrium studies employ the adsorbents used in this study in the investigation of their long-term effects.

Acknowledgement. The researchers would like to thank Mr. Roxzien Sesbreño and the staff of the Department of Science and Technology – Regional Office VI (DOST-VI). They would also like to extend their gratitude to Dr. Laureen Manalo & Mrs. Jessebel Gadot, both from the Office of the Vice Chancellor for Research and Extension, University of the Philippines - Visayas. The invaluable time, knowledge, and support they imparted have all contributed uniquely to the fulfillment of this study.

References

[1] Oliveira H. 2012. Chromium as an environmental pollution: insights on induced plant toxicity. J Bot. 2012: 1-8.

[2] Taberna, Jr. H, Nillos MG, Gamarcha L, Pahila I, Gastar A. 2014. Analysis of road-deposited sediments for heavy metal pollutants in bridge sidewalks of Iloilo City, Philippines. AES Bioflux. 6(1): 69-75.

[3] Taberna, Jr. H, Nillos MG, Pahila I, Arban JP. 2015. Distribution and geochemical behaviour of heavy metals (Cr, Cu, Ni and Pb) in Iloilo river estuarine sediments. AES Bioflux. 7(1): 11-17.

[4] Sarinas BG, Gellada L, Jamolague E, Teruñez M, Flores JRP. 2014. Assessment of heavy metals in sediments of Iloilo Batiano River, Philippines. Int J Environ Dev. 5(6): 543-546.

[5] Cabuga CC *et al.* 2017. Geometric morphometric and heavy metals analysis of flathead grey mullet (*Mugil cephalus*), from Agusan River, Butuan City, Philippines. J Biodiv Environ Sci. 11(1): 134-151.

[6] Solidum J, De Vera MJ, Abdulla AR, Evangelista J, Nerosa MJA. 2013. Quantitative analysis of lead, cadmium, and chromium found in selected fish marketed in Metro Manila, Philippines. Int J Environ Dev. 4(2): 207-212.

[7] Onchoke K, Sasu S. 2016. Determination of hexavalent chromium (Cr (VI)) concentrations via ion chromatography and UV-Vis spectrophotometry in samples collected from Nacogdoches Wastewater Treatment Plant, East Texas (USA). Adv Environ Chem.

[8] Bobade V, Eshtiagi N. 2015. Heavy metals removal from wastewater by adsorption process: a review. From APCChE 2015 Congress incorporating Chemeca 2015; 2015 Sep 27 – 2015 Oct 1, Melbourne, Australia.

[9] Sarinas BG, Gellada L, Jamolague E, Teruñez M, Flores JRP. 2014. Assessment of heavy metals in sediments of Iloilo Batiano River, Philippines. Int J Environ Dev. 5(6): 543-546.

[10] Bajinath L, Gautam V, Vadav VL. 2014. A comparative study of the removal efficiency of calcium hydroxide and sodium hydroxide as precipitating agents for chromium (III). J Civil Eng Environ Tech. 1(1): 17-20.

[11] Mathew BB, Jaishankar M, Biju VG, Beeregowda KN. 2016. Role of bioadsorbents in reducing toxic metals. J Tech. 2016: 1-13.

[12] Shin WS, Kang K, Kim YK. 2014. Adsorption characteristics of multi-metal ions by red mud, zeolite, limestone, and oyster shell. Environ Eng Res. 19(1): 1-8.

[13] Sthiannopkao S, Sreesai S. 2009. Utilization of pulp and paper industrial wastes to remove heavy metals from metal finishing wastewater. J Environ Manage. 90(2009): 3283-3289.

[14] Abeynaike A. Wang L. Jones M. Patterson D. 2011. Pyrolysed powdered mussel shells for eutrophication control: effect of particle size and powder concentration on the mechanism and extent of phosphate removal. Asia-Pac J Chem Eng. 6 231-243.

[15] Weerasooriyagedra MS, Kumar SA. 2018. A review of utilization of *Mollusca* shell for the removal of contaminants in industrial wastewater. Int J Sci Res Pub. 8(1): 282-287.

[16] Zukri NI, Khamidun MH, Sapiren MS, Abdullah S, Rahman MAA. 2017. Lake water quality improvement by using waste mussel shell powder as an adsorbent. 2018 IOP Conf Ser: Earth Environ Sci. 1-6.

[17] Hapinat HL. 2019. Waste from discarded oyster shells: a promising raw material for lime industry in the Philippines. FFTC Agricultural Policy Platform (FFTC-AP). Available online at: http://ap.fftc.agnet.org/index.php.

[18] Marin F, Le Roy N, Marie B. 2012. The formation and mineralization of mollusk shell. Frontiers in Bioscience. 1099-1125.

[19] Rahman NA, Said MIM, Azman S. 2017. Carbonized green mussel shell as heavy metal removal. Malay J Civ Eng. 29(1): 56-68.

[20] Darmokoesoemo H, Setianingsih FR, Putranto TWLC, Kusuma HS. 2016. Horn snail (*Telescopium* sp) and mud crab (*Scylla* sp) shells powder as low cost adsorbents for removal of Cu^{2+} from synthetic wastewater. J Chem. 9(4); 550-555.

[21] Darwin C, Padmavathi P. 2017. Preliminary assessment of calcium in six molluscan shells of Tamilnadu coast, India. Eco Env & Cons. 24(1): 302-305.

[22] Hamester MRR, Balzer Ps, Becker D. 2012. Characterization of calcium carbonate obtained from oyster and mussel shells and incorporation in polypropylene. Mat Res. 15 (2): 204-208.

[23] Mapa CS, Bautista R. 2019. Fisheries statistics of the Philippines 2016-2018. Philippine Statistics Authority.

[24] Sanchez-Hachair A and Hofmann A. 2018. Hexavalent chromium quantification in solution: Comparing direct UV-visible spectrometry with 1,5-diphenylcarbazide colorimetry. C R Chim. 21(2018): 890-896.

[25] Checa A. 2018. Physical and biological determinants of the fabrication of molluscan shell microstructures. Frontiers Marine Sci. 5: 1-21.

[26] Jain M, Garg VK, Kadirvelu K, Sillanpää M. 2016. Adsorption of heavy metals from multi-metal aqueous solution by sunflower plant biomass-based carbons. Int J Environ Sci Technol. 13(2016): 493-500.

[27] de Asudillo LR, Yen IC, Agard J, Bekele I, Hubbard R. 2002. Heavy Metals in Green Mussel (*Perna viridis*) and Oysters (*Crassostrea sp.*) from Trinidad and Venezuela. Arch Environ Contam Toxicol. 42(2002): 410-415.

[28] Gao YJ. 2013. Removal of Cadmium and Cobalt from Heavy Metal Solution Using Oyster Shell Adsorbent. Asian J Chem. 25(15): 8527-8540.

Determination of the phosphate adsorption potential of biochar derived from *Ananas comosus* (pineapple) peels in aqueous solution

CAELAN PHILIP B. DIAZ, NIKO EMMANUEL GOLO, NICOLE M. VILLALUNA, and ATHENES JOY PRESNO - ABAN

Philippine Science High School - Western Visayas Campus, Brgy. Bito-on, Jaro, Iloilo City 5000, Department of Science and Technology, Philippines

Abstract

The increased demand and use for phosphate around the world have caused the global phosphate level to rise. Adsorbents such as biochar are commonly used to remediate heavy metals, but research has also shown its potential to remediate excess nutrients. Pineapple peels were proven to contain magnesium which can aid phosphate adsorption and can be used as a potential biochar feedstock. The study aimed to determine the potential of pineapple peel derived biochar in adsorbing phosphates. Pineapple peel biochar were produced via pyrolysis at 300 °C, 400 °C, and 500 °C, and then characterized using a Fourier Transform Infrared (FTIR) spectrometer. Biochar analysis showed biochar decomposition as pyrolysis temperature was increased. Phosphate analysis showed positive adsorption rates at 25 ppm concentrations but showed negative adsorption rates at lower concentrations. The results showed a general inverse relationship between the biochar adsorption capacity and pyrolysis temperature which directly contradicts previous research.

Keywords: *pineapple peels, Ananas comosus, phosphate, adsorption, biochar*

Introduction. The increased industrial and agricultural demand and use for phosphate around the world caused the global phosphate levels to exceed the assimilation capacity in river basins which covers a total of 38% of the world's land surface area [1]. Locally, the phosphate levels in the local rivers have been nearing or have reached the 0.5 mg/L limit set by the Environmental Management Bureau [2].

Biochar is a pyrolyzed biomass used for remediation or sequestration purposes [3]. The speed and temperature of the pyrolysis of the biomass can affect the structure and functional groups that comprise the biochar. Biochar pyrolyzed at slower rates and lower temperatures tend to have more diversified organic characters including aliphatic and other types of molecular structures, more functional groups and a higher possible ion exchange capacity [4,5]. On the other hand, biochar pyrolyzed at higher temperatures has more pores. Therefore, it has a greater surface area yet is more carbonized and has less functional groups [5,6].

Biocharcoal have specific ions that can positively affect the biochar adsorption capacity of excess nutrients in the water, for example, correlation between the magnesium ions in the biochar and the phosphorus adsorption capacity of the biochar can be used as a basis for choosing the biomass stock for the production of biochar [5,6].

Pineapple peels have been used for the production of biochar for the remediation of chromium and oxytetracycline [8,9].

Since there are limited studies on the potential use of pineapple peel biochar on the remediation of excess phosphates, this study aimed to determine the potential of biochar derived from the peels of *Ananas comosus* (pineapple) pyrolyzed at different temperatures (300, 400, and 500°C) in adsorbing phosphates.

Studying the adsorption capacity of pineapple peels on phosphate can contribute to the current understanding of the relationship between the biochar adsorption capacity of a specific pollutant, and its structure and composition. The study specifically aimed to:

(i) characterize biochar pyrolyzed at 300, 400, and 500°C using Fourier Transform Infrared (FTIR) spectroscopy;

(ii) measure the phosphate concentration of phosphate solution samples before and after treatment with biochar;

(iii) calculate the adsorption potential of biochar by using the concentration of phosphates removed from the water; and

(iv) compare the adsorbed amounts of phosphates of the biochars pyrolyzed at 300, 400 and 500°C.

Methods. Pineapples were dried, powdered, and then pyrolyzed at three different temperatures - 300, 400, and 500 °C. The resulting treatments were referred to as PP300, PP400, and PP500. The yield of

How to cite this article:
CSE: Diaz CP, Golo NE, Villaluna N, Aban AJ. 2020. Determination of the phosphate adsorption potential of biochar derived from *Ananas comosus* (pineapple) peels in aqueous solution. Publiscience. 3(1):6-10.
APA: Diaz, C.P, Golo N.E., Villaluna N., & Aban AJ. (2020). Determination of the phosphate adsorption potential of biochar derived from *Ananas comosus* (pineapple) peels in aqueous solution. *Publiscience,* 3(1):6-10.

each sample was calculated and the adsorbents were characterized using FTIR analysis. The adsorption potential of the different biochars were determined through conducting five replicates of batch adsorption experiments, and calculating their removal rates and adsorption capacity after measuring the phosphate levels in the treated water using the 18th edition of American Public Health Association (APHA 1992) 4500-P standard methods for phosphate analysis [10]. Lastly, one-way analysis of variance (ANOVA) and paired t-Test were used to determine a significant difference among the means of the phosphate adsorption capacity of each biochar. All analyses unless otherwise stated were performed at the Biology and Chemistry Instrument laboratories at Philippine Science High School – Western Visayas Campus.

Pre-pyrolysis procedures. Pineapples were obtained from Leganes Public Market, Iloilo. The peels were thoroughly separated from the flesh by careful scraping. The peels were air-dried for 24 hours, and then oven-dried at 70°C for 12 hours. The oven-dried peels were ground using a blender and passed through a 1 mm sieve. Five grams of pineapple peels were weighed using an analytical balance, and were placed into ten constant-weighed ceramic crucibles for each pyrolysis temperature.

Pyrolysis. The powdered peels were stored in a plastic container with silica desiccant, and were brought to the Department of Science and Technology - Regional Standards and Testing Laboratory (DOST - RSTL) for slow pyrolysis. The crucibles were covered with lid to ensure oxygen-poor conditions, and charred under three different temperatures- 300, 400, and 500 °C using a muffle furnace, at a ramp rate of 5°C/minute. The crucibles were incubated at the peak temperature for 2 hours before cooling down to room temperature using a desiccator [8].

Ash and Biochar Separation. The resulting products of pyrolysis were immersed in 0.1M of HCl solution overnight. It was then rinsed with distilled water and oven-dried overnight at 60°C. After cooling down to room temperature, the solids were passed through a No. 100 mesh 149-µm sieve to obtain the final biochar samples [8]. The final samples were named PP300, PP400, and PP500, respectively. The biochar was stored in a desiccator until usage.

Biochar characterization. The functional groups present on the surface of the biochar were identified using Fourier Transform Infrared (FTIR) analysis, following the Attenuated Total Reflection (ATR) method for solids.

Sorption Tests. Five phosphate solutions were prepared by dissolving respective amounts (10, 20, 30, 40, 50 mg) of anhydrous monopotassium dihydrogen phosphate (KH_2PO_4) in 1 L distilled water. All glassware used were washed using 1:1 HCl and rinsed with distilled water to prevent contamination of other chemicals [10]. In separate Erlenmeyer flasks, 150 mL of each phosphate solution were treated with 0.3 g of biochar, shaken for 24 hours at 200 rpm using a mechanical shaker [11].

The agitated phosphate solutions were filtered with Grade 1 Whatman 11-µm filter paper, and then with 0.45-µm nylon membrane filters previously soaked in two liters of distilled water for 24 hours. The phosphate content of the treated solutions was determined using the stannous chloride acid method from APHA 1992 [10].

Spectrophotometry Analysis. The phosphate analysis was conducted by batches of five to maximize the capacity of the UV-1800 Shimadzu Ultraviolet–visible (UV-Vis) spectrophotometer. A volume of 25 mL of the phosphate solution samples were placed in 50-mL Erlenmeyer flasks. One (1) mL of the ammonium molybdate solution was added and mixed. Then, two drops of the stannous chloride solution were added and swirled. Samples were transferred to cuvettes within 5 to 15 minutes. Absorbance of samples were measured using a UV-Vis spectrophotometer at a wavelength of 650 nm [10]. The concentration limit of detection of the analysis was determined to be at 9.94 ppm.

Data Analysis. Using Microsoft Excel 2016, paired t-Test was conducted to determine if there is a significant difference between the means of the phosphate content of the solutions pre- and post-treatment of each biochar at each concentration. One-way ANOVA analysis was used to determine if there is a significant difference between the performance of each biochar. All analyses used a significance level (α) of 0.05.

Safety Procedure. Laboratory gowns, gloves and masks were worn every time chemicals were being handled. Excess $SnCl_2$ solution was turned over to the school's Chemistry Science Research Assistant (SRA). Solutions were disposed of in waste bottles which were labeled “Inorganic Waste”, and were turned over to the Chemistry SRA for proper disposal.

Results and Discussion. In Table 1, it is shown that as the pyrolysis temperature increases, the biochar yield decreases. This is mainly due to the cellulose-hemicellulose degradation and lignin decomposition as the pyrolysis temperature increases [12,14]. The degradation of cellulose is governed by parallel and competing steps that consequently produce products such as charcoal, water, tar and gas [13]. In addition, as the pyrolysis temperature increases, the increased decomposition of the organic matter of the biochar, the progressive concentration of inorganic compounds and the destructive volatilization of ligno-cellulosic matter led to the ashing of inorganic compounds and therefore caused further decrease in biochar yield [9]. This decrease in the biochar yield was also evident in related literature that pertained to the pyrolysis of pineapple peels and other biomass [7,9,12].

Table 1. Biochar yield of pineapple peels pyrolyzed at 300°C, 400° C, and 500° C.

Biochar	Yield (g)	Yield (%)
PP300	~ 14.9197	29.84%
PP400	~9.6137	19.23%
PP500	~8.3028	16.61%

These trends were also substantiated by the FTIR analysis which showed similar peaks and increasing transmittance. As seen in Figure 1, there is a notable decrease in the number of functional groups as temperature increases indicating the increased degradation of the pineapple peel at higher temperature. The results of the FTIR spectroscopy showed distinct peaks at about 3050, 1725, and 1610 cm^{-1}, signifying the presence of aliphatic alkane (C=C-C) and carbonyl groups (C=O). The individual peaks generated by C=O stretching at 1725 and 1610 cm^{-1} indicate possible formations of aliphatic and conjugated ketones (has C=C unit attached directly to the carbon of the carbonyl group) [14]. In addition, the peaks at 2300 and at 3050 cm^{-1} refer to the stretching of the alkyl functional group, and the molecular bonds of the C=C which denote presence of benzene rings, respectively.

FTIR analysis also showed that the transmittance of the C=C bonds increased slightly at biochar pyrolyzed at 400 °C but decreased at 500°C while there was a general increase of the transmittance of other functional groups as temperature increases. These changes might signify that most of the functional groups decreased in number as there are few bonds to absorb that light in the sample and therefore can transmit higher amounts of light. This decrease indicates the increased thermal degradation of the pineapple peel biochar due to increased energy availability which can destabilize the molecular bonds. Furthermore, previous studies showed that biochar prepared at higher temperatures exhibited lower (O/C) and (H/C) ratios, which corresponded to the loss of functional groups on biochar pyrolyzed at higher temperatures [7,9,11].

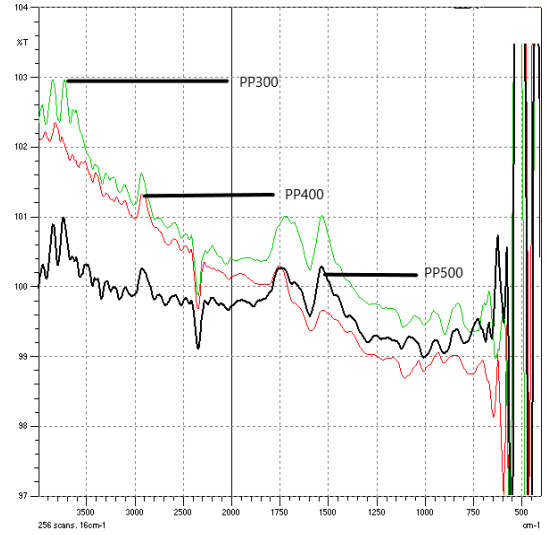

Figure 1. Zoomed FTIR spectra of PP300, PP400 and PP500.

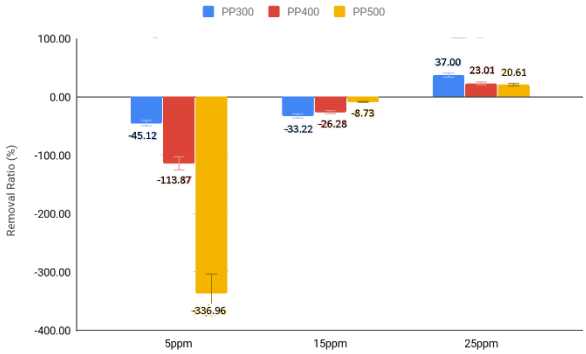

Figure 2. KH_2PO_4 removal ratio (%) of biochars PP300, PP400, and PP500.

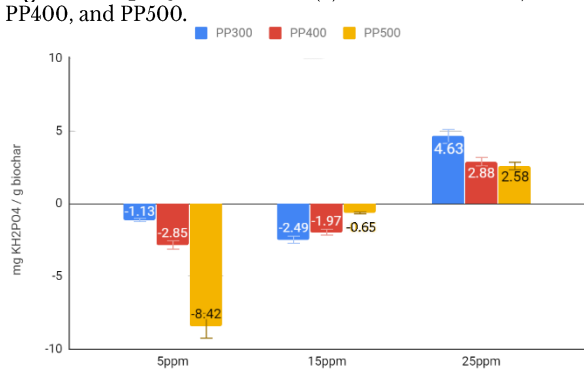

Figure 3. Adsorption capacity of PP300, PP400, and PP500 in different concentrations of phosphate solutions.

The predominantly negative results (-0.65 to -8.42 mg KH_2PO_4/g biochar) could suggest that using pineapple peel biochar for the overall remediation might be inefficient and cannot adsorb high amounts of pollutants. However, earlier studies using pineapple peel biochar for the adsorption of oxytetracycline and chromium (VI) showed positive potential in treating pollutants [8,9]. Although pineapple peel biochar was used for the remediation of other pollutants, it must be taken into consideration that pineapple peel biochar might not be suited for nutrient pollutant adsorption in general as biochar is often negatively charged, making it repel negatively charged ions such as phosphate [11]. However, previous research established that pineapple peels have 107 +/- 5.2 mg of magnesium per 100g of the peel in dried basis [10], and SEM analysis of Wang et al. [8] showed that amounts of magnesium ions were still present which have a positive effect in the adsorption capacity of phosphates [7,11]. Considering the previous literature regarding the use and chemical composition of pineapple peel biochar [8,9], together with the fact that the biochar used for the adsorption of 25 ppm phosphate solutions showed positive adsorption capacity, the inconsistent data cannot be attributed to the inefficiency of the pineapple peel biochar itself.

Furthermore, it should be noted that time during pyrolysis and agitation was standard in other research concerning the remediation of phosphates. According to Trazzi et al. [5], like adsorption, the desorption process of phosphate was influenced by the phosphate concentration in solution, carbonization temperature, and agitation time. This implies that the biochar pyrolyzed at higher temperatures, had longer agitation time in the phosphate solution and had been

utilized for the adsorption of more saturated phosphate solutions is more likely to undergo 50% desorption of phosphate [5], but the desorption of the biochar used does not seem to follow this trend.

Biochar also exhibits variable physicochemical properties that can directly influence adsorption such as pyrolysis temperature and biochar feedstock. The latter directly affects the chemical composition and surface characteristics that can influence phosphate sorption and desorption capacity causing varied and contrasting findings on the effect of biochar on phosphate (PO_4) sorption. For example, magnesium (Mg) enrichment of corn and peanut biochar enhanced the anion exchange capacity of phosphate [6,15].

The phosphate adsorption results showed that the standard deviation of all the replicates of the 5 mg/L concentration (σ = 3.66), regardless of pyrolysis temperature, was much higher than those of the replicates at 15 mg/L (σ = 0.98) and 25 mg/L (σ = 1.44). These results could imply inaccuracies in the concentrations used for the adsorption. This could be due to errors, human or otherwise, during the weighing of the solute, but it should be taken into consideration that the standard deviation generally decreases as the concentration increases which denotes a possible constant error during the weighing.

These erratic results may also be due to the possible desorption of phosphate, normal effects of the pyrolysis temperature, or the possible constant error during the weighing and preparation of the monopotassium phosphate solute. In addition, the long storage of the biochar can be a possible cause of the low phosphate adsorption rates. Research on the effect of biochar ageing on the adsorption of diuron and glyphosate herbicides by Zhelezova et al. [16] showed that the ageing of soil-biochar mixtures decreased the adsorption of both herbicides in comparison with freshly biochar-amended soil. This showed a relationship between the degradation of the biochar with the decrease of its adsorption capacity which might have caused the low adsorption rates of the pineapple peel biochar.

The high standard deviations and the conflicting adsorption results of different pyrolysis temperatures and phosphate concentrations mean results showing no cohesion, from which no conclusion can be made that can neither prove or disprove the hypothesis.

Limitations. The study included no characterization of the specific elemental composition and topography of the biochar using scanning electron microscopy and energy dispersive X-ray spectroscopy. Sorption isotherms used to determine adsorption kinetics were not applied in the study. The study also lacked the use of proper reference materials for blanks and pretrials.

Conclusion. The produced biochar showed decreasing yields and functional groups such as C=C, C-H, and C=O, which implied further biochar degradation, as pyrolysis temperature increased. The adsorption of phosphate increased from negative values to positive values as concentrations of the phosphate solutions increased. The high standard deviation and the pattern of adsorption values at lower concentrations imply desorption of phosphate, and errors that are more noticeable at lower phosphate concentrations. Based on these findings, there is no evidence to support nor to dismiss the efficiency of biochar as a phosphate adsorbent.

Recommendations. Further analysis is recommended for the determination of sorption kinetics and isotherms that establish the processes that govern the sorption capacity of the pineapple peel biochar. Furthermore, it is recommended that dilution should be used in order to make solutions with low concentrations to reduce the constant error of weighing apparatus. The addition of sorption pretrials and the usage of proper industrial or reference materials for blanks are also recommended.

Acknowledgement. The researchers would like to extend their gratitude towards the staff of the Department of Science and Technology - Region VI for their generosity and consideration to accommodate them in their laboratory.

References

[1] Mekonnen MM, Hoekstra AY. 2017. Global anthropogenic phosphorus loads to freshwater and associated grey water footprints and water pollution levels: a high-resolution global study. Water Resources Research. 53(1): 1-14.

[2] Environmental Management Bureau (EMB). 2017. Annual Assessment Report CY 2017.

[3] Woolf D, Amonette JK, Street-Perrott FA, Lehmann J, Joseph S. 2010. Sustainable biochar to mitigate global climate change. Nature Communications. (2010): 1- 9.

[4] Ma X, Zhou B, Budai A, Jeng A, Hao X, Wei D, Zhang Y ... 2016. Study of biochar properties by scanning electron microscope – Energy dispersive X-ray spectroscopy (SEM-EDX). Communication in Soil Science and Plant Analysis. 47(5): 593-601.

[5] Trazzi PA, Leahy JJ, Hayes MHB, Kwapinski W. 2015. Adsorption and desorption of phosphate on biochars. Journal of Environmental Chemical Engineering. 4 (2016): 37-46.

[6] Fang C, Zhang T, Li P, Jiang R, Wang Y. 2014. Application of magnesium modified corn biochar for phosphorus removal and recovery from swine wastewater. International Journal of Environmental Research and Public Health. 11(9): 9217–9237.

[7] Zeng Z, Zhang S, Li T, Zhao F, He Z, Zhao H, Yang X, ... 2013. Sorption of ammonium and phosphate from aqueous solution by biochar derived from phytoremediation plants. Journal of Zhejiang University-SCIENCE B (Biomedicine & Biotechnology). 14(12):1152-1161.

[8] Wang C, Gu L, Liu X, Zhang X, Cao L, Hu X. 2016. Sorption behavior of Cr(VI) on pineapple- peel-derived biochar and the influence of coexisting pyrene. International Biodeterioration & Biodegradation. 111: 78-84.

[9] Fu B, Ge C, Ye L, Luo J, Feng D, Deng H, Yu H. 2016. Characterization of biochar derived from pineapple peel waste and its application for sorption of oxytetracycline from aqueous solution. Bioresources. 11(4): 9017-9035.

[10] Greenberg AE, editor. Standard methods for the examination of water and wastewater. Washington: American Public Health Association; 1992.

[11] Yao Y, Gao B, Inyang B, Zimmerman A, Cae X, Pullammanappallil P, Yang L. 2011. Biochar derived from anaerobically digested sugar beet tailings: Characterization and phosphate removal potential. Bioresource Technology. 102(2011): 6273-6278.

[12] Parthasarathy P, Narayanan, KS, and Arockiam, L. 2013. "Study on kinetic parameters of different biomass samples using thermo gravimetric analysis," Biomass & Bioenergy. 58(1): 58-66. DOI 10.1016/j.biombioe.2013.08.004

[13] Shen D, Xiao R, Gu S, Zhang H. 2013. The overview of thermal decomposition of cellulose in lignocellulosic biomass. Environmental Science. DOI:10.5772/51883

[14] Figueredo C, Lopez H, Coser T, Vale A, Busato T Aguiar N, Novotny E, ... 2017. Influence of pyrolysis temperature on chemical and physical properties of biochar from sewage sludge. Archives of Agronomy and Soil Science. 112: 284-289.

[15] Morais DR, Rotta EM, Sargi SC, Bonafe EG, Suzuki RM, Souzaa NE, Matsushitaa M, Visentainer JV. 2017. Proximate composition, mineral contents and fatty acid composition of the different parts and dried peels of tropical fruits cultivated in Brazil. Journal of Brazilian Chemical Society. 28(2): 308-318.

[16] Zhelezova, A., Cederlund, H. and Stenström, J. 2017. Effect of biochar amendment and ageing on adsorption and degradation of two herbicides. Water, Air, & Soil Pollution. 228(6), p.216.

Column adsorption of cadmium (II) and lead (II) using rice husks and mango peels

KATRINA BIANCA T. BANDIOLA, JOSUA JAMES ANGELO Y. GALOTERA, JENN CHRISTEL C. SAMPIANO, and HAROLD P. MEDIODIA

Philippine Science High School - Western Visayas Campus, Brgy. Bito-on, Jaro, Iloilo City 5000, Department of Science and Technology, Philippines

Abstract

Cadmium (II) and lead (II) are commonly found in industrial wastewaters and have negative effects to the body and the environment with prolonged exposure. Conventional methods to remove these metals are costly and inefficient. An alternative method that is more economical is through adsorption, specifically through the use of fruit and vegetable peels. The adsorption efficiencies of a multi-adsorbent column setup composed of rice husk and mango peels, and single-adsorbent columns individually composed of rice husk and mango peels were determined and compared in the removal of cadmium and lead. The heavy metal solution with an initial concentration of 10 mg/L and 30 mg/L for lead and cadmium, respectively, and a pH of 6.0, was tested on the adsorbent column with a bed height of 15cm and a flow rate of ~10mL/min. It was determined that the combination setup had the lowest adsorption efficiency out of all three setups. This was attributed to a reduction on the masses of the adsorbents to control the bed height variable. The single adsorbent columns achieved a higher adsorption efficiency with rice husk at 94.661% for lead and the mango peel column at 80.860% for cadmium.

Keywords: *bed height, column adsorption, heavy metals, multi-adsorbent setup, agricultural wastes*

Introduction. Heavy metals found in industrial wastewater have been increasing over the years due to industrialization [1]. Among the heavy metals present, cadmium and lead are one of the most common heavy metals in industrial wastewater [2,3]. They are especially prevalent in the Iloilo Batiano River wherein the amount of heavy metals exceeded standard levels [4].

Conventional methods are costly and inefficient in removing heavy metals [5]. Thus, fruit and vegetable peels have been previously studied by researchers as potential adsorbents. Among household wastes, mango peels [2,6] and rice husks [5] are known to be capable adsorbents and are very cheap.

Two common methods in removing heavy metals are the batch and column methods. The column method is preferred since it tests the industrial scale applicability of an adsorbent [7].

Most column biosorption experiments used one type of adsorbent material. However, in some studies like that of Navaratne et al. [8], multiple adsorbents were utilized. Multiple adsorbents whether using the batch [9] or column [8] methods have been observed to increase the adsorption uptake of heavy metals when compared to single adsorbent setups. Although some adsorbents are efficient in removing a single type of heavy metal, industrial wastewater rather contains multi-metal species. Thus, evaluating a multi-adsorbent column setup in a solution containing multiple heavy metals is a more practical simulation to real-world industrial wastewater.

Only a few from previous studies have evaluated the capability of a column setup, composed of two different adsorbents, in adsorbing multiple heavy metals. Thus, the study utilized a multi-adsorbent column setup without well-defined layers. It is hypothesized that the column setup with multiple adsorbents will have a higher adsorption efficiency as compared to single adsorbent columns.

This study aimed to determine the adsorption efficiency of a fixed-bed column composed of rice husks and mango peels combined in equal proportions and compare it to the adsorption efficiency of a fixed-bed column with single adsorbents composed of only rice husks and only mango peels for the removal of cadmium (II) and lead (II) in the same aqueous solution. It specifically aimed to:

(i) determine the influent and effluent concentrations (mg/L) of cadmium (II) and lead (II); and

(ii) calculate and compare the percent adsorption (%) of the fixed-bed column setup composed of rice husks, mango peels, and a combination of both in adsorbing cadmium (II) and lead (II).

Methods. The rice husks and mango peels were washed, oven-dried, crushed, and weighed before

How to cite this article:
CSE: Bandiola KBT, Galotera JJAY, Sampiano JCC, Mediodia HP. 2020. Column adsorption of cadmium (II) and lead (II) using rice husks and mango peels. Publiscience. 3(1): 11-15.
APA: Bandiola, K.B.T., Galotera, J.J.A.Y., Sampiano, J.C.C., Mediodia, H.P. (2020). Column adsorption of cadmium (II) and lead (II) using rice husks and mango peels. *Publiscience.* 3(1): 11-15.

they were packed inside the column. Three hundred (300) mL of the heavy metal solution containing lead and cadmium was passed through each of the columns with an approximate flow rate of 10 mL/min. A total of three replicates were conducted for each column. The initial and final metal concentrations were analyzed using the Agilent 4200 Microwave Plasma-Atomic Emission Spectrometer (MP-AES) and were used to calculate for the adsorption efficiencies of the different setups. The data obtained were analyzed using One-Way ANOVA with LSD used as a post-hoc test.

Preparation of the adsorbents. One kilogram husks of *Oryza sativa* from Iloilo Central Market was initially washed with tap water and then with distilled water thrice by batches. After washing, the rice husks were oven-dried for eight hours at 70°C to remove any moisture. It was then ground using a blender. Ten kilograms of ripe mangoes, ranging from class four to five on the ripeness chart [15], was obtained from Iloilo Central Market. The mango peels were sliced into small squares and were initially washed with tap water by batch. It was then washed with distilled water thrice and was oven-dried for 72 hours at 70°C [2]. After drying, it was placed inside a plastic container and was crushed manually. Both the adsorbents were sieved to particles larger than 2 mm. After sieving, the adsorbents were stored in separate air-tight containers.

Preparation of metal solution. Solutions with a concentration of 10 mg/L and 30 mg/L for lead and cadmium respectively were prepared from the following salts: $3CdSO_4 \bullet 8H_2O$ (cadmium sulfate octahydrate, Scharlau) and $Pb(NO_3)_2$ (lead nitrate, Farco) [3]. Using an analytical balance, 60.44 mg of $3CdSO_4 \bullet 8H_2O$ and 47.95 mg of $Pb(NO_3)_2$ were weighed. The salts were then poured into three one-liter volumetric flasks. Deionized water was poured to mark into each of the volumetric flasks. The flasks were agitated until there were no visible solid salt particles in the solution. A pH of 6.0 was obtained using 0.1 M of hydrochloric acid. A strip of pH paper with an accuracy of 1 pH was used to determine the pH of the solution prior to adsorption. The three liter heavy metal solution was transferred and stored in a four-liter HDPE bottle.

Column Design. Before the columns were packed, they were washed with distilled water thrice and were left to air-dry. Using a wooden rod, glass wool was packed inside the column up to a height of 2 cm. After making sure that that layer was flat, the adsorbent layer (rice husks for setup A; mango peels for setup B; a 50:50 bed height combination of rice husk and mango peels for setup C) was then poured inside the column until a 15 cm layer was formed. The sides of the column were tapped for even distribution of the adsorbents. A final layer of glass wool with a height of 1cm was placed on top of the setup. As a primer, 100 mL of deionized water was passed through the column.

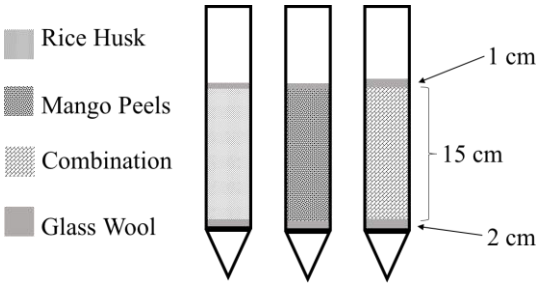

Figure 1. The schematic diagram of the column setups composed of A) rice husks only, B) mango peels only, and C) combination of rice husks and mango peels.

Column Adsorption Experiment. Three hundred mL of the heavy metal solution containing cadmium (II) and lead (II) was passed through the setup. Using a burette as an alternative to a peristaltic pump, the first batch of 50 mL of the 300 mL stock solution was poured into the burette using a funnel. After some of the 50 mL of the solution has finished passing through, the next 50 mL was added into the burette. The procedure was repeated six times. The effluent solution was collected in a 500 mL beaker. The procedure went on until the influent had been fully poured. The effluent solution was transferred from the beaker to an HDPE container for analysis. Concentrated nitric acid was added dropwise to the solution. The column adsorption experiments were done for all setups with each setup having three replicates.

Data Analysis. The heavy metal concentrations were analyzed using the Agilent 4200 MP-AES with a maximum sensitivity of 1 mg/L, and the minimum concentration it can detect is 0.001 mg/L and 0.003 mg/L for lead and cadmium, respectively at the Department of Science and Technology - Region VI. The standard method used was the direct aspiration and digestion of the samples that was done prior to analysis. The total percent adsorption was determined using the initial and final concentrations in mg/L of cadmium (II) and lead (II) ions present in the solution. The percent adsorption was calculated using the formula [8]:

$$Percentage\ Removal\ = \frac{Ci - `Cf}{Ci} \times 100$$

Where C_i is the initial concentration and C_f is the concentration of the metal ion present in the effluents collected from columns.

Statistical Analysis. A test for homogeneity was conducted for the adsorption capacities for the replicates of each setup. One-way ANOVA for the three means using the R Programming Language version 3.5.3 (March 2019) was used to analyze the adsorption efficiencies. A significance level of 0.05 was used. When a significant difference was observed, the Least Significant Difference (LSD) was used as a post-hoc test.

Safety Procedure. The leftover influents, effluents, and greywater collected from the washing were stored separately in properly-labeled air-tight polyethylene (PET) bottles and were handed over to the PSHS-WVC Science Research Assistant for proper storage and disposal. While the used adsorbents were

tightly wrapped with paper and were stored inside properly-labeled air-tight plastic bags. The liquid and solid wastes were stored separately. Both waste disposal methods were in accordance with the protocol of the Department of Science and Technology Region VI.

Results and Discussion. Presented in Table 1 are the mean ± standard deviation of the influent and effluent concentrations. The mean initial concentration of cadmium was 29.630 mg/L with a standard deviation of 0.668. The mean initial concentration of lead was 9.370 mg/L with a standard deviation of 0.014. Among the three setups, setup B achieved the lowest final concentration at 5.672±2.028 mg/L for cadmium adsorption. It was followed by setup A at 7.498±1.871 mg/L of cadmium and then, setup C at 10.242±0.956 mg/L of cadmium. Among the three setups, setup A achieved the lowest final concentration for lead at 0.050±0.387 mg/L. It was followed by setup B at 1.509±0.329 mg/L of lead and then, setup C at 1.975±0.324 mg/L of lead.

Table 1. Mean ± standard deviation of the concentrations (mg/L) of the influents and effluents for cadmium and lead.

Adsorbent	Cadmium (mg/L)	Lead (mg/L)
Initial	29.630 ± 0.668	9.370 ± 0.014
Rice Husk *(setup A)*	7.498 ± 1.871	0.050 ± 0.387
Mango Peel *(setup B)*	5.672 ± 2.028	1.509 ± 0.329
Combination *(setup C)*	10.242 ± 0.956	1.974 ± 0.324

The comparison between the adsorption efficiency for each setup is shown in Figure. 2. Among the three setups, setup A achieved the highest percent adsorption in removing lead at 94.66%. On the other hand, setup B achieved the highest percent adsorption for cadmium at 80.86%. For both heavy metals, setup C achieved the lower percentages adsorption.

As denoted by an asterisk (*) in Figure 2, it was determined that setup A has a significantly higher percent adsorption for lead compared to both setup B ($0.012 \leq 0.05$) and setup C ($0.002 \leq 0.05$). For cadmium adsorption, setup B was found to have a significantly higher percent adsorption compared to setup A and setup C. Additionally, there was a significant difference observed in the percent adsorption for the other two setups. Generally, the adsorption efficiencies of the single-adsorbent column setups were much higher than the combination setup.

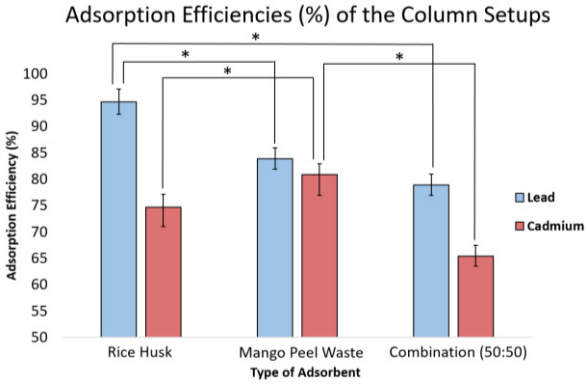

Figure 2. The percent adsorption (%) and standard deviations of each setup for cadmium and lead (* denotes that the $p \leq 0.05$, thus there is a significant difference between the means of the setup).

The results of the study suggest that both rice husks and mango peels vary in the efficiency of removal of a specific heavy metal in a multi-metal solution. It was also determined that the combination of these two adsorbents in the combination column setup reduced the adsorption efficiency.

The three columns were able to achieve adsorption efficiencies ranging from 65.438% to 94.661%. However, it was observed that setup C composed of both adsorbents having a 50:50 bed height ratio had a lower adsorption efficiency for both metals. The lower adsorption efficiency of a combination column setup can be attributed to the reduction of their adsorbent mass that specializes in the adsorption of a specific heavy metal [5]. Having a much lower adsorbent mass would result in less binding sites for the metal ions; thus, the total adsorption efficiency would also decrease. In conjunction with the study by Navaratne et al. [8], the multi-adsorbent setup did not have the highest efficiency. Instead, the single adsorbent column composed of brick clay had the highest adsorption efficiency for both cadmium and lead. Similarly, in this study, both the single adsorbent setups, the rice husk and mango peel columns, had the highest adsorption efficiencies compared to the combination setup in removing lead and cadmium, respectively. However, the results of this study are in contrast to the findings of Binabaj et al. [9] which determined that the multi-adsorbent batch setup had the highest adsorption efficiency compared to single adsorbent setups due to the diversity of the functional groups existing on the surfaces. A 50:50 adsorbent ratio was not guaranteed to produce the highest adsorption efficiency as observed in the study of Binabaj et al. [9] which conducted the batch method rather than the column. Their multi-adsorbent setup, composed of coal and zeolite, had the highest adsorption efficiency at a coal to zeolite ratio of 75:25.

The rice husk setup achieved the highest adsorption efficiency for lead at 94.661% with a standard deviation of 4.192%. The efficiency of rice husks in removing lead ions from water is mainly attributed to the presence of functional groups such as carboxyl, silanol, and hydroxyl wherein the different electronegativity charges enable the metal ion to attach itself unto the functional groups [5]. The

initial concentration of 10mg/L also has an effect on removal efficiency because having a lower concentration results in lesser saturation onto the available adsorption sites [5]. Similar to the results of this study, both Prabha and Udayashankara [5] and Sadon et al. [10] have identified rice husks as an efficient adsorbent in the removal of lead without being subjected to any form of chemical modification. Furthermore, it is worth noting that Sadon et al. [10] found multi-layered fixed-bed column setups to be more favorable in the adsorption of a multi-metal solution as compared to a single-layered setup which was what was utilized in this study.

The mango peel adsorbents achieved the highest adsorption efficiency for cadmium at 80.860% with a standard deviation of 6.845%. Mango peel adsorbents have high adsorption efficiencies due to the presence of hydroxyl and carboxyl functional groups which have different electronegativity charges [6,11]. The results of this study go in accordance with the result of the study of Iqbal et al. [2] which determined a high adsorption efficiency of mango peels for cadmium at 68.92 mg/g as well as for lead at 99.05 mg/g. Similar to the case of rice husk adsorbents, the removal efficiency of mango peel adsorbents can be affected by the initial concentration of the solution. At low metal concentrations, adsorption sites take up the available heavy metal more quickly due to the fewer metal ions competing for adsorption sites [11]. In this study, the adsorbent's uptake for lead is greater than cadmium since the initial concentration of the former is greater than the latter.

As observed in previous column studies, the adsorbent mass and column bed height could have also affected the individual efficiencies of each column. The adsorbent mass inside the column is proportional to the bed height. A taller bed height corresponds to a higher adsorbent mass and an increased surface area, hence, it results in a higher adsorption efficiency [5,11,12,13]. Thus, when the bed height is increased, there are more binding sites for the adsorbents which allows for an increased adsorption of heavy metal ions. Since the bed height was controlled, the combination column had lesser adsorbent masses to maintain a 15-cm bed height. At the same time, it is worth noting that increasing adsorbent mass does not always result in a higher adsorption efficiency. In a column setup with a higher bed height, all of the adsorbents may not be fully utilized [12,13]. This indicates that the adsorbent mass is in excess. Essentially, the amount of metal ions on the adsorbents and the amount of free ions remains constant even with the increase of the adsorbent mass. Determining the least possible amount of adsorbent to achieve maximum adsorption efficiency is significant in terms of economic viability [14]. Moreover, even though bed height is an important factor in column studies, adsorbent mass should also be looked into when implementing a multi-adsorbent column because the number of binding sites are also dependent on the adsorbent masses. It is important to consider that adsorbent masses for a certain bed height are different for each adsorbent due to the differences in their bulk density.

Lastly, it has been noted that when implementing a column setup, factors such as adsorbent mass, bed height, initial metal concentration, particle size, contact time, and pH level must be tested at different values in order to determine at which parameter values can the optimum adsorption efficiency be achieved.

Limitations. The study determined the potential use of multi-adsorbents in a column setup in removing multiple heavy metals. Primarily, it was focused on the comparison of the adsorption efficiencies of the (a) rice husk column, (b) mango peel column, (c) and the combination column composed of rice husk and mango peels. A burette was used instead of a peristaltic pump in controlling the influent flow rate due to material unavailability. pH paper was used to measure the pH because of the unavailability of a pH meter. Due to lack of resources, the study did not subject the column setups to positive and negative controls as well as different initial concentrations, adsorbent mass ratio, pH levels, flow rate/contact time, particle sizes, and there was no use of mathematical models and breakthrough curves.

Conclusion. It was determined that the single adsorbent column achieved the higher adsorption efficiency with rice husk at 94.661% for lead and the mango peel column at 80.860% for cadmium while the combination setup had the lowest adsorption efficiency which can be attributed to a reduction on the masses of the adsorbents to control the bed height variable. Since a reduction of adsorbent mass can affect the adsorption capability, the adsorption efficiency for the combination column was the lowest. Even though the combination column had a much lower efficiency, the use of multiple adsorbents in a column is a better design because it was considered to be capable of addressing multiple heavy metals; however, some design factors still need to be explored.

Recommendations. It is recommended to manipulate the ratio of the adsorbent mass in the combination column and test the column at different metal concentrations and pH levels to optimize operating parameters. Moreover, implementing a combination column with three or more adsorbents at different ratios in adsorbing multiple heavy metals may further expand the column design and including mathematical models and breakthrough curves can better explain the adsorption process.

Acknowledgement. The researchers would like to extend their gratitude to Mr. Roxzien Sesbreño for facilitating their data gathering at DOST-VI.

References

[1] Li Y, Zhou Q, Ren B, Luo J, Yuan J, Ding X, ... & Yao X. 2020. Trends and health risks of dissolved heavy metal pollution in global river and lake water from 1970 to 2017. Rev Environ Contam T. 251(2020): 1-24.

[2] Iqbal M, Saeed A, Zafar SI. 2009b. FTIR spectrophotometry, kinetics and adsorption isotherms modeling, ion exchange, and EDX

analysis for understanding the mechanism of Cd(2+) and Pb(2+) removal by mango peel waste. J Hazard Mater. 164(1): 161-71.

[3] Vera LM, Bermejo D, Uguña MF, Garcia N, Flores M, González E. 2019. Fixed bed column modeling of lead (II) and cadmium (II) ions biosorption on sugarcane bagasse. Environ Eng Res. 24(1): 31-37.

[4] Sarinas B, Gellada L, Jamolangue E, Teruñez M, Flores J. 2014. Assessment of heavy metals in sediments of Iloilo Batiano River, Philippines. IJESD. 5(6): 543-546.

[5] Prabha RT, Udayashankara TH. 2014. Removal of heavy metal from synthetic wastewater using rice husk and groundnut shell as adsorbents. IOSR-JESTFT. 7(11): 26-34.

[6] Iqbal M, Saeed A, Kalim I. 2009a. Characterization of adsorptive capacity and investigation of mechanism of Cu2+, Ni2+, and Zn2+ adsorption on mango peel waste from constituted metal solution and genuine electroplating effluent. Sep Sci Technol. 44(2009): 3770–3791.

[7] Romero-Cano LA, González-Gutiérrez LV, Baldenegro-Pérez LA, Carrasco-Marín F. 2017. Grapefruit peels as biosorbent: characterization and use in batch and fixed bed column for Cu(II) uptake from wastewater. J Chem Tech Biotech. 92(7): 1650–1658.

[8] Navaratne A, Priyantha N, Kulasooriya TPK. 2013. Removal of heavy metal ions using rice husk and brick clay as adsorbents–dynamic conditions. Int J Earth Sci Eng. 6(4): 807-811.

[9] Binabaj MA, Nowee SM, Ramezanian N. 2017. Comparative study on adsorption of chromium(VI) from industrial wastewater onto nature-derived adsorbents (brown coal and zeolite). Int J Environ Sci Tech. 15(7): 1509–1520.

[10] Sadon FN, Ibrahem AS, Ismail KN. 2014. Comparative study of single and multi-layered fixed bed columns for the removal of multi-metal element using rice husk adsorbents. J App Sci. 14(2014): 1234-1243.

[11] Ashraf MA, Mahmood K, Wajid A. 2011. Study of low cost biosorbent for biosorption of heavy metals. IPCBEE. 9(2011): 60-69.

[12] Amarasinghe BMWPK. 2011. Lead and cadmium removal from aqueous medium using coir pith as adsorbent: batch and fixed bed column studies. JTFE. 1(2011): 36-47.

[13] Jena S, Sahoo RK. 2017. Removal of Pb(II) from aqueous solution using fruits peel as a low cost adsorbent. Int J Adv Res Sci Eng Technol. 5(1): 5-13.

[14] Amin MT, Alazba AA, Shafiq M. 2017. Batch and fixed-bed column studies for the biosorption of Cu(II) and Pb(II) by raw and treated date palm leaves and orange peel. Global NEST J. 19(3): 464-478.

[15]Nambi VE, Thangavel K, Jesudas DM. 2015. Scientific classification of ripening period and development of colour grade chart for Indian mangoes (Mangifera indica L.) using multivariate cluster analysis. Scientia Horticulturae. 193(2015): 90-98.

The quantification of the correlation between water nitrogen level and the phosphorus uptake of *Chlorella sorokiniana* (freshwater green alga) in simulated nutrient-contaminated freshwater

JEFF LAWRENCE B. DERRAMAS, NINA BEATRIS C. GONZALEZ, TRISTAN TIMOTHY M. VILLAFLOR, and CATHERINE JOY A. MEDIODIA

Philippine Science High School - Western Visayas Campus, Brgy. Bito-on, Jaro, Iloilo City 5000, Department of Science and Technology, Philippines

Abstract

Eutrophication is a phenomenon wherein there is an oversaturation of nutrients, principally phosphorus and its partner nutrient nitrogen, in an ecosystem. It induces algal blooms which causes water anoxia and overall water quality deterioration. This has become an issue of increasing concern, especially in agricultural countries. Biological removal methods have proven to be cost-effective and efficient against this phenomenon, specifically microalgal bioremediation. Though microalgae have proven to remediate nitrogen and phosphorus, studies that investigate the effect of the presence of nitrogen on phosphorus removal are uncommon. In this study, the correlation between water nitrogen level and the phosphorus uptake of *Chlorella sorokiniana*, a locally available algae species, was investigated in simulated nutrient-contaminated freshwater. Batch cultures were exposed to treatments of 0, 5, 10, and 15 mg/L of nitrogen and a uniform amount of phosphorus for a period of 11 days, after which the samples were analyzed using UV-vis spectrophotometry. The results showed that a statistically significant positive correlation exists between water nitrogen level and percentage phosphorus removed.

Keywords: *Chlorella sorokiniana, eutrophication, limiting nutrients, nitrogen, phosphorus*

Introduction. Excess nutrient inputs from agricultural wastelands cause eutrophication which refers to the over-enrichment of lakes with limiting nutrients such as phosphorus (P) and nitrogen (N) [1,2,3]. Accumulating nutrients cause the overgrowth of algae and plants limiting sunlight and oxygen in water. It causes the aquatic environment to become oxygen-deficient [2], and negatively affects other oxygen-dependent aquatic species [4]. Widespread eutrophication due to nutrient input has become an increasing concern worldwide, and this is linked to increasing levels of industrial, urban, and agricultural activities such as land conversion and fertilizer use. It can be attributed as well to the increase in human population, demand for food, and nitrogen deposition in the recent years [1,4].

A wide array of treatments and technology for controlling eutrophication exists. However, biological remediation (bioremediation) methods, which use the uptake mechanisms of living organisms to consume and break down environmental contaminants such as nutrients, are favored over chemical methods of remediation because they are more cost-effective, and they produce less toxic waste and harmful by-products [4]. In this context, uptake refers to the movement or transfer of environmental contaminants into the tissues of biological organisms.

The usage of microalgae for bioremediation has become popular in recent research due to established findings proving their effectivity in remediating various types of contaminants, particularly phosphorus and nitrogen [5]. Biomass from microalgal bioremediation may also be used in post-experimental applications [6].

Chlorella sorokiniana, a locally available species of microalgae, has been proven to be able to remove organic pollutants [6]. It also has applications in the field of aquaculture such as its usage as fishmeal [7]. The significance of this species supports the need to further study it. Learning about its nutrient uptake mechanisms will give substantial information on the removal efficiency of certain nutrients. It can serve as beneficial information for the application of microalgal treatments for eutrophicated waters as well.

In the mitigation of eutrophication, nutrient control and reduction are essential. However, the control of multiple nutrients can be complicated by the effects of the presence of other nutrients impacting the uptake of another [1,2,3]. Nitrogen and phosphorus, as limiting nutrients that cause eutrophication, have been hypothesized to have a correlation that explains how they affect each other's uptake [1]. Along with this, the possibility of having various factors as to why nitrogen and phosphorus

How to cite this article:

CSE: Derramas JLB, Gonzalez NBC, Villaflor TTM. 2020. The quantification of the correlation between water nitrogen level and the phosphorus uptake of *Chlorella sorokiniana* (freshwater green alga) in nutrient-contaminated simulated freshwater. Publiscience. 3(1):16-20.

APA: Derramas, J.L.B., Gonzalez, N.B.C., Villaflor, T.T.M. (2020). The quantification of the correlation between water nitrogen level and the phosphorus uptake of *Chlorella sorokiniana* (freshwater green alga) in nutrient-contaminated simulated freshwater. *Publiscience, 3*(1):16-20.

could either hamper or assist the removal of each other exists [1,3,8].

Phosphorus removal characteristically has a high organic loading rate (OLR), which is a measure of the quantity of substrate or contaminant entering the system per unit time, and high sludge retention time (SRT), which is the average time a contaminant is contained in a system. Meanwhile, the removal of nitrogen possesses a low OLR and a high SRT. From those characteristics, a negative correlation can be expected between water nitrogen content and phosphorus uptake. Several studies, however, show that a positive relationship may also exist, more specifically an increase in nitrogen input may increase phosphorus uptake via stimulation of microalgal growth and metabolism rates and vice versa [9]. This shows that the relationship between nitrogen and phosphorus may be variable depending on the dominant effect of nutrient presence on uptake.

Though both nutrients contribute to eutrophication, it is suggested to focus on the removal of phosphorus rather than nitrogen. This is because nitrogen remediation is a more delicate process, susceptible to triggering nitrogen-fixing cyanobacterial blooms that result in adverse effects in the ecosystem and decreasing the activity of phosphorus removal in eutrophicated waters when unregulated. It also involves a prolonged timeframe for denitrification and nitrification. Thus, the cost is relatively high. Furthermore, phosphorus is regarded as a critical limiting factor in lakes, making its removal more costly but more beneficial to the environment on a long-term basis [3,4].

Studies investigating the individual remediation efficiency of phosphorus along with nitrogen are prevalent in recent research. However, studies on the remediation of both in relation to one another, specifically in the freshwater setting, are rare. There is a significant lack of research involving the relationship of nitrogen levels and the phytoremediation efficiency of phosphorus, especially in microalgal and water treatment studies. With this lack of information, this study sought to address the knowledge gap by conducting a study that aimed to describe and evaluate the correlation between water nitrogen content and phosphorus uptake of *Chlorella sorokiniana* in nutrient-contaminated freshwater in different levels of nitrogen. It specifically aimed to:

(i) measure the percentage of phosphorus removed by *Chlorella sorokiniana* in different levels of nitrogen using ultraviolet-visible (UV-Vis) spectrophotometry through the ascorbic acid method; and

(ii) quantify the correlation between the concentration of nitrogen input in the water and the percentage of phosphorus removed through Pearson R Correlation and Linear Regression.

Methods. The utilized algae culture was obtained, then subjected to microalgal cell counting. The four utilized treatment solutions were then prepared. After this, the replicate samples per treatment were prepared, then inoculated with algal culture. After an exposure period of 11 days based on the study of Patel [6], the samples were analyzed through UV-vis spectrophotometry through the ascorbic acid method, and absorbances were read at 880 nm. Obtained data was then ran through statistical analysis using Pearson R Correlation and Linear Regression.

Procurement of Microalgal Culture. A culture of *Chlorella sorokiniana* was purchased from SEAFDEC, Tigbauan, Iloilo. The culture was sealed in a plastic bottle for transport and was then stored in a refrigerator at 3°C prior to usage.

Counting of Microalgal Cells via Hemocytometer. Ten milliliters (10 mL) of the algae culture was pipetted into a test tube. It was then agitated in a vortex mixer for five seconds. Ten microliters (10 µL) of the culture was pipetted into slot A of the hemocytometer. Algae colonies in the five smaller squares of the hemocytometer's central square were counted. Colonies that overlapped between squares were not counted. The concentration of algae per milliliter was computed based on the number of microalgal cells per microliter (µL).

Preparation of Treatment Solutions. Four liters (4 L) of distilled water was measured and poured into a clean plastic container. After this, 57.3 mg of potassium dihydrogen phosphate (KH_2PO_4) was measured and mixed into the water via agitation to create the control (base) solution. One liter (1 L) of the KH_2PO_4 solution was then measured for each of the four treatments using a graduated cylinder and transferred into labelled beakers. From the separated solution, 180 mL was measured using a graduated cylinder and was transferred into each of the five Erlenmeyer flasks designated to hold the replicates of the control setup with the treatment containing 0 mg of nitrogen. The remaining 350 mL of the solution was stored inside a beaker. This process was then repeated for the three other treatments wherein 5 mg, 10 mg, and 15 mg of nitrogen as potassium nitrate (KNO_3) was added respectively to the one liter of base solution for each treatment.

Preparation of Batch Cultures. Twenty milliliters (20 mL) of *Chlorella sorokiniana* culture cultured in Conway medium was inoculated into each Erlenmeyer flask. The flasks were linearly arranged in a ventilated, isolated room. The cultures were subjected to light exposure with a 20-watt fluorescent lights distance of 40.64 cm (16 in) away from the flasks on a light/dark regimen with a 14/10 h simulation of the day and night light exposure cycle [6]. After submerging the connected tubing into the filled flasks, the water aerator, set on low, was switched on to induce agitation of the medium by continuously bubbling the air in the flasks. These conditions were maintained for the entire duration of the observation period.

Observation Period. The setup was monitored for a span of nine days. The lights were switched on and off at 6:26 AM and 8:26 PM, respectively. This simulated a 14/10-hour day and night cycle.

Ascorbic Acid Method. Fifteen milliliters (15 mL) of 36 N concentrated sulfuric acid (H_2SO_4) was diluted to 108 mL to form 5 N sulfuric acid.

Potassium antimonyl tartrate ($K_2Sb_2(C_4H_2O_6)_2$) solution was made through dissolving 1.37 g of the compound in 400 mL of distilled water in a beaker. Twenty grams (20 g) of ammonium molybdate ($(NH_4)_2MoO_4$) was also dissolved in 500 mL of distilled water. An ascorbic acid solution was prepared through mixing 1.76 g of ascorbic acid with 100 mL of distilled water in another beaker. A combined reagent was then made through mixing 50 mL of 5 N sulfuric acid, 5 mL of potassium antimonyl tartrate solution, 15 mL of the ammonium molybdate solution and 30 mL of ascorbic acid solution, for a total of 100 mL of combined reagent that was used for the chemical analysis of the samples [10].

From each sample, 50 mL of the solution was pipetted into an Erlenmeyer flask. One drop of phenolphthalein indicator was added. If a red color developed, 5 N H_2SO_4 was added drop by drop to discharge the color. Eight milliliters (8 mL) of the combined reagent was added to the samples and mixed thoroughly. This process was repeated for each individual replicate for all treatments.

UV-vis Spectrophotometry. After the 20-minute exposure to the combined reagent, the absorbance of each sample was measured at 880 nm, using distilled water as a blank solution for reference. After the individual analysis of the samples per replicate, the absorbance of the Conway medium content in the samples was analyzed and then subtracted from the sample absorbances, providing the values for the phosphorus remaining in the samples, disregarding the phosphorus content of that of the Conway medium.

$$A_{actual} = A_{sample} - A_{Conway}$$

Where: A_{sample} *= absorbance of sample*
A_{Conway} *= absorbance of Conway medium*
A_{actual} *= absorbance of sample disregarding Conway*

Computation of Phosphorus Concentration. The Beer-Lambert Law was used to compute for the concentration of phosphorus remaining in the samples based on their absorbances as shown below.

$$A_{actual} = \mathcal{E}\, c\, L$$

Where: A_{actual} *= absorbance of sample disregarding Conway*
$\mathcal{E}$ *= molar extinction coefficient*
L *= path length of light*
c *= concentration of chemical*

Data Analysis. The data was analyzed through Pearson R Correlation and Linear Regression analysis using the IBM Statistical Package for the Social Sciences (SPSS®) application.

Safety Procedure. After the conduct of the experiment, the remaining algae culture and glassware were filled with bleach solution and were left for 24 hours as prescribed by standard protocol. After the 24-hour exposure period, the glassware were then washed and rinsed thoroughly with detergent and running water followed by a final rinsing using distilled water. The excess solutions from chemical analysis were poured into a container labeled accordingly to be turned over to the Science Research Assistant (SRA) of the school for proper storage and disposal. The glassware that were used for culturing and UV-Vis analysis were subjected to autoclaving to eliminate any microorganisms that may still be present even after the conduct of the experiment.

Results and Discussion. Shown in Table 1 is the mean percentage ± standard deviation of phosphorus removed by the replicates exposed to each nitrogen level treatment. Percentage values were determined through calculation of the change in concentration over the initial concentration of phosphorus in the solution.

Table 1. Mean ± standard deviation of the percentages of phosphorus removed by the algae in different levels of nitrogen.

Nitrogen Level (mg/L)	Percent Removed (%)
0	90.40 ± 2.497
5	91.96 ± 0.946
10	93.26 ± 0.606
15	93.64 ± 0.861

The average removal percentages were seen to increase in treatments of higher concentrations of nitrogen input. This is illustrated in Figure 1 below.

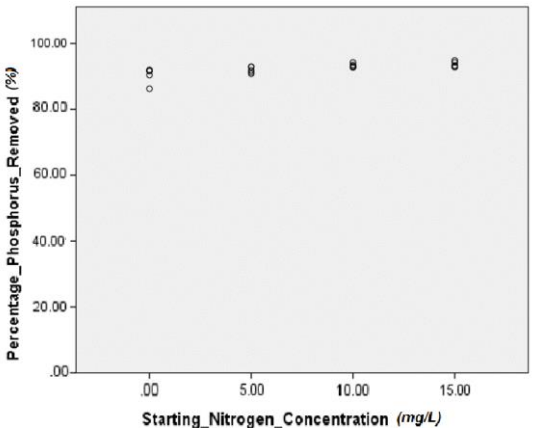

Figure 1. Scatterplot of phosphorus removed from samples for each nitrogen level.

The trend exhibited indicated a positive relationship between the involved variables.

The Pearson R correlation analysis was conducted to determine: (1) the strength of the linear correlation between water nitrogen content and phosphorus uptake, and (2) the type of correlation that exists between the variables, which may be either positive or negative.

The Pearson R correlation was run at a 95% confidence interval. The p-value derived from the data was 0.001, a value less than the significance level (0.01), indicating a significance in the results. The resultant coefficient from the test is a positive value of 0.694.

A value of 0.694 in the Pearson R correlation test indicates that a positive correlation exists between nitrogen input and phosphorus removal. This confirms that in the case of this study, the increase of one variable leads to an increase of another. Nitrogen input and phosphorus removal are found to be directly proportional.

The Linear Regression was used to represent the correlation between water nitrogen content and phosphorus uptake as a graph or linear function which shows their relationship as variables. A significant difference between the mean value of sample groups was first evaluated in order to proceed with the linear regression analysis.

A linear equation where x is the nitrogen level and y is the amount of phosphorus removed was derived from the linear regression analysis of the data conducted at a 95% confidence interval (p=0.05). This equation is shown below.

$$y = 0.2213x + 90.66$$

The equation mathematically models the relationship between water nitrogen level and phosphorus uptake of *Chlorella sorokiniana.* It can be observed that a positive correlation exists between nitrogen level and the amount of phosphorus removed as illustrated by Figure 2.

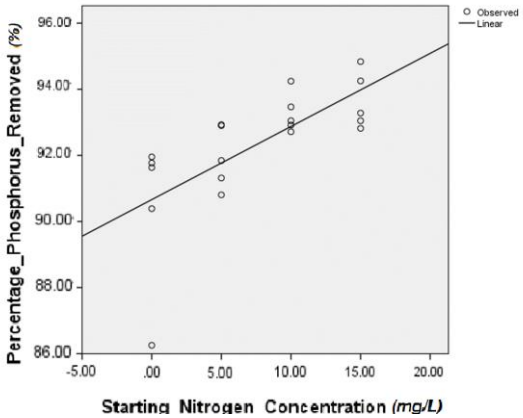

Figure 2. Linear representation of the relationship between water nitrogen level and phosphorus removed.

The linear equation, having a positive slope, is an indicator of a positive relationship between the variables and shows that as the nitrogen level increases, so does the amount of phosphorus removed from the water.

The relationship and effects of water nitrogen levels on the uptake of phosphorus are dependent on the dominant mechanism of their uptakes relative to each other's presence, which may vary between species. The mechanisms behind the removal of phosphorus and nitrogen may be attributed to their uptake through microalgal biological processes such as nitrification and denitrification, and stripping phenomena such as ammonia volatilization and phosphorus precipitation [5]. Ammonia volatilization is the conversion of ammonium into ammonia gas at high pH levels [11]. Biological phosphorus removal is done by phosphorus-accumulating organisms (PAOs) like algae through the absorption dissolved phosphorus in wastewater and storing them as granules (precipitate) within the cells [12]. These phenomena are induced by photosynthetic microalgal growth alongside the adsorption on the cell surface of the algae. Aside from uptake, adsorption to the cell surface is among the most significant processes in the removal of phosphate by algae. Phosphate removal and biomass production are known to positively correlate [5]. Despite this, various studies show differing hypothetical understanding as to what the effect of remediating both phosphorus and nitrogen is.

One point of basis for prediction of the possible dominant relationship between the uptake of the two nutrients of an algal species is the differences in the SRT and the OLR required for the efficient bioremediation of nitrogen and phosphorus. Nitrogen, requiring a low OLR, interferes with the efficiency of the loading of phosphorus, whose uptake requires a higher, more rapid rate of entry into the algal cells. On the other hand, phosphorus has a characteristically low SRT, which means that it is not retained in the algal cells for a prolonged period in its remediation. Nitrogen, having a high SRT, has a tendency to interfere with the efficiency of the outflow of P from the algal cell as it is retained longer, and has a less rapid rate of outflow itself [3]. Due to the interplay of these factors, a negative trend and correlation between phosphorus uptake and nitrogen concentration may exist.

However, studies such as those by Graciano [8], Bennett [9], and Xin et al. [13] have shown that positive trend and correlation between these two variables may be observed. Bennett [9] discusses that increasing the presence of phosphorus and nitrogen, nutrients essential for plant and algae growth, increases the rate of growth of an organism, leading to an increase of nutrient demand to sustain its growth, and ultimately resulting to an overall increased rate of the uptake of the two nutrients.

In the case of the results of this study, the statistical analysis of the data shows that a positive correlation exists between water nitrogen content and phosphorus uptake of *Chlorella sorokiniana* which is aligned with the results of the three aforementioned studies.

Limitations. The scope of the procedures in the study is limited to the usage of laboratory simulated freshwater. The simulation of freshwater medium utilized in the experiment constituted of only four major components: phosphorus (in the form of KH_2PO_4), nitrogen (in the form of KNO_3), Conway medium which is a nutrient replete culturing medium, algae, and distilled water. Other constituents linked to natural freshwater such as additional nutrient input, pH, and temperature are not included in the scope of the study and procedures.

Conclusion. It was determined that the replicates exposed to the treatment with the highest N content (15 mg/L) exhibited the highest percentage of phosphorus removal at 93.64%. In contrast, the replicates exposed to the treatment with the lowest N content (0 mg/L) exhibited the lowest percentage of phosphorus removal at 90.40%. A positive

relationship between nitrogen content and phosphorus removal was observed to exist represented by the linear equation, $y = 0.2213x + 90.66$. This may have been caused by accelerated microalgal growth stimulated by the presence of increasing concentrations of growth-stimulating nutrients.

Recommendations. It is recommended to implement measures to minimize inaccuracies due to human error such as the usage of a timed electrical switch for turning the lights on and off for the 14/10 day and night cycle simulation. It is also recommended for the procedures of the study to be conducted using naturally sourced freshwater from local sources. Lastly, the conduct of a study of similar nature involving the testing of more nitrogen levels is recommended to produce a more accurate representation of the linear relationship between the nitrogen input and phosphorus uptake.

Acknowledgement. The researchers would like to extend their gratitude to Mrs. Annie Franco and the staff of SEAFDEC-VI for their guidance in the conduct of the study.

References

[1] Carpenter SR. 2005. Eutrophication of aquatic ecosystems: bistability and soil phosphorus. Proc Natl Acad USA [Internet]. [cited 2018 Aug 11]; 102(29): 10002-10005. Available from:http://www.pnas.org/content/pnas/102/29/10002.full.pdf.DOI:10.1073pnas.0503959102.

[2] Schindler DW, Hecky RE, Findlay DL, Stainton MP, Parker BR, Paterson MJ, Beaty KG, Lyng M, Kasian SEM. 2008. Eutrophication of lakes cannot be controlled by reducing nitrogen input: results of a 37-year whole-ecosystem experiment. Proc Natl Acad USA [Internet]. [cited 2018 Aug 11]; 105(32): 11254 11258. Available from: http://www.pnas.org/content/pnas/105/32/11254.full.pdf

[3] Wang H, Wang H. 2009. Mitigation of lake eutrophication: loosen nitrogen control and focus on phosphorus abatement. Prog Nat Sci [Internet]. [cited 2018 Aug 11]; 19(2009) 1445-1451. Available from: https://www.sciencedirect.com/science/article/pii/S1002007109002391. DOI:10.1016/j.pnsc.2009.03.009.

[4] Salgueiro JL, Perez L, Maceiras R, Sanchez A, Cancela A. 2016. Bioremediation of wastewaters using *Chlorella vulgaris* microalgae: phosphorus and organic matter. Int J Environ Res. 10(3): 465-470.

[5] Delgadillo-Mirquez L, Lopes F, Taidi B, Pareau D. 2016. Nitrogen and phosphate removal from wastewater with a mixed microalgae and bacteria culture. Biotechnol Rep. 11(2016): 18-26.

[6] Patel A, Barrington S, Lefsrud M. 2012. Microalgae for phosphorus removal and biomass production: a six species screen for dual-purpose organisms. GCB Bioenergy. 4(2012): 485-495.

[7] Barone R, Sonoda D, Lorenz E, Cyrino J. 2017. Digestibility and pricing of *Chlorella sorokiniana* meal for use in tilapia feeds. Sci Agr 75(3): 184-190. Xin L, Hu HY, Sun YX. Effects of different nitrogen and phosphorus concentrations on the growth, nutrient uptake, and lipid accumulation of a freshwater microalga Scenedesmus sp. 2010. Bioresour Technol. 101(14):5494-500

[8] Graciano C, Goya JF, Frangi JL, Guiamet JJ. 2006. Fertilization with phosphorus increases soil nitrogen absorption in young plants of Eucalyptus grandis. For. Ecol. Manag. 236(2): 20.

[9] Bennett WF. 1958. Effect of nitrogen on phosphorus absorption by corn. Iowa State College. 1-179.

[10] Clesceri LS, Eaton AD, Greenberg AE. 1992. Standard methods for the examination of water and wastewater. American Public Health Association. 18th. Washington, DC (WA). 1015 15th Street, NW. p. 115.

[11] Freney JR, Simpson JR, Denmead OT. 1983. Gaseous Loss of Nitrogen from Plant-Soil Systems. 9(1): 1–32. DOI:10.1007/978-94-017-1662-8_1

[12] Ross M. 2013. What every operator should know about biological phosphorus removal. Operator Essentials. 48-50.

[13] Xin L, Hu HY, Sun YX. 2010. Effects of different nitrogen and phosphorus concentrations on the growth, nutrient uptake, and lipid accumulation of a freshwater microalga Scenedesmus sp. Bioresour Technol. 101(14):5494-5500.

MAKAPTAN

ANTIBACTERIAL STUDIES

MAKAPTAN represents sickness in the Visayan folklore. Even today, we are plagued with diseases that continue to trump modern medicine; nonetheless, breakthroughs in the medical field has afforded us increased understanding of such diseases and continue to guide us in developing the necessary treatments. This section deals with antibacterial agents that could be used in tandem with proper hygiene and modern drug-delivery systems in response to drug-resistant pathogens.

These studies are part of the Health Research and Development Agenda with focus on discovering and/or developing drugs that target bacteria. It aims to contribute to the repository of research by proposing evidence-based solutions to pressing health problems, as well as methods that maximizes available resources in the country.

BASED ON: Harmonized National Research and Development Agenda (HNRDA)

Formulation of liquid soap incorporated with *Mangifera indica* (mango) leaf extracts and evaluation of its antibacterial activity against *Staphylococcus* spp.

CERYL GRACE B. HEMBRA, RYA CESSNA B. HENDERIN, MAUREEN COSETTE G. PAREÑAS, and RAMON ANGELO N. SINCO

Philippine Science High School - Western Visayas Campus, Brgy. Bito-on, Jaro, Iloilo City 5000, Department of Science and Technology, Philippines

Abstract

After triclosan-containing soaps were banned by the United States Food and Drug Association due to health and environmental risk, the need for an alternative antibacterial agent arised. Leaves of *Mangifera indica* (mango) contain phytochemicals which promote antibacterial activity. This study aimed to determine whether *M. indica* leaves extract can be an alternative antibacterial agent for triclosan. There were three set-ups in this study namely formulated soaps with no antibacterial agent for soap base, triclosan, and *M. indica* extract. The set-ups were evaluated using the parameters pH, density, foam stability and free caustic alkali (FCA) along with antibacterial evaluation against *Staphylococcus* spp. Soap formulations passed the parameters except FCA. The antibacterial evaluation showed that soap with triclosan obtained the highest zone of inhibition (7.40±0.20 mm) followed by *M. indica* (6.87±0.06 mm). The results suggested that the formulated soap with *M. indica* extract cannot be used as an alternative to triclosan.

Keywords: *triclosan, agar well diffusion method, hot saponification process, free caustic alkali, zone of inhibition*

Introduction. *Mangifera indica*, commonly known as mango, is used as an alternative treatment for diarrhea, anemia, asthma, and cough among other ailments [1]. One of the several research works that have been conducted on its leaves is the phytochemical screening and antibacterial activity of *M. indica* extracts where phytochemicals such as alkaloids, tannins, and flavonoids were found to be present in ethanolic mango leaf extracts [1]. These phytochemicals have antibacterial properties [2] and could be the reason for the plant's efficiency in inhibiting the growth of bacteria such as *Staphylococcus aureus* [3]. It has been observed in the study of Krishnananda and Shabaraya [4] and Zakaria et al. [5] that the concentration that yields the greatest diameter of the zone of inhibition against *S. aureus* is 100 mg/mL, followed by 50 mg/mL.

S. aureus is a common bacterium frequently isolated from the nose of humans. It causes skin infections. When left untreated, disorders associated with this organism may progress into a wide range of conditions such as tissue infections, pneumonia, wound, joint, and/or bone infections. Less than 20% of *S. aureus* which were isolated mostly from the wounds and abscesses of admitted patients of a tertiary hospital in Bacolod City, exhibited resistance to chloramphenicol, tetracycline, and ciprofloxacin but with excellent susceptibility to linezolid [6]. Infections caused by *S. aureus* could be transmitted from one person to another through direct contact. A simple way to prevent the transmission is by thorough washing of hands with antibacterial soap. However, commercial soaps usually use synthetic antibacterial agents that are potentially harmful to the user and to the environment.

Triclosan (TCS) and triclocarban (TCC) are antibacterial agents commonly found in personal care products such as hand disinfecting soaps [7]. After the discharge of these personal care products into domestic sewage, TCS or TCC may reach the environment due to their incomplete removal in wastewater treatment plants or direct discharge of wastewater without treatment [7]. Thus, an antibacterial soap that does not use these chemicals is needed to reduce health risks.

The study aimed to formulate three liquid soaps namely no antibacterial agent for the negative control, triclosan for the positive control and *M. indica* leaf extract for the treatments, and to test its antibacterial activity against *Staphylococcus* spp. It specifically aimed to:

(i) determine the physicochemical properties of the formulated liquid hand soaps using the parameters pH, density, foam stability and free caustic alkali;

(ii) determine antibacterial activity exhibited by the formulated soaps against *Staphylococcus* spp. using agar-well diffusion method; and

(iii) determine if there is a significant difference between the zones of inhibition of the formulated soap.

Methods. This research was conducted to formulate three soaps: the base soap, the soap with triclosan, and the soap with *M. indica* extract and test their antibacterial activity against *Staphylococcus* spp. as well as their physicochemical parameters and compare them to the standards. There were three

How to cite this article:
CSE: Hembra CG, Henderin RC, Pareñas MC, Sinco RA. 2020. Formulation of liquid soap incorporated with *Mangifera indica* (mango) leaf extract and evaluation of its antibacterial activity against *Staphylococcus* spp. *Publiscience.* 3(1):22-26.
APA: Hembra, C.G., Henderin, R.C., Pareñas, M.C. & Sinco, R.A. (2020). Formulation of liquid soap incorporated with *Mangifera indica* (mango) leaf extract and evaluation of its antibacterial activity against *Staphylococcus* spp. *Publiscience,* 3(1):22-26.

phases in the methods including the extraction of *M. indica* leaves, the formulation of liquid soaps, and the antibacterial testing of the soaps. The data in the antibacterial test were then analyzed using one-way ANOVA.

Collection and Identification of Samples. The mature *M. indica* leaf samples were collected from Orchard Valley, Tigum Barrio Road, Pavia, Iloilo and were stored in a mesh bag. Prior to identification, the samples were identified by the Department of Agriculture (DA) in Sta. Barbara, Iloilo.

Extraction and Concentration. The *M. indica* leaf samples were washed with tap water twice then rinsed with distilled water to remove unwanted residues [4]. Based on the methods of Zakaria et al. [5], the leaves were oven-dried; however, the drying period was extended to four days because the leaves were not crisp dry after 24 hours of oven drying. The leaves were then cut into small pieces using a pair of scissors and were powdered using a Hanabishi kitchen blender. The powdered samples were then macerated for 72 hours using 95% ethanol as the solvent, and the resulting mixture was filtered using Whatman no. 1 filter paper [8], properly positioned inside a glass funnel. After which, the remaining solvent was evaporated using Biobase RE100-Pro rotary evaporator at 40°C with 100 rpm [5].

Liquid Soap Formulation. The soap formulation was based on the modified hot saponification process by Widyaningsih et al. [9]. The liquid soap base was formulated by heating 21.4% (w/w) of palm oil to 80°C. The potassium hydroxide (KOH) solution was separately prepared by dissolving 4.29% (w/w) of KOH to 10.0% (w/w) of distilled water. The KOH solution was then poured into the heated palm oil. The process was exothermic, so the solution was allowed to cool down to 80°C. After which, 1.07% (w/w) of sodium lauryl sulfate (SLS) and paraben were added into the solution. The soap solution was then stirred at 600rpm - 700 rpm until the stir bar was no longer able to rotate. Upon reaching this state, the solution was manually stirred using a stirring rod until a semi-solid consistency was achieved. The weight of the semi-solid solution was then measured using a top loading balance. To dilute the soap, distilled water was added to the solution while being heated. The amount of the added distilled water had tripled the initial recorded weight of the solution. For the positive control, 4.29 x 10^{-5}% (w/w) of triclosan was added to 21.4% (w/w) of liquid soap base. For the preparation of the soap with the crude extract, the temperature of the soap base was first lowered to 40°C. After which, 0.536% (w/w) of *M. indica* extract was incorporated into the 21.4% (w/w) of liquid soap base and was mixed using a magnetic stirrer until the solution was homogeneous.

Physicochemical Test for Liquid Soap. The pH test was done in triplicates and was based on the standard protocol recommended by American Oil Chemists' Society (AOCS) [10]. Using buffer solutions of pH 4.00, 7.00 and 10.00, the EUTECH pH700 pH meter was calibrated. After calibration, the probe was dipped into 10% solutions of each of the formulated soaps. The obtained pH value was then recorded.

The density of each soap solution was determined by initially weighing 10mL of each solution using the Sartorius top loading balance. The obtained mass was divided to 10mL to calculate for the density.

For the assessment of foam stability, 10 mL of each soap solution was prepared and then mixed in a vortex for five (5) minutes. The foam height produced was measured using a ruler with ±0.5 mm precision. After allowing the solution to stand for five (5) minutes, the foam height was measured again. Foam stability was measured using the formula [11]:

$$\text{Foam stability} = (\text{final foam height} / \text{initial foam height}) \times 100$$

For the determination of free caustic alkali, 5 g of each soap solution was prepared and dissolved in 30 mL ethanol. After dissolution, three (3) drops of phenolphthalein indicator and 10 mL of 20% barium chloride ($BaCl_2$) was added into each of the solutions. After thorough mixing, each solution was then titrated with 0.05 M sulfuric acid (H_2SO_4). Free caustic alkali was determined using the formula [12]:

$$FCA = (0.31 \times W) / VA$$

wherein W is the weight of the liquid soap and VA is the volume of H_2SO_4 used during titration.

Antibacterial Test for Liquid Soap. The agar well diffusion assay was performed in triplicates. The *Staphylococcus* spp. cultures were obtained from Philippine Science High School - Western Visayas Campus. Cultures of *Staphylococcus* spp. were inoculated separately on solidified agar on each petri dish by streaking using a wire loop. Three (3) wells of six (6) mm diameter and five (5) mm depth were made into the solidified agar using a sterile borer. About 100 mg/ml^{-1} of each test liquid soap was dispensed into separate wells using a 100ug micropipette [13]. The plates were then incubated at 37°C for 24 hours. The sensitivity of the test organisms to the treatments was determined by measuring the diameter of the zone of inhibition surrounding the wells. After incubation, the diameters of the zones of inhibition were measured with a ruler read to the nearest mm [13]. In the event that the zone was irregular, the colony closest to the center of the disc (radius) was measured and doubled to get the diameter.

Data Analysis. For calculations, p-values were calculated using Statistical Package for Social Sciences (SPSS) Version 13.0 applying one-way ANOVA with statistical significance set at 5% to prove if there is a significant difference between the formulated soaps.

Safety Procedure. Gloves and lab gowns were worn throughout the conduct of the experiment to avoid contamination of the samples and bacteria. Tabletops where the activities were performed were disinfected with a 10% solution of hypochlorite [15]. Disposal of *Staphylococcus* spp. waste was in accordance with the regulations set by the University of San Agustin. All chemicals and hazardous waste were collected in tightly closed, leak-proof containers that were kept closed except when adding waste. Biological materials such as cultures and

contaminated glasswares were autoclaved before proper disposal.

Results and Discussion. This research project was conducted to formulate an antibacterial soap using *M. indica* leaf extract as an antibacterial agent. Three soaps were developed using hot process and were tested against *Staphylococcus* spp. using the agar well diffusion method. The positive control was incorporated with triclosan as its antibacterial agent, the other with *M. indica* leaf extract, and the negative control has no antibacterial agent. All soaps were evaluated with the following physicochemical parameters: pH, free caustic alkali, density, and foam stability. The values were then gathered and were compared to the standards of Handrayani et al. [12] for liquid soap.

Physicochemical Test Results. The recorded pH of the soap base was 10.27 ± 0.03 while the soap with triclosan obtained 10.25 ± 0.04. These values are comparable as reflected in Table 1. The soap with *M. indica* leaves extract as an antibacterial agent with the pH 10.07 ± 0.03 showed a lower value compared to the two. For the foam stability, the soap base obtained 96.67% which was the highest value while triclosan and *M. indica* extract obtained the same value which was 93.75%. The soap base also obtained the highest density value (1.01 g/mL) followed by the extract (0.97 g/mL). For the free caustic alkali, *M. indica* extract obtained the highest value (0.06%) followed by triclosan (0.05%).

Table 1. The values for pH, foam stability, density, and free caustic alkali of the formulated soaps.

	Soap Base	Triclosan	*M. indica* Extract	Standard Value
pH	10.27± 0.03	10.25±0.04	10.07±0.03	9.00-11.00
Foam Stability (%)	96.67	93.75	93.75	80.00 - 100.00
Density (g/mL)	1.01	0.96	0.97	1.01 - 1.10
Free Caustic Alkali (%)	3.10	4.96	5.58	≤ 2.00

pH. All the pH values for each of the formulated soaps were within 9-11 which is the standard range for the pH of soaps based on the National Agency for Food and Drug Administration and Control (NAFDAC) [15]. Since the saponification process involves the use of base KOH in order to form fatty acid salts with the triglyceride palm oi, the obtained basic pH of the soap solutions were anticipated. It is important that the pH is within the set standard value since lower or higher values than that may cause skin irritation and imbalance in the normal bacterial flora of the skin because the soap reacts with the acidic layer of the skin by neutralizing it to protect it against bacteria and viruses [15,16].

Density. The obtained density values of the formulated soaps have negligible differences. However, only the soap base passed the set standard values of 1.01-1.10 g/ml set by National Indian Standard (NSI) [9]. The concentration and chemical properties of raw materials used in formulating the soap influence the density. high molecular weight of soap resulting from the combined amounts of raw materials results in high density [12]. Based on the results, triclosan and *M. indica* soaps produced lower densities compared to the soap base. Since the raw materials used for each soap formulation are the same except for the antibacterial agent, the results suggest that the addition of triclosan and *M. indica* affected the density of the soap.

Foam stability. Results for the foam stability of the formulated soaps reflected that the soap base is more stable compared to the two other soap formulations. Foaming does not increase the efficiency of soap in removing dirt; however, consumers enjoy the foam produced [17]. The characteristic of the foam is also influenced by the addition of foam stabilizers, fatty acid and surfactant to the soap. The use of sodium lauryl sulfate (SLS) as a surfactant in the formulated soaps allowed the foam to be more stabilized. However, an excess of SLS may cause skin irritation [12]. In the results, triclosan and *M. indica* soap produced lower foam stability compared to the soap base which suggests that addition of antibacterial agents decreases the foam stability of soap

Free Caustic Alkali. All the formulated soaps did not pass the ≤2.00% standard value set by the International Standards Organization (ISO) [18,19]. This may be caused by the unfinished alkali hydrolysis during saponification as this process results in an excess of alkali which causes a rise in pH. To neutralize the excess alkali, the addition of triglycerides to or a reduction of 5% - 10% from the original amount of KOH to be added may be done [20]. High amounts of excess alkali in soap may result in dryness, scaling, and irritation of the skin since it saponified the fats and oils in the skin which serves as a protection [21].

Antibacterial Evaluation Results. The results of the antibacterial test presented in Table 2 show that the positive control soap with triclosan as its antibacterial agent obtained the highest zone of inhibition (7.40±0.20 mm) against *Staphylococcus* spp. The formulated soap with *M. indica* yielded the second highest zone of inhibition (6.87±0.06 mm). The negative control with no antibacterial agent showed the lowest zone of inhibition (6.60±0.14 mm). The three formulated soaps showed significant differences in the antibacterial activity against *Staphylococcus* spp ($p>0.05$). In the study of Aiello et al. [20], *S. aureus*, a species of the genus *Staphylococcus,* is known to be susceptible to triclosan at low concentrations (2µg/mL). However, the results contradicted the conclusion of their study because the *Staphylococcus* spp. are resistant to the soap containing triclosan and *M. indica* extract.

The concentrations used for triclosan which was 2 µg/mL based on the study of Fan et al. [23] was much smaller compared to the concentration used with *M. indica* leaf extract which was 25 mg/mL based on the study of Krishnananda and Shabaraya [4]. Comparing the two concentrations along with their effect on the bacteria, triclosan had a better antibacterial performance considering that its concentration was smaller compared to *M. indica.*

Table 2. Mean and p-value of the inhibition zones (mm) produced by the three replicates in the agar-well diffusion.

	Soap Base	Triclosan	*M. indica* Extract
Mean (mm)	6.60±0.14	7.40±0.20	6.87±0.06
P-value		0.0041	

The antibacterial performance of the soaps incorporated with triclosan and *M. indica* leaf extract is not comparable. One-way analysis of variance (ANOVA) of the antibacterial activity of the soap formulated using SPSS Statistics indicated that there is a significant difference between the results of the antibacterial tests for the three soaps.

The antibacterial activity of the soap base was unexpected because no antibacterial agent was incorporated into the soap. However, it contradicts the results of the study conducted by Kim et al. [24] wherein the plain soap tested had no significant difference on its antibacterial activity compared to the soap with triclosan. The negative control should not have a zone of inhibition or should have a small zone. However, the soap base resulted in a zone with a size close to that of the soap with the extract. These results were obtained after 24 hours. The contact of the hands and soap while washing is normally just about a minute. Therefore, it cannot be concluded that the triclosan soap performs better than the mango extract unless an actual hand washing test is conducted.

Limitations. This study was limited to the assessment of the antibacterial activity of the liquid soap base, the liquid soap with triclosan and liquid soap with *M. indica* leaf extracts. The *M. indica* leaves were collected from Orchard Valley, Pavia, Iloilo. The antibacterial activity of the soap was only tested against *Staphylococcus* spp. The following physicochemical parameters were used to evaluate the formulated soaps: pH, density, foam stability and free caustic alkali. The extracted leaf samples were not tested against *Staphylococcus* spp. Previous literature were relied upon to support the claim that the *M. indica* extract has antibacterial activity against *Staphylococcus* spp. Due to the lack of studies which clearly describe the formulation of soap, the process was adjusted based on the availability of resources during the conduct of the study.

Conclusion. *Staphylococcus* spp. are resistant to the three formulated soaps. Based on the statistical analysis of the antibacterial activity, there is a significant difference among the zones of inhibition of the three soaps. Thus, *M. indica* leaf extract cannot be used as an alternative for triclosan as an antibacterial agent. The physicochemical properties of the soaps were all in the range of the standard values for soap. Since all three soaps have the same base ingredients, most of the values for the tests were similar. However, all three soaps did not pass the free caustic alkali test. This may be caused by the unfinished alkali hydrolysis during saponification as this process results in an excess of alkali.

Recommendations. To further improve the results of the study, it is recommended that the formulation and the antibacterial test be done immediately after the extraction of the *M. indica* leaf extracts. It is also recommended that a different oil would be used for future research and formulation of the soaps. Varieties of oil determined to exhibit antibacterial activity could be used as a substitute for palm oil. Studying the antibacterial effects of soaps using different oils is also recommended. Different antibacterial tests will also result in different inhibition zone sizes. Since the study is meant to compare the antibacterial activity of the antibacterial agents when incorporated in soap, it is recommended that the concentrations for each antibacterial agent would be the same in order to compare the antibacterial activity directly. For the antibacterial testing, the use of spread plate method is recommended to ensure that the bacteria is evenly distributed on the plate. The use of a caliper is also recommended in measuring the diameter to ensure the accuracy of the data obtained. This will provide a more accurate comparison between the inhibitions of the soaps. Quality control on the antibacterial testing such as the incubation period of the MHA agar and nutrient broth should also be done to have a more reliable and accurate result.

Acknowledgement. The researchers of this study are grateful for the following people who offered their service and support to make this research project possible: Mr. Albert Cachuela and his staff in Orchard Valley for giving their time in helping the researchers obtain our leaf samples; Mr. Stephen Sabinay of West Visayas State University for assisting the researchers and imparting his knowledge on the extraction process; and Mr. Matthew Tubola and his colleagues from the Gregor Mendel Research Laboratory of the University of San Agustin who lend their time, effort and knowledge during the antibacterial evaluation for this study.

References

[1] Mohammed AH, Na'inna SZ, Yusha'u M, Salisu P, Adamu U, Garba SA. 2016. Phytochemical screening and antibacterial activity of *Mangifera indica* extracts. J Microbio Res. 1(1):23-28.

[2] Barbieri R, Coppoa E, Marchese A, Dagliac M, Sobarzo-Sánchez E, Nabavif SF, Nabavif SM. 2017. Phytochemicals for human disease: an update on plant-derived compounds antibacterial activity. Microbio res. 196(1). 44–68.

[3] Mustapha AA, Enemali MO, Olose M, Owuna G, Ogaji JO, Idris MM, Aboh VO. 2014. Phytoconstituents and antibacterial efficacy of Mango (*Mangifera indica*) leaves extract. J Med Plants Stu. 2(5):19-23.

[4] Krishnanada KK, Shabaraya AR. 2016. Comparison of antibacterial activity of leaves extracts of *Tectona grandis, Mangifera indica,* and *Anacardium occidentale*. Int j curr pharm res. 9(1):36-39.

[5] Zakaria Z A, Mat Jais A M, Sulaiman M R, Mohamed S S P, Riffin S. 2006. The in vitro antibacterial activity of methanol and ethanol extracts of Carica papaya flowers and *Mangifera indica* leaves. J pharmacology toxicology. 1(3):278-283.

[6] Juayang AC, de los Reyes GB, de la Rama AG, Gallega CT. 2014. Antibiotic resistance profiling of *Staphylococcus aureu*s isolated from clinical specimens in a tertiary hospital from 2010 to 2012. Interdiscip perspect infect dis. 2014(1):1-4.

[7] Chalew T, Halden R. 2009. Environmental exposure of aquatic and terrestrial biota to triclosan and triclocarban. 45(1):4-1.

[8] Diso S, Ali M, Mukhtar S, Garba M. 2017. Antibacterial activity and phytochemical screening of *Mangifera indica* (mango) stem and leaf extracts on clinical isolates of methicillin resistant *Staphylococcus aureu*s. J Ad Med Pharma Sci. 13(1):1–6.

[9] Widyaningsih S, Chasani M, Diastuti M, Novayanti M. 2018. Formulation of antibacterial liquid soap from nyamplung seed oil (*Calophyllum inophyllum* L) with addition of *Curcuma heyneana* and its activity test on *Staphylococcus aureus.* Mater Sci Eng. 349(1):1-9.

[10] American Oil Chemists' Society (AOCS). 1997. Official and recommended practices of the AOCS. AOCS Press Publication.

[11] Osei-Bonsu K, Shokri N, Grassia P. 2015. Foam stability in the presence and absence of hydrocarbons: from bubble-to bulk-scale. Colloid Surf A Physicochem Eng Asp. 481 (1):514–526.

[12] Handrayani L, Aryani R. 2015. Liquid bath soap formulation and antibacterial activity test against *Staphylococcus aureus* of Kecombrang (*Etlingera elatior* (Jack) R.) Flos Extracts. Curr Pharma Mat Ana. 2(1):17-22.

[13] Bbosa GS, Kyegombe DB, Ogwal-Okeng J, Bukenya-Ziraba R, Odyek O, Waako P. 2007. Antibacterial activity of *Mangifera indica* (L.). Afri J Eco. 45(1):13–16.

[14] Rutala, W. A., & Weber, D. J. (2005). Disinfection, sterilization, and control of hospital waste. Mandell, Douglas, and Bennett's principles and practice of infectious diseases. 2(1):3294-3309.

[15] Vivian OP, Nathan O, Osano A, Mesopirr L, Omwoyo WN. 2015. Assessment of the physicochemical properties of selected commercial soaps manufactured and sold in Kenya. J App Sci. 4(8):433–440.

[16] Oyedele AO, Akinkunmi EO, Fabiyi DD, Orafidiya LO. 2017. Physicochemical properties and antimicrobial activities of soap formulations containing *Senna alata* and *Eugenia uniflora* leaf preparations. J Med Plants Res. 11(48):778-787.

[17] Warra AA, Wawata LG, Gunu SY, Atiku FA. 2011. Soap preparation from Soxhlet extracted Nigerian cotton seed oil. Adv Appl Sci Res. 2(5):617-623.

[18] Idoko O, Emmanuel SA, Salau AA, Obigwa PA. 2018. Quality assessment of some soaps sold in Nigeria. Nigeria J Tech. 4(37):1137-1140.

[19] Betsy KJ, Jilu M, Fathima R, Varkey JT. 2013. Determination of alkali content and total fatty matter in cleansing agents. Asian J Sci Tech. 1(2):8-18.

[20] Popescu V, Soceanu A, Dobrinas S, Stanciu G, Epure DT. 2011. Quality control and evaluation of certain properties for soaps made in Romania. Sci St Res. 12(3):257.

[21] Nangbes JG, Zukdimma NA, Wufem BM, Lawam TD, Dawan NN. Quality survey and safety of some toilet soaps in the Nigerian market: a case study of B/Ladi, Bokkos and Panshin, Plateau state. J App Chem. 7(7):29-35.

[22] Aiello AE, Marshall B, Levy SB, Della-Latta P, Larson E. 2004. Relationship between triclosan and susceptibilities of bacteria isolated from hands in the community. Antimicrob Agents Chemother. 48(8): 2973–2979.

[23] Fan F, Yan K, Wallis N, Reed S, Moore T, Rittenhouse S, DeWolf W, Huang J, McDevitt D, Miller W, et al. 2002. Defining and combating the mechanisms of triclosan resistance in clinical isolates of *Staphylococcus aureus.* Antimicrob Agents Chemotherapy. 46(11):3343-334.

[24] Kim SA, Moon H, Lee K, Rhee MS. 2015. Bactericidal effects of triclosan in soap both in vitro and in vivo. J Antimicrob Chemotherapy. 70(12):3345-3352.

Antibacterial activity of copper-chitosan complexes against zoonotic *Vibrio parahaemolyticus*

HARVEY C. LOQUIAS, REIGEN R. PLACIDO, and HAROLD P. MEDIODIA

Philippine Science High School - Western Visayas Campus, Brgy. Bito-on, Jaro, Iloilo City 5000, Department of Science and Technology, Philippines

Abstract

Copper-chitosan (Cu-Ch) complexes can be used as antibacterial agents against zoonotic microorganism strains. This study assessed the antibacterial activity of Cu-Ch complexes synthesized via a chemical method outlined by Usman et al. [7,8] against zoonotic *Vibrio parahaemolyticus* using disk diffusion assay. The complexes were characterized using Ultraviolet-Visible (UV-VIS) and Fourier Transform Infrared (FTIR) spectrophotometry. Characterization results indicate the formation of Cu-Ch complexes during synthesis, but not nanoparticles. The synthesized Cu-Ch complexes exhibited no antibacterial activity against *Vibrio parahaemolyticus*, suggesting that they are ineffective antimicrobials against zoonotic microorganisms. Further studies can look into their antibacterial activity against other types of microorganisms.

Keywords: *chitosan, copper, nanocomplexes, Vibrio parahaemolyticus, zoonotic*

Introduction. Metal nanoparticles and nanocomplexes have been synthesized from cost-efficient metals such as copper (Cu) and tested for antimicrobial activity [1,2,3,4]. However, copper rapidly oxidizes upon exposure to the atmosphere which can result in the formation of oxides, aggregation and decreased activity [5,6,7]. To counter the problem of agglomeration and rapid oxidation of copper, Usman et al. [8] synthesized pure copper nanoparticles in the presence of a chitosan stabilizer through a chemical process.

Chitosan (Ch), a modified carbohydrate polymer derived from chitin, has been used with metal nanoparticles as a chelating agent to retard oxidation and increase antimicrobial activity [9]. The presence of chitosan has been found to improve the antimicrobial activity of copper nanoparticles due to its stabilizing effect on copper [4, 10,11]. There are also no reports of bacteria resisting or developing resistance against this biopolymer [12].

Copper-Chitosan (Cu-Ch) nanocomplexes have possible applications for treatment of zoonotic and resistant organisms and biofilms. Tests by Usman et al. [7] and Syame et al. [13] have shown that Cu-Ch nanocomplexes can exhibit antibacterial activity on resistant gram-positive bacteria such as Methicillin-Resistant *Staphylococcus aureus*. Despite reports of Cu-Ch nanocomplexes exhibiting greater antimicrobial activity against gram-negative bacteria, a number of zoonotic gram-negative strains as well as other gram-positive strains have yet to be subjected to antimicrobial tests with Cu-Ch complexes.

Vibrio parahaemolyticus is a gram-negative target bacterial species to monitor according to the Philippine Antimicrobial Resistance Surveillance Plan for the Animal Health Sector (2018-2020). It has been found to cause gastroenteritis and septicemia on humans both directly and indirectly exposed *to V. parahaemolyticus* infected animals such as oysters [14] and shrimps [15]. It has also caused diseases in aquaculture organisms such as shrimp [16,17] and abalone [18].

Although there are a number of studies investigating the antimicrobial activity of copper-chitosan nanocomplexes [4,7,8,10] and a number of susceptibility studies conducted on *V. parahaemolyticus* [19,20,21,22], as far as can be ascertained, no research has yet been performed to test the antibacterial activity of copper-chitosan complexes against *V. parahaemolyticus*.

To address this, the study aimed to assess the antibacterial activity of researcher-synthesized copper-chitosan complexes against zoonotic *Vibrio parahaemolyticus* via disk diffusion assay and characterize them in terms of Ultraviolet-Visible Spectra (surface plasmon resonance peaks), absorbance spectra, and morphology for the complexes exhibiting the highest antimicrobial activity. It specifically aimed to:

(i) measure the zone of inhibition of researcher-synthesized Cu-Ch complexes against zoonotic *Vibrio parahaemolyticus* using disk diffusion assay;

(ii) characterize researcher-synthesized Cu-Ch complexes in terms of:
- (a) surface plasmon resonance peaks;
- (b) FTIR / Transmittance spectra; and
- (c) morphology (size, shape, agglomeration) for the Cu-Ch complex treatment exhibiting the highest antibacterial activity; and

(iii) determine the viability of researcher-synthesized Cu-Ch complexes as nanoparticles in comparison with
- (a) surface plasmon resonance peaks in the range 500-600 nm as outlined by Mallick et al. [23] and Usman et al. [7];
- (b) blue shifts and decreased intensity peaks in FTIR Spectra as outlined by Usman et al. [7,8]; and
- (c) diameter size in the range of 50-270nm for the 0.1% Cu-Ch NPs, in the range of 5-50nm for the 0.2% Cu-Ch NPs, and in the range of ~2-50nm for the 0.5% Cu-Ch

How to cite this article:
CSE: Loquias HC, Placido RR, Mediodia HP. 2020. Antibacterial activity of copper-chitosan complexes against zoonotic *Vibrio parahaemolyticus.* Publiscience. 3(1):27-31.
APA: Loquias, H.C., Placido, R.R., & Mediodia, H.P. (2020). Antibacterial activity of copper-chitosan complexes against zoonotic *Vibrio parahaemolyticus. Publiscience*, 3(1):27-31.

NPs; predominantly spherical in shape; and polydispersed in agglomeration, as outlined by Usman et al. [7,8] for the Cu-Ch complex treatment exhibiting the highest antibacterial activity.

Methods. Copper-chitosan complexes were synthesized via a chemical method outlined by Usman et al. [7,8] and subjected to both antimicrobial tests using the standard disk diffusion method as outlined by the Clinical and Laboratory Standards Institute (CLSI, Performance Standards for Antimicrobial Disk Susceptibility Tests; Approved Standard 11th Edition, 2012) and characterization using UV-VIS and FTIR Spectrophotometry.

Materials. Laboratory grade copper (II) sulfate ($CuSO_4$), acetic acid, ascorbic acid, barium chloride ($BaCl_2$), sulfuric acid (H_2SO_4), and sodium hydroxide (NaOH) were provided by the Science Research Assistant in Philippine Science High School-Western Visayas Campus (PSHS-WVC). Analytical grade hydrazine (N_2H_4) was purchased from Sigma-Aldrich Pte Ltd. Laboratory grade chitosan was purchased from KAN Phytochemicals Pvt. Ltd. *Vibrio parahaemolyticus* was sourced from the Philippine National Collection of Microorganisms (PNCM) at the University of the Philippines - Los Baños College, Los Baños, Laguna.

Chemical Synthesis. Ten (10) mL of $CuSO_4 \cdot 5H_2O$ (0.05 M) was added to 40 mL of acetic acid solution (0.1 M) containing chitosan (0.1, 0.2, and 0.5 wt%). After constant stirring and refluxing at around 100°C-140°C for 20 minutes, 0.5 mL of ascorbic acid (0.05 M) was added, and the solution was stirred for 20 minutes at room temperature. Two (2) mL of NaOH (0.6 M) was then added, obtaining a darker blue-green solution after stirring for another 20 minutes. Then 0.5 mL of N_2H_4 (0.05M) was added and the solution was stirred for five (5) minutes. The pH was kept at an average of 8.0 throughout the process. The solution was centrifuged at 10,000 G for 10 minutes and washed with acetone (90%, v/v). The precipitate was vacuum dried at 50°C for 18 hours.

Antibacterial Assay. Mueller-Hinton (MH) Agar was utilized as culture media. The copper-chitosan complexes (0.1, 0.2, 0.5 wt% chitosan content) were suspended in distilled water and loaded onto blank sterilized Whatman No. 1 filter paper disks. Ciprofloxacin-loaded antibacterial discs (5 ug) and distilled water loaded onto blank sterilized Whatman No. 1 filter paper disks served as the positive and negative controls, respectively. Chitosan was also loaded onto blank sterilized Whatman No. 1 filter paper disks, totaling 6 treatments. The experiment was carried out in triplicate and the diameters of the zones of inhibition (in mm) were measured after incubating for 16-18 hours at 35±2°C in ambient air.

Characterization. The synthesized Cu-Ch complexes were characterized in terms of Ultraviolet-Visible Spectra (surface plasmon resonance) and Absorbance Spectra using a UV-1800 Shimadzu UV Spectrophotometer (Ultraviolet-Visible Spectrophotometry) and an IRAffinity-1S Shimadzu Fourier Transform Infrared (FTIR) Spectrophotometer.

Data analysis. The susceptibility of *V. parahaemolyticus* to the complexes was determined based on the CLSI test interpretation document M45-Methods for Antimicrobial Dilution and Disk Susceptibility Testing of Infrequently Isolated or Fastidious Bacteria. Results of the characterization of the synthesized complexes were analyzed by comparison to previously published articles, specifically on the UV-Vis and FTIR results of Mallick et al. [23], Zhou et al. [24], Huang et al. [25], Shameli at al. [26], Usman et al. [7], and Sportelli et al. [27].

Safety procedure. The handling of *V. parahaemolyticus* was performed under a biosafety cabinet in the Department of Science and Technology VI (DOST VI) Microbiology laboratory. Organic and inorganic chemical waste were disposed separately in designated containers found in PSHS-WVC. Biohazard waste from the antibacterial testing phase was properly disposed with the aid of laboratory personnel from DOST VI, following their protocol for disposal.

Results and Discussion. The complexes (0.1 wt%, 0.2 wt%, 0.5 wt%) and the pure chitosan solution (50% w/v) did not exhibit bacterial inhibition. As shown in Table 1, the negative and positive controls resulted in 6mm and 30mm diameter zones of inhibition, respectively. Non-uniform radii of inhibition around the 0.2% discs (2.45mm, 3.10mm, and 1.35mm) were observed but were not interpreted as zones of inhibition as stated in the CLSI M45 guide document. *V. parahaemolyticus* is resistant to the Cu-Ch complexes and pure chitosan, and susceptible to ciprofloxacin (5ug). Spectrophotometric analysis of the researcher-synthesized Cu-Ch complexes suggests formation of Cu-Ch complexes and non-formation of Cu-Ch nanoparticles. The Cu-Ch complexes were not subjected to morphological characterization as they did not exhibit antibacterial activity against the test organism.

Table 1. Summary of the antibacterial and characterization results of the study.

Treatment	Antibacterial activity (Zone of inhibition in mm)	Copper Complex formation	NP formation
Ciprofloxacin (+)	Susceptible (30 mm)	-	-
Distilled Water (-)	Resistant (6 mm)	-	-
Pure Ch	Resistant (6 mm)	-	-
0.1 wt% Ch content	Resistant (6 mm)	Y	N
0.2 wt% Ch content	Resistant (6 mm)	Y	N
0.5 wt% Ch content	Resistant (6 mm)	Y	N

Legend: Y = formation; N = non-formation

The synthesized Cu-Ch complexes are not identified to be nanoparticles due to the lack of a surface plasmon resonance (SPR) peak in the

500-600 nm range of the UV-Vis absorbance spectra of the complexes (Figure 1), as well as a lack of decreased intensity peaks and a significant peak in the 600-700 cm^{-1} range of the FTIR spectra (Figure 2) [7,26,27]. Cu-Ch nanoparticles are known to show absorbance in the range of 500–600 nm of their UV-Vis spectra [7]. Copper-polymer nanoparticles by Mallick et al. [23] also showed UV-VIS absorbance peaks at the 500-600 nm range.

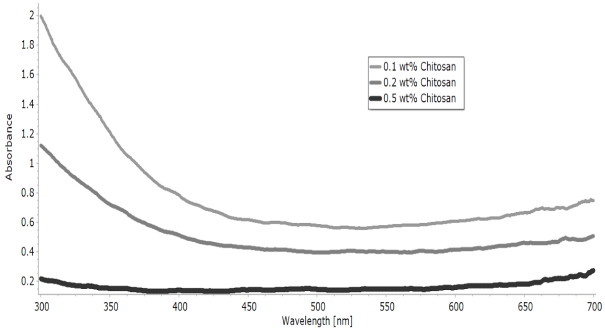

Figure 1. UV-VIS Absorbance spectra of copper-chitosan complexes (0.5 wt%, 0.2 wt%, 0.1 wt% chitosan content).

Decreasing intensity peaks and peaks in the 600-700 cm^{-1} range are also characteristic in the FTIR spectra of Cu-Ch nanoparticles [32]. The presence of peaks at 3310 cm^{-1} , 3317 cm^{-1}, and 3315 cm^{-1} indicate N-H and O-H bonds, both of which are present due to the characteristic structure of chitosan [28]. Stretches observed at 2360 cm^{-1} indicate the presence of C-N and C-C triple bonds which were found to be present in the complexes [7,24]. The 2000-1450 cm^{-1} region contains peaks corresponding to double bond stretching vibrations. The presence of blueshifts indicates that ligand groups of chitosan are combined with the surface of Cu NPs [28]. Furthermore, no color change was observed after the addition of the reducing agent (N_2H_4), indicating that no nanocomplexes were formed [7,8]. Li et al. [28] states this is possibly due to the concentration of the reducing agent that was unable to reduce the synthesized complexes into nanoparticles.

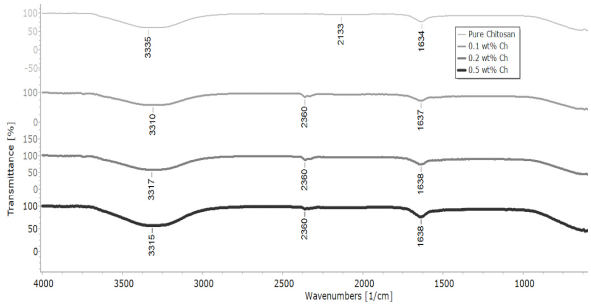

Figure 2. Processed fourier transform infrared spectra of Ch and Cu-Ch complexes (0.5 wt%, 0.2 wt%, 0.1 wt% Ch content).

Factors such as pH, metal concentration, and metal/ligand ratio influence the complexation of metal species and polymers [29]. While chitosan has been observed to exhibit good metal ion uptake, in crosslinked and uncrosslinked forms [30], it is also known to form a complex with copper in conditions below pH 6.1 due to its poor solubility in alkaline media [10]. However, complexation in acidic conditions results in chitosan protonation which significantly reduces the affinity of the sorbent for the uptake of metal cations [31]. Incomplete capping or instability of the synthesized complexes can be attributed to the pH 8.0 level maintained in the synthesis process modeled after the chemical procedure of Usman et al. [7,8].

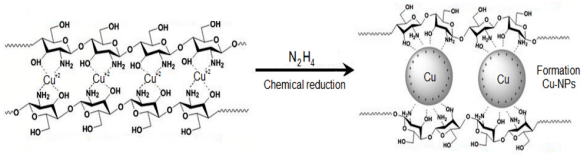

Figure 3. Molecular structure of Cu-Ch complexes (left) and Cu-Ch nanocomplexes (right) after chemical reduction presented by Usman et al. [7].

Pure chitosan and the Cu-Ch complexes exhibited no antibacterial activity against *V. parahaemolyticus* that was susceptible to ciprofloxacin (5ug), which exhibited activity resulting in an inhibition zone of 30 mm. This coincides with previous literature stating pure chitosan does not have antimicrobial activity in alkaline media due to its poor solubility above pH 6.5 [7]. The inhibitory activity of pure chitosan can be linked to changing the bacterial cell membrane permeability, and poorly soluble chitosan is unable to penetrate outer bacterial membranes as a macromolecule [29,32].

The lack of activity of the synthesized Cu-Ch complexes is in contrast with the synthesized nanocomplexes of Usman et al. [7] which exhibited antibacterial activity. Huang et al. [32] showed that despite a synergistic effect on the antibacterial activity of copper and chitosan, Cu-Ch complexes exhibit less antibacterial activity compared to Cu-Ch nanoparticles. Mekhalia and Bouzid [29] posits that chitosan, as a macromolecule, is unable to pass the outer membrane of bacteria which functions as a permeability barrier against macromolecules. Unlike their macromolecule counterparts, smaller chitosan molecules such as nanocomplexes can diffuse into the bacterial cells through pervasion and disrupt normal physiological activity, resulting in cell death. The coordination bonding between the functional groups of the chitosan molecules and copper ions may weaken a bond near the coordinating site and cause some weak points on the chitosan chain, resulting in smaller chitosan molecules [10]. This coincides with how the antibacterial activity of previously synthesized Cu-Ch nanocomplexes [7,8,27] has been attributed to morphology, specifically decreased size and increased surface area. The UV-VIS and FTIR spectra of the synthesized complexes in this study both indicate non-formation of nanoparticles. Improvement of coordination bonding between the chitosan polymer and the copper ions, and thus decreasing complex sizes, may be achieved with higher concentrations of the reducing agent [28].

On the resistance exhibited by the test organism, a previous study by Gordon et al. [33] showed that *V. parahaemolyticus* can recover from stress induced by copper. The same study also found proteins in copper-induced *V. parahaemolyticus* cultures similar to extracellular copper-binding proteins found in *Vibrio alginolyticus,* which may be one of the defense mechanisms of *V. parahaemolyticus* against copper. This coincides with the results of the study of Chari

et al. [34] where copper nanoparticles tested against *V. parahaemolyticus* exhibited no antibacterial activity against the test organism.

Limitations. The results only reflected the activity of Cu-Ch as complexes and not as nanoparticles. Furthermore, results only reflected the activity of the complexes against *V. parahaemolyticus*. Only the Kirby-bauer method was used to test for antibacterial activity, which investigated activity at one concentration.

Conclusion. Results indicated that Cu-Ch complexes, in contrast to Cu-Ch nanoparticles synthesized by Usman et al. [8,7] exhibit no antibacterial activity against zoonotic *Vibrio parahaemolyticus*.

Recommendations. Due to the observed non-activity of the complexes against *V. parahaemolyticus*, further tests may consider other compounds exhibiting different modes of action compared to Cu-Ch complexes. Antibacterial activity of the complexes against other types of microorganisms may be investigated, especially against Gram-positive bacteria. An assay investigating the minimum inhibitory concentration (MIC) of the complexes may be utilized to investigate the activity of the complexes at other concentrations and in direct contact with the test organism. Morphological testing of Cu-Ch complexes and further tests comparing the antibacterial activity of Cu-Ch coordination complexes and Cu-Ch nanoparticles are also recommended for further studies. Further studies are suggested to employ measures to monitor the temperature of the reflux setup at 120 ˚C during the synthesis process.

Acknowledgement. The researchers would like to extend their gratitude to the following: to Dr. Czarina Nobleza and Dr. Stephen Sabinay for their assistance in conceptualizing and conducting this research, to the Department of Health and Department of Agriculture for providing data for conceptualization, to the Department of Science and Technology- Region VI and the University of the Philippines- Visayas for allowing the researchers to work in their laboratories, to Mr. Joeben Gabutanga for his assistance the procurement of their test organism, and to everyone who supported this research.

References

[1] Yoon KY, Byeon JH, Park JH, Hwang J. 2007. Susceptibility constants of *E. coli* and *B. subtilis* to silver and copper nanoparticles. Sci Total Environ. 373(2007):*572-575*.

[2] Ruparelia JP, Chatterjee AK, Duttagupta SP, Mukherji S. 2008. Strain specificity in antimicrobial activity of silver and copper nanoparticles. Acta Biomaterialia. 4(3):707-716.

[3] Ramyadevi J, Jeyasubramanian K, Marikani A, Rajakumar G, Rahuman AA. 2012. Synthesis and antimicrobial activity of copper nanoparticles. Mater lett. 71: 114-116.

[4] Du WL, Niu SS, Xu YL, Xu ZR, Fan CL. 2009. Antibacterial activity of chitosan tripolyphosphate nanoparticles loaded with various metal ions. Carbohydr Polym. 75(3): 385-389.

[5] Balela MDL, Amores KLS. 2015. Formation of highly antimicrobial copper nanoparticles by electroless deposition in water. Sci Diliman. 27(2):10-20.

[6] DeAlba-Montero I, Guajardo-Pacheco J, Morales-Sánchez E, Araujo-Martínez R, Loredo-Becerra GM, Martínez-Castañon GA, Ruiz F, Compeán-Jasso ME. 2017. Antimicrobial properties of Copper nanoparticles and amino acid chelated Copper nanoparticles produced by using a soya extract.

[7] Usman MS, El Zowalaty ME, Shameli K, Zainuddin N, Salama M, Ibrahim NA. 2013. Synthesis, characterization, and antimicrobial properties of copper nanoparticles. Int J Nanomed. 2013(8):4467-4479.

[8] Usman MS, Ibrahim NA, Shameli K, Zainuddin N, and Yunus WM. 2012. Copper nanoparticles mediated by chitosan: synthesis and characterization via chemical methods. Molecules. 2012(17): 14928-14936.

[9] Al-Dhabaan FA, Shoala T, Ali AA, Alaa M, Abd-Elsalam K. 2017. Chemically-produced copper, zinc nanoparticles and chitosan–bimetallic nanocomposites and their antifungal activity against three phytopathogenic fungi. IJAT. 13(5):753- 769.

[10] Qi L, Xu Z, Jiang X, Hu C, Zou X. 2004. Preparation and antibacterial activity of chitosan nanoparticles. Carbohyd Res. 339(16): 2693-2700.

[11] Manikandan A, Sathiyabama M. 2015. Green synthesis of copper-chitosan nanoparticles and study of its antibacterial activity. J Nanomed Nanotechnol. 6(1): 1-5.

[12] Divya K, Vijayan S, George TK, Jisha MS. 2017. Antimicrobial properties of chitosan nanoparticles: mode of action and factors affecting activity. Fiber Polym. 18(2): 221-230.

[13] Syame OM , Mohamed WS, Mahmoud RK and Omara ST. 2017. Synthesis of copper-chitosan nanocomposites and their applications in treatment of local pathogenic isolates bacteria. Orient J Che. 33(6):2959-2969.

[14] McLaughlin JB, DePaola A, Bopp CA, Martinek KA, Napolilli NP, Allison CG, Murray SA, Thompson EC, Bird MM, Middaugh JP. 2005. Outbreak of *Vibrio parahaemolyticus* gastroenteritis associated with Alaskan oysters. N Engl J Med. 353(14): 1463-1470.

[15] Daniels NA, MacKinnon L, Bishop R, Altekruse S, Ray B, Hammond RM, Thompson S, Wilson S, Bean NH, Griffin PM, Slutsker L. 2000. *Vibrio parahaemolyticus* infections in the United States, 1973–1998. J Infect Dis. 181(5): 1661-1666.

[16] Alapide-Tendencia EV, Dureza LA. 1997. Isolation of *Vibrio spp.* from Penaeus monodon (Fabricius) with red disease syndrome. Aquaculture. 154(2): 107-114.

[17] Joshi J, Srisala J, Truong VH, Chen IT, Nuangsaeng B, Suthienkul O, Lo CF, Flegel TW, Sritunyalucksana K, Thitamadee S. 2014. Variation in *V. parahaemolyticus* isolates from a single Thai shrimp farm experiencing an outbreak of acute hepatopancreatic necrosis disease (AHPND). Aquaculture. 428(2014): 297-302.

[18] Liu PC, Chen YC, Huang CY, Lee KK. 2000. Virulence of *Vibrio parahaemolyticus* isolated from cultured small abalone, *Haliotis diversicolor supertexta*, with withering syndrome. Lett Appl Microbiol. 31(6): 433-437.

[19] Han F, Walker RD, Janes ME, Prinyawiwatkul W, Ge B. 2007. Antimicrobial susceptibilities of *V. parahaemolyticus* and *V. vulnificus* isolates from Louisiana Gulf and retail raw oysters. Appl Environ Microbiol. 73(21): 7096-7098.

[20] Shaw KS, Goldstein RER, He X, Jacobs JM, Crump BC, Sapkota AR. 2014. Antimicrobial susceptibility of *Vibrio vulnificus* and *Vibrio parahaemolyticus* recovered from recreational and commercial areas of Chesapeake Bay and Maryland Coastal Bays. PLoS One. 9(2): e89616.

[21] Letchumanan, V, Yin WF, Lee LH, Chan KG. 2015. Prevalence and antimicrobial susceptibility of *V. parahaemolyticus* isolated from retail shrimps in Malaysia. Front Microbiol. 6(33).

[22] Stevens D, Higbee J, Oberhofer T, Everett D. 1979. Antibiotic susceptibilities of human isolates of *V. parahaemolyticus*. Antimicrob Agents Chemother. 16(3):322-324.

[23] Mallick K, Witcomb MJ, Scurrell MS. 2006. In situ synthesis of copper nanoparticles and poly (o-toluidine): a metal–polymer composite material. Eur Polym J. 42(3): 670-675.

[24] Zhou YG, Yang YD, Guo XM, Chen GR. 2003. Effect of molecular weight and degree of deacetylation of chitosan on urea adsorption properties of copper chitosan. J App Polym Sci. 89(6); 1520-15.

[25] Huang H, Yuan Q, Yang X. 2004. Preparation and characterization of metal–chitosan nanocomposites. Colloids Surf B. 39(1-2); 31-37.

[26] Shameli K, Ahmad MB, Yunus WMZ., Rustaiyan A, Ibrahim NA. Zargar M, Abdollahi Y. 2010. Green synthesis of silver/montmorillonite/ chitosan bionano-composites using the UV irradiation method and evaluation of antibacterial activity. Int J Nanomed. 5(2010): 875887.

[27] Sportelli M, Volpe A, Picca R, Trapani A, Palazzo C, Ancona A, Lugarà P, Trapani G, Cioffi N. 2016. Spectroscopic character-rization of copper-chitosan nano-antimicrobials prepared by laser ablation synthesis in aqueous solutions. Nanomaterials. 7(1):6.

[28] Li Y, Li B, Wu Y, Zhao Y, Sun L. 2013. Preparation of carboxymethyl chitosan/copper composites and their antibacterial properties. Mater Res Bull. 48(2013).

[29] Mekhalia S, Bouzid B. 2009. Chitosan-Copper (II) complex as antibacterial agent: synthesis, characterization and coordinating bond-activity correlation study. Physcs Proc. 2(3): 1045-1053.

[30] Sobahi TR, Abdelaal MY, Makki MS. 2014. Chemical modification of chitosan for metal ion removal. Arab J Chem. 7(5): 741-746.

[31] Guibal E. 2004. Interactions of metal ions with chitosan-based sorbents: a review. Sep Purif Technol. 38(1): 43-74.

[32] Huang Y, Huang J, Cai J, Lin W, Lin Q, Wu F, Luo J. 2015. Carboxymethyl chitosan/clay nanocomposites and their copper complexes: fabrication and property. Carbohydr Polym. 134(2015).

[33] Gordon AS, Howell LD, Harwood V. 1994. Responses of diverse heterotrophic bacteria to elevated copper concentrations. Can J Microbiol. 40(5): 408–411.

[34] Chari N, Felix L, Davoodbasha M, Ali AS, Nooruddin T. 2017. In vitro and in vivo antibiofilm effect of copper nanoparticles against aquaculture pathogens. Biocatal Agric Biotechnol. 10: 336-341.

MAGWAYEN

HEALTH AND TOXICITY

MAGWAYEN is revered as the deity governing the seas and death. She is believed to ferry the souls of the reposed into the afterlife. Vectors, much like Magwayen, behaves as carriers – spreading diseases, causing sickness, and compromising health. This section recognizes the paramount importance of identifying, monitoring, and controlling such vectors, which could become the difference between life and death. Included here are studies exploring possible alternatives to traditional bacterial stains and mosquito larvicides.

These studies fall under the Health Research and Development Agenda, with focus on research that could potentially improve lives as they propose countermeasure against disease vectors, as well as alternative materials, substances, and/or methods that have minimal effect on non-target organisms.

BASED ON: Harmonized National Research and Development Agenda (HNRDA)

The utilization of methanolic *Bixa orellana* (Annatto) seed extract as substitute for safranin in Gram staining

SAM DANIEL T. VENTURINA, JOSH ZAVION A. COMUELO, WAYNE ROCQ A. SAMANIEGO, and FERNANDO CHRISTIAN JOLITO III

Philippine Science High School - Western Visayas Campus, Brgy. Bito-on, Jaro, Iloilo City 5000, Department of Science and Technology, Philippines

Abstract

The routine use of safranin, a synthetic dye, in Gram staining raises a number of environmental and safety concerns. This study evaluates the utility of the methanolic extract of *Bixa orellana* (Annatto) seeds as replacement for safranin as counterstain in Gram staining. Pure and mixed bacterial smears of *Escherichia coli* and *Staphylococcus aureus* were stained with Annatto and safranin. The staining showed that the *Bixa orellana* extract did not stain the bacteria in any of the slides. Results show that the pH of the extract was found to be acidic at 5.92 in comparison to safranin, which was basic at 7.44. The inability of the extract to stain the bacteria may be attributed to its acidic pH which makes it unable to bind to the acidic cell wall of the bacteria.

Keywords: *annatto, bixin, safranin, Gram staining, methanol*

Introduction. At present, due to increasing environmental consciousness among commercial dyers and small textile exporters, interest has shifted towards the utilization of naturally-sourced colour pigments in food materials, pharmaceuticals and textiles, as an alternative to their synthetic counterparts [1]. Although synthetic dyes are produced from cheap sources and show superior fastness properties, their usage cause pollution and can be harmful to humans [2]. Natural dyes, in contrast, are less hazardous and eco-friendly [3].

Dyes are used in Gram staining, which is a process which uses basic stains to impart color to bacteria [4]. It uses a primary stain and a counterstain to differentiate gram-positive and gram-negative bacteria. However, commonly used stains such as safranin and crystal violet are synthetically made. Gram staining is primarily used in histopathology for primary identification of bacteria, as such information is useful in deciding the appropriate treatment for patients [5].

Unlike most organic compounds, dyes possess color because they absorb light in the visible spectrum (400–700 nm), have at least one chromophore or colour-bearing group, have a conjugated system, i.e. a system of connected p orbitals with delocalized electrons in a molecule, and exhibit resonance of electrons, which is a stabilizing force in organic compounds [6]. Stains are examples of a dye which has the ability to impart colour to tissues. However, the pH of a stain affects its ability to adhere to a specific tissue thus, basic structures have better affinity towards acidic stains while acidic structires have better affinity towards basic stains due to their nature.

B. orellana (Annatto), a dye yielding plant, is known for its lack of toxicity and its high tinctorial value [7]. Annatto dyes are widely used in the food, pharmacological and cosmetic industries due to the intensity of their colours, their greater stability and the wide variety of tones [8]. According to a study by Lauro [9], bixin, the liposoluble component of Annatto, amounts to about 80% of the plant's carotenoids.

Bixin, the main colorant found in the seeds of *Bixa orellana*, is an example of a dye with the capacity to absorb light. Studies have shown that bixin is soluble in organic solvents with medium polarity [10]. The studies conducted by Attokaran [11], Rahmalia et al. [12], and Scotter [13] have explained that bixin is soluble to most polar organic solvents. A study conducted by Braide et al. [14] using methanolic crude extract of *Bixa orellana* with NaOH and glacial acetic acid was unable to stain bacteria. Methanol is a suitable reconstituting agent and solvent for extraction because a study conducted by Husa et al. [15] found that methanol results in the highest bixin yield in comparison with water, hexane, and acetone due to its ability to dissolve the cell membrane in comparison to the other aforementioned solvents.

The aforementioned hazards that synthetic dyes possess [2] provides an avenue for exploring alternatives. While there has been research on using plant-based dyes as alternatives to commercial bacterial stains [14], the utility of bixin from *Bixa orellana* as a replacement for safranin has not been explored.

The present study proposed to investigate *Bixa orellana*, for its potential in being a substitute for safranin in Gram staining. It specifically aimed to:

(i) compare the UV-Spectra of the *Bixa orellana* extract at 50ppm to Bixin;

(ii) compare the pH of the stock solutions of both *Bixa orellana* and safranin; and

(iii) compare the staining capabilities (visibility and color intensity) of both Annatto and safranin.

If the *Bixa orellana* extract is proven to be a dye comparable to safranin in terms of effectiveness as a bacterial stain, it would be beneficial to the

How to cite this article:
CSE: Venturina SD, Comuelo JZ, Samaniego WR, Jolito FC. 2020. The utilization of methanolic *Bixa orellana* seed extract as substitute for safranin in Gram staining. Publiscience. 3(1):33-36.
APA: Venturina, S.D., Comuelo, J.Z., Samaniego, W.R., & Jolito, F.C. (2020). The utilization of methanolic *Bixa orellana* seed extract as substitute for safranin in Gram staining. *Publiscience,* 3(1):33-36.

environment, as the use of plant dyes as an alternative can lead to more environmentally-friendly practices.

Methods. The study was conducted to evaluate the potential of the *Bixa orellana* methanolic extracts as a substitute to safranin. Bixin, one of the primary dye components of *Bixa orellana* extracts, was extracted utilizing methanol (CH_3OH) as the solvent. For the preparation of *Bixa orellana*, the seeds were collected then ground. The seeds were then macerated in methanol and stirred using a magnetic stirrer. The extracts were then placed in a rotary evaporator to remove the methanol solvent and to acquire crude extract. Gram staining was then performed using *S.aureus* and *E. coli* as test organisms. The stains were viewed using a Digital Microscope and evaluated their staining capability in comparison to safranin.

Preparation of Materials. The *Bixa orellana* seeds were separated by hand then washed with distilled water and sterilized in a hot air oven at 60˚C for 24 hours. The seeds were then crushed using a blender.

Extraction. One hundred grams (100g) of the pulverized seeds were added to 1 L of methanol (CH_3OH) and stirred for 12 hours using a magnetic stirrer and stored without sunlight at room temperature for another 12 hours. The extract was then filtered using Whatman Filter Paper No. 1 and was placed in an IKA RV10 Rotary Evaporator at 40 ˚C until the methanol had leaving solid crude extract remained. The extract was then stored in a refrigerator prior to staining.

Test for pH. Crude extract of mass 0.25g was dissolved in 10 mL of methanol (CH_3OH). Its pH was then measured using a pH meter.

UV-Vis Spectroscopy. Crude extract of mass 0.25g was dissolved in 10 mL of methanol (CH_3OH). The absorbance of the reconstituted solutions was then measured with a UV-Vis spectrophotometer at 300-650 nm and compared to the expected absorption maxima from the study of Silva et al. [16].

Reconstitution of extract. Crude extract of mass 2.5g was dissolved in 50ml of methanol to form the solution.

Staining. A drop of normal saline solution was placed on the slide. Using an inoculating needle, the cultured bacteria was smeared on the slide and allowed to dry. The slide was then passed quickly over the flame of an alcohol lamp three times. The slide with the heat fixed smear was then flooded with crystal violet for one minute and was then rinsed with distilled water. The smear was gently flooded with Gram's iodine for one minute and was then rinsed with distilled water. The smear was then decolorized using a 50 v/v% mixture of acetone and alcohol. The slide was then flooded with safranin as counterstain and left to stand for one minute. The slide was then rinsed with distilled water [17]. The process was repeated using the methanol-reconstituted *Bixa orellana* extract as a counterstain. For safranin, 30 slides consisting of 10 slides of mixed *E. coli* and *S. aureus* bacteria, 10 slides of *S. aureus*, and 10 slides of *E. coli* were stained. Another 30 of slides were stained with *Bixa orellana* extract as counterstain instead of safranin.

Safety procedure. The use of personal protective equipment such as laboratory gowns, safety goggles, gloves and masks in the laboratory was observed at all times. The solvents and bacteria were stored in sealed containers with proper labels for clear identification. The materials used to handle *S. aureus* and *E. coli* were sterilized in an autoclave prior to use. The handling of bacteria was performed in a biosafety level 2 laboratory. The bacteria cell cultures were properly labeled and stored in an incubator.

Results and Discussion. The study aimed to investigate the use of *Bixa orellana* methanolic extract as a substitute for safranin in Gram Staining. Specifically, it aims to compare the pH of the stock solutions of both *Bixa orellana* and safranin, compare the UV-Spectra of the bixin extracts, and compare the staining capabilities of both *Bixa orellana* and safranin. 60 slides were stained and evaluated. The two stains: *Bixa orellana* extract and Safranin were used to stain the bacteria. The slides were evaluated and compared.

Measurement of pH. The pH of the Methanol extract was found to be acidic at 5.92 while the safranin solution was found to be basic at pH 7.44. The ability to stain certain structures is determined by the pH values of the stain. Safranin is an example of a basic dye, which easily release OH^- ions and readily accept H^+ ions, this leaves the stain positively charged and ready to adhere to negatively charged molecules like the polyphosphated nucleic acids and proteins found in the cell wall of bacteria [18]. The results suggest that the *Bixa orellana* extract was not able to stain the bacteria because of its acidic pH, which is in agreement with Prescott et al. [17], which posits that the pH of the dye may alter staining effectiveness since the nature and degree of the charge on cell component changes with pH. It then follows that acidic structures are stained by basic dyes while basic structures are stained by acidic dyes [19]. This is also in agreement with a study conducted by Chukwu et al. [20], wherein modified Henna extracts with acidic pH were unable to stain the bacterial cells while Henna extracts oxidized with potassium permanganate had a better counter staining reaction due to its neutral pH as stated in the study.

UV-Vis Spectroscopy. In Fig. 1, the UV–Vis absorbance spectrum is shown for the extract reconstituted with methanol. The absorption peaked at 425.64nm, which is in good agreement with the expected absorption maxima for bixin which are at 429 nm, 457 nm, and 487 nm [14]. This indicates that bixin was extracted. The presence of bixin indicates that the methanolic extract has the potential to stain bacterial cells because unlike most organic compounds, bixin, is an example of a dye because it has a chromophore, which is characterized by a conjugated system and extended delocalized system [21]. Bixin also contains an auxochrome, which are groups that increase the color absorption of a chemical, represented by the hydroxyl group [21].

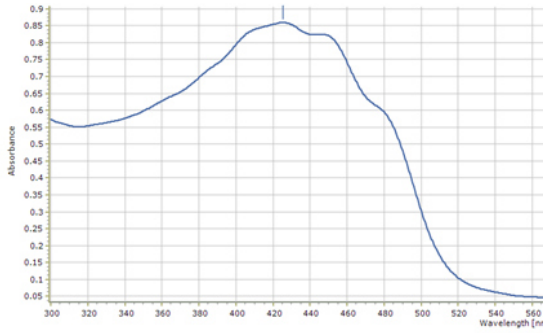

Figure 1. The graph of the UV-Vis Spectra for the methanolic *Bixa orellana* extract.

Staining. The evaluation of mixed bacterial smears as shown in Table 1 showed that *S.aureus* counterstained with Annatto stain had no traces of color other than the violet from the crystal violet stain. This conforms with the expected coloration for the Gram Staining of *S.aureus.* Gram-positive bacteria are expected to retain the color of the primary stain with no traces of the counterstain because it has a thicker peptidoglycan layer which shrinks and traps the primary stain-mordant complex during decolorization [20]. Gram-positives possess cell membranes with low permeability to iodine in alcoholic solution. This, combined with the low alcohol solubility of the dye-iodine compound, can be the cause of the retention of the primary stain [4]. Gram-negative bacteria is expected to be colorized by the counterstain as its thinner peptidoglycan layer is unable to retain the primary stain-mordant complex during decolorization while the counterstain binds itself to the bacteria [4]; however, the *E.coli* in the mixed bacterial smears counterstained with the acidic Annatto stain appeared to be decolorized showing no color compared to the sample counterstained with safranin which was stained red due to its inability to bind to the bacterial cell wall.

Table 1. *S.aureus* and *E.coli* samples stained using safranin and the methanolic *Bixa orellana* extract.

	S. aureus	*E.coli*	Mixed
Safranin	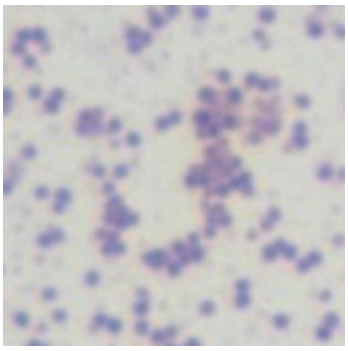	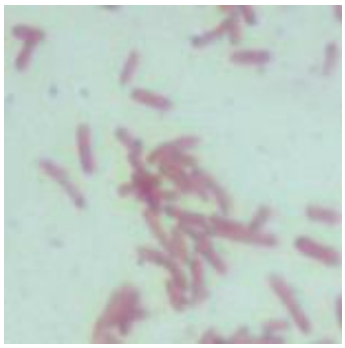	
Bixa orellana extract	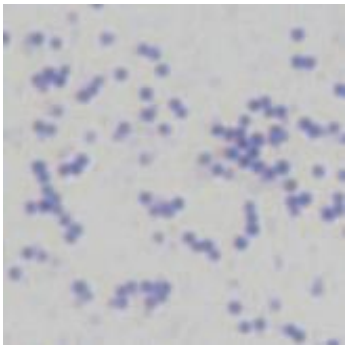	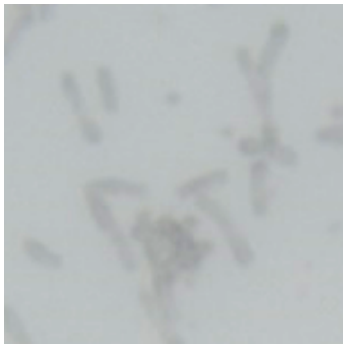	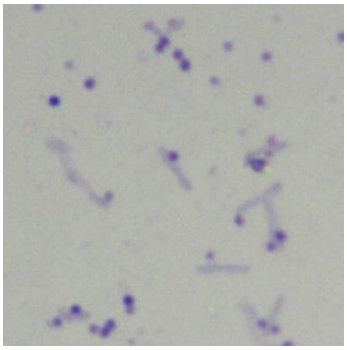

Limitations. The study is limited to the assessment of the staining capability of *Bixa orellana* extract with the bacteria *E. coli* and *S. aureus,* and its comparison to safranin utilizing pH, UV-Vis color spectra, and staining capability as parameters for the comparison. No other test organisms were used in this study. Only the methanolic extract was used to stain the test organisms. For staining, only one licensed medical technologist evaluated the slides. The actual size of the bacteria was not measured.

Conclusion. The methanolic extract of *Bixa orellana* (Annatto) was investigated for its use as an eco-friendly alternative to safranin in Gram staining. The Annatto extract failed to stain the *E. coli* samples, which remained colourless after staining. The acidic pH of the Annatto stain had no staining affinity with the acidic structure of the bacterial cell wall. Conversely, safranin, a basic stain, had better staining affinity towards the acidic structures of *E.coli*. The *Bixa orellana* extracts therefore cannot replace safranin as a counterstain for Gram staining. However, due to its capacity to absorb light as a dye, it has the potential to be used as a stain. This can be explored by future studies given that it is adjusted to have the optimal parameters of a bacterial stain.

Recommendations. The replication of this study with more focus on the pH of the stain is recommended, so that the relationship between the pH and the staining capability of the extract can be better observed. The pH of the Annatto stain was not adjusted as the study focuses on baseline parameters. This may have been a factor to the results of the staining. It is therefore possible that the adjustment of the pH, through addition of treatments, may yield positive results. For future research, we recommend the use of other plant extracts for Gram staining. More concentrations may be used in order to further test their capabilities as an alternative stain.

Acknowledgement. The authors would like to acknowledge the University of San Agustin MedTech Lab for providing the necessary materials for the study.

References

[1] Tripathi G, Mukesh K, Yadav M, Upadhyay P, Mishra S. 2015. Natural dyes with future aspects in dyeing of textiles: a research article. Int J PharmaTech Res. 8(1): 96-100.

[2] Haji A. 2010. Functional dyeing of wool with natural dye extracted from *Berberis vulgaris* wood and *Rumex hymenosepalus* root as biomordant. Iran J Chem Eng. 29(3): 55-59

[3] Meena Devi VN, Ariharan VN, Nagendra Pasad P. 2013. Annatto: eco-friendly and potential source for natural dye. Int Res J Pharm. 4(6): 106-108. 10.7897/2230-8407.04623

[4] Davies J, Anderson G, Beveridge T, Clark H. 1983. Chemical mechanism of the Gram stain and synthesis of a new electron-opaque marker for electron microscopy which replaces the iodine mordant of the stain. J bacteriol. 156. 837-45. 10.1128/JB.156.2.837-845.1983.

[5] Ryan KJ, Ray CG. 2004. Sherris Medical Microbiology (4th ed.). New York City(NY): McGraw Hill. p. 232f.

[6] Abrahart EN. 1977. Dyes and their intermediates. Oxford: Pergamon Press.

[7] Giridhar P, Akshatha V, Parimalan R. 2014. Review on Annatto Dye Extraction, Analysis and Processing – A Food Technology Perspective. J Sci Res. 3(2): 327-348.

[8] Silva FG, Gamarra, C Oliveira A, Cabral F. 2008. Extraction of bixin from annatto seeds using supercritical carbon dioxide. Braz J Chem Eng. 25(2):419-426.

[9] Lauro GJ. 1991. A primer on natural colours. Cereal FoodWorld. 36:949–953.

[10] Cardarelli CR, de Toledo Benassi M, Mercadante AZ. 2008. Characterization of different annatto extracts based on antioxidant and colour properties. J Food Safety. 41(9):1689-1693.

[11] Attokaran M. 2017. Natural food flavors and colorants. Hoboken (NJ): John Wiley & Sons

[12] Rahmalia W, Fabre JF, Mouloungui Z. 2015. Effects of cyclohexane/acetone ratio on bixin extraction yield by accelerated solvent extraction method. Procedia Chemistry. 14. 455-464. 10.1016/j.proche.2015.03.061.

[13] Scotter M. 2009. The chemistry and analysis of annatto food colouring: A review. Food Additives & Contaminants: Part A. 26. 1123-1145. 10.1080/02652030902942873.

[14] Braide W, Akobundu C, Nwaoguikpe RN, Njiribaeko LC. 2010. The use of extracts from four local Nigerian plants for the staining of selected bacteria and mold. Afr J Microbiol. Res. 5(1): 79-86.

[15] Husa NN, Hamza F, Said HM. 2018. Characterization and storage stability study of bixin extracted from *Bixa orellana* using organic solvent. 2018 IOP Conf. Ser.: Mater. Sci. Eng. 358 012035

[16] Silva MG, Garcia AL, Brito ES, Nogueira PR. 2018. The Annatto Carotenoids and the Norbixin Absorption Coefficient. Rev Inst Adolfo Lutz. 7(7):1-8.

[17] Prescott LM, Harley JP, Klein DA. 1999. Microbiology. New York City (NY): McGraw-Hill

[18] Horobin RW. 1975. Biological stains and their uses. J.S.D.C 91:4-14. 10.111/j.1478-4408.1975.tb02314.x.

[19] Ochei J, Kolhatkar A. 2000. Medical laboratory science: theory and practice. New York City (NY): Tata McGraw-Hill Education

[20] Halilu H, Chukwu O, Odu C, Chukwu D, Chidozie I. 2011. Application of extracts of Henna (Lawsonia inermis) leaves extracts as counter stain. Afr J Microbiol Res. 5(21). 10.5897/JMR10.418.

[21] The Dye Spectrum. New Scientist. Reed Business Information. 122 (1665): 52. May 1989. ISSN 0262-4079.

Larvicidal activity of *Citrofortunella microcarpa* (calamansi) peel essential oil against third and early fourth instar *Aedes aegypti*

MA. ANNA E. CARIGABA[1], MARY ANGELI J. LEONIDA[1], CARYL JANE C. MASCULINO[1], CATHERINE JOY A. MEDIODIA[1], and ALICIA G. GARBO[2]

[1]*Philippine Science High School - Western Visayas Campus, Brgy. Bito-on, Jaro, Iloilo City 5000, Department of Science and Technology, Philippines*
[2]*Department of Science and Technology – Industrial Technology Development Institute, DOST Compound, General Santos Avenue, Bicutan, Taguig City*

Abstract

This study evaluated the larvicidal activity of *Citrofortunella microcarpa* (calamansi) peel essential oil (EO) against third and early fourth instar *Aedes aegypti*. Larvicidal assay was performed against the test organisms to determine the efficacy of the essential oil at 8 ppm, 9 ppm, 10 ppm, and 11 ppm concentrations. Data on the larval mortality after 24 hours of exposure were analyzed using Probit Analysis. Results from the bioassay revealed that calamansi peel EO in 95% ethanol possessed great larvicidal potential with an estimated LC_{50} of 8.89 ppm and LC_{90} of 10.57 ppm. This implies that calamansi peel EO is effective at low concentrations against third and early fourth instar *Ae. aegypti* mosquito larvae and may be used as a potentially safer and alternative biolarvicide posing minimal harmful effects to non-target organisms.

Keywords: *bioassay, biolarvicide, Citrofortunella microcarpa, essential oil, limonene*

Introduction. Mosquitoes transmit many diseases, including but not limited to yellow fever, malaria, several forms of encephalitis, filariasis, and chikungunya. One of the most notable diseases transmitted by mosquitoes worldwide, particularly *Aedes* species, is dengue hemorrhagic fever. It is a viral disease that causes mild to severe fever, which can be potentially life-threatening [1]. In the Philippines, reported cases of dengue from January to August 2019 have reached 271, 480 cases nationwide, 213% higher compared to the same reporting period in 2018 according to a report from the Department of Health (DOH) [2]. Particularly in Region VI, there have been 45, 345 reported dengue cases from January to August 2019, which is 475% higher compared to the previous year.

Controlling mosquitoes, particularly *Aedes* sp. which are vectors of pathogenic diseases that harm humans, has been the predominant subject of several new studies. The life cycle of a mosquito involves four stages: egg, larva, pupa, and adult. The larval stage of a mosquito is subdivided into four substages: first instar, second instar, third instar, and fourth instar. Mosquito control involves targeting the adult mosquito through spraying chemical insecticides or by killing mosquito larvae before entering the adult stage, where they are the most vulnerable, through synthetic larvicides or botanical extracts as an alternative [1]. Insect repellents and/or pesticides containing active ingredients such as N,N-Diethyl-meta-toluamide (DEET) are frequently used. However, adverse effects of DEET have been reported [3,4], with some being severe enough to cause sensory disturbances. In addition, DEET, which is available worldwide in various formulations including aerosols, creams, lotions, and sprays at concentrations ranging from 5% to 100%, is not recommended for children, because exposure to high concentrations of DEET can cause encephalopathy as well as other side effects [5].

Pesticides and insect repellents are common in almost every household. These products do not only contain DEET but other harmful chemicals and substances as well. Continued use of these pesticides against disease-carrying mosquitoes has harmful and adverse effects on the health of the people and the environment as a whole [6]. Two of the basic chemical classes of insect repellents include the following: (1) synthetic chemicals including DEET and picaridin and (2) botanical oils such as citronella oil and eucalyptus oil [5]. Other various types of substances that are both natural and synthetic have also been discovered and used to protect humans from mosquito bites [7].

Essential oil (EO) is one of the natural-based products that are being recently developed because it contains an abundant amount of bioactive compounds that have the potential against the developmental stages of mosquitoes. For example, limonene is a nerve toxin found to be effective against insects by hyperstimulating their motor neurons. Citrus plants, one of the primary sources of EOs, possess insecticidal properties due to the presence of the compound D-limonene in abundant amounts [8,9].

How to cite this article:
CSE: Carigaba MAE, Leonida MAJ, Masculino CJC, Mediodia CJA, Garbo AG. 2020. Larvicidal activity of *Citrofortunella microcarpa* (calamansi) peel essential oil against third and early fourth instar *Aedes aegypti*. Publiscience. 3(1):37-41.
APA: Carigaba, M.A.E., Leonida, M.A.J., Masculino, C.J.C., Mediodia, C.J.A. & Garbo, A.G. (2020). Larvicidal activity of *Citrofortunella microcarpa* (calamansi) peel essential oil against third and early fourth instar *Aedes aegypti*. *Publiscience, 3*(1):37-41.

Among the plants related to citrus, calamansi is common, native, and widely cultivated here in the Philippines. Oftentimes, only the fruit itself is being utilized, then the rest, including the peels, are thrown away [10]. Therefore, to maximize the use of the plant, calamansi peels were chosen for this study.

This study promotes the use of a natural-based product, particularly an alternative biolarvicide, as a means of mosquito control by killing *Ae. aegypti* larvae before it can develop into an adult mosquito and become a vector of dengue. Moreover, this alternative biolarvicide poses little to no harmful effects to the environment as well as non-target organisms unlike synthetic counterparts.

This study aimed to evaluate the larvicidal activity of *Citrofortunella microcarpa* (calamansi) peel essential oil against third and early fourth instar *Aedes aegypti*. It specifically aimed to:

(i) determine the limonene content present in the calamansi peel essential oil by subjecting it to gas chromatography-mass spectrometry;

(ii) evaluate the larvicidal activity of the calamansi peel essential oil against third and early fourth instar *Ae. aegypti* by measuring the mortality rate; and

(iii) compare the results of larval mortality rate using Probit Analysis.

Methods. This was an experimental type of research which was composed of two phases. The first phase involved the purchasing of commercially available steam distilled calamansi peel essential oil (EO) and the verification of the purchased EO. The second phase involved the actual experiment and conduct of the test. This phase included the collection of the test organisms, its acclimatization process, the conduct of the preliminary testing, and the final confirmatory testing. The preliminaries were necessary to establish the range of concentrations that would give larval mortality from 10% to 90%. Each of the treatments: the calamansi peel EO in acetone, calamansi peel EO in 95% ethanol, positive control, and negative controls had four replicates. The positive control used for this study was Abate® 1SG while the negative controls included 95% ethanol, acetone, and dechlorinated water. The preparation of the set-ups was done in this phase. After the preparation, the concentration of the EOs were applied to the set-ups. Larvicidal activity of the calamansi peel EO was evaluated by the measurement of the mortality rate of the test organism introduced. The results obtained were tabulated. It was then analyzed using Probit Analysis. The duration of the data gathering was one week.

Acquiring of Essential Oils. One hundred (100) mL of Calamansi Essential Oils extracted from the fruit's peels via steam distillation was commercially purchased. A Material Safety Data Sheet (MSDS) was issued upon purchasing.

Gas Chromatography. Twenty (20) mL of the essential oil was subjected to Gas Chromatography - Mass Spectrometry Test for Limonene in order to determine the limonene content present in the product.

Collection of Mosquito Larvae. The total number of larvae was determined from the range of concentrations obtained from the preliminary testing. However, 20 larvae (a combination of third and early fourth instar) were used for each set-up both during the preliminary testing and confirmatory testing.

Acclimatization Process of Mosquito Larvae. The *Ae. aegypti* larvae used in the study were cultured in the DOST-ITDI Entomology Section Insectary and were reared according to their standard procedures following the guidelines provided by the World Health Organization (WHO). The larvae were reared at a laboratory condition of 25 ± 2°C and a relative humidity of 70% ± 10%.

Preparation of Mosquito Larvae Set-ups. Using a pasteur pipette, batches of 20 third and early fourth instar *Ae. aegypti* larvae were transferred to 100 mL glass beakers each containing 50 mL of dechlorinated water. Small, unhealthy, or damaged larvae were removed and replaced as they are not considered to be valid test organisms, following the guidelines of World Health Organization.

Preparation of Stock Solution. Two stock solutions of 10,000 ppm each (0.1 mL extract in 10 mL acetone and 0.1 mL in 10 mL 95% ethanol) were prepared. Ethanol and acetone were used as solvents because the essential oil is not miscible in water, if applied directly.

Preparation of the Positive and Negative Controls. Abate® 1SG was used as a positive control, whereas set-ups with dechlorinated water, acetone, and 95% ethanol were used as negative controls. These controls were then tested against third and early fourth instar *Ae. aegypti* mosquito larvae.

Bioassay. In the preliminary testing, the third and early fourth instar *Ae. aegypti* mosquito larvae were exposed to a wide range of test concentrations to establish a set of concentrations that would give larval mortality from 10% to 90%. The results were also compared to the negative controls to determine whether the dilution of the extract with the solvents had an effect on the mortality of the test organisms. For each concentration, at least four replicates were prepared.

For the final confirmatory test, the test organisms were exposed to concentrations ranging from 8 ppm to 11 ppm. After 24 hours, the mortality of the mosquito larvae for each set-up was recorded. The mortality rate was calculated using the following formula:

$$Mortality\ Rate = \frac{Number\ of\ dead\ larvae}{Number\ of\ larvae\ introduced} \times 100$$

The larvae were probed with a pasteur pipette and if there was no response from the larvae, it was considered dead. In calculating the percentage mortality, moribund larvae which is the larvae that is approaching death, was counted too and was added

to the total number of dead larvae. Moribund larvae were qualified as those incapable of rising to the surface. They did not show any reaction when the water was disturbed.

Data Analysis. Probit Analysis is a type of regression that was used to analyze the obtained results. The recorded values were plotted in a spreadsheet, wherein all the values of concentration used in the final confirmatory test were converted into the logarithm of the concentration and all the mean percentage larval mortality were transformed into probit values in order to obtain the linear equation that would estimate the LC_{50} and LC_{90} values.

Biosafety Procedures and Waste Disposal. All laboratory protocols were strictly observed throughout the conduct of the experiment, which included the wearing of laboratory gowns, safety gloves, face masks, and proper handling of laboratory equipment. Proper waste disposal was observed and done according to the institution's rules. The stock solution was disposed as chemical waste. Hot water was poured on the mosquito larvae prior to its disposal as biohazard waste.

Results and Discussion. This study aimed to evaluate the larvicidal activity of calamansi peel EO against third and early fourth instar *Ae. aegypti*. Larvicidal bioassay was performed with concentrations ranging from 8 to 11 ppm. Results were observed after 24 hours. After the data analysis, the lethal concentration values obtained were compared to determine which treatment achieved the lowest value, indicative of high efficacy of the treatment.

Gas Chromatography. Results from the Gas Chromatography-Mass Spectrometry test showed that the limonene content of calamansi peel EO is 83.1%w/w, indicating a substantial amount of limonene. The limonene present caused the larvicidal activity of calamansi peel EO. A study by Cheong et al. [9] reported that calamansi peels were composed of limonene. Limonene is known to cause the plants' larvicidal activity. Thus, it entails that it caused the death of the mosquito larvae [12,13,14]. This active compound is a nerve toxin that kills insects on contact by acting upon their sensory cells, leading to hyperstimulation of motor neurons [8]. One of the factors accounting for differences between this study's and related study's results may be the species of plant and the plant part used. Plant extracts have various insecticidal and medicinal values depending on the compound present [16]. In addition to that, Mahanta et al. [11] stated that major compounds of the essential oil along with its quality and quantity is one of the significant factors that can determine the insecticidal activity of a different plant essential oil.

Larvicidal Activity. Table 1 shows the mean percent larval mortality after 24 hours of exposure from varying concentrations of the calamansi peel EO in acetone and calamansi peel EO in 95% ethanol at 8 ppm, 9 ppm, 10 ppm, and 11 ppm, the LC_{50} and LC_{90}, and the positive control and negative control group for comparison. As the dose per treatment increases, mean % mortality also increases. As shown in Table 1, 11.0 ppm of the calamansi peel EO in acetone has the highest mean % mortality having a value of 92.14%. Then, it was followed by 10.0 ppm, 9.0 ppm and lastly 8.0 ppm. The same trend was observed in the calamansi peel EO in 95% ethanol, having a value of 94.28% mortality at 11.0 ppm. The larval mortality in the positive control, Abate® 1SG Mosquito Larvicide, was observed at a concentration ranging from 0.1 ppm to 0.5 ppm with the larval mortality rate from 8.0 ± 5.7% to 94.95 ± 3.54% within exposure period of 24 hours (Table 1). No larval death was observed in the negative controls using acetone alone, 95% ethanol alone, and dechlorinated water alone within an exposure period of 24 hours.

Table 1. Larvicidal activity of calamansi peel EO against third and early fourth instar *Ae. aegypti* after 24 hours (n=20).

Treatments	Dose (ppm)	Mean % Mortality ± SD
Calamansi Peel EO in Acetone	8.00	11.43 ± 4.76
	9.00	52.85 ± 7.56
	10.00	84.29 ± 9.76
	11.00	92.14 ± 6.36
Calamansi Peel EO in 95% Ethanol	8.00	22.14 ± 13.18
	9.00	50.88 ± 8.26
	10.00	82.14 ± 8.59
	11.00	94.28 ± 5.34
Positive Control (Abate® 1SG mosquito larvicide)	0.10	8.00 ± 5.70
	0.20	41.00 ± 8.90
	0.30	77.00 ± 7.58
	0.40	91.00 ± 7.41
	0.50	94.95 ± 3.54
Negative Control (Dechlorinated Water)	0.00	0.00
Negative Control (Acetone)	11.00	0.00
Negative Control (95% Ethanol)	11.00	0.00

Calamansi peel EO possessed significant toxicity based on the mortality of the third instar and early fourth instar *Ae. aegypti* mosquito larvae. It was reported in a previous study by Pansit et al. [1] that calamansi is a more potent larvicide compared to other plant extracts. In line with this, according to the results of this study, calamansi peel EO showed promising larvicidal activity against *Ae. aegypti* mosquito larvae.

Comparing the Larvicidal Activities. As shown in Table 2, the larvicidal activity of calamansi peel EO in acetone and calamansi peel EO in 95% ethanol of this study were compared to the larvicidal activity of different plant extracts of the other studies. Comparing each of the treatments' lethal concentrations, the lowest LC_{50} and LC_{90} values were obtained by the calamansi peel EO in 95% ethanol having 8.89 ppm for its LC_{50} and 10.57 ppm for its LC_{90}. Then, it was followed by the calamansi peel EO in acetone having an LC_{50} value of 9.08 ppm and LC_{90} value of 10.58 ppm. Other citrus species as reported by similar studies, *Citrus grandis*, *Citrus*

aurantium peel EO and *Citrus paradisi* and other plant extracts such as *Hyptis suaveolens* in acetone, *Hyptis suaveolens* in ethanol and *Leucas aspera* obtained lethal concentrations greater than 30.0 ppm [11,13,15,16].

Table 2. Lethal concentrations of the different treatments.

Treatments	LC_{50} (ppm)	LC_{90} (ppm)
Calamansi Peel EO in Acetone	9.08	0.58
Calamansi Peel EO in 95% Ethanol	8.89	0.57
Positive Control (Abate® 1SG mosquito larvicide)	0.21	0.40
Negative Control (Dechlorinated Water)	0.00	0.00
Negative Control (Acetone)	0.00	0.00
Negative Control (95% Ethanol)	0.00	0.00
Citrus grandis peel [11]	61.04	-
Citrus aurantium peel EO [13]	31.20	73.83
Citrus paradisi peel EO [13]	35.71	70.23
Leucas aspera [15]	44.02	73.24
Hyptis suaveolens in Acetone [16]	95.66	196.76
Hyptis suaveolens in Ethanol [16]	78.88	193.49

Calamansi peel EO in acetone and calamansi peel EO in 95% ethanol were able to obtain low concentrations compared to the other plant extracts because of the abundance of limonene. Plants with limonene are more efficient than plants without limonene when it comes to larvicidal activity [11,12,13]. This study has proven that the kind of major compounds present in the extract determine the differences in insecticidal activity of plant. The dominant compounds found in *C. grandis* are nootkatone and eudesmol [11] in contrast with the findings of this study where limonene is found to be dominant. In the study done by Sanei-Dehkordi et al. [13], it was found that *C. aurantium* contains 94.81% limonene and it obtained LC_{50} value of 31.20 ppm and LC_{90} value of 73.83 ppm. This is in line with this study because Sanei-Dehkordi et al. [13] also stated that high presence of limonene showed effective larvicidal activity. Other studies by Oumarou et al. [16] and Elumalai et al. [15] did not use citrus species, thus, limonene is not present in their plant sample. This means that a different extract was used which affected the larvicidal activity of the plant. Furthermore, the difference in results with previous studies may also be due to difference in the species of mosquito used. The mosquitoes used in other studies were not limited to third and early fourth instar *Ae. aegypti*, as in the study by Sanei-Dehkordi et al. [13] for example *Anopheles stephensi* was used. This may account for the lethal concentration being higher in the said study than that found in this one. In the study of Oumarou et al. [16], they used *Anopheles gambiae*, the resulting lethal concentration being 78.88 ppm in contrast with this study's lowest lethal concentration which is 8.89 ppm. It is important to note the factors that can affect the findings of the study which include the test organism and the plant used since the differences may have an impact in the results obtained.

Limitations. This study was conducted primarily for the purpose of evaluating the larvicidal activity of *Citrofortunella microcarpa* (calamansi) peel EO against third and early fourth instar *Aedes aegypti*. The conduct of the study was limited only to the third and early fourth instar larval stages of the *Ae. aegypti* mosquito considering that these are stages where the mosquito larvae are most vulnerable. This study was also limited to the essential oil from peels of *C. microcarpa* fruit. The calamansi peel EO used in the study was commercially purchased. The EO was specifically tested to determine the amount of limonene present in the product, hence, other components of the EO were not discussed.

Conclusion. The present study which evaluated the larvicidal activity of *C. microcarpa* (calamansi) peel essential oil is found to be effective at low concentrations against third and early fourth instar *Ae. aegypti* mosquito larvae. Therefore, it can be used as an alternative to the commercially available larvicide.

Recommendations. It is recommended to increase the number of replicates for each concentration in order to eliminate outliers. A smaller range of intervals between concentrations may also be tested for larvicidal activity observation for more accurate results. It is also recommended to test the calamansi peel EO against other types of mosquitoes. The EO that was used in this study was commercially purchased, therefore it is also suggested to perform the manual extraction of the EO via steam distillation. Only the limonene content of the EO was determined, thus it is also recommended to subject it to other tests to determine other compounds also present in the product.

Acknowledgement. The researchers would like to thank Mrs. Alicia Garbo, the Entomology Section Head of DOST-ITDI Standards and Testing Division, for the supervision she provided during their one-week data gathering. The researchers further thank their families, especially their parents, for the encouragement and support from start to finish of this study.

References

[1] Pansit NR, Avila STR, Calumba JR. 2018. Larvicidal activity of *Citrofortunella microcarpa* (Lemonsito) and *Carica papaya* (papaya) extracts against the dengue-vector mosquito, *Aedes* sp.. Int J Mosq Res. 5(4):51-58.

[2] Department of Health (DOH), 2019. Monthly Dengue Report [Internet]. [Cited 13 August 2019.] Available from http://bit.ly/300bPL2.

[3] Corbel V, Stankiewicz M, Pennetier C, Fournier D, Stojan J, Girard E, Dimitrov M, Molgo J, Hougard JM, Lapied B. 2009. Evidence for inhibition of cholinesterases in insect and mammalian nervous systems by the insect repellent deet. BMC Biology, 7(47). https://doi:10.1186/1741-7007-7-47.

[4] Swale DR, Sun B, Tong F, Bloomquist JR. 2014. Neurotoxicity and mode of action of N,N-diethyl-metatoluamide (DEET). PLoS ONE. 9(8): e103713. Doi: 10.1371/journal.pone.0103713.

[5] Yoon JK, Kim K, Cho Y, Gwon Y, Cho HS, Heo Y, Park K, Lee Y, Kim M, Oh Y, et al. 2015. Comparison of repellency effect of mosquito repellents for DEET, citronella, and fennel oil. J Parasitol Res. 2015(1):1-7.

[6] Sritabutra D, Soonwera M. 2013. Repellent activity of herbal essential oils against *Aedes aegypti* (Linn.) and *Culex quinquefasciatus* (Say). Asian Pac J Trop Dis. 3(4):271-276.

[7] Effiom OE, Avoaja DA, Ohaeri CC. 2012. Mosquito repellent activity of phytochemical extracts from peels of Citrus fruit species. Global J Sci Frontier Res. 12(1):1-5.

[8] Karr LL, Coats JR. 1988. Insecticidal properties of d-limonene. J Pesticide Sci. 13(2):287-290.

[9] Cheong MW, Chong ZS, Liu SQ, Zhou W, Curran P, Yu B. 2012. Characterisation of calamansi (*Citrus microcarpa*). Part I: volatiles, aromatic profiles and phenolic acids in the peel. Food Chem. 134(2012):686-695.

[10] Morte MYT, Acero LH. 2017. Potential of Calamansi (*Citrofortunella microcarpa*) fruit peels extract in lowering the blood glucose level of streptozotocin induced albino rats (*Rattus albus*). Int J Food Eng. 3(1):29-34.

[11] Mahanta S, Khanikor B, Sarma R. 2017. Potentiality of essential oil from *Citrus grandis* (Sapindales: Rutaceae) against *Culex quinquefasciatus* Say (Diptera: Culicidae). J Entomol Zoology Stud. 5(3):803-809.

[12] Kweka E, Lima TC, Marciale C, Pergentino de Sousa D. 2016. Larvicidal efficacy of monoterpes against the larvae of *Anopheles gambiae*. Asian Pac J Trop Biomed. 6(4):290-294.

[13] Sanei-Dehkordi A, Sedaghat MM, Vatandoost H, Abai MR. 2016. Chemical compositions of the peel essential oil of *Citrus aurantium* and its natural larvicidal activity against the malaria vector *Anopheles stephensi* (Diptera: Culicidae) in comparison with *Citrus paradisi*. J Arthropod-Borne Dis. 10(4):577-585.

[14] Hazarika H, Tyagi V, Krishnatreyya H, Kishor S, Karmakar S, Bhattacharyya DB, Zaman K, Chattopadhyay P. 2018. Toxicity of essential oils on *Aedes aegypti*: A vector of chikungunya and dengue fever. Int J Mosq Res. 5(3):51-57.

[15] Elumalai D, Hemalatha P, & Kaleena PK. 2017. Larvicidal activity and GC–MS analysis of *Leucas aspera* against *Aedes aegypti*, *Anopheles stephensi* and *Culex quinquefasciatus*. J Saudi Society of Agri Sci. 16(4):306-313.

[16] Oumarou MK, Younoussa L, Nukenine EN. 2018. Toxic effect of *Chenopodium ambrosoide*s, *Hyptis suaveolens* and *Lippia adoensis* leaf methanol extracts and essential oils against fourth instar larvae of *Anopheles gambiae* (Diptera: Culicidae). Int J Mosq Res. 5(1):61-66.

Publiscience Vol. 3 Issue 1

The use of *Clitoria ternatea* (blue ternate) ethanolic extract as a potential stain for bacteria

CHERIL B. TRIOL, ATHENA THERESE V. DIONELA, ANGELA ISABELLE D. ECUBE, and CATHERINE JOY A. MEDIODIA

Philippine Science High School - Western Visayas Campus, Brgy. Bito-on, Jaro, Iloilo City 5000, Department of Science and Technology, Philippines

Abstract

Most synthetic microbial stains are pollutants that pose carcinogenic, mutagenic and teratogenic health risks. Thus, this study aimed to investigate the ability of *Clitoria ternatea* ethanolic extract as a potential stain for bacteria. The extract was utilized in the simple staining and Gram staining of *Staphylococcus aureus*, *Escherichia coli*, and mixture of the two. The properties of the stain such as presence of anthocyanin, pH level, color, and solubility of the extract were determined. The staining ability of the extract, in terms of visibility of cell walls and color intensity, was determined through frequency count that showed that majority of the replicates had defined cell walls with incomplete uptake of stain in simple staining and Gram staining. *Clitoria ternatea* ethanolic extract has the potential to impart stain on *Staphylococcus aureus* and *Escherichia coli* bacteria through simple staining and Gram staining; however, due to the incomplete uptake of stain by the bacteria, it cannot be considered as an alternative to commonly-used bacterial stains. Hence, the researchers recommend the development of a new staining technique for the potential stain.

Keywords: *Clitoria ternatea, dyes, stain, anthocyanin, ethanolic extract*

Introduction. Dyes, natural or synthetic, are substances that are soluble in a medium and are usually used to give a desired color to non-food materials [1,2,3,4], such as animal and plant tissues, and microbes to make them visible and distinct [5,6]. Microorganisms viewed under the microscope need to be fixed and stained to improve visibility, emphasize morphological features, and sometimes preserve them [1]. In microbiology, this process is known as staining [3].

In staining bacteria, bacterial smears are initially made to fix bacteria on the slide [1]. Most stains for bacteria are cationic as they bind to negatively-charged structures such as the bacterial cell wall. Because of the opposite charges of both the stain and bacterial cell wall, the stain adheres to the surface of the bacterial cells [7]. Currently, most microbial stains in use are chemically synthesized due to its convenience [4,8]. However, they pose a threat to the environment and human health [9] as some synthetic dyes contain allergenic components [3,4] and toxic heavy metals, contributing to land, water and air pollution [3]. For example, crystal violet, a dye that has been extensively used as a biological stain, is regarded as a toxic biohazard substance that causes serious environmental and health problems [2].

Because of this, researchers are searching for alternative dyes for staining microbial cells, which are not hazardous to living things [3,9]. Research show that extracts for the production of dyes can be obtained from natural sources such as plants [3,6,10], animals, and the soil [4]. According to recent studies, natural dyes from plants are used as histological stains for tissue components [3,9]. These natural dyes are known to be convenient, cheaper, safe, non-toxic, eco-friendly, renewable and biodegradable [3,6].

Plant extracts contain natural phenolic compounds that are structurally related to a family of water-soluble pigments known as anthocyanins [11]. Anthocyanin compounds are flavonoids found in the flower petals, fruits and leaves of several plants, and are known to be the plant's main colorant molecule [12]. It contains flavylium cation that is its chromophore [13]. The color stability of these compounds depends on several factors such as chemical structure and pH [13,14]. Cationic or basic stains are called so because their coloring agent is located in the basic part of the compound while the acidic radical is inactive [15]. They also carry a positive charge and stains negatively-charged elements [16]; thus, many of them are considered as Lewis acids or electron acceptors [17]. On the other hand, anionic or acidic stains have their coloring agent located in the acidic part of the compound [15], and they carry a negative charge that stains positively-charged elements [16]. Thus, many of them are considered as Lewis bases or electron donors [17]. With anthocyanins having a positive charge [11], they are considered to be the key compound causing the staining ability of several plant extracts [18], especially in staining negatively-charged structures such as those of bacterial cell walls. Thus, plants with the presence of anthocyanin can potentially be a source of natural histological stains.

Clitoria ternatea, commonly known as blue ternate, is a strangling and climbing herb commonly used as a medicinal plant due to its wide range of pharmacological activities and phytochemicals, including anthocyanin [11,18]. Anthocyanin

How to cite this article:
CSE: Triol CB, Dionela ATV, Ecube AID, Mediodia, CJA. 2020. The use of *Clitoria ternatea* ethanolic extract as a potential stain for bacteria. Publiscience. 3(1):42-47.
APA: Triol, C.B., Dionela, A.T.V., Ecube, A.I.D., & Mediodia, C.J.A. (2020). The use of *Clitoria ternatea* ethanolic extract as a potential stain for bacteria. *Publiscience, 3*(1):42-47.

compounds of blue ternate plants are commonly found in their flowers as they are responsible for the flowers' red violet-blue color [14]. The ability of *Clitoria ternatea* as a stain is not much given focus and studies on it are limited. A study conducted by Suebkhampet and Sotthibandhu [11] utilized the aqueous crude extract of *Clitoria ternatea* as a stain for blood smears; however, its capacity to stain microorganisms such as bacteria is yet to be explored.

This study aimed to investigate the ability of the ethanolic extract of *Clitoria ternatea* flowers as a potential stain for bacteria. Specifically, it aimed to:

(i) test the ethanolic extract of *Clitoria ternatea* for the presence of anthocyanin;

(ii) determine the properties of ethanolic extract of *Clitoria ternatea* such as (a) pH level, (b) color, and (c) solubility, and compare them to the properties of crystal violet, a conventional bacterial stain;

(iii) use the ethanolic extract of *Clitoria ternatea* to stain Gram-positive *Staphylococcus aureus*, Gram-negative *Escherichia coli*, and mixture of the two bacteria using the simple staining and Gram staining method; and

(iv) evaluate the ability of ethanolic extract of *Clitoria ternatea* to stain Gram-positive *Staphylococcus aureus*, Gram-negative *Escherichia coli*, and mixture of the two bacteria in terms of (a) visibility of cell walls, and (b) color intensity.

Methods. This is an exploratory study. *Clitoria ternatea* flowers were oven-dried, macerated in ethanol and filtered. The crude extract was obtained and reconstituted with ethanol. The properties of the extract were determined and compared to crystal violet. The ethanolic extract and crystal violet was used to stain S*taphylococcus aureus, Escherichia coli*, and mixture of the two bacteria through simple and Gram staining. Positive control using crystal violet and negative control without any stain were also prepared. The staining ability of both the ethanolic extract and crystal violet were evaluated by a licensed professional using a modified rubric.

Ethanolic Extraction. The collected *C. ternatea* flowers were separated petal by petal, washed with distilled water and oven-dried at 75°C for 24 hours [12]. The powdered petals were macerated in 95% ethanol with 1:10 mass to volume ratio. The mixture was filtered using No. 41 Whatman filter paper and subsequently filtered using No. 1 Whatman filter paper [11]. The filtered extract was then subjected to rotary evaporation to obtain the crude extract, which was dissolved again in 95% ethanol in a 1:1 mass-of-extract-to-volume-of-solvent dilution ratio.

Test for the Presence of Anthocyanin. The ethanolic extract of *C. ternatea* was tested for the presence of anthocyanin. A change from the original color of the extract to orange-red to blue-red color upon addition of 1% (v/v) hydrochloric acid (HCl) was used as an indicator for the presence of anthocyanin in the extract [19].

Assessment of Physical and Chemical Properties. The following properties were assessed: pH, color, and solubility. The pH values of the ethanolic extract of *C. ternatea* and crystal violet were measured using a pH meter. The color of both stains were determined based on the Pantone Colour Matching System. For the solubility of ethanolic extract in water, one mL of distilled water was added to one mL of ethanolic extract, and the solution was checked if both liquids are miscible where there is no distinction between the two liquids in the mixture.

Preparation of Bacterial Smears and Staining. *Staphylococcus aureus, Escherichia coli*, and mixture of the two bacterial smears were prepared in a biosafety cabinet. The ethanolic extract was used as primary stain for the experimental set-up in the simple staining of *S. aureus* and *E. coli,* and in the Gram staining of *S. aureus, E. coli* and mixture of the two bacteria [20]. Crystal violet, on the other hand, was used for the positive control. Other parts of the simple staining and Gram staining method were not modified. Negative control without any stain was also prepared.

Data Analysis. The evaluation of the visibility of cell walls of bacteria and their color intensity utilized nominal scale data, with values from zero to three, and are based on a rubric modified from Sridhara et al. [21]. Frequency count was used to describe the stain performance of the extract and of crystal violet in terms of visibility of bacterial cell walls and the color intensity. The bacterial smears were evaluated, and the results were verified by a licensed medical technologist.

Safety Procedure. During the conduct of the research, the use of appropriate personal protective equipment (PPE) was observed, and hand hygiene was performed regularly. Chemicals and bacteria were handled properly according to their MSDS. For the disposal of bacterial smears, all slides were collected, autoclaved and turned over to the science research assistant (SRA) in charge of the laboratory.

Results and Discussion. The ethanolic extract obtained a positive result in the test for the presence of anthocyanin. Both the ethanolic extract and crystal violet have low pH, have different shades of violet in color, and are soluble in water. For the staining ability of ethanolic extract through simple staining, majority of the Gram-positive *S. aureus* and Gram-negative *E. coli* replicates had defined cell walls but with incomplete uptake of stain. For the Gram staining, *S. aureus* and mixture of the two bacterial smears had replicates with defined cell walls but incomplete uptake of stain. *E. coli* replicates had defined cell walls, and the bacteria were properly differentiated.

Presence of Anthocyanin. The color of the ethanolic extract changed from deep violet to deep red, which indicates the presence of anthocyanin in the extract. The use of ethanol as the solvent during extraction optimizes anthocyanin extraction [18], and is reported to perform better compared to using water as the solvent [6,9,21]. Flavylium cation is the basic chromophore of anthocyanin [13]. It is electron deficient and highly reactive [22]. The positive charge in its structure gives it the capacity to bind to

the negatively-charged bacterial cell walls [11,18], thus imparting color to the bacteria. However, several factors may influence the stability of this compound including light, temperature, and the compound's chemical structure and pH [14]. In this study, all factors except pH were controlled.

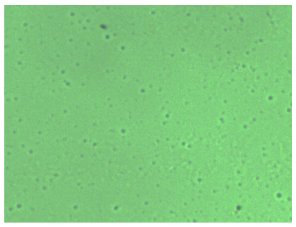

Plate 1. *S. aureus* stained with the ethanolic extract using simple staining.

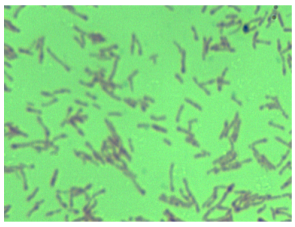

Plate 2. *E. coli* stained with the ethanolic extract using simple staining.

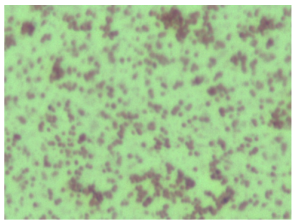

Plate 3. *S. aureus* stained with the ethanolic extract using Gram staining.

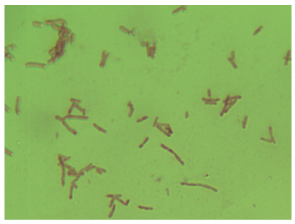

Plate 4. *E. coli* stained with the ethanolic extract using Gram staining.

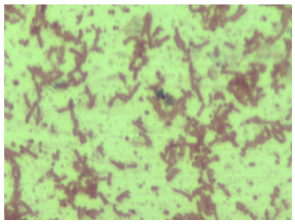

Plate 5. Mixture of *S. aureus* and *E. coli* stained with the ethanolic extract using Gram staining.

pH. Crystal violet staining solution was reported to have a low pH with a value of 5.43 whereas the ethanolic extract of *C. ternatea* was also reported to have a low pH with a value of 4.75.

In staining, the pH of the stain affects the nature and degree of the charge on specific tissue structures [1,4], influencing the ability of the stain to adhere to it [21]. It is known that tissue elements are attracted to the oppositely-charged ions of the stain [4]. The magnitude of the electrostatic charges to be imparted by the dye to the cell component is affected by the pH of the stain [16]. Bacteria are generally stained better with cationic stains due to their anionic cell walls.

Crystal violet is a cationic dye [2,16]. Its major structural form is a monovalent cation that serves as its principal form in solid state and in aqueous solution across a wide range of pH values. As the pH changes, the positive charge in the central carbon atom is delocalized by resonance of the three nitrogen atoms present in the molecule, making it more stable [2]. Crystal violet dissolved in water has a pH range of 2.5 to 3.5 at 10 g/L at 20°C [23]. The reported pH value of crystal violet, which is 5.43, coincides with the expected acidic pH.

The pH value of the ethanolic extract, which is 4.75, is low and acidic. Ethanol, the solvent of extraction, is known to have a slightly basic pH value; however, in the study of Sridhara et al. [21] and Itodo et al. [24], ethanolic extracts are reported to have acidic pH values. This coincides with the acidic pH of the ethanolic extract of *C. ternatea*. A factor that affects the pH of anthocyanin is the structure of the compound, which also influences its color. The flavylium cation in the compound has conjugated double bond that causes the delocalization of the positive charge leading to multiple resonance structures. Anthocyanin at pH 1.0 is red. When pH is between 1.0 and 4.0, discoloration from red to violet occurs, and colorless carbinol base would be formed. This will then undergo water catalyzed-tautomerization to produce chalcone. At pH 4.0 to 6.0, the structure changes into anhydrobase that gives an extension of conjugation to its structure, causing a color change from violet to blue with stronger intensity [14].

Having acidic pH values, both crystal violet and the ethanolic extract of *C. ternatea* are considered as Lewis acids, which make them cationic stains with good staining affinity towards the anionic bacterial cell walls [16,17]. The staining affinity of the acidic ethanolic extract is supported by the study of Sridhara et al. [21] wherein the ethanolic extracts of *Hibiscus* at an acidic pH of 5.7 gave optimal staining in the negatively-charged cytoplasm of tissues. It is also substantiated by the study of Itodo et al. [24] that concludes that the cytoplasmic staining ability of the onion skin extract solution was due to its highly acidic pH.

Color. Crystal violet is known to be blue-violet in color [2]. It is an example of a quinonoid dye with a quinonoid ring as its chromophore and an auxochrome that is responsible for its color and staining properties [15]. It was observed that the corresponding color of crystal violet based on Pantone Colour Matching System is Pantone 2685. The ethanolic extract of *C. ternatea*, on the other hand, was observed to have a deep violet (Pantone 276) color that is from the anthocyanin compound. Both crystal violet and ethanolic extract are violet in color, which is useful for the evaluation of the color intensity of the ethanolic extract as it is relative to the positive control, crystal violet.

The color of crystal violet depends on its acidity. It is yellow at a strongly acidic pH of 0 and is green at a pH of 1.0. When dissolved in water, its color is blue-violet or vibrant purple. The vibrant purple color of crystal violet is caused by the delocalization of the positive charge present in the central carbon atom of crystal violet across the double bonds in the benzene rings that stabilizes the carbonation [2].

The color of the ethanolic extract also depends on the acidity of anthocyanin present in it [12,14]. Anthocyanin in acidic conditions is red in color [11,14], which explains the change of color of the ethanolic extract from deep violet to deep red upon the addition of the strong acid, HCl. As the pH increases, the structure of the compound changes, and discoloration occurs [14]. The pH value of the ethanolic extract that is 4.75 lies near pH 4.0, and the extract has a violet color. This agrees with the study

of Saptarini et al. [14] that states that at pH 4.0, the color of the anthocyanin compound changes from red to violet. Similar with crystal violet, the color change of the dye is caused by the delocalization of the positive charge present in the molecule across the conjugated double bond that gave some resonance to its structure, thus stabilizing the flavylium cation [14].

The color of both crystal violet and ethanolic extract is influenced by the pH of their dye molecule, and their colors are different at a distinct pH [2,14]. This may be attributed to the difference in their nature and structure. Both stains contain different molecules; thus, they have different spacing of energy levels. This affects the absorption of the visible light radiation in the electromagnetic spectrum that causes dyes to appear colored. This spacing is influenced by the degree of delocalization of the bonding electrons of the molecule [25]. This may cause the different shades of violet in both stains.

Solubility. *C. ternatea* ethanolic extract was soluble in water. It was comparable to crystal violet, which is known to be water-soluble. Due to the positive charge in the flavylium cation of anthocyanin [13], its structure is considered as polar. Thus, the ethanolic extract is soluble in polar solvents such as water [14].

Visibility of Cell Walls. The staining ability in terms of cell wall visibility is based on the uptake of the stain by the bacteria. A complete uptake of the stain means the bacterium shows its regular and expected shape where Gram-positive *S. aureus* must be round and purple whereas Gram-negative *E. coli* must be rod and pinkish-red. For the positive control for simple staining, all replicates of *S. aureus* and *E.coli* had bacterial cells with defined cell walls and complete uptake of stain, as in Figure 1. *S. aureus* bacteria stained with ethanolic extract through simple staining showed that 11 out of 15 replicates had defined cell walls with incomplete uptake of stain whereas only four out of 15 replicates had defined cell walls with complete uptake of stain. The *E. coli* bacteria stained using ethanolic extract through simple staining had 12 out of 15 replicates with defined cell walls but incomplete uptake of stain whereas three out of 15 replicates had defined cell walls with complete uptake of stain.

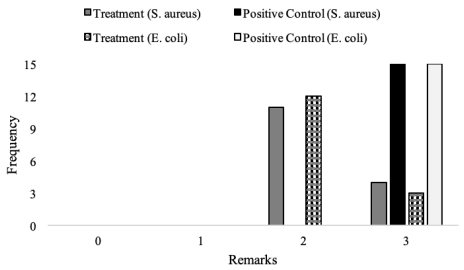

0 - Cell walls defined and has no color
1 - Cell walls defined but has no color
2 - Cell walls defined with incomplete uptake of stain
3 - Cell walls defined with complete uptake of stain

Figure 1. Staining ability of *Clitoria ternatea* ethanolic extract on *S. aureus* and *E. coli* through simple staining.

For the Gram staining, crystal violet was able to stain all of the replicates for the *S. aureus* and mixture of the two bacterial smears with defined cell walls and complete uptake of stain whereas no trace of crystal violet is visible on all replicates of *E. coli* bacterial smears, as in Figure 2. *S. aureus* stained with ethanolic extract had 14 out of 15 replicates with defined cell walls and incomplete uptake of stain whereas only one replicate had defined cell walls but only exhibits pinkish-red color that can be attributed to the counterstain, safranin. For the Gram staining of *E. coli*, all of the replicates had defined cell walls with proper differentiation between Gram-positive bacteria and Gram-negative bacteria because it exhibited the expected pinkish-red color. All 15 replicates of mixture of the two bacterial smears stained with ethanolic extract through Gram staining had defined cell walls with incomplete uptake of stain.

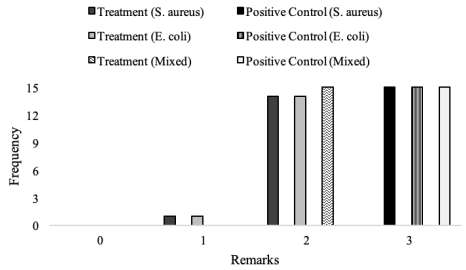

0 - Cell walls not defined
1 - Cell walls defined and the cells are pinkish-red (*E. coli*) and purple (*S. aureus*)
2 - Cell walls defined with incomplete uptake of stain (both *S. aureus* and *E. coli*)
3 - Cell walls defined and properly differentiated where *S. aureus* cells are purple and *E. coli* cells are pinkish-red

Figure 2. Staining ability of *Clitoria ternatea* ethanolic extract on *S. aureus, E. coli,* and mixture of the two bacteria through Gram staining.

The results showed that the ethanolic extract of *C. ternatea* is a potential bacterial stain because it was able to impart color to the bacteria, although the uptake is incomplete. Its staining ability may be attributed to comparable results between the ethanolic extract and crystal violet in terms of staining factors such as pH, color, and solubility. Its ability to impart color can be attributed to the presence of anthocyanin and an acidic pH, suggesting that it has a cation that binds with the anionic bacterial cell wall. However, the results suggest that, currently, the ethanolic extract cannot be used as an alternative to crystal violet as there was an incomplete uptake of the stain. One factor that may have affected the uptake of stain was the staining procedure used that was a standardized procedure in staining bacteria using synthetic dyes such as crystal violet. The ethanolic extract may require its own developed staining procedure [11] due to its chemical structure and compatibility with counterstains, which may be different from synthetic dyes [21].

Color Intensity. The color intensity checks the contrast between the specimen and the background since stains are used to enhance contrast in the microscopic image [3]. The intensity of the color contrast is correlated with the purity of the stain, thus affecting its staining efficacy [25]. A darker stain can provide better contrast between the stained specimen and the lightly-colored background.

The color intensity of the ethanolic extract was evaluated in comparison to the color intensity of crystal violet in staining Gram positive *S. aureus* and

Gram negative *E. coli*. For the simple staining of *S. aureus*, the ethanolic extract had lighter color compared to crystal violet in 11 out of 15 replicates. Equal color intensity between the ethanolic extract and crystal violet was observed in 4 replicates out of 15. For the simple staining of *E. coli* bacteria, 13 out of 15 replicates stained with ethanolic extract through Gram staining had a lighter color on bacteria compared to crystal violet whereas three out of 15 replicates stained with ethanolic extract had equal color intensity to crystal violet, as in Figure 3.

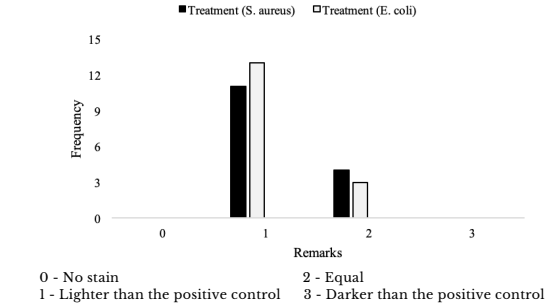

Figure 3. Color intensity of *Clitoria ternatea* ethanolic extract on *S. aureus* and *E. coli* through simple staining.

For the Gram staining, the color intensity was evaluated relative to the positive control. For *S. aureus* and mixture of the two bacterial smears, the color intensity of the ethanolic extract was evaluated based on the visibility and intensity of smears stained with crystal violet while the *E. coli* bacterial smears were evaluated based on the absence of purple stain or the intensity of the counterstain. All replicates of *S. aureus* and mixture of the two bacterial smears were observed to exhibit lighter color compared to crystal violet while *E.coli* bacterial smears had an equal color intensity compared to the positive control of stained *E.coli* bacterial smears, as in Figure 4.

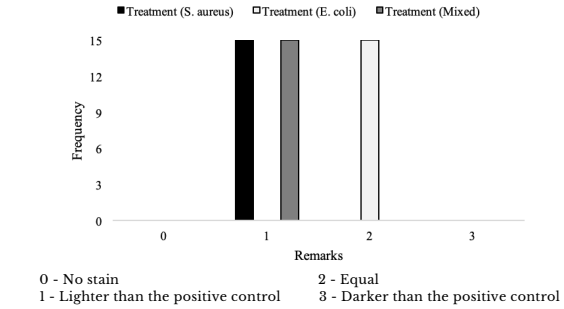

Figure 4. Color intensity of *Clitoria ternatea* ethanolic extract on *S. aureus, E. coli*, and mixture of the two bacteria through Gram staining.

Staining is performed to impart color to bacterial cells in order to highlight its morphological features [4] and to create contrast in the image viewed with the aid of a microscope [3]. Despite the ethanolic extract having a deeper shade of violet than crystal violet, it generally had a lighter color. This indicates that crystal violet, being a conventional biological stain [2], created a better contrast between the background and the bacterial cells compared to that of the ethanolic extract. The color intensity is affected by dye impurities [25], which may be present in the ethanolic extract. These impurities influence staining by altering the intensity of coloration imparted by the stain or by changing staining patterns, and the nature and staining mechanism [25]. The standardised staining procedure used that was designed for synthetic dyes may also attribute the lighter color imparted by the ethanolic extract on bacteria.

Limitations. Only three properties of the ethanolic extract were evaluated namely pH, color, and solubility. The test for the presence of anthocyanin was the only phytochemical screening done. The Pantone Colour Matching System, a standardized color reproduction system used in industries, was used due to unavailability of color charts for microbial stains. Due to the lack of standardized rubrics for evaluation, the researchers modified a rubric from Sridhara et al. [21] and had it verified by only one licensed medical technologist. The staining ability of the extract was also evaluated using one Gram-positive and one Gram-negative bacteria only.

Conclusion. Based on the findings of the study, the *Clitoria ternatea* ethanolic extract has the potential to stain Gram-positive *Staphylococcus aureus* and Gram-negative *Escherichia coli* bacteria through simple staining. Also, it has the potential to stain and differentiate *S. aureus*, *E. coli* and mixture of the two bacteria using the Gram staining method. However, despite comparable results in the pH, color and solubility of the ethanolic extract and crystal violet, it cannot currently be used as an alternative bacterial stain because it was not able to stain the bacteria as effectively as the positive control in terms of the visibility of bacterial cell walls and color intensity.

Recommendations. The researchers recommend: (1) the development of a new staining technique for the potential stain; (2) the determination of other phytochemicals and functional groups present in the ethanolic extract; (3) the preparation of more oven-dried flowers to be soaked in order to accommodate more number of replicates per set-up; and (4) having varying concentrations for the potential stain.

Acknowledgement. The authors would like to thank the Department of Agriculture, the Department of Science and Technology - Region VI, and Ms. Myrna Sarmiento, Ms. Abigail Perez and Ms. Gem Pamulag of the University of San Agustin for giving permission to work in their laboratory, and transact in the said institutions. Special thanks are also expressed to Mrs. Cherry Rose D. Haro for being the external evaluator to validate the results of this research. Huge appreciation is also expressed to the various households in Igbaras and Oton, Iloilo for providing the authors with *Clitoria ternatea* flowers.

References

[1] Braide W, Akobundu C, Nwaoguikpe R, Njiribaeko L. 2011. The use of extract from four local Nigerian plants for the staining of selected bacteria and moulds. Afr J Microbiol Res. 5(1): 79-86.

[2] Mani S, Bharagava RN. 2016. Exposure to crystal Violet, its toxic, genotoxic and carcinogenic effects on environment and its degradation

and detoxification for environmental safety. Rev Environ Contam Toxicol. 237: 72-97.

[3] Adeyemo S, Akinloye A, Adekanmi G. 2017. The use of plant dyes for microbial staining and identification: an eco-friendly and non-toxic alternative method. J Adv Biol Biotechnol. 16(4):1-10.

[4] Olise N, Enweani I, Oshim I, Urama E, Ngwoke C. 2018. The use of extract from Nigerian indigenous plants as staining techniques in bacteriology, mycology and histopathology. Int J Plant Res. 8(1):15-24.

[5] Chukwu O, Odu C, Chukwu D, Hafiz N, Chidozie V, Onyimba I. 2011. Application of extract of henna (*Lawsonia inamis*) leaves as a counter stain. Afr J Microbiol Res. 5(21): 3351-3356.

[6] Cheng C, Saad S, Abdullah R. 2014. Alternative staining using extract of hibiscus (*Hibiscus rosa-sinensis* L.) and red beet *(Beta vulgaris* L.) in diagnosing ova of intestinal nematodes (*Trichuris trichiura* and *Ascaris lumbricoides*). Eur J Biotechnol Biosci. 1(5):14-18.

[7] [NIOS] National Institute of Open Schooling. 2012. Common staining technique. [Internet]. Module. Microbiology. Available from:https://nios.ac.in/media/documents/dmlt/Microbiology/Lesson-02.pdf

[8] Ihuma J, Asenge G, Abioye J, Dick S. 2012. Application of methanolic extract from *Hibiscus sabdariffa* Linn. as a biological staining agent for some fungal species. Int J Plant Anim Environ Sci. 2(2):254-259.

[9] Akinloye A, Illoh H, Olagoke A. 2010. Screening of some indigenous herbal dyes for use in plant histological staining. J For Res. 21(1):81-84.

[10] Grover N, Patni V. 2011. Extraction and application of natural dye preparations from the floral parts of *Woodfordia fruticosa* (Linn.) Kurz. Indian J Nat Prod Resour. 2(4):403-408.

[11] Suebkhampet A, Sotthibandhu P. 2013. Effect of using aqueous extract from butterfly pea flowers (*Clitoria ternatea l.)* as a dye on animal blood smear staining. Suranaree J Sci Technol. 19(1):15-19.

[12] Wang H, Li P, Zhou W. 2014. Dyeing of silk with anthocyanins dyes extract from *Liriope platyphylla* fruits. J Text. 2014: 1-9.

[13] Held B, Tang H, Natarajan P, da Silva CP, de Oliveira Silva V, Bohne C, Quina FH. 2016. Cucurbituril inclusion complexation as a supramolecular strategy for color stabilization of anthocyanin model compounds. Roy Soc Ch. 2016(15):752-757.

[14] Saptarini N, Suryasaputra D, Nurmalia H. 2015. Application of butterfly pea (*Clitoria ternatea* Linn) extract as an indicator of acid-base titration. J Chem Pharm Res. 7(2):275-280.

[15] Ochei J, A. 2008. Medical laboraty science: Theory and practice. New Delhi. Tata McGraw-Hill Publishing Lmtd. 438 p.

[16] Salleh M, Mahmoud D, Karim W, Idris A. 2011. Cationic and anionic dye adsorption by agricultural solid wastes: a comprehensive review. Desalination. 2011: 1-13.

[17] Puchtler H, Meloan S, Spencer M. 1985 Current chemical concepts of acids and bases and their application to anionic ("acid") and cationic ("basic") dyes. Histochemistry 82(1985): 301–306.

[18] Leong C, Azizi M, Taher M, Wahidin S, Lee K , Tan W, Tong W. 2017. Anthocyanins from *Clitoria ternatea* attenuate food-borne penicillium expansum and its potential application as food biopreservative. Nat Prod Sci. 23(2):1-7.

[19] Guevara BQ. 2005. A guidebook to plant screening: Phytochemical and biological. Manila: Research Center for the Natural Sciences, University of Santo Tomas. 156 p.

[20] Merck Microbiology Manual. 12th Ed. 2010. Kenilworth (NJ): Merck.

[21] Sridhara SU, Raju S, Gopalkrishna AH, Haragannavar VC, Latha D, Mirshad R. *Hibiscus*: A different hue in histopathology. J Med Radiol Pathol Surg. 2016(2):9-11.

[22] Janeiro P, Brett AMO. 2007. Redox behavior of anthocyanins present in V*itis vinifera L.* Electroanalysis. 19(17): 1779 – 1786.

[23] Sigma-Aldrich Corporation. 2014. Crystal violet. [Internet]. Material Safety Data Sheet. Available from: https://www.nwmissouri.edu/naturalsciences/sds/c/Crystal%20Violet.pdf

[24] Itodo SE, Oyero S, Umeh EU, Ben A, Etubi MD. 2014. Phytochemical properties and staining ability of red onion (*Allium cepa*) extract on histological sections. J Cytol Histol. 5(6): 1-4.

[25] Bancroft JD, Gamble M. 2008. Theory and practice of histological techniques. [Internet]. China: Churchill Livingstone Elsevier. 725 p. Available from: https://bit.ly/34M0LUg

Publiscience Vol. 3 Issue 1

The effects of acetyl l-carnitine on the prevention of platelet storage lesions

SAMANTHA LAUREN E. ALVAREZ and ZENNIFER L. OBERIO

Philippine Science High School - Western Visayas Campus, Brgy. Bito-on, Jaro, Iloilo City 5000, Department of Science and Technology, Philippines

Abstract

Platelet storage lesion is the degradation of platelets when stored in an external environment, causing a loss in platelet viability, in turn, causing their low availability. The aim of the study is to compare the effects of l-carnitine with its derivative acetyl l-carnitine with respect to platelet count, mean platelet volume, pH, and platelet shape change. Three blood bags were used and separated into three setups: l-carnitine, acetyl l-carnitine, and saline, and were stored at 20 to 24°C. Platelet count and mean platelet volume were determined by using a hema-analyzer, and pH was determined by using a pH meter. Platelet morphology was assessed by collecting stained samples and observed under a microscope, where regular and irregular platelets were recorded. One-way ANOVA analysis for mean platelet volume, pH and morphology did not show any significant difference ($p>0.05$) among the setups, indicating that there is insufficient evidence to conclude that acetyl l-carnitine can be used as a platelet preservative.

Keywords: *platelet storage lesions, platelet preservation, l-carnitine, acetyl l-carnitine, platelet storage*

Introduction. Platelet storage lesion (PSL) is a term that covers the progressive degradation of platelets in storage [1]. This degradation is seen with the lowering of pH, platelet count and volume, and changes in platelet morphology, and accordingly there is a significant societal motivation to decrease PSLs. Whereas current platelet-storage protocols are deemed adequate, there are nevertheless societal gains to be achieved by examining alternatives. These gains include cost-per-day-of-storage, collection and disposal costs, and the associated administrative costs.

PSLs cause platelet metabolism inadequacy thus reducing the efficiency of intracellular metabolism. This further causes the platelet's shelf-life to decrease to only five to seven days [2]. The true cause of PSL has not been clearly understood; however, it has been observed to be linked to lactic acid accumulation and platelet aggregation [3]. Additionally, it has been shown that heightened metabolic activity within the platelet contributes to the production of PSLs [3].

There is research on preserving platelets using preservatives, one being l-carnitine. L-carnitine is a common ergogenic acid due to its importance in the conversion of fat into energy [4]. It can change the metabolic pathway in platelet mitochondria from glycolysis to ß-oxidation, which uses fatty acids instead of glucose to make energy available at the cellular level [1]. The use of fatty acids instead of carbohydrate complexes lowers lactic acid accumulation and thus lowers the chance of PSLs occurring in the platelets. Studies have shown that l-carnitine is a significantly effective platelet preservative [1,5] and its derivative, acetyl l-carnitine (ALCAR), has its uses in the medical field. ALCAR is also able to metabolize fats to make energy available at the cellular level; however, it is mainly used to treat neurological diseases such as cerebral ischemia [6], a condition wherein there is a reduction in the supply of blood to the brain. ALCAR is vital for mitochondrial lipid transport which is important for the mitochondria's function [7]. Additionally, ALCAR has anti-aging abilities for cells [7,8] and is more effective than l-carnitine against oxidative stress [9]—the excess of production of free radicals vis-à-vis the body's capacity to neutralize them— which is a factor in producing PSLs. L-carnitine itself has been proven to be a successful platelet preservative; however, further research is needed to determine whether its derivatives exhibit the same results [5].

ALCAR is less expensive than l-carnitine; but, that alone does not signal efficacy. The motivation of researching ALCAR is to determine whether decreased per-unit application cost is dominated by shorter storage periods or increased PSLs or a combination thereof.

The study aimed to determine the effects of ALCAR as a preservative against PSLs in comparison to the tested l-carnitine. It specifically aimed to:

(i) determine platelet count, mean platelet volume, platelet pH, and platelet morphology with respect to platelet concentrates treated with 1mL each of 15mM ALCAR, saline as the negative control, and l-carnitine as the positive control at Days 0 (before treatment), 3 and 5 after application of preservatives; and

(ii) compare mean change (with respect to Day 0) of platelet count, mean platelet volume, platelet pH, and platelet morphology at Days 0, 3, and 5 among the different treatments and control.

How to cite this article:
CSE: Alvarez SLE, Oberio, ZL. 2020. The effects of acetyl l-carnitine on the prevention of platelet storage lesions. Publiscience. 3(1):48-52.
APA: Alvarez, S.L.E., & Oberio, Z.L. (2020). The effects of acetyl l-carnitine on the prevention of platelet storage lesions. *Publiscience, 3*(1):48-52.

Methods. The study aimed to determine if ALCAR is an effective platelet preservative and to compare its efficacy with l-carnitine. Platelet count, mean platelet volume, platelet pH, and platelet morphology was observed and analyzed to determine the efficacy of l-carnitine and ALCAR. Platelet samples were obtained and separated into three blood bags to be treated with ALCAR, l-carnitine, and saline for five days. The first three parameters were measured on Days 0, 3, and 5 using a hema-analyzer and platelet morphology was observed on Day 5.

Materials. Platelet concentrates (PCs) was isolated from whole blood using a large, specialized centrifuge at a soft spin of 110 rpm then a hard spin of 1000 rpm both for 15 minutes at 20-24 °C . The platelets were separated into three bags and stored at 20-24 °C. Citrate Phosphate Dextrose Adenine (CPDA-1) was already introduced inside the blood bag upon being purchased as it is the standard chemical which lines the bag specifically to work as a preservative. L-carnitine and ALCAR, obtained from in powdered form from Now Foods and iHerb respectively, and were each dissolved in sterile normal saline to produce 1 mL of 15 mM of l-carnitine and ALCAR solutions. After PC extraction, the preservatives were thoroughly mixed with the PCs by gently shaking the blood bag. The local blood bank that assisted with the study by supplying healthy blood samples, equipment, and guidance requested not to be named in the research paper for confidentiality purposes. Models and other specific settings of equipment used are not mentioned under the blood bank's request.

Sampling. Blood samples were acquired from a local blood bank agency at Day 0. From each of the three donors, 450 mL of blood was extracted by a phlebotomist in a triple bag. CPDA-1 contained in the bag was used as an anticoagulant after blood extraction. The blood bank ensured that no contaminants or pathogens that can affect the results were present in the samples by analysis of Transfusion Transmitted Infections (TTIs). In order to ensure confidentiality, no name, age, sex, or any other personal data of the donor was given to the researchers.

Extraction of Platelet Concentrate. The platelets were extracted by a medical technologist via the platelet-rich plasma method to obtain the PCs.

The blood unit was subjected to a soft spin of 110 rpm for 15 minutes using a large, specialized centrifuge machine. Afterwards, the platelet-rich plasma was collected and transferred to the first satellite bag then subjected to a hard spin of 1000 rpm for 15 minutes. Both spins were conducted in a blood centrifuge at 20-24 °C. Separation of PC from platelet-poor plasma was done using a plasma separator by transferring the platelet-poor plasma to the primary bag. PCs with a volume of 60-70 mL was obtained from the procedure, to be used for one replicate each. The obtained PCs were tested by medical technicians to see if the platelets were infected with any disease (i.e. malaria, AIDS, hepatitis, etc.). The healthy PCs were stored at 20-24 °C with constant gentle agitation using a platelet agitator.

Separation of Setups. Each PC was used for one replicate of each setup. Blood extraction was done on a quadruple bag to enable the use of three setups: ALCAR, l-carnitine, and saline.

Before storage in the agitator, the PC was separated into three parts, each approximately at a volume of 60mL. The PC in the first satellite bag was transferred and equally divided to all three satellite bags. Approximately 60 mL PC each was transferred to both the second and the third satellite bags. The first bag became the negative control setup, the second the positive control and the third for the ALCAR variable setup. The primary bag was used to contain unwanted red blood cells and platelet-poor plasma, which was returned to the blood bank.

The negative control setup consisted of the PC with 1mL saline solution. The positive control setup consisted of the PC and 1mL of 15mM l-carnitine.

Storage and Preservation. CPDA-1 has been added during blood extraction at around 63 mL per blood unit in order to prevent coagulation. The samples were stored at a volume of 20 mL at 20-24 °C with constant gentle agitation in their respective satellite bags. Three replicates were prepared, and each replicate consisted of the three setups: l-carnitine (positive control), saline (negative control), and ALCAR.

The chosen concentration for the preservatives used in the study was 15 mM based on a pilot study of Deyhim et al. [1] in determining the best concentration and volume of l-carnitine in preserving PCs.

L-carnitine solution was prepared by dissolving the l-carnitine powder in sterile, normal saline at a concentration of 15 mM. A volume of 1 mL l-carnitine solution was added to the positive control setup [1]. ALCAR was prepared and added to the variable setup the same way as l-carnitine. The preservatives were added to the PCs one day after blood extraction.

One mL of l-carnitine and ALCAR each were introduced into the platelet bag via aseptic infusion one day after extraction. Insulin syringes were used after filtering the preservative solution through a 0.22 μm filter. Sterile normal saline was used in order to dissolve the l-carnitine and ALCAR powders. As a control, an equal volume of 1 mL of saline was also added to the third setup. The site of puncture was sealed and a stripper was used to mix the preservative with the blood bag contents. A biosafety cabinet level II located in a nearby hospital from the site of storage was used. Transportation of samples was done using an approved Styrofoam box and was returned after application of preservatives.

Data Gathering. After extraction, platelet count and mean platelet volume were measured by running a sample of 1mL through the hema-analyzer three times and taking the average. The pH was tested using a pH meter by sampling a 1mL volume of the PCs and washing the bulb of the pH meter after every measurement. All successive measurements were taken on Days 3 and 5 of storage.

Platelet morphology was analyzed by photographing microscope smears of the platelets in each setup and manually counting the ratio of

activated platelets to the total number of platelets. For a qualitative comparison, microscopic analysis of the samples involving the shape and concentration of platelet change was also done to show their shape and configurations. Discoid and irregular shapes were noted among the platelets. Six photographs were taken from each slide and were gridded and printed into paper for manual counting. A four-by-four area was used to count the platelets. The number of irregularly-shaped platelets was divided by the total number of platelets to obtain the percent change of platelet morphology.

Statistical Analysis. One-way ANOVA and paired t-test (α=0.05) was used to compare the mean changes of Day 0 and Day 3, and Day 3 and Day 5 between all setups. Post-hoc tests were conducted to see if there were any significant differences. The results were verified by a statistics teacher of Philippine Science High School – Western Visayas Campus.

Safety Procedure. The researchers wore the necessary personal protective equipment such as lab gowns, surgical gloves, and lab goggles. Proper grooming (i.e. hair was short/tied up) was observed. The researchers followed the standard operating procedure of the American Association of Blood Banks, under the supervision and guidance of a hematology professional. Platelet samples, and instruments used for blood extraction and preservative application were treated and handled as biohazards and were safely disposed. Sharp objects, i.e. blood syringes, were disposed in their respective containers. The waste bags were discarded to specific medical waste contractors.

Results and Discussion. The aim of the study is to determine the effects of ALCAR on the prevention of PSLs by observing the treated platelets' platelet count, mean platelet volume, platelet pH, and change in platelet morphology. An error was made in the preparation of the l-carnitine and ALCAR solutions wherein the study used 1mL of 15 mM preservative solution then mixed with their respective PCs. This resulted in a final concentration much lower than 15 mM and thus may have contributed to the inconclusive results collected. Instead of 15 mM concentration, 1mL stock preservative concentration of 1000 mM should have been used to make the final and intended 15 mM concentration.

Despite the dubious results, there is potential value in observing the effects of small concentrations of preservatives on platelets, and hence they are presented. Other than the major flaw in the preservative preparation and application method, it is possible there are other factors that had an effect on the results.

Platelet Count. The saline setup had a smaller platelet count compared to the l-carnitine and ALCAR setups on Day 0, but each setup equalized from Day 3 of storage onwards. Days 3 and 5 showed similar results, with the biggest change on the saline setup. Day 0 showed no samples with platelet count higher than $1x10^5/mm^3$. Days 3 and 5 showed platelet counts greater than $2x10^5/mm^3$. There was an insignificant increase in platelet count between all measurements.

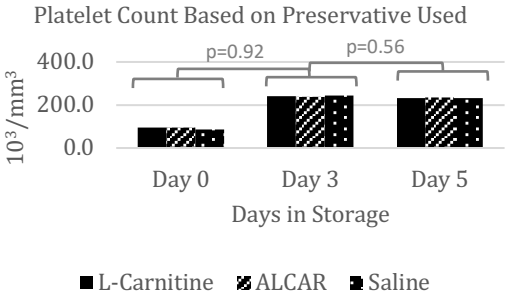

Figure 1. Platelet count means ($10^3/mm^3$) on Days 0, 3, and 5 of storage with three replicates of L-Carnitine (solid), ALCAR (lined), and Saline (dotted).

An anomaly was observed during the experiment wherein there was an increase in platelet count from Day 0 to Day 3 instead of a decrease. For this reason, the data could not be analyzed to accurately represent the effects of the preservatives on platelet count. It is unknown exactly why this occurred in the experiment. So far, no related research has been found to explain this phenomenon, therefore the data cannot be analyzed. It is possible that this was due to the measurement on the first day, where platelet count was low even during preliminary experiments.

Mean Platelet Volume Mean platelet volume measurements were taken at the same time as platelet count. The gathered data for all setups were 5.5 μm^3 on Day 0, 5.8 μm^3 on Day 3, and 6.1 μm^3 on Day 5 which were all below the normal range of values between 7.2 μm^3 and 11.7 μm^3 [10]. A trend whereby the volume of the platelets increased was observed during subsequent analyses.

Mean platelet volume of ALCAR setup was highest in Day 5 during preservation. L-carnitine consistently resulted in the lowest values among all measurements.

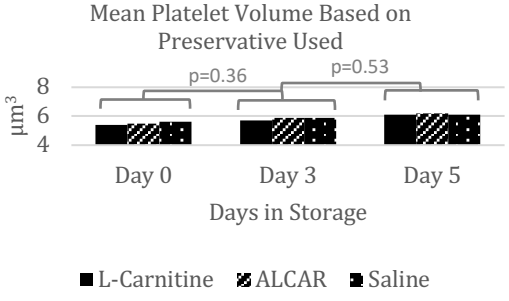

Figure 2. Mean platelet volume means (μm^3) on Days 0, 3, and 5 of storage with three replicates of L-Carnitine (solid), ALCAR (lined), and Saline (dotted) each.

Statistical analysis showed insignificant differences in mean platelet volume among all setups.

Platelet pH. L-carnitine dropped from 6.7 to 6.6 on Day 5 while ALCAR dropped from 6.7 to 6.6 on Day 3 of storage. Saline dropped from 6.6 on Day 3 to 6.5 on Day 5. This data is all within the normal range of values between 6.4 and 7.4 [11] and

shows insignificant difference between Days 0 and 3 and Days 3 and 5.

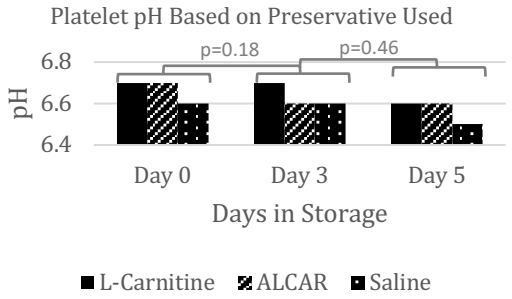

Figure 3. Platelet pH means on Days 0, 3, and 5 of storage with three replicates of L-Carnitine (solid), ALCAR (lined), and Saline (dotted).

Platelet Morphology. Statistical analysis showed that the platelet morphology results are statistically insignificant between all setups.

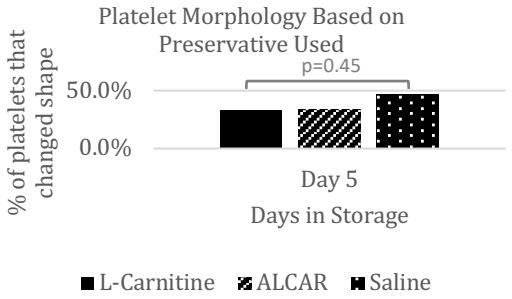

Figure 4. Platelet morphology means on Day 5 of storage with three replicates of L-Carnitine (solid), ALCAR (lined), and Saline (dotted) treatments each.

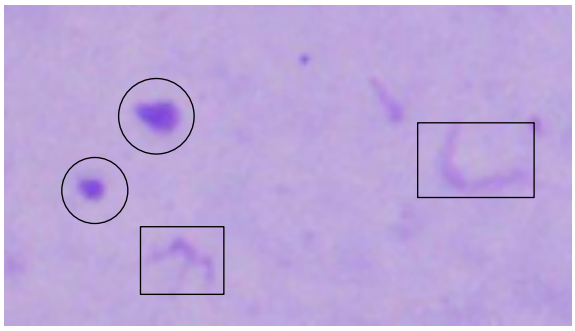

Plate 1. Regular (circled) and irregular (boxed) platelets taken from a platelet sample.

All results showed an insignificant difference in mean platelet volume, platelet pH, and platelet morphology among all setups all throughout the five-day observation period. This is because five days is the standard storage period for platelets. Previous studies showed that platelets were observed not to have significant decrease in quality during this period [12,13,14,15]. Multiple studies have since explored more options on preventing PSLs and thus increasing platelet shelf-life [14,15].

In previous literature, the focused factors included the acidity of the platelet medium and the metabolic activity of the platelets. With the current technology used for platelet storage, there is an increase in number of studies observing the metabolic activity of platelets. In the body, platelets derive up to 80% of their energy through ß-oxidation [1]. The energy from ß-oxidation comes from fatty acids, reducing the reliance on glucose. In vitro, however, requires different mechanisms. Prevention of platelet activation is necessary for long term storage and increased platelet viability. Platelet metabolism shifts to glucose during storage, increasing lactate concentration, which is a byproduct of the metabolic pathway. This accumulation leads to the decrease of plasma pH, inducing platelet activation [1].

The studies of Deyhim et al. [1] and Sweeney et al. [12] used l-carnitine to prolong platelet shelf-life. By switching the metabolism of platelets from depending on glucose to fatty acids, the metabolites that are produced during glucose metabolism, primarily lactate, is eliminated. This change can help prevent the lowering of the pH inside the blood bag, minimizing platelet storage lesion. The study that was conducted followed these observations and tested to see whether another chemical such as ALCAR could be capable of obtaining similar results. The final data showed that not only is there an insignificant difference in comparison to l-carnitine, but that it cannot be conclusively said that ALCAR is a viable platelet preservative.

In the study of prolonging platelet shelf-life, platelet storage lesion is the biggest hurdle against the loss of platelet viability. It does not stem from a single variable, but instead involves multiple factors that influence platelet degradation [1,14,16]. In order to improve platelet shelf life, factors such as temperature, agitation, medium acidity, and oxygen permeability are needed to be considered. Understanding the mechanisms of platelet storage lesion involves understanding each of these factors and more in order to know their roles in maintaining platelet viability.

Limitations. The methods had the fundamental flaw of preparing the wrong concentration which may have resulted in insignificant data.

Conclusion. All four parameters showed no significant results during the entire observation period. It can be concluded that this study did not yield enough information to say that ALCAR is effective in improving platelet viability.

Recommendations. Future studies must use 1mL of stock l-carnitine solution and ALCAR solution of 1000 mM each rather than 15 mM in order to achieve to achieve more accurate results. The researchers also recommend the use of the Kruskal Wallis and Wilcoxon tests to analyze the data due to its small sample size.

Acknowledgement. This research would not have been possible without the efforts of: Philippine Red Cross - Western Visayas Chapter, with Dr. Dennise Roy Pasadilla as the blood center manager; Mrs. Rose Ababao, for assisting the researchers through the preliminary studies of the research and

allowing the researchers to use her home microscope; Johannes Tré Maquiling and John Mark Villanueva, for being the researchers' groupmates in the academic year 2017-2018; and Michelle Peneranda PhD in Pathobiology and research scientist of UiT The Arctic University of Norway for her recommendation on future steps correcting the preservative preparation and application as indicated in the discussion.

References

[1] Deyhim MR, Mesbah-Namin SA, Yari F, Taghikhani M, Amirizadeh N. 2014. L-carnitine effectively improves the metabolism and quality of platelet concentrates during storage. Ann Hematol. 94:671–680. doi: 10.1007/s00277-014-2243-5

[2] Sahlin K. 2011. Boosting fat burning with carnitine: an old friend comes out of the shadow. J Physiol. 1509-1510. doi: 10.1113/jphysiol.2011.205815

[3] Bode AP. 1990. Platelet activation may explain the storage lesion in platelet concentrates. Blood Cells. 16(1): 109-126. Available from: http://bit.ly/2RdSfsl

[4] Jain S, Singh SN. 2015. Effect of L-carnitine Supplementation on Nutritional Status and Physical Performance under Calorie Restriction. Indian J Clin Biochem. 30(2): 187-193. doi: 10.1007/s12291-014-0437-1

[5] Mohammadi M, Talasaz AH, Alidoosti M. 2016. Preventive effect of l-carnitine and its derivatives on endothelial dysfunction and platelet aggregation. ESPEN. 15: 1-10. doi: 10.1016/j.clnesp.2016.06.009

[6] Malaguarnera M. 2012. Carnitine derivatives: Clinical usefulness. Curr Opin Gastroent. 28(2): 166-176. doi: 10.1097/MOG.0b013e3283505a3b

[7] Curran MWT, Olson J, Morhart M, Sample D, Chan KM. 2016. Acetyl-L-carnitine (ALCAR) to enhance nerve regeneration in carpal tunnel syndrome: study protocol for a randomized, placebo-controlled trial. Trials. 17(200). doi: 10.1186/s13063-016-1324-2

[8] Tanaka Y, Sasaki R, Fukui F, Waki H, Kawabata T, Okazaki M, Hasegawa K, Ando s. 2004. Acetyl-L-carnitine supplementation restores decreased tissue carnitine levels and impaired lipid metabolism in aged rats. J. Lipid Res. 45: 729-735. doi: 10.1194/jlr.M300425-JLR200

[9] Wang CH, Wang SS, Ko WJ, Chen YS, Chang CY, Chang RW, Chang KC. 2013. Acetyl-l-Carnitine and Oxfenicine on Cardiac Pumping Mechanics in Streptozotocin-Induced Diabetes in Male Wistar Rats. PLoS One. 8(7): e69977. doi: 10.1371/journal.pone.0069977

[10] Demirin H, Ozhan H, Ucgun T, Celer A, Bulur S, Cil H, Gunes C, Yildirim HA. 2011. Normal range of mean platelet volume in healthy subjects: Insight from a large epidemiology study. Thromb Res. 128(4): 358-360. doi: 10.1016/j.thromres.2011.05.007

[11] Dekkers DWC, De Curper IM, Van der Meer P, Verhoeven AJ, de Korte D. 2007. Influence of pH on stored human platelets. Transfusion. 47(10): 1889-1895. doi: 10.1111/j.1537-2995.2007.01412.x

[12] Sweeney JD, Blair AJ, Cheves TA, Dottori S, Arduini A. 2000. L-carnitine decreases glycolysis in liquid-stored platelets. Transfusion. 40(11):1313-1319. doi: 10.1002/jca.21207

[13] Shrivastava M. 2009. The platelet storage lesion. Transfus Apher Sci. 41(2):105-113. doi: https://doi.org/10.1016/j.transci.2009.07.002

[14] Subota V, Vučetić D, Balint B, Mujišković Z, Vojvodić D, Pejović J, Mandić-Radić S. 2007. Evaluation of Platelet Activation Parameters as Quality Markers for the Stored Platelets. JMB. 26(4):280-284. doi: 10.2478/v10011-007-0034-4

[15] Gupta A, Chandra T, Kumar A. 2010. Evaluation of random donor platelets at different temperatures for an ex-tended shelf life. Biomed Res. 21 (4):433-436. Available from: http://bit.ly/38s2vTd

[16] Richard NN, Mwamba MP, J G, Rajab J. 2014. Quality Parameters of Platelet Concentrate at Kenyatta National Hospital's Blood Transfusion Unit. Int J Blood Res Disord. 1(1):35-40. doi: 10.12691/ijhd-1-1-7

L A L A H O N

A G R I C U L T U R E

LALAHON is respected by the ancient Visayans as their protector against natural calamities and the bringer of bountiful harvest. With the rising incidence of natural calamities and the continued increase of the population, agriculture – as the provider of sustenance to humanity – must face these challenges with resilience and confidence. This section explores different methods that may improve agricultural products, providing insight on crop production, seed priming, and pest control.

These studies fall under the Aquatic, Agriculture, and Natural Resources (AANR) Research and Development Agenda. These studies address research for agricultural resources, moving towards the goal of developing good agricultural practices and eco-friendly pest management.

BASED ON: Harmonized National Research and Development Agenda (HNRDA)

Seed germination potential of different local varieties of *Oryza sativa* (rice) as affected by different seed priming methods

MIKKO LEGURPA, MARIUS LEGURPA, and ZENNIFER OBERIO

Philippine Science High School - Western Visayas Campus, Brgy. Bito-on, Jaro, Iloilo City 5000, Department of Science and Technology, Philippines

Abstract

Seed priming is a technique used to improve the overall germination behavior of rice through the imbibition of solutions. This study aimed to investigate the effects of different priming methods on two local varieties of *Oryza sativa* (rice). This study employed three different priming methods using mannitol, glycerol, and sorbitol on red and black varieties of *Oryza sativa* and compared the germination behavior between primed and unprimed seeds. The researchers compared three different parameters such as germination percentage, germination index, and shoot/root ratio by performing a Kruskal-Wallis test using SPSS. Seeds primed with mannitol in black rice resulted in a significant difference in the germination index and shoot/root ratio compared to unprimed seeds. Seeds primed with glycerol in red rice resulted in a significant difference in the germination index compared to unprimed seeds.

Keywords: *seed priming, imbibition, germination percentage, germination index, shoot/root ratio*

Introduction. Seed priming is a technique used to improve the overall germination behavior of rice. This is done by starting all processes necessary for germination but inhibit radicle protrusion preventing the seed to germinate. Osmotic solutions are used in order to partially hydrate seeds up until a point necessary for germination process to start but not enough for radicle protrusion [1].

Priming has shown to increase resistance in crops against both biotic and abiotic stresses [2]. Multiple studies conducted on seed priming have yielded mostly positive results with most of them focusing on studying the effects of multiple types of stresses, be it biotic or abiotic, along with different crop varieties and priming agents [3,4,5].

There are several types of seed priming including hydropriming, halopriming, osmopriming, and hormonal priming, and all have shown great promise in improving seed germination [6]. Osmopriming utilizes osmotic sugars to induce germination in seeds. This specific method has shown great potential, with polyethylene glycol being one of the most common solutions used [7,8]. A previous study has shown a significant difference between osmopriming and hydropriming when it comes to seed germination [9]. However, there are still knowledge gaps found in this field. Some priming agents are yet to be tested on rice or compared against other agents. Also, the effect of seed priming on multiple local rice varieties has not been tested.

Commonly used rice varieties include Rc 216, Rc 160, Rc 300, and Rc 222. However, due to the lack of research regarding high-value rice varieties, the researchers chose to investigate the black and red rice varieties. In this study, the effects of different osmopriming methods on different rice varieties were investigated and compared.

For this study, the parameters germination percentage, germination index, and shoot/root ratio for each rice cultivar treated with the different osmopriming methods (mannitol, glycerol and sorbitol), the number of seeds that germinate every day, and the length of the seedling, shoot and root on the seventh day were measured. Using these parameters, the germination percentage, germination index and shoot/root ratio were computed. These were used to compare the effect of different osmopriming methods on seed germination within each cultivar.

This research aimed to investigate the effects of different osmopriming methods (mannitol, glycerol and sorbitol) on the seed germination behavior of two local varieties (red and black) of *Oryza sativa* (rice). Specifically, it aimed to:

(i) determine the parameters for each rice cultivar treated with the different osmopriming methods such as the number of seeds that germinate every day and the length of seedling, shoot, and root on the seventh day;

(ii) compute for the parameters for each rice cultivar treated with the different osmopriming methods such as germination percentage, germination index, and shoot/root ratio; and

(iii) compare the effect of different osmopriming methods on seed germination parameters within each cultivar in terms of germination percentage, germination index, and shoot/root ratio.

How to cite this article:
CSE: Legurpa, MP, Legurpa, MP, Oberio, ZL. 2020. Seed germination potential of different local varieties of *Oryza sativa* (rice) as affected by different seed priming methods. Publiscience. 3(1): 54-58.
APA: Legurpa, M.P., Legurpa, M.P. & Oberio, Z.L. (2020). Seed germination potential of different local varieties of *Oryza sativa* (rice) as affected by different seed priming methods. *Publiscience, 3*(1): 54-58.

Methods. This study tested the effects of three different priming methods using mannitol, glycerol and sorbitol with specific concentrations on two different local varieties of rice (red and black). Several germination parameters were used to test the seed priming effects on seed germination. The methods were done in correspondence with the International Rice Research Institute (IRRI), Los Baños, Laguna.

This study was conducted in one of the laboratories of Philippine Science High School - Western Visayas Campus' (PSHS-WVC) SLRC Building over a 16-day period, including a 10-day germination test.

Three different priming methods and one unprimed control for each variety were used in the study. The concentrations indicated below were based on previous studies on seed priming [11,12]. Table 1 shows the priming agent, concentration, and treatment numbers.

Table 1. Priming agents, concentrations, and treatment.

Treatment Number	Priming Agent	Concentration*
1	mannitol	2%
2	glycerol	5%
3	sorbitol	0.25 M

* References: [11] Seed priming alleviated salt stress effects on rice seedlings by improving Na+/K+ and maintaining membrane integrity; and [12] Effects of different priming methods and duration on seedling characters maize (Zea mays L.)

Seeds, Priming Agents, and Equipment. Black and red rice seeds were purchased from a local farm. The priming agents mannitol, glycerol, and sorbitol were all obtained from Patagonian Enterprises. The beakers, stirring rods, Petri dishes, flasks and graduated cylinders were all from PSHS-WVC's Chemistry Science Research Assistant (SRA).

Moisture Content Test. Seeds were tested for their moisture content at Western Visayas Agricultural Research Center (WESVIARC). A grain moisture tester (Riceter f511) was used to measure the moisture content. The test chamber was filled with seeds, then the handle was turned to crush the grain, and the moisture content was instantly provided. Optimum moisture content for rice is at 14.0% or lower after drying.

Preparation of Priming Agents. Twenty-five grams of mannitol was measured using an analytical balance (Shimadzu aux-220), then dissolved in 500 mL of water in a 2 L beaker and stirred using a stirring rod in order to achieve the desired 2% concentration. A 100 mL graduated cylinder was used to measure 25 mL of glycerol and 475 mL of water to create a 5% glycerol solution, and both solutions were mixed using a stirring rod in a 2 L beaker. The same process was repeated to achieve a 0.25 M sorbitol solution using 15 mL of sorbitol and 485 mL of water.

Treatment of Seeds. During the priming process, the seed weight to solution volume ratio of 1:5 was used. Using 100 g of seeds from each variety, the seeds were soaked in 5% solution of glycerol for 24 h. The same was done for mannitol and sorbitol. Soaked seeds were then recovered from the solution, spread on a metal tray with paper towels and allowed to dry for 24 h. The seeds were then brought to WESVIARC to have their moisture contents measured, following the same methods as the first test.

Germination Test. A total of eight (8) setups were used for the two varieties (red and black). Three different priming agents and a control of untreated seeds were used in each variety. Twenty-five seeds were sown in one 90 mm Petri dish which contained one layer of Whatman No. 2 filter paper moistened with 10 mL of water which was measured using a syringe. Each setup had three replicates which were made up of six Petri plates each. A total of 150 seeds were used in each replicate and 144 Petri plates were used for the study.

Every day, at 7:00 AM and at 3:00 PM, seeds were watered as needed to maintain a 100% moisture level using a syringe. Natural light was allowed to enter through the windows while an artificial source of light was turned on from 7:00 AM to 6:00 PM. External factors were also observed and recorded such as the temperature, presence of insects, animals or any other factor that might affect the study. At 3:00 PM, the number of germinated seeds were recorded. A seed was deemed to have germinated once it reached a radicle length of 2 mm which was measured using a vernier caliper.

Measuring of Seedling Shoot and Root Length. On the seventh day of the experiment, the seedling shoot and root length were measured. The two longest germinated seeds in each Petri plate were chosen, and their length was measured using a vernier caliper.

Calculation of Parameters. The germination percentage, germination index and shoot/root ratio were calculated using the formulas stated by Li [13] and Wilson [14];

$$Germination\ Percentage = (GS/ST) \times 100$$

where GS is the total number of germinated seeds and ST is the total number of seeds tested.

$$Germination\ Index = \sum (Gt/Dt)$$

where Gt is the number of germinated seeds on day t and Dt is the time corresponding to Gt in days.

$$Shoot/Root\ Ratio = SL : RL$$

where SL is the length of the shoot and RL is the length of the root.

Data Analysis. Using IBM SPSS Statistics, a Kruskal-Wallis test was conducted with a significance level of 0.05 to examine the differences in the

germination behavior of *Oryza sativa* according to the priming technique used. It was followed by a Dunn Test for pairwise comparisons in a post hoc manner.

Safety Procedure. Before the conduct of the study, the chemical safety data sheet of chemicals to be used were reviewed. During the conduct of the study, the proper use of personal protective equipment was observed inside the laboratory and proper precautions were followed. The chemicals obtained were placed inside appropriate containers and were handled properly according to their safety protocol. After the conduct of the experiment, the seedlings were thrown away properly into the garbage bins, and chemical wastes were properly disposed.

Results and Discussion. During the moisture content test, red rice yielded a moisture content of 12.6% while black rice yielded a moisture content of 14.0% which are both within the optimal 14.0% moisture content. The moisture content should be within the optimal percentage in order to proceed to priming.

The table below shows the results of the germination test for red rice. The germination percentage of the primed seeds relative to the unprimed seeds showed an overall increase. The means of the germination index of the primed seeds were comparable to one another and were higher than those of the unprimed seeds. The means of the shoot/root ratio were also comparable.

Table 2. The germination percentage and the germination index at the end of the 10 d experiment and the shoot/root ratio on the seventh day of the experiment sorted into four groups according to the priming technique (mean ± standard error) for RED RICE.

Treatment	Germination %	Germination index*	Shoot/Root Ratio
Mannitol	98.00 ± 0.00	49.30 ± 0.25	0.85 ± 0.05
Glycerol	98.00 ± 0.77	49.44 ± 0.23 a	0.85 ± 0.06
Sorbitol	98.00 ± 1.02	50.33 ± 0.83	0.82 ± 0.10
Unprimed	97.56 ± 0.80	44.44 ± 1.34 a	0.81 ± 0.05

* Means followed by the same letter are significantly different at $p \leq 0.05$ (Dunn Test).

A significant difference ($h = 8.273$, $p = 0.041$) was found between the germination index of red *Oryza sativa* seeds that were primed with glycerol and the unprimed seeds based on pairwise comparison of treatments. This would mean that priming with glycerol does indeed lead to a better germination index compared to non-priming.

The test showed that there was no significant difference between germination percentage and shoot/root ratio between primed and unprimed seeds.

Table 3 shows the results of the germination test for black rice. Similar to the red variety, the germination percentage of the primed seeds relative to the unprimed seeds showed an overall increase. The means of the germination index of the primed seeds were comparable to one another and were higher than those of the unprimed seeds. The shoot/root ratio among all treatments vary with mannitol having the lowest shoot/root ratio and unprimed seeds having the highest.

Table 3. The germination percentage and the germination index at the end of the 10 d experiment and the shoot/root ratio on the seventh day of the experiment sorted into four groups according to the priming technique (mean ± standard error) for BLACK RICE.

Treatment	Germination %	Germination index*	Shoot/Root Ratio*
Mannitol	97.78 % ± 0.45	47.92 ± 0.74 a	0.93 ± 0.04 a
Glycerol	96.45% ± 0.80	44.29 ± 0.37	1.28 ± 0.14
Sorbitol	97.58 % ± 0.22	46.02 ± 0.49	1.46 ± 0.12
Unprimed	93.11 % ± 1.74	36.58 ± 0.19 a	1.75 ± 0.17 a

* Means followed by the same letter are significantly different at $p \leq 0.05$ (Dunn Test).

A significant difference ($h = 9.974$, $p = 0.019$) was found between the germination index of black *Oryza sativa* seeds that were primed using mannitol and unprimed seeds based on pairwise comparison of treatments. This would mean that priming with mannitol does indeed lead to a better germination index compared to non-priming for black *Oryza sativa* seeds.

A significant difference ($h = 8.435$, $p = 0.038$) was found between the shoot/root of seeds primed with mannitol and unprimed seeds.

The test showed that there was no significant difference between germination percentage between primed and unprimed seeds.

Seed priming has been used to reduce the time between seed sowing and seedling emergence, and to synchronize that emergence [15]. Primed seeds have shown to have earlier, more uniform and sometimes greater germination and seedling establishment and growth [16]. Currently, many rice varieties have been tested with priming such as Inpago 8, Situ Bagendit, IR64 and more. Seed priming using mannitol, glycerol, and sorbitol has not yet been tested on local varieties such as red and black varieties. Investigation of the effects of seed priming on red and black rice will allow a better understanding of seed priming and its effects.

A significant difference in the germination index (GI) of both red and black rice varieties was found. In red rice, the GI of seeds treated with glycerol had a significant difference among the GI of unprimed seeds. In black rice, the GI of seeds treated with mannitol had a significant difference compared to the GI of unprimed seeds. These results are consistent with the results of a previous study [3],

where primed aerobic cultivars were compared with unprimed aerobic cultivars, showed an improved GI. This could be attributed to how the priming process works, wherein seeds that have undergone seed priming have already completed the processes necessary for germination without the occurrence of the germination itself [1]. This gives the primed seeds an advantage for an earlier germination compared to the unprimed seeds, thus increasing the speed of germination and the germination index.

Germination percentage has shown to have no significant difference among the treatments and the control, although there was an observed increase in the germination percentages of primed seeds when compared to the germination percentage of the unprimed seeds over a period of ten days. The lack of significant difference goes against the existing literature which has shown a significant difference in the germination percentage of seeds with the use of priming in different crops such as maize, wheat, rice, and canola [17,18]. Granted that the seeds were obtained from one source, the seeds could have had similar seed quality, which refers to the physical, physiological and genetic attributes that determine the performance of the seed [19], and could be influenced by both genetic background and environmental conditions of the mother plant during seed development [20]. Priming, despite being able to speed up the germination process and therefore increasing resistance against biotic and abiotic resources [21], cannot salvage seeds from undergoing the deterioration process [22].

Regarding the shoot/root ratio between primed and unprimed seedlings, there was no significant difference in red rice varieties. However, there was a significant difference in black rice with mannitol-primed seeds having the minimum shoot/root ratio. The results for the black rice variety are supported by a previous study [23], which shows that seed priming caused a significant difference in the shoot/root ratio. However, the results of this study led to a lower shoot/root ratio of seeds primed with mannitol compared with unprimed seeds. This indicates a longer root than shoot after seven days. The shoot/root ratio is defined as the ratio of the amount of plant tissues that have supportive functions to the amount of those that have growth functions [24]. Previous studies have shown that plants show different reactions based on different limitations in the environment. For example, root growth is favored when there is a lack of nitrogen, phosphorus, or sulfur [25].

Biotic factors that could affect germination such as insects and pests were present. While these factors were not fully controlled, the researchers employed several techniques to minimize their effects such as using an insecticide chalk to line the perimeter around the set-up, closing the windows to prevent insects from infesting the seedlings, distributing water equally among all Petri dishes, and using an artificial source of light from 7:00 AM to 6:00 PM while allowing natural light to enter through the windows.

Limitations. This study was limited to the germination stage alone, and while germination is one of the initial factors influencing yield, there are still other factors during the other stages of crop production that should be considered such as infestations and forces of nature. Abiotic factors such as light, moisture content, and temperature are largely dependent on nature and could not be controlled. Therefore, temperature was measured and recorded every day at 3:00 PM using a room thermometer. Also, several natural factors could not be controlled such as the presence of pests and sunlight exposure.

Conclusion. This study had shown that seed priming does indeed have a significant effect on some of the germination behaviors of *Oryza sativa* — specifically its germination index and in the case of black rice, its shoot/root ratio — but does not affect the germination percentage. Mannitol is the best priming agent for black rice, while glycerol is the best priming agent for red rice.

Recommendations. For future experiments similar to this study, a longer period for the data gathering is recommended. The crop yield may also be another parameter to measure and compare in future studies. Other priming agents and other varieties could also be employed in future studies on the subject.

Acknowledgement. The researchers would like to thank the following people for aiding them during their study: Hope G. Patricio for sharing her valuable insights into their study; the WESVIARC technicians for allowing them and teaching them how to use the grain moisture meter; Dr. Myrna Libutaque for her valuable help in statistical analysis of their data; Norma Pongan who contacted Mr. Edgar Tono who provided both the red and the black rice seeds; and their parents, Marlon and Cecilia Legurpa, who assisted them throughout the conduct of their research.

References

[1] Taylor AG, Allen PS, Bennett MA, Bradford KJ, Burrisand JS, Misra MK. 1998. Seed enhancements. Seed Sci. Res. 8: 245-256.

[2] Borges AA, Jiménez-Arias D, Expósito-Rodríguez, M, Sandalio LM, Pérez JA. (2014). Priming crops against biotic and abiotic stresses: MSB as a tool for studying mechanisms. Frontiers in plant science, *5*, 642. doi:10.3389/fpls.2014.00642.

[3] Abdallah EH, Musa Y, Mustafa M, Sjahril R, Kasim N, Riadi M. 2016. Seed germination behaviors of some aerobic rice cultivars (*Oryza Sativa L*) after priming with polyethylene glycol-8000 (Peg-8000). Int J of Scientific & Technology Res; *5*(2): 227-234.

[4] Sadeghi H, Khazaei F, Yari L, Sheidaei S. 2011. Effect of seed osmopriming on seed germination behavior and vigor of soybean (*Glycine max L.)*. ARPN J of Agri and Bio Sci. 6(1): 39-43.

[5] Hasan MN., Salam MA, Chowdhury MI, Sultana M, Islam M. 2016. Effect of osmopriming on germination of rice seed. Bangladeshi J Agri Res. 41(43): 451-460.

[6] Nawaz J, Hussain M, Jabbar A, Nadeem GA, Sajid M, Subtain M, Shabbir M. 2013. Seed priming a technique. Int. J of AGRI and Crop Sci. 6 (20): 1373-1381.

[7] Salehzade H, Shishvan MI, Ghiyasi M Forouzin F, Siyahjani AA. 2009. Effect of seed priming on germination and seedling growth of wheat (*Triticum aestivum L.)* Res J of Bio Scie. 4(5): 629 - 631.

[8] Dezfuli PM, Sharif-zadeh F, Janmohammadim M. 2008. Influence of priming techniques on seed germination behavior of maize inbred lines (*Zea mays. L)* ARPN Journal of Agricultural and Biological Science. (3)3: 25.

[9] Abdallah EH, Musa Y, Mustafa M, Sjahril R, Kasim N, Riadi M. 2016. Comparison between hydro-priming and osmo-priming to determine the period needed for priming indicator and its effect on the germination percentage of aerobic rice cultivars (Oryza sativa L.). AGRIVITA Journal of Agricultural Science. 2016. 38(3): 222-230.

[10] Bandumula N. 2017. Rice production in Asia: key to global food security. Proceedings of the National Academy of Sciences, India Section B: Biological Sciences. ;88(4):1323–1328. doi:10.1007/s40011-017-0867-7

[11] Theerakulpisut P, Kanawapee N, Panwong B. (2017). Seed priming alleviated salt stress effects on rice seedlings by improving Na+/K+ and maintaining membrane integrity. International Journal of Plant Biology, 7(1). doi:10.4081/pb.2016.6402.

[12] Debnath A, Chaurasia AK., Bara BM, Vishwas S, Saxena R. 2017. Effects of different priming methods and duration on seedling characters maize (*Zea mays L.)* Seeds. J of Pharmacognacy and Phytochemistry. 6(4); 348-351.

[13] Li Y. (2008). Effect of salt stress on seed germination and seedling growth of three salinity plants. Pakistan Journal of Biological Sciences. 2008;11(9):1268–1272. doi:10.3923/pjbs.2008.1268.1272

[14] Wilson J, A Review of evidence on the control of shoot: root ratio, in relation to models, *Annals of Botany*, Volume 61, Issue 4, April, Pages 433-449.

[15] Parera AC, Cantliffe DJ. 1994. Pre-sowing seed priming. Hortic. Rev. 16109-148.

[16] Bradford KJ. 1986. Manipulation of seed water relations via osmotic priming to improve germination under stress conditions. Hort. Sci. 21 11051112.

[17] Basra SMA, Farooq M, Wahid A, Khan MB. 2006. Rice seed invigoration by hormonal and vitamin priming. Seed Science and Technology. 34(3) 753-758(6).

[18] Ghiyasi M, Seyahjani AA, Tajbakhsh M, Amirnia R, Salehzadeh H. 2008. Effects of osmopriming on polyethylene glycol 8000 on germination and seedling growth of wheat (*Triticum aestivum L.)* seeds under salt stress. Res J of Bio Sci. 3(10): 1249-1251.

[19] Hampton JG. (2002). What is seed quality? Seed Sci. Technol. 30 1–10.

[20] Hampton JG, Boelt B, Rolston MP, Chastain TG. (2013). Effects of elevated CO2 and temperature on seed quality. J. Agr. Sci. 151 154–162. Doi: 10.1017/S0021859612000263.

[21] Mustafa H, Mahmood T, Ullah A, Sharif A, Bhatti A, Nadeem M, Ali R. 2017. Role of seed priming to enhance growth and development of crop plants against biotic and abiotic stresses. Section Plant Sciences (2):1-11.

[22] Mwale S, Hamusimbi C, Mwansa K. 2003. Germination, emergence and growth of sunflower (*Helianthus annuus L.*) in response to osmotic seed priming. Seed Science and Technology ;31(1):199–206. doi:10.15258/sst.2003.31.1.21.

[23] Khan MB, Gurchani MA, Hussain M, Freed S, Mahmood K. 2011. Wheat seed enhancement by vitamin and hormonal priming. Pak. J. Bot., 43(3): 1495-1499, 2011.

[24] Allaby M. 2006. A Dictionary of Plant Sciences. Oxford University Press. Doi: 10.1093/acref/9780198608912.001.0001

[25] Ericsson T. 1995. Growth and shoot: root ratio of seedlings in relation to nutrient availability. Developments in Plant and Soil Sciences: (62) 205-214.

The effect of salt stress on growth parameters of *Oryza sativa* (rice) variety NSIC Rc 442

ELAINE S. GEROCHE[1], NICO ANGELO O. SOMBIRO[1], JEREMY LANCE P. VILLEGAS[1], ANGELO P. OLVIDO[1], and HOPE G. PATRICIO[2]

[1]*Philippine Science High School - Western Visayas Campus, Brgy. Bito-on, Jaro, Iloilo City 5000, Department of Science and Technology, Philippines*
[2]*College of Agriculture, Resources, and Environmental Sciences – Central Philippine University, Jaro, Iloilo City 5000, Philippines*

Abstract

Salinity is one of the leading causes of crop yield loss worldwide. The presence of harmful cations and anions in the soil through seawater intrusion is the main cause of soil salinization in the Philippines. With this, the study focused on the effect of three types of salts: NaCl, KCl, and $CaCl_2$ on the germination stage of rice. Three different salts with three different concentrations along with a negative control were utilized for the setup. Three replicates were utilized for each treatment. Three Petri dishes were utilized per replicate, each containing fifty seeds. Salt solutions were prepared at three different salinity levels (4, 6, and 8 dS/m). Seeds were allowed to grow for 10 days and germination parameters were measured and recorded thereafter. All data were analyzed using One-way ANOVA at 95% confidence level. Germination percentage showed no significant difference among salts and salinity levels. All the lengths of the shoots and roots, and fresh weights of seeds exposed to NaCl, KCl, and CaCl2 at varying salinity levels showed significant differences.

Keywords: *salt stress, Oryza sativa, sodium chloride, potassium chloride, calcium chloride*

Introduction. The cultivated *Oryza sativa* (rice plant) is a grass of the *Gramineae* family. It is an important crop worldwide, responsible for being the major source of carbohydrates for nearly half of the world's population [1]. It grows in a wide range of environments, particularly centered around Asian countries such as China, India, and the Philippines. Currently, biotic and abiotic stresses such as soil pH, rainfall, salinity, insects, fungi, and diseases are the leading cause of crop failure and decrease in average yield [2]. Of these factors, salinity is among the most widespread problems encountered in rice production worldwide due to its prevalence in coastal fields and irrigations.

For agricultural production, irrigation of the land with salinity is a major menace to modern agriculture, resulting in imbalance and crop failure. According to Vibhuti et al. [2], seed germination decreased from 100% in control to 65% in 20 dS/m. Although most of these results are based on sodium chloride (NaCl), it is hypothesized that other salts have similar effects, but to different degrees [3]. Many studies have used NaCl solutions to study salinity tolerance in the germination of *Oryza sativa* [1,4,5], but little information exists regarding the effect of other salts on the germination of rice seeds.

The most common salts found in irrigation water are the following: sodium chloride (NaCl), sodium sulfate (Na_2SO_4), sodium bicarbonate ($NaHCO_3$), magnesium sulfate ($MgSO_4$), calcium sulfate ($CaSO_4$), calcium chloride ($CaCl_2$), potassium chloride (KCl), and potassium sulfate (K_2SO_4) [6]. Soils usually have these high concentrations due to a number of factors, including expanding urbanization [7] and seawater intrusion [8]. Although seawater intrusion is the main source of salinity in the Philippine setting, other factors such as agricultural malpractice should be taken into consideration. With this status in the Philippine soils, increasing concentrations of salts may inhibit plant growth especially in its germination period since it is the earliest stage of plant development.

This study aimed to determine the effect of increasing salinity levels of sodium chloride (NaCl), potassium chloride (KCl), and calcium chloride ($CaCl_2$) on the germination parameters of *Oryza sativa* (rice) variety NSIC Rc 442. It specifically aimed to:

(i) compare the germination percentage, germination rate (also known as the periodic germination percentage), and germination time of rice seeds exposed to different types of salts (NaCl, KCl, and $CaCl_2$) at increasing salinity levels (control, 4 dS/m, 6 dS/m, and 8 dS/m);

(ii) measure the mean length of roots and shoots of 10 seedlings exposed to different types of salts (NaCl, KCl, and $CaCl_2$) at increasing salinity levels (control, 4 dS/m, 6 dS/m, and 8 dS/m) per setup after 10 d;

(iii) measure the fresh weight of shoots and roots of at least 10 seedlings exposed to different types of salts (NaCl, KCl, and $CaCl_2$) at increasing

How to cite this article:
CSE: Geroche ES, Sombiro NAO, Villegas JLV, Olvido AP, Patricio HG. 2020. The effect of salt stress on growth parameters of *Oryza sativa* (rice) variety NSIC Rc 442. Publiscience. 3(1): 59-62.
APA: Geroche, E.S., Sombiro, N.A.O., Villegas, J.L.V., Olvido, A.P., & Patricio, H.G. (2020). The effect of salt stress on growth parameters of *Oryza sativa* (rice) variety NSIC Rc 442. *Publiscience*, 3(1): 59-62.

salinity levels (control, 4 dS/m, 6 dS/m, and 8 dS/m) after 10 d; and

(iv) compare the leaf color of the seedlings after 10 d.

Methods. Three different salts with three different concentrations, along with a negative control, were utilized for the setup. Three replicates were utilized for each treatment. Three Petri dishes were utilized per replicate, each containing fifty seeds. Salt solutions were prepared at three different salinity levels (4, 6, and 8 dS/m) [9]. Seeds were allowed to grow for 10 days and germination parameters were measured and recorded thereafter. All germination parameters were analyzed using One-way ANOVA at 95% confidence level using SPSS ver. 23.

Seed Acquisition, Pre-germination, and Quality Testing. Seeds of the variety NSIC Rc 442 utilized in the experiment were acquired from Western Visayas Agricultural Research Center (WESVIARC). Moisture content determination was conducted in the same institution. The desired moisture content range was from 8% to 14%. Seeds were then soaked in distilled water for 48 h. Seed quality testing was done by identifying pure and impure seeds [10].

Germination Experiment. Seeds were allowed to germinate for 10 days. Three types of salt and four treatments in each salt type were utilized, namely the control, 4 dS/m, 6 dS/m, and 8 dS/m treatment [9]. In each treatment, there were three replicates with three Petri dishes for each. Fifty seeds were placed in each Petri dish along with 20 mL of their specific salt solutions on day 0 of germination. Each day, 5 mL of distilled water is added. Parameters such as humidity and ambient temperature were recorded thrice a day at 8:00 AM, 12:00 PM, and 4:00 PM. Seeds were exposed to sunlight from 8:00 AM to 4:00 PM, and exposed to artificial light from 4:00 PM to 8:00 AM. Germination parameters (germination rate and time) were recorded accordingly and daily. Germination percentage, length of shoots and roots, fresh weight of shoots and roots, and leaf color were recorded after germination.

Computation of Parameters. Germination percentage and germination rate were solved using the following formulas:

$$\text{Germination Rate} = [(GR_0 \times GR_1)/50] \times 100;\ \text{wherein}$$
GR_0 = *Total number of germinated seeds today.*
$GR1$ = *Total number of germinated seeds yesterday.*

$$\text{Germination Percentage} = (TG/TS) \times 100;\ \text{wherein}$$
TG = *Total number of germinated seeds.*
TS = *Total number of tested seeds.*

Statistical Analysis. Data were analyzed using one- way Analysis of Variance (ANOVA) at a 95% confidence interval (α = 0.05) performed using Statistical Packages for the Social Sciences (SPSS) version 23. Least Significant Difference Post-Hoc Test was performed after One-way ANOVA.

Safety Procedure. During the implementation, the use of protective equipment such as face masks, nitrile gloves and lab gowns was always observed. For the disposal, all seedlings were washed with running water and disposed inside a black trash bag. All salt solutions were placed inside a plastic bottle, and placed inside the trash bag, alongside the seedlings. All Petri dishes were washed with dishwashing soap, and treated with 70% isopropyl alcohol, then left to dry overnight.

Results and Discussion. Germination percentage was not significantly affected by the type of salt and salinity levels, whereas germination rate decreased with increase in salinity level, regardless of the type of salt. Shoot length under the NaCl and KCl treatments decreased with increasing salinity level. Also, the root length decreased as the salinity level increased. For the $CaCl_2$ treatment, the shortest root and shoot length was at 4 dS/m. Fresh weight of roots and shoots was significantly affected by both the type of salt and salinity levels. Increasing the salinity level resulted in a decrease in the mean fresh weight of roots and shoots.

These findings may be attributed to the high Na^+ and Cl^- concentrations that cause the stomata to be less responsive allowing various plant injuries and growth inhibition. The role of K^+ is necessary for osmoregulation and protein synthesis, maintaining cell turgor and stimulating photosynthesis while externally supplied Ca^{2+} has been shown to ameliorate the adverse effects of salinity especially in osmotic adjustment and growth. Both K^+ and Ca^{2+} are required to maintain the integrity and functioning of cell membranes but would induce stress and injury at toxic levels [11].

Germination Percentage. No significant difference was found between all treatments, including the control (Table 1). All treatments had a germination percentage greater than 90%. Supposedly, increasing salinity levels would show a decrease in the germination percentage [2,4,5]. This opposing result could be due to the qualifications of a seed to be considered "germinated" which requires the main radicle to be at least 2 mm in length.

Germination Rate. The rate of germination was delayed with an increase in salinity level, leading to different germination times. Most seeds treated with

Table 1. The effect of salinity concentration and type of salt on the germination percentage.

Type of Salt	Concentration		
	4 dS/m	6 dS/m	8 dS/m
	Germination Percentage (%)		
NaCl	96.67 ± 1.11	95.33 ± 1.29	96.89 ± 0.68
KCl	95.78 ± 0.91	94.67 ± 1.53	95.78 ± 1.02
$CaCl_2$	94.67 ± 1.45	96.00 ± 0.82	95.56 ± 1.14
Control	96.67 ± 0.49	96.67 ± 0.49	96.67 ± 0.49
P-value	0.362	0.375	0.601

4 dS/m achieved a 50% germination percentage on the 2nd day while those treated with 8 dS/m achieved the same percentage by the 4th day.

Effects on root and shoot lengths. Root and shoot lengths were significantly affected by salt type and concentration. For seedlings treated with NaCl and KCl, both root and shoot lengths decreased with increasing concentration (Tables 2, 3, & 4). For seedlings under $CaCl_2$, maximum root and shoot length was achieved at 6 dS/m, while the shortest was at 4 dS/m. Reduction of shoot length is a common phenomenon of rice and other crop plants grown in highly saline conditions [12]. The decrease in shoot length is due to the reduction in physiological availability of water with an increase in solute suction or accumulation of toxic ions within the seedlings [13]. Balkan et al. [5] also reported that root length decreased at increasing salinity levels starting from 4 dS/m which might be due to greater inhibitory effects of different salts to root growth [12,14].

Effects on mean fresh weight. Fresh weight of roots and shoots was significantly affected by the type of salt and salinity levels (Tables 2, 3, & 4), which could be attributed to root and shoot lengths of the different treatments. Increasing salinity levels resulted in a decrease in mean fresh weight of roots and shoots, as supported by Balkan et al. [5], Rahman et al. [12], and Vibhuti et al. [2].

Fresh weight of roots and shoots under NaCl and KCl treatments decreased with increasing salinity levels. In the case of $CaCl_2$, the lowest mean fresh weight of roots and shoots was attained at 4 dS/m, followed by 8 dS/m, and 6 dS/m. This shows that different salts have different effects, depending on the type of salt used and its respective concentration.

Limitations. Due to time constraint, this study has only pursued to observe the effects of salinity on germination parameters. There is also a limitation in the objectives of the study, as leaf color was originally part of the results. Due to the 21-day minimum period for valid leaf color results, the use of the leaf color chart provided was not applicable to the seedlings.

Conclusion. The different salts induced significantly stunted the growth of physiological parameters of rice during the germination stage. Also, the degree of this effect increased with salinity concentration, but the extent differed per salt. With increasing salinity concentrations, germination percentage, shoot and root length, and mean fresh weight were adversely affected. For seeds treated with NaCl and KCl, increasing concentrations resulted to a decrease in value of recorded parameters. For seeds treated with $CaCl_2$, seeds showed better performance at 6 dS/m, while it achieved the lowest values at 4 dS/m.

Table 2. The effect of different types of salts at 4 dS/m on the investigated traits.

Salt	Lag (days)	Shoot Length (mm)	Root Length (mm)	Mean Fresh Weight (g)
NaCl	3 days	55.57 ± 3.17 a	24.69 ± 3.39 a	0.2110 ± 0.0222 ab
KCl	3 days	53.38 ± 4.86 a	23.22 ± 3.00 a	0.1900 ± 0.0239 ac
$CaCl_2$	4 days	42.09 ± 2.16 b	6.694 ± 0.77 b	0.1379 ± 0.0100 c
Control	~	77.38 ± 2.21 c	36.49 ± 1.78 c	0.2520 ± 0.0117 b

*Means followed by the same letter are not significantly different at P = 0.05 (LSD Test).

Table 3. The effect of different types of salts at 6 dS/m on the investigated traits.

Salt	Lag (days)	Shoot Length (mm)	Root Length (mm)	Mean Fresh Weight (g)
NaCl	4 days	35.57 ± 3.19 a	12.66 ± 3.10 a	0.1023 ± 0.0127 ab
KCl	3 days	34.67 ± 3.94 a	11.36 ± 1.58 a	0.1257 ± 0.0225 ac
$CaCl_2$	4 days	50.54 ± 1.28 b	12.54 ± 1.44 a	0.1857 ± 0.0126 c
Control	~	77.38 ± 2.21 c	36.49 ± 1.78 b	0.2520 ± 0.0117 b

*Means followed by the same letter are not significantly different at P = 0.05 (LSD Test).

Table 4. The effect of different types of salts at 8 dS/m on the investigated traits.

Salt	Lag (days)	Shoot Length (mm)	Root Length (mm)	Mean Fresh Weight (g)
NaCl	4 days	23.12 ± 1.42 a	5.389 ± 1.09 a	0.0681 ± 0.0106 a
KCl	4 days	18.10 ± 0.70 a	5.072 ± 0.27 a	0.0541 ± 0.0064 a
$CaCl_2$	4 days	46.07 ± 2.13 b	7.989 ± 0.63 a	0.1634 ± 0.0162 b
Control	~	77.38 ± 2.21 c	36.49 ± 1.78 b	0.2520 ± 0.0117 c

*Means followed by the same letter are not significantly different at P = 0.05 (LSD Test).

Recommendations. It is recommended that the setup will have more number of salts and salinity levels to utilize. It would also be best if the study is conducted in a soil setup and would be extended until yield to further imitate the natural environment and to measure more parameters for more conclusive data.

Acknowledgement. The researchers would like to express their gratitude to Prof. Hope G. Patricio for helping them in planning and designing their research. They would also like to thank the Western Visayas Integrated Agricultural Research Center for providing them with the registered seeds and for allowing them to use their facilities and the Department of Agriculture- LGU Oton for providing them with the leaf color chart. The researchers also thank their parents, for providing them with financial assistance and assisting them with their endeavors throughout the conduct of their research study. Without them, none of this would be possible. To God be all the glory.

References

[1] Mokhtar SME, Samb A, Moufid AO, Boukhary AOMS, Djeh TKO. 2015. Effect of different levels of salinity on germination and early seedling growth of three rice varieties cultivated in Mauritania. Int J Agri Crop Sci. 8(3): 346-349.

[2] Vibhuti, Shahi C, Bargali K, Bargali SS. 2015. Seed germination and seedling growth parameters of rice (*Oryza sativa*) varieties as affected by salt and water stress. Ind J Agri Sci. 85(1): 102-108.

[3] Tavili A, Biniaz M. 2009. Different salts effects on the germination of *Hordeumvulgare* and *Hordeumbulbosum*. Pak J Nutr. 8(1): 63-68.

[4] Ologundudu AF, Adelusi AA, Akinwale RO. 2014. Effect of salt stress on germination and growth parameters of rice (*Oryza sativa* L.). Not Sci Biol. 6(2): 237-243.

[5] Balkan A, Genctan T, Bilgin O, Ulukan H. 2015. Response of rice (*Oryza sativa* L.) to salinity stress at germination and early seedling stages. Pak J Agri Sci. 52(2): 453-459.

[6] Ghosh B, Ali N, Gantait S. 2016. Response of rice under salinity stress: A review update. J Res Rice. 4(2): 1-8.

[7] Rahim Z, Parveen G, Mukhtar N, Natasha Kiran. 2019. Salinity (Sodium and Potassium chloride) influence on germination and growth factors of wheat (*Triticumaestivum*). Pure Appl Biol. 8(3): 2044-2050.

[8] Almaden CRC, Baconguis RDT, Camacho JV, Rola AC, Pulhin JM, Ancog RC. 2019. Determinants of adaptation for slow-onset hazards: The case of rice-farming households affected by seawater intrusion in Northern Mindanao, Philippines. Asia J AgriDevel 16(1): 117-132.

[9] Abrol IP, Yadav JSP, Massoud FI. Salt-affected soils and their management. Food Agri Org. 1(1).

[10] CESD. 2013. Seed Quality Training Manual. Int Rice Res Inst. 1(1): 1-23.

[11] Nawaz K, Hussain K, Majeed A, Khan F, Afghan S, Ali K. 2010. Fatality of salt stress to plants: morphological, physiological, and biochemical aspects. Afr J Biotechnol. 9(34): 5475-5480.

[12] Rahman MS, Miyake H, Takeoka Y. 2001. Effect of Sodium Chloride on seed germination and early seedling growth of rice (*Oryza sativa* L.). Pak J Biol Sci. 4(3): 351-355.

[13] Rad HE, Aref F, Rezaei M. 2012. Response of rice to different salinity levels during different growth stages. Res J ApplSciEng Tech. 4(17): 3040-3047.

[14] Hakim MA, Juraimi AS, Begum M, Hanafi MM, Ismail MR, Selamat A. 2010. Effect of salt stress on germination and early seedling growth of rice (*Oryza sativa* L.). Afr J Biotechnol. 9(13): 1911-1918.

Potential antifeedant bioactivity of *Anethum graveolens* (dill) essential oil against *Cochlochila bullita* (lace bugs) on *Ocimum kilimandscharicum* (sweet basil)

GIDEON BENEDICT F. BENDICION[1], AARON PHILIP C. DAEL[1], SOPHIA KARINA S. GENTEROLA[1], ATHENES JOY P. ABAN[1], and MA. VICTORIA C. SEREDRICA[2]

[1]*Philippine Science High School - Western Visayas Campus, Brgy. Bito-on, Jaro, Iloilo City 5000, Department of Science and Technology, Philippines*
[2]*Central Philippine University - College of Agriculture and Resources and Environmental Science, Lopez Jaena St. Iloilo City, Philippines 5000*

Abstract

Anethum graveolens (dill) has been known to have insecticidal activity on several insect pests. Studies state that components of the essential oil of *Anethum graveolens*, which are mainly composed of carvones and limonenes, can be used as antifeedant against insect pests. This study used the essential oil of *Anethum graveolens* in order to determine whether it has potential antifeedant bioactivity against *Cochlochila bullita* (lace bugs) on *Ocimum kilimandscharicum* (sweet basil). Three (3) setups containing eighteen (18) *Cochlochila bullita* were subjected to four concentrations, 100, 200, 400, and 800ppm, of *Anethum graveolens* essential oil and two control groups for a period of 48 hours. Results showed that there was no significant difference in the number of frass spots observed in 200ppm, 400ppm, and 800ppm, with those of the control groups. The 100ppm concentration had a significantly higher number of frass spots but showed no antifeedant bioactivity. These results indicated that *Anethum graveolens'* essential oil does not have antifeedant bioactivity against *Cochlochila bullita*.

Keywords: *antifeedant, lace bugs, Anethum graveolens, essential oil, Ocimum kilimandsharicum*

Introduction. The Philippines is mainly an agricultural country that produces a variety of food crops such as rice and corn and a variety of different plants that serve medical and herbal purposes. One of these plants is *Ocimum kilimandscharicum,* also known as basil, which is a popular spice and medicinal herb. Basil's different plant parts have different uses and benefits [1]. Basil has been studied to contain a wide range of essential oils, phenolic compounds, and a wide array of other chemical components that help give the plant its aroma and flavor [2]. According to Sathe et al. [1], the basil plant, which includes the *ocimum* family, is heavily infested by several pests such as whitefly *Aleurodicus dispersus* and aphid *Macrosiphum sp*. However, it is the pest, *Cochlochila bullita,* a species of lace bugs, that causes the most damage [3] by sucking the nitrogen-rich plant fluids causing the leaves to wilt and eventually die [4].

Management of lace bugs includes repeated applications of organophosphorus, synthetic pyrethroid, imidacloprid, thiamethoxam, or acetamiprid insecticides [5]. However, pesticide poisoning is still one of the global health problems and contributes to environmental concerns [6]. It is estimated that five million people die every year as a result of intentional, accidental and occupational exposures worldwide [7]. Therefore, an alternative organic solution must be discovered. Plants such as *Anethum graveolens* have long been harvested in order to study their components and their effects on insect pests.

Anethum graveolens is proven to be a source of effective insecticides. *Anethum graveolens* essential oil contained thirteen bioactive components such as carvone, trans-dihydrocarvone, dill ether, phellandrene, and limonene [8]. Carvone and limonene were considered the major components for the cytotoxicity of *Anethum graveolens*. According to Babri et al. [9], the essential oil of *Anethum graveolens* was efficient against *Periplaneta americana*, *Musca domestica*, and *Tribolium castenum* and carvone and limonene were two major components of the oil. Yildrim et al. [10] confirmed that carvone and limonene had greater insecticidal activity when dosage and exposure time were increased. Carvone attained 100% mortality at 30µl after 24 hours. Furthermore, a previous study [11] showed that carvone and limonene, which are the major constituents in *Anethum graveolens'* fruit, are monoterpenes. A previous study [12] that used essential oils of *Hedychium* species, whose major components were monoterpenes, had significant insecticidal activity against azalea lace bugs. Current evidence indicates that monoterpenoids may act on various types of insects, particularly affecting their nervous systems.

Plants have chemical components in their leaf extracts that are a source of insecticide. The plant *Anethum graveolens*, or dill, has had its leaf and seed extracts studied for its insecticidal potential and thus, had been used against aphids [13], beetles and cockroaches [9]. These studies reinforce the statement that plants have chemical components that are of insecticidal value and are therefore good sources of insecticides. This knowledge establishes

How to cite this article:
CSE: Bendicion GBF, Dael APC, Genterola SKS, Aban AJP, Seredrica MVC. 2020. Potential antifeedant bioactivity of *Anethum graveolens* (dill) essential oil against *Cochlochila bullita* (lace bugs) on *Ocimum kilimandscharicum* (sweet basil). Publiscience. 3(1): 63-67.
APA: Bendicion G.B.F, Dael A.P.C., Genterola S.K.S., Aban A.J.P., & Seredrica M.V.C. (2020). Potential antifeedant bioactivity of *Anethum graveolens* (dill) essential oil against *Cochlochila bullita* (lace bugs) on *Ocimum kilimandscharicum* (sweet basil). *Publiscience, 3*(1): 63-67.

that plant extracts could further be studied and/or applied to several other kinds of insect species in order to determine their insecticidal activity.

Any effect that leads to the decreased consumption of food is considered as antifeedancy. This can range from a variety of effects and modes of action depending on the chemical and the target pest. Kordan and Gabrys [14] stated that insect feeding can be preingestional (affecting gustatory senses involved in finding food), ingestional (affecting the digestive system), or postingestional (long-term effects affecting future consumption of food). According to a study by Schlyter et al. [15], carvone is known to have antifeedant properties against *Hylobius abietis* and *Hylobius pales*. The study suggested that carvone had antifeedant effects linked to olfactory (smell) and gustatory (taste) senses depending on the volatility of the carvone analogue used.

Antifeedancy was chosen for the study due to the visual damage caused by *Cochlochila bullita* feeding on basil leaves. Black frass spots, curled and dried leaf tips, loss of entire leaves, and diminished flower production lowers the selling value of affected basil plants. Avoiding damage caused by the feeding allows the basil plants to stay in prime condition to be sold.

Although previous research by Sakhanokho et al. [12] has shown that essential oil rich in monoterpenes are effective against *Stephanitis pyrioides* (azalea lace bugs), as far as the researchers can ascertain, none of the previous research has been able to test the potential antifeedant bioactivity of the essential oil of *Anethum graveolens*.

This study encouraged research on finding a naturally derived product that is able to act as a pesticide, through antifeedant bioactivity, against *Cochlochila bullita* that infest the plant *Ocimum kilimandscharicum*. Furthermore, the data and information that this study produced will add baseline knowledge to future researchers about insecticidal activity of *Anethum graveolens* against *Cochlochila bullita*. It specifically aimed to:

(i) assess the antifeedant bioactivity of the essential oil of *Anethum graveolens* on *Ocimum kilimandscharicum* by counting the total number of frass spots on the leaves per treatment; and

(ii) determine if there is a significant difference in antifeedant bioactivity among the treatments and the negative control group using One-Way ANOVA.

Methods. The experiment consisted of four major stages: (1) collection and rearing of *Cochlochila bullita* (lace bugs), (2) dilution of essential oil concentrations, (3) antifeedant assay, and (4) data analysis. *Anethum graveolens'* essential oil was obtained and shipped from the United States. A certificate of analysis containing gas chromatography - mass spectrometry test results was also provided. Lace bugs were collected from Orchard Valley, Pavia, Iloilo, and reared in a greenhouse created by the researchers at Philippine Science High School - Western Visayas Campus based on the methods of previous studies [1,16,17]. The lace bugs were confirmed in the College of Agriculture and Resources and Environmental Science in Central Philippine University. The dilution for the essential oil concentrations was based on a previous study by Khosravi and Sendi [18]. The basil leaves were soaked in four (4) different concentrations of essential oil that were prepared with a dilution of 0.4% dimethyl sulfoxide (DMSO), which serves as an emulsifier, and a control group consisting of distilled water. Three replicates were made for each setup. The number of frass spots per basil leaf was then counted manually at six (6) hour intervals for forty-eight (48) hours as part of the raw data. The raw data was then analyzed using IBM Statistical Package for the Social Sciences Statistics (SPSS) 23.

Collection and rearing of lace bugs. Basil plants were procured from 3 Sunshine Garden, Tagbak, Jaro, Iloilo City. They were verified by an entomologist at Central Philippine University. The basil plants were then transported to and raised in an improvised greenhouse created at Philippine Science High School - Western Visayas Campus (10°45'10.1"N 122°35'15.9"E). For four days, the basil plants were watered every morning and afternoon. *Cochlochila bullita* colonies were collected from basil plants located at Orchard Valley, Pavia, Iloilo (10°46'09.7"N 122°33'03.8"E). Adult lace bugs were collected by cutting the entire basil leaves on which the lace bugs were situated on using scissors and were placed inside plastic box containers which were covered with perforated cling wrap. The lace bugs were then transported to the greenhouse and placed onto the basil leaves. The basil plants were transferred inside the laboratory in the Student Learning Resource Center Building at Philippine Science High School - Western Visayas Campus. The lace bugs were acclimatized inside the laboratory for three days [1,16]. Male and female adult lace bugs were collected from the basil plants for the antifeedant assay. As described by Sajap and Peng [4], adult lace bugs were classified according to sex using a hand microscope.

Dilution of essential oil concentrations. The essential oil of *Anethum graveolens* was acquired from Plant Therapy Essential Oils Corporate, 510 2nd Ave S, Twin Falls, ID 83301, the United States of America through Lazada PH, an online shopping site, as the medium. The essential oil concentrations were diluted according to a previous study [18] in which 0.01, 0.02, 0.04, and 0.08 mL of essential oil were mixed separately in 0.4 mL of dimethyl sulfoxide (DMSO) emulsifier inside a 100 ml volumetric flask. Distilled water was added into the volumetric flask until the final volume of 100 mL was reached. This provided a 100 mL solution of 100, 200, 400, and 800ppm concentrations of essential oil. A negative control group of distilled water was also prepared.

Antifeedant assay test. Three mature leaves (fourth or fifth leaves from the bottom of a branch) of one *Ocimum kilimandscharicum* were placed inside an 11 cm diameter petri dish, with their stalks covered in sections of moist paper towel. This constituted one replicate. There were three replicates in total [17]. The basil leaves which the lace bugs were placed on were exposed to a concentration of

essential oil from *Anethum graveolens* through dipping for ten seconds and then air-dried, whereas the negative control was only dipped in water [19]. Three adult lace bugs (two females and one male) were starved for at least six hours prior to the experiment [20] and then released into each petri dish. All petri dishes were then covered with their friction-fitting lid. The dishes were arranged in a randomized complete block design. The lace bugs were put under a photoperiod of 14:10 (L:D) hours [17]. Observations on the number of frass spots on the leaves per treatment were conducted every six (6) hour interval for two (2) days [21].

Statistical Analysis. After every six (6) hour interval, the leaves were assessed for damage by counting the number of frass spots. Frass spot numbers are highly correlated with leaf damage and serves as an index for the amount of *Cochlochila bullita* feeding on the basil [17]. The number of frass spots per leaves per treatment was recorded and analyzed using One-Way ANOVA. The means were separated using Fisher's protected least significant difference (LSD) test.

Safety Procedure. The experiment was conducted inside a laboratory at Philippine Science High School - Western Visayas Campus. The researchers wore lab gowns, gloves, and face masks in order to avoid exposure and contamination during the handling of the essential oils. The researchers followed the advice given by the supervising entomologist, especially on the proper handling and disposing of the lace bugs. The petri dishes that contained the basil leaves and the lace bugs were inserted with damp tissue paper in order to keep the lace bugs from going out of the petri dish as advised by the consultant entomologist. After experimentation, the lace bugs were disposed by drowning them in water and rinsing them down the drain. The unused dilutions of dill essential oil were poured into a properly labeled plastic container.

Results and Discussion. This section is divided into two parts: (1) number of frass spots, and (2) antifeedant bioactivity.

Number of frass spots. Frass spots on the leaves were observed and counted from each treatment and control group. The mean number of frass spots on each treatment was compared with the other treatments and the control groups. Using One-way ANOVA, all treatments except for the 100ppm treatment showed no significant difference in the mean number of frass spots between each other and with the control groups. The mean number of frass spots recorded from the 100ppm concentration's treatments were significantly higher compared to the other treatment concentrations and the control groups. This indicates that more feeding occurred on these particular treatment's leaves.

The results of the study showed that treatments with 200ppm, 400ppm, and 800ppm concentrations of *Anethum graveolens* essential oil showed no significant difference with that of the negative control group. This was analyzed from the number of frass spots observed on the 200ppm, 400ppm, and 800ppm treatments. Only the 100ppm treatment concentration was recorded to have had a significantly higher ($p \leq 0.05$) number of frass spots as compared to the negative control group. Because frass spots were used to measure the damage to the basil leaves due to their correlation to leaf damage [17], this indicated that more feeding occurred in the 100ppm treatment.

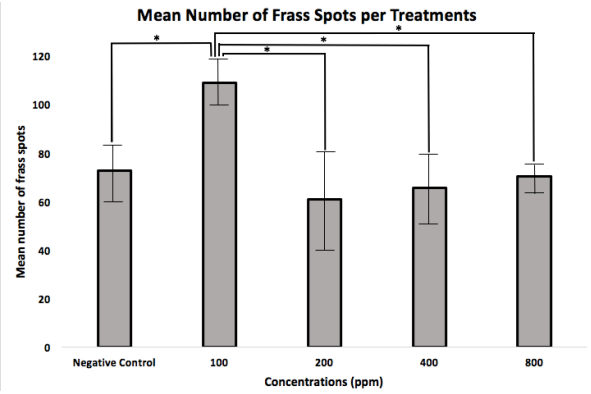

Figure 1. The total mean number of frass spots correlated with treatment concentration after 48 hours (* denotes that the $p \leq 0.05$, thus there is a significant difference between means of the frass spots).

Antifeedant bioactivity. The results of Fisher's protected LSD test showed there was no antifeedant bioactivity observed between the four treatments and the control groups. Based on these results, *Anethum graveolens* essential oil did not show antifeedant bioactivity against *Cochlochila bullita*.

The result of this study is in conjunction with a study conducted by Kumar et al. [22], which investigated the bio-efficacy of plant essential oils and insecticides against *Cochlochila bullita* on *Ocimum basilicum*. The study revealed that karanj oil and neem oil containing monoterpenes were least effective in reducing the lace bug population in comparison to the synthetic pesticides prophenophos, imidacloprid, and malathion. Due to the insecticidal activity of essential oils being linked to their terpene contents, it is possible that terpenes are ineffective against *Cochlochilla bullita*.

The concentrations (100ppm, 200ppm, 400ppm, 800ppm) used for this study was based on a study conducted by Khosravi and Sendi [18], wherein toxic effects of the essential oils of *Thymus vulgaris L.* (garden thyme) and *Lavandula angustifolia L.* (lavander) were observed against the elm leaf beetle *Xanthogaleruca luteola*. However, the concentrations used for this study were lower compared to the *Hedychium* essential oil concentrations used against azalea lace bugs in an earlier study by Sakhanokho et al. [12].

According to Fatope et al. [13], the major cytotoxic components of *Anethum graveolens* include carvone, dihydrocarvone, and limonene. The study of Ibrahim et al. [23] found that monoterpenes such as limonene found in plants or artificial food of herbivorous insects can positively and negatively influence the food consumption of different types of insects. The study of Alfaro et al. [24] found that the limonene concentrations stimulated feeding for another insect pest, *Pissodes strobi*, when at low

concentrations. They mentioned that some monoterpenes may act as synergists for nonvolatile feeding stimulants at low concentrations, but act as feeding inhibitors at higher concentrations. The significantly higher feeding observed in 100ppm treatment, compared to the other treatments with higher concentrations, may be attributed to each treatment's concentration of limonene content of the *Anethum graveolens* essential oil, of which the 100ppm treatment had the lowest concentration.

In addition to four (4) treatment concentrations and a negative control group, an additional treatment with three replicates consisting of 0.4% DMSO emulsifier and distilled water was utilized and had undergone the process simultaneously along with the other treatments.

Most studies involving the use of dimethyl sulfoxide primarily used it as a negative control [25] or as a solvent [26]. Additionally, a study by Orchard et al. [27], which studied the influence of different carrier oils on the antimicrobial and cytotoxic effects of different essential oils, simply used DMSO as a solvent for its negative control, which was seawater, to mimic a natural environment. The use of DMSO as the negative control in this study was done to determine whether or not DMSO, the emulsifier, would have any effect on the antifeedant bioactivity of *Anethum graveolens* against *Cochlochila bullita*.

Limitations. *Anethum graveolens* essential oil was commercially purchased online with a certificate of analysis acquired from the online seller. The lace bugs in the bioassay test was limited to the adult stage of their life cycle. Additionally, the age of these adult lace bugs was not controlled. The age of the *Ocimum kilimandscharicum* (sweet basil) plants for the experiment was not determined due to the limited number of basil plants that could be procured. The study measured the antifeedant bioactivity based on the frass spots observed. There was no positive control used in the experiment due to lack of a known product that causes antifeedancy against *Cochlochila bullita*.

Conclusion. The statistical analysis showed no antifeedant bioactivity against lace bugs. Thus, it can be concluded that there is no antifeedant bioactivity in the essential oil of *Anethum graveolens* against *Cochlochilla bullita* when used at concentrations of 100, 200, 400, and 800ppm.

Recommendations. The results obtained from the present investigation suggest that further studies on promising organic plant based essential oils must be studied regarding their potential antifeedant bioactivity against *Cochlochila bullita*. In order to further develop this study, future researchers are recommended to: (i) increase the amount of concentration of *Anethum graveolens* essential oil in the treatments to be used; (ii) consider how to culture *Cochlochila bullita* to take into account the life stage and age of the lace bugs to be subjected to experimentation; (iii) increase the number of replicates in order to make the data more reliable; (iv) maintain the temperature inside the laboratory at an optimal temperature range for lace bug development which is 19°C-33°C [28]; (v) take into account the age of the basil plants that will be utilized during the bioassay test; and (vi) consider the amount of limonene present in the treatments.

Acknowledgement. The researchers would like to extend their utmost gratitude to the people and organizations who have made this study successful. These include Iloilo Research Outreach Station at Sta. Barbara, Iloilo for helping them identify their basil plants, and Orchard Valley at Pavia, Iloilo for giving them permission to collect *Cochlochila bullita* (lace bugs) for their experiment. The researchers would also like to express their utmost gratitude to their entomologist, Prof. Ma. Victoria Seredrica, for without her assistance and guidance, this study would not be possible.

References

[1] Sathe TV, Sathe NT, Ghodake D, Sathe A. 2014. Sucking insect pests and medicinal value of Tulsi, *Ocimum sanctum L.* (Lamiaceae). Indian Journ. of Appl. Res. 4(3):31-33

[2] Joshi RK. 2014. Chemical composition and antimicrobial activity of the essential oil of *Ocimum basilicum L.* (sweet basil) from Western Ghats of North West Karnataka, India. Anc Sci Life. 2014 Jan-Mar; 33(3): 151–156. doi: 10.4103/0257-7941.144618.

[3] Zala MB, Patel BN, Vegad NM. 2016. Report on incidence of lace wing bug, *Monanthia globulifera* Walker on sweet basil (*Ocimum basilicum* L.) in middle Gujarat. Current Biotica.10(3):258-260.

[4] Sajap A, Peng T. 2010.The lace bug *Cochlochila bullita (Stål)* (Heteroptera: Tingidae), a potential pest of *Orthosiphon stamineus Bentham* (Lamiales: Lamiaceae) in Malaysia. *Insecta Mundi*. Paper 654. http://digitalcommons.unl.edu/insectamundi/654

[5] Kim CS, Park JD, Byun BH, Park Il Chae CS. 2000. Chemical control of sycamore lace bug, *Corythucha ciliata* (Say). J. of Kor. For. Soc. 89: 384-388.

[6] Devine G, Furlong M. 2007. Insecticide use: Contexts and ecological consequences. Agri Human Values. 24: 281-306.

[7] Kim K, Kabir E, Jahan SA. 2018. Exposure to pesticides and the associated human health effects. Sci Total Environ. 575:525–535.

[8] Sharopov F, Wink M, Gulmodorov I, Isupov S, Zhang H, Setzer W. 2013. Composition and bioactivity of the essential oil of *Anethum graveolens* L. from Tajikstan.Int J Med Arom Plants.3(2): 125-130.

[9] Babri RA, Khokhar I, Mahmood Z, Mahmud S. 2012. Chemical composition and insecticidal activity of the essential oil of *Anethum graveolens* L.Sci.Int.(Lahore). 24(4):453-455.

[10] Yildrim E, Emsen B, Kordali S. 2013. Insecticidal effects of monoterpenes on *Sitophilus zeamais Motschulsky* (Coleoptera: Curculionidae). J. of Appl Bot and Food Qual 86, 198 - 204 (2013), doi:10.5073/JABFQ.2013.086.027

[11] Jana S, Shekhawat GS. 2010.*Anethum graveolens* An Indian traditional medicinal herb and spice.Pharmacogn Rev.4(8):179–184.

[12] Sakhanokho H, Sampson B, Tabanca N, Wedge D, Demirci B, Baser K, Bernier U., Tsikolia M., Agramonte N., Beenel J., Chen J., Rajasekaran K., Spiers J. 2013. Chemical composition, antifungal and insecticidal activities of *Hedychium* essential oils. Mol.2013(18): 4308-4327.

[13] Fatope MO, Marwah RG,Onifade AK, Ochei JE, Al Mahroqi YKS. 2008. 13C NMR Analysis and Antifungal and Insecticidal Activities of Oman Dill Herb Oil. Pharmaceutical Biology, 44:1, 44-49, DOI: 10.1080/13880200500530716

[14] Kordan B, Gabrys B. 2013. Feeding deterrent activity of natural monoterpenoids against larvae of the large white butterfly *Piersis brassicae* (L.). Pol. J. Natur. Sc. 28 (1): 63-69.

[15] Schlyter F, Smitt O., Sjodub K, Hogberg HE, Lofqvist J. 2004. Carvone and less volatile analogues as repellent and deterrent antifeedants against the pine weevil, *Hylobius abietis*. JEN 128(9/10) doi:10.1111/j.1439-0418.2004.00889.610–619.

[16] Rojht H, Meško A, Vidrih M, Trdan S. 2009. Insecticidal activity of four different substances against larvae and adults of sycamore lace bug (*Corythucha ciliata* [Say], Heteroptera, Tingidae). Acta agriculturae Slovenica, 93 - 1, maj 2009 str. 31 - 36.

[17] Nair S, Braman SK, Knauft DA. 2012.Host Plant Utilization Within Family Ericaceae by the Andromeda Lace Bug *Stephanitis takeyai* (Hemiptera: Tingidae). J. Environ. Hort. 30(3):132–136

[18] Khosravi R, Sendi JJ. 2013. Toxicity, development and physiological effect of *Thymus vulgaris* and *Lavandula angustifolia* essential oils on *Xanthogaleruca luteola* (Coleoptera: *Chrysomelidae*). Jour. of King Saud Univ. 25, 349-355.

[19] Shukla P, Vidyasagar SPV, Aldosari SA, Abdel-azim M. 2012. Antifeedant activity of three essential oils against the red palm weevil, *Rhynchophorus ferrugineus*. Bulletin of Insectology 65 (1): 71-76, 2012 ISSN 1721-8861

[20] Schoonhoven LM. 1982. Biological Aspects Of Antifeedants.*Ned. Entomol. Vet. Amsterdam*. 31; 57-69.

[21] JeniLapinangga N, Bunga JA, Sonbai JHH, Da Lopez YF. 2018. Utilization of Local Vegetable Materials To Control *Cylasformicarius* Pest Plant Power Plants. Jour of Agri and Vet Sci. 11(6):58-62

[22] Kumar S, Kumar N, Kumar A. 2017. Bio-efficacy of botanical and insecticides for management of lace bug, *Cochlochila bullita (Stål)* on sweet basil, *Ocimum basilicum* L. Annals of Plant Protection Sciences (25)1:57-59

[23] Ibrahim MA, Kainulainen P, Aflatuni A, Tiilikkala K, Holopainen JK. 2001. Insecticidal, repellent, antimicrobial activity and phytotoxicity of essential oils: With special reference to limonene and its suitability for control of insect pests (Review), Agricultural and Food Science in Finland, 10(3): 243-260

[24] Alfaro RI, Pierce HD Jr., Borden JH, Oehlschlager, AC. 1980. Role of volatile and nonvolatile components of Sitka spruce bark as feeding stimulants for *Pissodes strobi* Peck (Coleoptera: Curcullionidae). Canadian Journal of Zoology 58: 626–632.

[25] Bosnić T, Softić D, Grujić-Vasić J. 2006. Antimicrobial Activity of Some Essential Oils and Major Constituents of Essential Oils. Acta Medica Academica 2006; 35:19-22.

[26] Andrade MA, Cardoso MG, Batista LR, Freire JM, Nelson DL 2011. Antimicrobial activity and chemical composition of essential oil of *Pelargonium odoratissimum*. Revista Brasileira de Farmacognosia Brazilian Journal of Pharmacognosy 21(1): 47-52. DOI: 10.1590/S0102-695X20110050000009

[27] Orchard A, Kamatou G, Viljoen AM, Patel N, Mawela P, van Vuuren SF. 2019. The Influence of Carrier Oils on the Antimicrobial Activity and Cytotoxicity of Essential Oils. Evidence-Based Complementary and Alternative Medicine. DOI: 10.1155/2019/6981305

[28] Ju RT, Wang F, Li B. 2011. Effects of temperature on the development and population growth of the sycamore lace bug, *Corythucha ciliata.* J. of Ins. Sci 11(1): 16. https://doi.org/10.1673/031.011.0116

Isolation, characterization and screening of bacterial endophytes from *Zea mays L. var. rugosa* (sweet corn) Sugar King variety with biotechnological potential in agriculture

DANILEE JOSHUA S. HALABA, JONATHAN S. MOLINOS, JP P. SUPERFICIAL and ANDREA LUCYLE BELA-ONG

Philippine Science High School - Western Visayas Campus, Brgy. Bito-on, Jaro, Iloilo City 5000, Department of Science and Technology, Philippines

Abstract

This study aimed to determine the plant growth promoting activities exhibited by bacterial endophytes isolated from the roots of *Zea mays L. var. rugosa* (sweet corn) Sugar King. A total of eight different bacterial strains were isolated and characterized through Gram staining and screened for a positive reaction for nitrogen fixation, ammonia production and zinc solubilization through the use of Jensen's media, peptone water with Nessler's reagent, and zinc incorporated media, respectively. Results showed that Gram-negative bacteria were the dominant group. Colony characterization showed that circular forms comprised the majority. Similarly, the colonies with entire forms and either pulvinate or flat elevation were recurrent throughout the isolates. Cell characterization revealed that all isolates were rod in shape. The plant growth promoting screenings revealed that all isolates were plant growth promoters. All were found to be positive for ammonia production and zinc solubilization; however, none were found to be positive for nitrogen fixation.

Keywords: *endophytes, nitrogen fixation, ammonia production, zinc solubilization, Zea mays L. var. rugosa*

Introduction. Endophytes are organisms, often fungi and bacteria, that live between living plant cells [1]. They are defined as microorganisms that could be isolated from surface-sterilized plant tissues and do not visibly harm host plants. Endophytism is a universal phenomenon, and it is likely that all plants harbor endophytic bacteria [1]. There have been studies on the characterization and testing of endophytic bacteria for their beneficial effects on plants. It has been shown that some species of endophytic bacteria were able to produce indole-3-acetic acid which can promote plant growth [3]. Endophytic bacteria can also do nitrogen fixation in order to assist plants in obtaining nitrogen, which they use to promote growth development. Other plant growth enhancing capabilities were characterized by the ability to produce siderophores, ammonia, phytohormones, inorganic phosphate solubilization and biocatalyst like cellulase, amylase and protease [14]. Endophytic bacteria are also capable of being a biocontrol agent due to a mechanism of antibiosis which makes substances to be used against organisms that are harmful to the host plant [11]. In order for the endophytic bacteria and its host plant to have a symbiotic relationship, it is essential for the host plant to supply metabolites and nutrients to the endophyte and for the endophyte to produce auxins and do other plant growth promoting activities such as nitrogen fixation and phosphate solubilization. In order to be able to fully utilize these microorganisms, screening of endophytic bacteria having plant growth promoting abilities is necessary.

Corn is one of the staple food crops in the Philippines. Most of the corn sold in markets today are hybrids due to the advanced traits they have over natural corn. The *Zea mays L. var. Rugosa* (sweet corn) Sugar King variety was selected for the study due to its early maturity, uniform large cobs, good husk protection, and a strong plant habit designed for most weather conditions. These traits are considered as the possible benefits of the plant growth promoting activities that were screened for.

Using culture-dependent isolation techniques and standard procedures for the testing of plant growth promoting factors of the bacteria, the study focused on the characterization and screening of endophytic bacteria present in the roots of the corn hybrid variety *Zea mays L. var. rugosa* (sweet corn) Sugar King. The samples were characterized based on colony morphology, cell morphology and Gram stain. Bacterial strains from the isolated samples were not identified. Bacterial samples were inoculated into selective media to test for plant growth promoting activities. Jensen's media, peptone water, and zinc incorporated media were used to screen nitrogen fixing, ammonia producing and zinc solubilizing bacteria, respectively. The plant growth promoting activities associated with each cultured bacteria were also determined.

The study aimed to isolate, characterize, and screen endophytic bacteria present in the roots of *Zea mays L. var. rugosa* (sweet corn) Sugar King variety for plant growth promoting activities, which can be used as biofertilizers. It specifically aimed to:

How to cite this article:
CSE: Halaba DJ, Molinos J, Superficial J, Bela-ong AL. 2020. Isolation, characterization and screening of bacterial endophytes from *Zea mays L. var. rugosa* (sweet corn) Sugar King variety with biotechnological potential in agriculture. Publiscience. 3(1):68-72.
APA: Halaba, D. J. S., Molinos, J. S., Superficial, J. P., & Bela-ong, A.L. (2020). Isolation, characterization and screening of bacterial endophytes from *Zea mays L. var. rugosa* (sweet corn) Sugar King variety with biotechnological potential in agriculture, *Publiscience*, 3(1):68-72.

(i) isolate endophytic bacteria from Sugar King variety sweet corn using culture-dependent isolation methods;

(ii) characterize endophytic bacteria isolated from Sugar King variety sweet corn using culture-dependent isolation methods; and

(iii) screen the endophytic bacteria for plant growth promoting factors such as ammonia production, nitrogen fixation, and zinc solubilization.

Methods. Sweet corn gathered from Barangay Agutayan, Sta. Barbara, Iloilo were screened for possible activities on nitrogen fixation, ammonia production, and zinc solubilization. A total of nine samples were randomly selected and three mixed culture plates were generated from the gathered samples. The three mixed culture plates contained eight pure bacterial strains and each were then characterized based on their colony morphology, cell morphology and Gram stain. Each bacterial strain was tested for positivity in nitrogen fixation, ammonia production, and zinc solubilization through the use of selective media.

Preparation of Growth Media. Trypticase Soy Agar (TSA) and Trypticase Soy Broth (TSB) were used as growth media for the isolated bacterial endophytes. Three media bottles were each filled with 20 g of TSA and 500 mL of distilled water while another was filled with 6 g of TSB and 200 mL of distilled water. The mixtures were then boiled using a hot plate and continuously stirred using a sterile glass stirring rod until a clear solution was formed. After boiling, the solutions were sterilized in an autoclave at 121° C for 15 minutes, then was allowed to cool down for 3-4 minutes before being distributed. Sixty standard sized Petri dishes were filled with the TSA solution until the bottom of each dish was fully covered while 20 sterile test tubes were each filled with 10 mL of the TSB solution. The plates and test tubes were then allowed to rest for a few minutes before being stored at 2-8° C in a refrigerator.

Preparation of Selective Media. Jensens's media, peptone water, and zinc incorporated media were used for the screening of nitrogen fixation, ammonia production and zinc solubilization, respectively. In making Jensens's media, the procedure by Richard et al. [16] was followed. Twenty grams of sucrose, 1g of dipotassium phosphate, 0.500g of magnesium sulphate, 0.500g of sodium chloride, 0.100g of ferrous sulphate, 2g of calcium carbonate and 15g of agar were suspended in 1L of distilled water in a culture bottle. In making peptone water, the guideline reported by Jorgensen et al. [9] was followed. In a culture bottle, 10g of peptone and 5g of sodium chloride were suspended in 1L of distilled water. In making zinc incorporated media, the procedure by Kamran et al. [10] was followed. Half a gram of zinc chloride was suspended in 500 mL of TSA in a culture bottle. The three mixtures were then boiled using a hot plate and continuously stirred using a sterile glass stirring rod until a clear solution was formed. After boiling, the solutions were sterilized in an autoclave at 121° C for 15 minutes, then was allowed to cool down for 3-4 minutes, before being labelled and stored at 2-8° C in a refrigerator.

Sample Gathering. Samples of Sugar King variety sweet corn roots (SCR) were gathered from Brgy. Agutayan of Sta. Barbara, Iloilo. Nine root samples were gathered randomly and stored in polythene bags inside a cooler partially filled with ice, in order to minimize bacterial activity, before being transferred to the Microbiology Laboratory of PSHS-WVC.

Surface Sterilization. Following the procedure for surface sterilization by Youseif [18], samples were surface sterilized with 70% ethyl alcohol and bathed in 1% sodium hypochlorite for two minutes. The outside surface of the samples was inoculated onto TSA plates to check for sterilization efficiency. Respective samples from agar plates that showed no signs of microbial growth were gathered and smashed together using a mortar and pestle in preparation for the serial dilution.

Serial Dilution. Three sets of three test tubes, labelled 10^{-1},10^{-2}, and 10^{-3}, respectively, were filled with 9 mL of 0.9% saline solution. One gram of the sample was added to each of the test tube labelled 10^{-1}. Before the sample settled, 1 mL of the suspension was transferred into the test tubes labeled 10^{-2} using a micropipette. The procedure was repeated once again to achieve a concentration of 10^{-3}.

Isolation of Mixed Culture. One drop of the diluted samples from the test tubes labelled 10^{-3} was pipetted onto one side of an agar plate. Using an inoculating loop heat-sterilized using an alcohol lamp, the sample was streaked on the agar plate using the quadrant streak method. The agar plates were then incubated for 24 hours at 37° C. The plates were placed upside-down during the incubation period to avoid the interference of condensation in the growth of the microbes. After the incubation period, the colony morphology of the microbial plates was observed. Those with the same morphology were classified as the same colonies before the isolation of pure cultures to avoid multiple cultures of the same bacteria.

Isolation of Pure Culture (TSA). For the agar culture, a sterile inoculating loop was used to transfer bacteria from the mixed culture plate to another agar plate. The bacteria were then streaked using the quadrant streak method and incubated at 37°C for 24 hours.

Isolation of Pure Culture (TSB). A stock culture for each isolated colony was prepared. A sterile inoculating loop was gently touched to the surface of an existing colony to gather the bacteria. The loop was then inserted into the broth, moving the loop back and forth to ensure the inoculation of the bacteria to the media. The broth was then incubated at 37°C for 24 hours. Pure culture colonies were necessary for the biochemical testings as bacteria may react differently in isolation than when it is combined with other species.

Colony morphology. Colony morphology was observed before and after the isolation of pure culture bacterial colonies to ensure that the colonies isolated were correct. The shape, margin, elevation, size, color, and texture of the bacterial colony were identified. This determined the groupings, based on the similarities of their characteristics, for the isolation of pure culture colonies.

Cell morphology. Microscopy was conducted to determine the shape and arrangement of the bacterial cell.

Gram staining. From each pure culture colony grown, a bacterial smear was prepared. Smears were prepared by heat fixing bacteria onto a sterile glass slide. Following the procedure of Jorgenson et al. [9], the smears were then saturated with the following reagents: the primary stain crystal violet for 1 minute; Gram's iodine solution for 1 minute; 95% ethanol for 5 seconds; and the counterstain safranin for 1 minute rinsing the glass slide with distilled water after the addition of each reagent. During microscopy, purple-stained bacteria were considered Gram-positive while pink-stained bacteria were considered Gram-negative.

Screening Nitrogen Fixation. The procedure for nitrogen fixation screening by Ebeltagy et al. [5] was followed. Nitrogen-free malate agar (Jensen's media) was used in the screening for nitrogen fixation with bromothymol blue (BTB) acting as an indicator [8]. The isolates were then incubated at 37°C for 24 hours. Isolates with blue colored zones were marked as nitrogen fixers.

Screening Ammonia Production. The procedure for ammonia production screening by Richard et al. [16] was followed. Isolates were inoculated into 10 mL peptone water in separate test tubes, then incubated for 2-3 days at 28 ± 2 degrees Celsius. After the addition of 0.5 ml of Nessler's reagent, isolates that produced a brown-yellow discoloration were marked positive for ammonia production.

Screening Zinc Solubilization. The procedure for zinc solubilization screening by Kamran et al. [9] was followed. Zinc chloride ($ZnCl_2$) medium plates were used in the screening for zinc solubilization. The isolates were aseptically inoculated as a spot on the respective medium plates and covered with aluminum foil. They were then incubated in the dark at 28° C for one day. The presence of clear zones around the colony indicated the presence of zinc solubilizing strains.

Data Analysis. The basis for positive results in each screening was from past articles [9,10,16]. Evaluation of results were done through visual assessment and were verified by a licensed medical technologist.

Safety Procedure. While in the process of isolation and handling of bacteria, proper lab equipment such as lab gowns, sterile gloves, and masks were used to ensure the prevention of contamination and infection of bacteria. Used gloves, tissues, and other trash were properly disposed into designated disposal bins inside the Microbiology Laboratory of PSHS-WVC. Bacteria cultures were properly decontaminated with 10% sodium hypochlorite. Work areas were disinfected with 70% ethyl alcohol after working.

Results and Discussion. Results obtained from the study revealed that *Zea mays L. var. rugosa* (sweet corn) Sugar King variety harbors culturable endophytic bacteria. Eight bacterial strains were isolated from the sweet corn roots (SCR). All isolates were characterized based on their colony morphology, cell morphology, and Gram stain (Table 1). Five of the isolates (SCR 2, SCR 3, SCR 4, SCR5 and SCR 7) were Gram-negative (Figure 1) while three (SCR 1, SCR 6, and SCR 8) were Gram-positive (Figure 2).

Table 1. Morphological characteristics of individual strains.

Isolate*	Colony Morphology	Cell Morphology	Gram +/-
SCR 1	Circular, Lobate, Umbonate, Moderate, Brown, Smooth	Rod	Gram +
SCR 2	Rhizoid, Rhizoidal, Flat, Moderate, White, Rough	Rod	Gram -
SCR 3	Irregular, Entire, Flat, Small, White, Smooth	Rod	Gram -
SCR 4	Circular, Lobate, Raised, Moderate, Dark, Brown, Smooth	Rod	Gram -
SCR 5	Circular, Entire, Pulvinate, Moderate, Brown, Rough	Rod	Gram -
SCR 6	Circular, Entire, Pulvinate, Small, Orange, Smooth	Rod	Gram +
SCR 7	Circular, Entire, Pulvinate, Moderate, Brown, Smooth	Rod	Gram -
SCR 8	Irregular, Lobate, Flat, Moderate, Brown, Smooth	Rod	Gram +

*Nomenclature was given based on the crop and tissue type isolated which is sweet corn root (SCR).

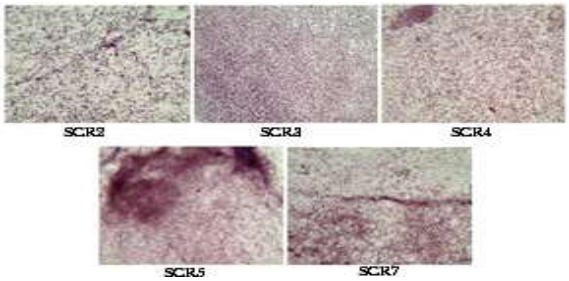

Figure 1. Isolates of the sweet corn root (SCR) that did not retain the crystal violet stain indicating it as Gram-negative.

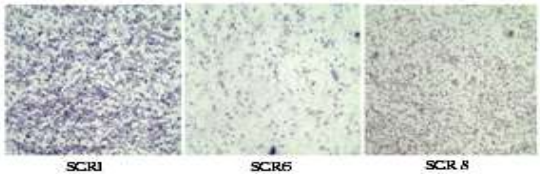

Figure 2. Isolates of the sweet corn root (SCR) that did retain the crystal violet stain indicating it as Gram-positive.

For the characterization of the bacteria based on colony and cell morphology as well as Gram Stain, results showed that the endophytic bacteria lcommunity of the Sugar King sweet corn was composed of both Gram-positive and Gram-negative bacteria. Gram-negative stain, circular form, entire margin, pulvinate and flat elevations, and rod shape predominated among all isolates.

The functional potentialities in relation to plant growth promoting activities of root isolates were assessed. Strains were tested in vitro for their ability to conduct three plant growth promoting activities such as ammonia production, nitrogen fixation and zinc solubilization (Table 2).

Table 2. Presence of plant growth promoting activities in endophytic bacteria from *Zea mays* roots.

Isolate*	Ammonia Production	Nitrogen Fixation	Zinc Solubilization
SCR 1	Present	Absent	Present
SCR 2	Present	Absent	Present
SCR 3	Present	Absent	Present
SCR 4	Present	Absent	Present
SCR 5	Present	Absent	Present
SCR 6	Present	Absent	Present
SCR 7	Present	Absent	Present
SCR 8	Present	Absent	Present

*Nomenclature was given based on the crop and tissue type isolated which is sweet corn root (SCR).

The results demonstrated that the endophytic bacterial community isolated were all capable of producing ammonia, with SRC 2 and SRC 3 exhibiting maximum production. Marques et al. [13] suggested that the ammonia produced by endophytes is beneficial for the root and shoot elongation, consequently increasing plant biomass. Presence of these endophytes may have contributed to the large cobs and sturdy structure characterized by the sweet corn Sugar King variety. Nitrogen fixation is another biological process that plants undergo in order to take in nitrogen. It is an important biological process wherein bacteria convert molecular nitrogen, which plants cannot utilize, into usable forms like ammonia [15]. None of the strains isolated were able to fix nitrogen during the screening. This may be either due to all isolates being not really able to fix nitrogen or an error was conducted during the screening, specifically during the formulation of the selective media. All endophytic isolates of *Zea mays L. var. rugosa* were observed to be zinc solubilizers. So far, the *Bacillus spp.* and *Pseudomonas spp,* both of which are rods, are the only bacterial species from maize crops that were reported to be zinc solubilizers as they form a clear halo zone [10]. Reports from past studies have confirmed that zinc solubilizing strains significantly improved the activity of enzymes, plant growth, yield attributes and successfully biofortified maize grains aside from the increase in zinc content [9].

Endophtic bacteria are tissure specific, but not plant specific [18], meaning that the strains isolated from the study could be utilized as bio-fertilizers, which are becoming more and more popular in many countries, for many crops. Biofertilizers are natural products carrying living organisms derived from plant organs or soil itself, so they do not have any ill effects on soil health or the environment, unlike chemical fertilizers. In modern agriculture, chemical fertilizers have degraded the fertility of soil making it unsuitable for raising crop plants. In addition, the intensive use of these inputs has also led to severe health and environmental hazards such as soil erosion, water contamination, pesticide poisoning, falling groundwater table, water logging and depletion of biodiversity. Although chemical fertilizers are more commonly used, bio-fertilizers are more practical and beneficial to farmers and agriculturalists. Saeed et al. [17] reported that biofertilizers increased yield, yield components and growth promotion better than chemical fertilizers. Biofertilizers naturally activate the microorganisms found in the soil. Being cheaper, more effective and environmentally friendly, biofertilizers are gaining importance for use in crop production, restoring the soil's natural fertility and protecting it against drought, soil diseases and therefore stimulate plant growth. This shows that biofertilizers that utilize plant growth promoting endophytes are practically and economically better than chemical fertilizers. Endophytic bacteria isolated from *Zea mays L. var. rugosa* exhibiting capabilities for plant growth promotion (specifically ammonia production and zinc solubilization) could have potential use for biotechnological purposes in agriculture, in particular, as biofertilizers.

Limitations. The data presented in the study is exclusive to the sweet corn hybrid variety *Zea mays L. var. Rugosa.* The selective media used in the study were verified by only one licensed medical technologist. Due to the lack of resources, the researchers were not able to identify the isolated bacterial strains.

Conclusion. The present study showed that Zea *mays L. var. rugosa* (sweet corn) Sugar King variety is home for diverse plant growth promoting bacterial endophytes. Being able to showcase plant growth promoting activities, inoculation of maize plants with these endophytic representatives may result to a more stimulated plant growth and increased biomass production compared to uninoculated plants. The present study suggests the potential application of these endophytes in agricultural traits that could result in reduced input costs due to the use of agro-chemicals, better production yield and health, and in a way, may lead to improved soil quality and fertility. However, further field experiments and actual identification of the representative endophytes are encouraged to support the findings of the study.

Recommendations. It is recommended to add screenings for other important plant growth promoting activities such as indole acetic acid production and phosphate. Future researchers of similar field can use other corn hybrids as the plant sample to see differences in the resulting isolated bacteria. It is also recommended to consult experts on how to make the various growth media to be used for screening to further legitimize the results.

Increasing the sample size can improve the quality of the gathered data being a more accurate representation of the endophytic bacterial community from the sample site. For the success of biofertilizer technology and the utilization of endophytes, further research and development is needed to understand the mechanisms of action of various biofertilizers and to find out more competent endophytic strains and carrier materials to make agriculture practices more sustainable and economical. Finally, identification of bacterial strains is recommended to further strengthen the legitimacy of the study.

Acknowledgement. The researchers would like to give their thanks to the staff of the DOST-Region VI who entertained their inquiries and assisted them with patience and politeness. The researchers would also like to express their thanks to the people of the Department of Agriculture - Sta. Barbara for giving assistance to the researchers, and to Mr. Alex Alemane for being generous in the provision and collection of the samples.

References

[1]Correa-Galeote D, Bedmar EJ and Arone GJ .2018. Maize endophytic bacterial diversity as affected by soil cultivation history. Front. Microbiol. 9:484.

[2] Disi J, Zebelo S, Kloepper J, Fadamiro H. 2018. Seed inoculation with beneficial rhizobacteria affects European corn borer (Lepidoptera: Pyralidae) oviposition on maize plants. Entomological science. 21(1):48-58.

[3] Duangpaeng A, Phetcharat P, Chanthapho S, Boonkantong N, Okuda N. 2012. The study and development of endophytic bacteria for enhancing organic rice growth. Procedia Engineering. 32: 172-176.

[4] Ek-Ramos M, Gomez-Flores R, Orozco-Flores A, Rodriguez-Padilla C, Gonzalez-Ochoa G, Tamez-Guerra P. 2019. Bioactive products from plant-endophytic gram-positive bacteria. Front Microbiol. 10: 463

[5] Ebeltagy A, Nishioka K, Sato S, Ye B, Hamada T, Isawa, Mitsui H, Minamisawa K. 2001. Endophytic colonization and in planta nitrogen fixation by a *Herbaspirillum sp.* isolated from wild rice. Appl Environ Microbiol. 67: 5285-5293.

[6] Ferreira N, Mazzuchelli R, Pacheco A, Araujo F, Antunes J, Araujo A. 2018. *Bacillus subtilis* improves maize tolerance to salinity. Ciência Rural. 48(8).

[7] Geetha K, Venkatesham E, Hindumathi A, Bhadraiah. 2014. Isolation, screening and characterization of plant growth promoting bacteria and their effect on *Vigna Radita* (L.) R. Wilczek. Int J Curr Microbiol App Sci. 3(6): 799-809.

[8] Gothwal R, Nigam V, Mohan M, Sasmal D, Ghosh P. 2007. Screening of nitrogen fixers from rhizospheric bacterial isolates associated with important desert plants. Aookied Ecology and Environmental Research. 6(2): 101-109.

[9] Jorgensen JH, Pfaller MA, Carroll KC, Funke G, LAndry ML, Richter SS, Warnock DW. 2015. Manual of Clinical Microbiology. 11(1)

[10] Kamran S, Shahid I, Baig DN, Rizwan M, Malik KA, Mehnaz S. 2017. Contribution of Zinc Solubilizing Bacteria in Growth Promotion and Zinc Content of Wheat. *Front Microbiol*. doi:10.3389/fmicb.2017.02593

[11] Kandel S et al. 2017. An *In vitro* study of bio-control and plant growth promotion potential of Salicaceae Endophytes. Front Microbiol. 8: 386.

[12] Kauffmann F and Møller V. 1955. On amino acid decarboxylases of Salmonella types and on the KCN test. Acta pathologica et microbiologica Scandinavica. 36(2):173-8.

[13] Marques A, Pires C, Moreira H, Rangel A, Castro P. 2010. Assessment of the plant growth promotion abilities of six bacterial isolates using Zea mays as indicator plant. Soil Biology and Biochemistry. 42(8):1229-35.

[14] Nawangshi A, Damayanti I, Wiyono S, Kartika J. 2011. Selection and characterization of endophytic bacteria as biocontrol agents of tomato bacterial wilt disease. Biosciences. 18(2): 66 – 70.

[15] Passari A, Mishra V, Leo V, Gupta V, Singh B. 2016. Phytohormone production endowed with antagonistic potential and plant growth promoting abilities of culturable endophytic bacteria isolated from *Clerodendrum colebrookianum* Walp. Microbiol. 193: 57-73.

[16] Richard P, Adekanmbi A, Ogunjobi A. 2018. Screening of bacteria isolated from the rhizosphere of maize plant (*Zea mays* L.) for ammonia production and nitrogen fixation. Microbiol. 12(34): 829-837.

[17] Saeed K, Ahmed S, Hassan I, Ahmed P. 2015. Effect of bio-fertilizer and chemical fertilizer on growth and yield in cucumber (Cucumis sativus) in green house condition. Pak J Biol Sci. 18(3):129-34.

[18] Youseif S. 2018. Genetic diversity of plant growth promoting rhizobacteria and their effects on the growth of maize plants under greenhouse conditions. Annals of Agriculture Sciences. 63 (2018): 25-3

SUMALONGSON

AQUATIC AND NATURAL RESOURCES

SUMALONGSON is a figure in the Visayan pantheon responsible for the rivers and seas. Much of the world is composed of water, housing numerous organisms essential in the balance of the ecosystem and the sustenance of the human population. This section contains studies that identify potential risks, and addressing emerging issues affecting aquaculture, fisheries, and forestry.

These studies fall under the Agriculture, Aquatic and Natural Resources (AANR) Research and Development Agenda. These address research for aquatic and natural resources geared towards the improvement of the community.

BASED ON: Harmonized National Research and Development Agenda (HNRDA)

Publiscience Vol. 3 Issue 1

Mapping mangrove forest land cover change in Jaro Floodway, Iloilo City using Google Earth imagery

MARY YSHABELLE M. FLORES, and ARIS C. LARRODER

Philippine Science High School - Western Visayas Campus, Brgy. Bito-on, Jaro, Iloilo City 5000, Department of Science and Technology, Philippines

Abstract

The construction of the Jaro Floodway was completed in 2011 to divert the floodwater from the Jaro River towards the Iloilo Strait. Its construction may pose a threat to the nearby mangrove forest due to its large-scale anthropogenic disturbance. This study aims to determine the effect of the floodway to the nearby mangrove forest in terms of its areal change. Google Earth imagery was downloaded for the years 2005, 2009, 2012, 2014, 2016, and 2018. The images were digitized in Quantum Geographic Information System (QGIS) and classified into four thematic classes, namely, mangrove, non-mangrove, fishpond, and water. Mangrove cover increased throughout the years measuring 8.98 (2005), 9.35 (2009), 11.39 (2012), 16.60 (2014), 26.82 (2016), and 42.98 ha (2018). The general increase in mangroves is attributed to a combination of factors such as sedimentation rate and mangrove planting efforts. Its construction led to the formation of a new delta which the mangroves currently thrive in.

Keywords: *mangrove colonization; sedimentation; remote sensing; mapping; satellite imagery*

Introduction. Mangroves in the Philippines have significantly decreased by 51% throughout the years, where it amounted to approximately 500, 000 hectares in 1918 and about 256, 000 hectares in 2010 [1,2,3,4]. Anthropogenic disturbances, illegal logging, urban development, agriculture, aquaculture, and natural disasters (e.g. storm surges, tsunamis, flooding) are the primary causes which have been attributed to the degradation of mangroves in the Philippines [4,5]. However, environmental factors such as wave action, duration and depth of tidal inundation, salinity, sediment accretion, and ground subsidence might have also influenced the colonization of the mangroves [2]. Studies such as those of Albano [2], Long et al. [3,4], Dan et al. [6], Fromard et al. [7], Heumann [8], and Nascimento et al. [9] have used remote sensing to measure the mangrove cover in the study area.

The construction of the Jaro Floodway was completed in 2011 with the goal to minimize the flooding in Iloilo City by diverting the floodwater from the Jaro River to the Iloilo Strait. It is 4.8 km long and 82 m wide and designed to protect the city against a 20-year flood return period [10]. However, its construction may pose a threat to the nearby mangrove forest due to its large-scale anthropogenic disturbance, which may lead to an overall change in ecological processes in the area such as water current movements, sedimentation, and salinity shifts. Possible causes that can be attributed to the change in mangrove cover will be determined by examining the large-scale environmental change as seen from the series of satellite images. Results of the study can contribute in providing insights on how mangroves adapt to environmental changes.

Types of remote sensing data may vary, each having a significant purpose to analyze an area from a distance. There are numerous ways that remote sensing technology has been applied in the different fields of sciences, which include: applications in land use/land cover mapping, geologic and soil mapping, agriculture, forestry, rangeland, water resources, snow and ice mapping, urban and regional planning, wetland mapping, wildlife ecology, archaeology, environmental assessment, disaster assessment, and landform identification and evaluation [11,12].

As stated by Kuenzer et al. [13], remote sensing (RS) has been widely proven to be essential in monitoring and mapping threatened mangrove ecosystems. Examples of remote sensing systems that have been utilized for mangrove forest studies include the use of aerial photography, or satellite images provided by Landsat, SPOT, MODIS, ASTER, etc. [8]. Landsat images were used by Long et al. [4] to estimate the mangrove cover for the entire Philippine archipelago during 1990, 2000 and 2010 to be approximately 269, 256, and 241 kilohectare, respectively.

This research determined the change in area covered by mangrove for the years 2005, 2009, 2012, 2014, 2016, and 2018 in Brgy. Bito-on, Jaro, Iloilo City before and after the construction of the Jaro Floodway using freely available high-resolution satellite images from Google Earth. It specifically aimed to:

(i) determine the area of the mangrove forest in the Jaro Floodway in Brgy. Bito-on, Jaro, Iloilo City using Quantum Geographic Information System (QGIS); and

How to cite this article:
CSE: Flores MYM, Larroder AC. 2020. Mapping mangrove forest land cover change in Jaro Floodway, Iloilo City using Google Earth imagery. Publiscience. 3(1):74-77.
APA: Flores, M.Y.M., & Larroder, A.C. (2020). Mapping mangrove forest land cover change in Jaro Floodway, Iloilo City using Google Earth imagery. *Publiscience, 3*(1):74-77.

(ii) determine the rate of mangrove colonization in the Jaro Floodway in Brgy. Bito-on, Jaro, Iloilo City by adapting the formula used by Albano [2].

Methods. The methods was divided into three steps: (1) georeferencing of satellite images from the years 2005, 2009, 2012, 2014, 2016, (2) digitization of each georeferenced satellite image and image classification into four thematic classes, namely, mangrove, water, non-water, and fishpond areas and, (3) calculation for the rate of mangrove colonization.

Study area. The study area included the mangrove cover area at the mouth of the Jaro Floodway in Brgy. Bito-on, Jaro, Iloilo City as in Figure 1. A grid with a 200 m spacing bounded by geographic coordinates 122.5836°E, 10.7487°N and 122.5982°E, 10.7361°N was created in QGIS software, version 3.4.6. The grid served as a guide in downloading high resolution images from Google Earth for the years 2005, 2009, 2012, 2014, 2016 and 2018.

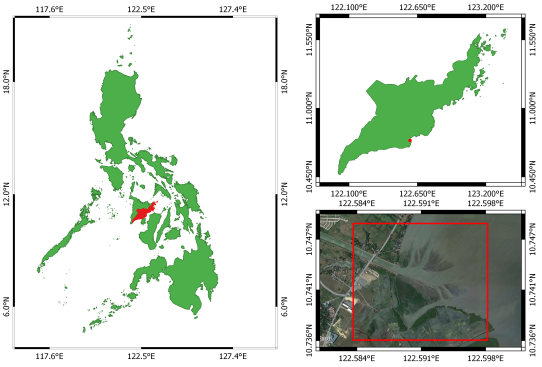

Figure 1. Study area.

Satellite image georeferencing. Satellite images as of December 2018 were georeferenced using Google Earth Pro, version 7.3.2 and Smart Geographic Information System (SmartGIS) 2019, version 19.11. Images were available for the years 2005, 2009, 2012, 2014, 2016, and 2018. The georeferenced images were saved as a Geospatial Tagged Image File Format (GeoTIFF), then imported as a raster layer to QGIS for digitization.

Digitization and image classification. The georeferenced images for each year were then classified into four (4) thematic classes using visual interpretation namely water, fishpond, mangrove, and non-mangrove areas. Water was identifiable as a dark blue color in the satellite image. Fishpond areas were rectangular shaped with a well-planned distribution, as seen through the satellite image. Mangroves were identifiable in the satellite images as green regions along the coast. These are the only plant species which could thrive on the salinity of the brackish water. Other areas which do not fit the criteria for the other three thematic classes were classified into a non-mangrove area. Every thematic class was then manually traced over using QGIS and saved as a shapefile layer. After the digitization process, the area of each thematic class, which was measured in hectares, was automatically determined by the software. An ocular inspection was also conducted in order to verify the classified areas.

Mangrove colonization rate. The rate of mangrove colonization for the years 2005-2009, 2012-2014, 2014-2016, and 2016-2018 was calculated using the formula used by Albano [2]:

$$CR_x = \frac{MC_b - MC_a}{b - a}$$

where CR_x is the average rate of mangrove areal cover change (ha/yr) or colonization rate of x, MC_a is the mangrove areal cover for the earliest year a, and MC_b is the mangrove areal cover for the most recent year b.

Results and Discussion. The construction of the Jaro Floodway began in 2008 and was completed in 2011. After its construction, mangrove cover steadily increased throughout the years as in Figure 2. In 2005, mangrove cover was measured to be 8.98 ha, this increased by 34.00 ha by 2018 to 42.98 ha.

Figure 2. Area of mangrove cover in the Jaro Floodway from 2005 to 2018.

Mangrove colonization rate has also increased from 2005 to 2018, as observed in Figure 3, wherein the slope of the line steadily increases. It can also be observed that from 2009 to 2012 and 2016 to 2018 there is a notable increase in mangrove colonization in the area. Overall, the colonization rate of mangroves in the Jaro Floodway increased by 7.99 ha/yr from 2005-2009 and 2016-2018.

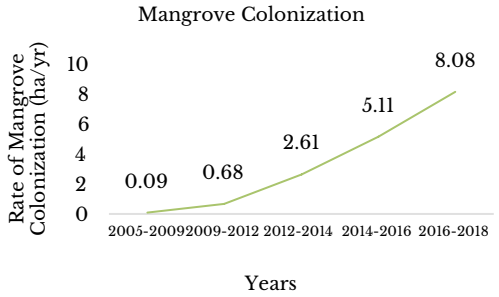

Figure 3. Rate of mangrove colonization in the Jaro Floodway from 2005 to 2018.

The extent of mangrove colonization depends on various environmental factors such as availability of propagule or seedling source, wave action, duration and depth of tidal inundation, and salinity [1]. In this study, the rate of mangrove colonization after the construction of the Jaro Floodway is mainly attributed to sedimentation [2,14]. Bathymetric charts available from the National Mapping and Resource Information Authority show that the water depth at the river mouth section of the Jaro Floodway before it was constructed is approximately 1 m, which is too deep for the propagules to grow. Thus, sedimentation played a major role by reducing the water depth to the optimal depth needed for mangroves to grow, which resulted in an increase in mangrove cover from 9.35 ha in 2005 to 42.98 in 2018. This study does not imply that an abrupt change in sediment accumulation is beneficial for the environment but rather emphasizes that mangroves increased from this environmental change.

There have been mangrove planting efforts in the study site that were initiated by the government. The Department of Public Works and Highways reported that a total of 13,000 seedlings were planted along the coasts of Barangay Bito-on. Personal communication with the Department of Environment and Natural Resources also reported that there are annual mangrove planting efforts after the Jaro Floodway was constructed. However, there are no reports on the survival of the planted seedlings. Despite this data gap, it is still likely that natural colonization took place because mangroves are known to colonize unutilized areas at a fast rate. Albano [2] reported that unutilized fishponds in selected barangays of Guimaras and Sorsogon, were naturally colonized by mangroves at a rate of 2,305 $m^2/_{yr}$ in 2006-2012 and 1,890 $m^2/_{yr}$ in 2000-2015, respectively. Nascimento et al. [9] also reported that mud deposition at the mouth of the Amazon River lead to an increase in mangrove cover by more than 700 km^2 in 12 years. Although the results of this study indicate that there was an increase in the mangrove cover, the contribution of mangrove planting efforts and natural colonization could not be quantified because of the lack of field data. However, in the case of natural colonization, the most likely propagule and seedling source is the nearby mangrove forest located at the mouth of the Jaro River.

Limitations. The study determined the area of mangrove cover and rate of mangrove colonization in the Jaro Floodway; thus, the species of the mangroves present in the area were not identified. Calculation for the rate of sediment accumulation could not be quantified with the methods used.

Conclusion. Mangrove cover increased after the Jaro Floodway was constructed. Sedimentation from the Jaro Floodway led to the formation of a new delta lobe that increased the area covered by mangroves from 9.35 (2005) to 42.98 ha (2018). Results of the study can contribute in providing insights on how mangroves adapt to environmental changes. Government offices can also use the results in the study in future decision making and aid in the development of rehabilitation projects.

Recommendations. Further studies regarding the survey of the presence of mangroves in the area and comparative studies between the number of naturally colonized mangroves and planted mangroves could be conducted. Quantifying sedimentation in the area may also be investigated.

Other sources of satellite imagery data and georeferencing software can also be used for the conduct of the study. When using a different source for the satellite imagery data, it is advised that the earliest and most recent available satellite image of the study site should be downloaded. There should also be a specific time interval for every acquired satellite image for the computation of the mangrove colonization rate.

Acknowledgement. The researcher would like to thank the involvement of Dr. Fernando P. Siringan and Mr. Paul Caesar M. Flores from the University of the Philippines, Marine Science Institute and Mr. Jose Marie Tumasis and Mrs. Gloria M. Flores from the Department of Environment and Natural Resources in Region VI for their assistance and guidance during the conduct of the study.

References

[1] Samson MS, Rollon RN. 2008. Growth performance of planted mangroves in the Philippines: revisiting forest management strategies. AMBIO: J Hum Environ. 37(4): 234-240.

[2] Albano G. 2017. Mangrove colonization of selected unutilized fishponds in Barangay Sabang, Sibunag, Guimaras and Juban, Sorsogon. University of the Philippines – Diliman. 1(2017):1-80.

[3] Long J, Giri C. 2011. Mapping the Philippines' mangrove forests using landsat imagery. Sensors; 11(2011):2972-2981.

[4] Long J, Napton D, Giri C, Graesser J. 2014. A mapping and monitoring assessment of the Philippines' mangrove forests from 1990 to 2010. J Coastal Res; 30(2):260-271.

[5] Alongi, DM. 2008. Mangrove forests: resilience, protection from tsunamis, and responses to global climate change. Estuar Coast Shelf Sci. 76(1):1-13.

[6] Dan TT, Chen CF, Chiag SH, Ogawa S. 2016. Mapping and change analysis in mangrove forest by using landsat imagery. ISPRS J Photgramm Remote Sens. 3(8):109-116.

[7] Fromard F, Vega C, Proisy C. 2004. Half a century of dynamic coastal change affecting mangrove shorelines of French Guiana: a case study based on remote sensing data analyses and field surveys. Mar Geol. 208:265–80.

[8] Heumann, BW. 2011. Satellite remote sensing of mangrove forests: Recent advances and future opportunities. Prog Phys Geogr. 35(1): 87-108.

[9] Nascimento WR, Souza Filho PWM, Proisy C, Lucas RM, Rosenqvist A. 2013. Mapping changes in the largest continuous Amazonian mangrove belt using object-based classification of multisensor satellite imagery. Estuar Coast Shelf Sci. 117:83–93.

[10] Dodman D, Mitlin D, Co JR. 2010: Victims to victors, disasters to opportunities: community-driven responses to climate change in the Philippines. IDPR 32, 1-26.

[11] Campbell JB, Wynne RH. 2011. Introduction to remote sensing. Guilford Press.

[12] Lillesand T, Kiefer RW, Chipman J. 2015. Remote sensing and image interpretation. John Wiley & Sons.

[13] Kuenzer C, Bluemel A, Gebhardt S, Quoc TV, Dech S. 2011. Remote sensing of mangrove ecosystems: A review. Remote Sensing. 3(5):878-928.

[14] Woodroffe, C.D., Rogers, K., McKee, K.L., Lovelock, C.E., Mendelssohn, I.A., Saintilan, N. 2016: Mangrove sedimentation and response to relative sea-level rise. Annu. Rev. Mar. Sci. 8, 243-266.

Monogenean and cestode infestation in the gills and intestines of *Clarias gariepinus* (African catfish) in Zarraga, Iloilo and *Chanos chanos* (Milkfish) in Dumangas, Iloilo

BEVERLY MAE L. CONSTANTINO, LANDER R. GUILLERGAN, CARL WILLIAM P. YABUT, and VIRNA JANE M. NAVARRO

Philippine Science High School - Western Visayas Campus, Brgy. Bito-on, Jaro, Iloilo City 5000, Department of Science and Technology, Philippines

Abstract

In the Philippines, *Clarias gariepinus* (African catfish) and *Chanos chanos* (milkfish) are two economically important fish species. Studies conducted by Echem et al. (2018) and Agbabiaka et al. (2017), respectively have suggested that both of these species have high mean intensity and prevalence of parasites which can cause mortalities in fish. The study aimed to identify and determine the prevalence and mean intensity of parasites present in *Clarias gariepinus* and *Chanos chanos* in Zarraga and Dumangas, Iloilo, respectively. The gills and intestines of 30 fish samples from each species were dissected and examined under a microscope. It was found that *Dactylogyrus spp.* and *Gyrodactylus spp.*, both monogeneans, infected the gills of both species. Meanwhile, varied species of cestodes were only present in the intestines of *Clarias gariepinus*. A positive correlation was found between the number of parasites present, and the length and weight of *Clarias gariepinus,* while no correlation was observed in *Chanos chanos*. This may be explained by the difference in the environmental preference of the fishes.

Keywords: *Cestodes, correlation, mean intensity, monogenean, prevalence*

Introduction. Fish is among the most widely cultured food items in the country as it is a common source of protein. Diseases brought about by parasites are one of the main reasons for the decrease in fish supply [1]. This usually results in huge economic losses among fish farmers and fish hatchery owners. In the country, *Chanos chanos* is generally considered as one of the main aquaculture products [2]. On the other hand, *Clarias gariepinus* (African catfish) is also one of the most abundant cultured species in the country [3].

Clarias gariepinus [4] and *Chanos chanos* [1] are known to be susceptible to parasites. However, the degree of parasitism varies among these species. The diversity and composition of parasites that infest fish such as *Clarias gariepinus* and *Chanos chanos* vary depending on several factors such as water quality, diet, habitat, and weight and length of the fish [5,6].

Zarraga and Dumangas, Iloilo are the two main producers of *Clarias gariepinus* and *Chanos chanos* in the province, respectively. Several studies have been conducted concerning the parasitism in *Clarias gariepinus* and *Chanos chanos*. However, those that address parasite prevalence in the province are limited. This study aims to determine the mean intensity and prevalence rate and identify the types of parasites present in *Chanos chanos* from Dumangas, Iloilo and *Clarias gariepinus* from Zarraga, Iloilo. The data obtained in this study may help local fish farmers in selecting treatments for their farms.

The study aimed to identify the types of parasites present in *Clarias gariepinus* in Zarraga, Iloilo, and *Chanos chanos* in Dumangas, Iloilo.

It specifically aimed to:

(i) identify the parasites present in *Clarias gariepinus* and *Chanos chanos*;

(ii) determine the prevalence of parasites present;

(iii) determine the mean intensity of parasites present;

(iv) correlate the weight of the fish to the number of parasites present; and

(v) correlate the length of the fish to the number of parasites present.

Methods. The data gathering was composed of three phases: sample collection, sample preparation, and fish dissection and examination. Sample collection involved the purchase, collection, and transportation of *Clarias gariepinus* and *Chanos chanos* samples from their respective fish farms to the Microtechnique Laboratory in Southeast Asian Fisheries Development Center (SEAFDEC), Tigbauan, Iloilo. Sample preparation involved euthanizing, measuring, and identifying the sexes of the fish samples before dissection. Fish dissection and examination involved the dissection and evisceration of the fish samples, examination of the gills and intestines, and data recording. Prevalence

How to cite this article:

CSE: Constantino BM, Guillergan L, Yabut CW, Navarro VJ. 2020. Monogenean and cestode infestation in the gills and intestines of *Clarias gariepinus* (African catfish) in Zarraga, Iloilo and *Chanos chanos* (Milkfish) in Dumangas, Iloilo. Publiscience. 3(1):78-83.

APA: Constantino, B.M., Guillergan, L., Yabut, C.W., & Navarro, V.J. (2020). Monogenean and cestode infestation in the gills and intestines of *Clarias gariepinus* (African catfish) in Zarraga, Iloilo and *Chanos chanos* (Milkfish) in Dumangas, Iloilo. *Publiscience*, 3(1):78-83.

and mean intensity of parasites in each of the fish samples were calculated by formulas provided by Bush et al. [7]. Pearson Correlation Test was then performed using IBM Statistical Package for the Social Sciences Statistics Version 22 (SPSS) to determine the relationship between the number of parasites present and the length and weight of the fish samples from each fish species.

Sample Collection. A total of 30 live fish samples per fish species were directly purchased from their respective fishponds. Samples were purchased in groups of 10 as these are the maximum number that could be dissected per day. Fish samples were stored in aerated fry bags, along with water from the pond where the samples were harvested [8]. Fry bags were transported in large buckets, with a total number of five (5) samples per bucket [8]. This method was repeated until 30 *Clarias gariepinus* and 30 *Chanos chanos* samples were collected and examined. *Clarias gariepinus* and *Chanos chanos* samples were then transported to the Microtechnique Laboratory of SEAFDEC/AQD in Tigbauan, Iloilo for the dissection and examination of the gills and intestines.

Sample Preparation. The fish samples were sedated using 2.4 mL phenoxyethanol with a concentration of 200 ppm diluted in five (5) liters of water inside the fry bags [9]. The total length (TL) of each fish was then taken using a ruler with a 1-mm precision [8] Each fish sample was then weighed using an Asuki TB-300 digital weighing scale with a one (1) mg precision [8].

Fish dissection and examination. Fish samples were dissected by first cutting the left and right operculae open. The gill arches were then cut and removed from the cavity using dissecting scissors and tweezers. The gill filaments were cut from the gill arches, placed on a glass slide, and covered with a cover slip. An incision was then made from the anus of the fish up to its mouth, exposing the digestive tract [10]. The fish samples were then eviscerated. The small and large intestines were removed, and placed on a petri dish filled with freshwater for *Clarias gariepinus*, and seawater for *Chanos chanos to* mimic the salinity of the fish pond where the fish species were collected. The gill filaments were examined under the Olympus BX51 compound light microscope, and the Howell Binocular Compound Microscope at 40x and 100x magnification. Photographs of parasites in the gills were taken at 100x magnification. The intestines were examined under the Howell Binocular Stereomicroscope. Parasites found in the gills and intestines were identified up to the genus level based on morphology, using the book Health Management in Aquaculture by Cruz-Lacierda et al. [11], and further verified by the Fish Health Section of SEAFDEC/AQD. After identification, parasites were counted based on their types.

Data Analysis. The parasites were then quantified by calculating the prevalence and mean intensity. The formula for prevalence is shown below.

$$Prevalence = \frac{Number\ of\ infected\ samples}{Number\ of\ samples}\ X\ 100$$

Mean intensity can be calculated using the equation:

$$Mean\ intensity = \frac{Total\ number\ of\ parasites}{Number\ of\ infected\ samples}$$

The length and weight of the fish samples were then correlated to the number of parasites present in each fish species using the Pearson Correlation Test in SPSS.

Safety Procedure. Before dissection of *Clarias gariepinus* samples, spines located along the pectoral fins were removed by cutting them using dissecting scissors. The spines contain venom that causes swelling and increased blood flow to the affected area. Improper handling of *Clarias gariepinus* could result in potential injuries during the dissection of the fish. After dissection and examination, used fish samples were properly disposed according to SEAFDEC protocols. Samples were buried in a vacant lot in SEAFDEC/AQD, Brgy. Buyu-an, Tigbauan, Iloilo.

Results and Discussion. The results and discussion is composed of six (6) parts: parasites present, prevalence, and mean intensity; attachment sites; *Clarias gariepinus* weight and length-parasite relationship; *Chanos chanos* weight and length-parasite relationship; parasitism comparisons between *Clarias gariepinus* and *Chanos chanos*; and water parameters that may have affected the extent of parasitism in each fish species.

Parasites present, prevalence, and mean intensity. Overall, all fish samples of *Clarias gariepinus* were infected with at least one type of parasite, while no parasite was recorded for 16 out of 30 samples of *Chanos chanos*. Table 1 shows that *Clarias gariepinus* was parasitized by three different parasites, namely, *Dactylogyrus spp.* (monogenean, Fig. 1A), *Gyrodactylus spp* (monogenean, Fig. 1B), and Cestode (Fig. 1C). Among the parasites that were recorded, two types were also found to parasitize *Chanos chanos*, which include *Dactylogyrus spp.* (monogenean), and *Gyrodactylus spp* .(monogenean) as summarized in Table 2. Cestodes were only found to be present in *Clarias gariepinus*.

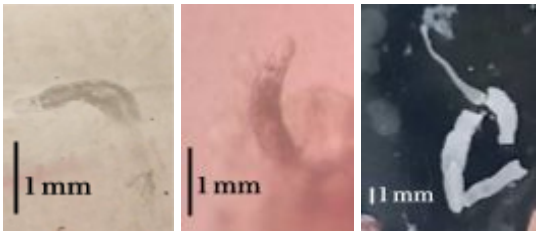

A B C

Figure 1. Parasites present in the fish samples: (A) Monogenean [*Dactylogyrus spp.*]; (B) Monogenean [*Gyrodactylus spp.*]; and (C) Cestodes.

Attachment sites. Attachment sites of the parasites in each fish species are shown in Tables 1 and 2. *Dactylogyrus spp.* (monogenean), and *Gyrodactylus spp* . (monogenean) were found attached to the gills of all fish samples for both *Clarias gariepinus* and *Chanos chanos*. Cestodes were only found in the intestines of *Clarias gariepinus*.

Table 1. Parasites found in *Clarias gariepinus.*

Parasites recorded	Site of attachment	TP*	inf**
Dactylogyrus spp. (monogenean)	Gills	1157	30
Gyrodactylus spp. (monogenean)	Gills	61	15
Cestode	Intestines	32	5

**TP* number of parasites, ***inf* number of infected samples

Table 2. Parasites found in *Chanos chanos.*

Parasites recorded	Site of attachment	TP*	inf**
Dactylogyrus spp. (monogenean)	Gills	19	12
Gyrodactylus spp. (monogenean)	Gills	1	1

**TP* number of parasites, ***inf* number of infected samples

The prevalence (%) and mean intensity (MI) of parasites present in *Clarias gariepinus* and *Chanos chanos* are shown in Table 3. *Dactylogyrus spp.* (monogenean) was found to be the most prevalent parasite infecting both fish species, followed by *Gyrodactylus spp.* (monogenean), and finally Cestodes for *Clarias gariepinus*. *Dactylogyrus spp.* (monogenean) had the greatest MI among other types of parasite for *Clarias gariepinus* and *Chanos chanos*. The parasite exhibited an MI of 39 parasites per sample in *Clarias gariepinus* and two (2) parasites per sample in *Chanos chanos*. *Dactylogyrus spp.* (monogenean) has an MI of four (4) parasites per sample in *Clarias gariepinus*, and an MI of one (1) parasite per sample in *Chanos chanos*, the least MI of parasites in both species. Meanwhile, Cestodes exhibited an MI of six (6) parasites per fish sample in *Clarias gariepinus.*

Table 3. Prevalence and mean intensity of parasites present.

	Clarias gariepinus		*Chanos chanos*	
Parasites present	%*	MI**	%*	MI**
Monogenean (*Dactylogyrus spp.*)	100	39	40	2
Gyrodactylus spp. (monogenean)	50	4	3.33	1
Cestode	16.67	6	-	-

*% prevalence, ***MI* mean intensity

Clarias gariepinus weight and length-parasite relationship. Among the two fish species, *Clarias gariepinus* was the most infected, hosting three types of parasites, and a total of 1250 parasites in 30 samples. The correlation of catfish weight and length to the number of parasites present in the fish are shown in Figure 2. The correlation coefficients (r) of the length and weight to the number of parasites were 0.639 and 0.622 respectively. A positive correlation of the weight and length to the number of parasites present was found to be significant at α=0.01. With this, the correlation of the weight and length of catfish to the number of parasites present can be described as moderate since the values of r fall between the range of 0.40-0.69 [12].

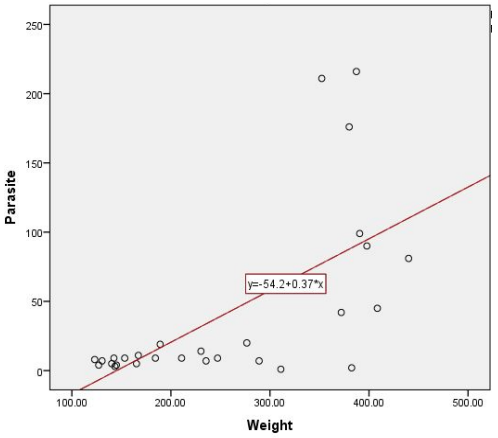

Figure 2. The graph shows the correlation of catfish weight to the number of parasites (r=0.639).

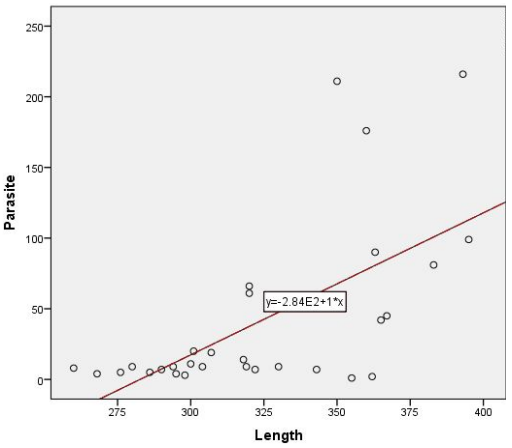

Figure 3. The graph shows the correlation of catfish length to the number of parasites (r=0.622).

Chanos chanos weight and length-parasite relationship. Chanos chanos exhibited a lower prevalence and MI of parasites present than *Clarias gariepinus*. Among the three parasites observed, *Chanos chanos* hosted only two types, with a total number of 20 parasites found for all fish samples. No significant correlation between the weight and length of *Chanos chanos* and the number of parasites was observed.

Clarias gariepinus and *Chanos chanos* both had the presence of *Dactylogyrus spp.* (monogenean) and *Gyrodactylus spp.* (monogenean) in the gills. Of the two fish species examined, only *Clarias gariepinus* had a presence of cestodes in its intestines.

The presence of parasites in the fishes may be explained by the water quality of the pond where the fishes were sourced from. When the water parameters differ from the ideal conditions of the fish species, slow growth, inability to reproduce, and the increased risk of parasite infestation due to decreased immunity is expected. Along with this, unfavorable water conditions allow for the easy proliferation of parasites in the water system. Some of these parameters include the salinity, temperature, and dissolved oxygen of the water in the pond. [13]. Also, a similarity in diet, habitat, and

feeding capacity of the host may have affected the presence and abundance of these parasites [14].

Parasites were observed to be more prevalent in the gills, than in the intestines. This is because the gills are in direct contact with the water where the fish is exposed to [15]. The gills are more likely to catch more parasites, especially monogeneans because of its threadlike filaments which makes it easy for monogeneans to hook and attach to [16]. Additionally, most parasites present in the fishes were monogeneans. Monogeneans are ectoparasitic flatworms, which mostly infect only the skin and the gills of the fish [11].

The absence of cestodes in *Chanos chanos* may be due to the salinity of the water where the fish is found. This is because cestodes usually infest freshwater fishes, such as catfish, carps, and snakeheads, while *Chanos chanos* is a euryhaline fish [11]. The difference in the water salinities in which the two organisms exist may have contributed to the minimal parasitism in *Chanos chanos*. Furthermore monogeneans exist mostly in temperatures optimal for catfish growth, which may explain the parasite prevalence in the samples [17,18,19]. In contrast, *Chanos chanos* exists in environments with high levels of dissolved oxygen. Dissolved oxygen (DO) can also affect the extent of the parasitism by supporting the immunity of the host fish against parasitic infestations [20]. Along with this, fishes that are exposed to environmental systems which have low DO and high turbidity, such as *Clarias gariepinus*, are more vulnerable to parasite infestation [21].

It was found that both the length and weight of *Clarias gariepinus* had a positive correlation to the number of parasites present in the fish species. This is supported by the study of Khalil et al. [22], which indicated that the larger the fish, the larger the surface area that the parasites can attach to, leading to an increase in parasitism. The study of Amare et al. [1] also showed a positive correlation between the number of parasites present and the size of the fish. The results of Oscar et al. [6] also showed a high number of monogeneans present in the gills and a positive correlation between the length and weight of the fish to the number of parasites present.

No significant correlation was observed between the size and number of parasites present in *Chanos chanos*. This is inline with the findings of Echem et al. [2], which reported a negative correlation between the size of the milkfish and the number of parasites present. This is because monogeneans infesting the fish are not present in their optimum habitat for growth. Monogeneans mostly infest freshwater fishes, while *Chanos chanos* is a euryhaline fish. The difference in the tolerance to saltwater of the parasite and the fish species may have affected the extent of monogenean parasitism in the fish [11].

Treatments for the parasitism depend upon the type of parasites present. Treatments for monogenean infestation include Praziquantel (PZQ), hydrogen peroxide, formalin, potassium permanganate, hyposalinity and hypersalinity, and restocking. Meanwhile, cestode infestations are usually treated using PZQ and niclosamide.

Praziquantel (PZQ) is a selective drug used for the treatment of trematode, cestode, and monogenean infections only in ornamental fishes, and is not approved by the US Food and Drug Administration (USFDA) for the use in fishes that are being consumed [23,24]. Hydrogen peroxide, formalin, and potassium permanganate have also been used in the aquaculture industry as immersion treatments against disease-causing organisms, including ectoparasites [25,26,27]. Hyposalinity and hypersalinity are osmotic shock treatments used against parasitic infestations, especially monogenean, in certain fish species by decreasing or increasing the salinity of the water bath where the fishes are exposed to [23,28]. Disinfection in aquaculture involves emptying, drying, and disinfecting the tanks or ponds where the fishes are cultured [23]. Niclosamide is a drug which belongs to the family of medicines called anthelmintics, which are generally used to treat worm infections, like cestodes [29].

Limitations. The examination of fish parts for the presence of parasites was only limited to the gills and intestines of both fish species. The samples were also limited to *Clarias gariepinus* and *Chanos chanos* cultured and obtained from one fish farm in Zarraga, Iloilo, and one fish farm in Dumangas, Iloilo respectively. The sample size for each fish species was limited to 30 samples. *Clarias gariepinus* samples were commercially available, however, *Chanos chanos* samples were collected using aerated fry bags to transport the samples to the laboratory as suggested by the fish farm owner. This was to assure that milkfish samples were alive once they arrived at the laboratory to be dissected and examined.

Conclusion. *Dactylogyrus spp.* (monogenean) exhibited a high prevalence rate and mean intensity in *Clarias gariepinus*, while it exhibited a moderate prevalence rate and low mean intensity in *Chanos chanos*. Meanwhile, *Gyrodactylus spp*. (monogenean) exhibited moderate and low prevalence rates and mean intensities for *Clarias gariepinus* and *Chanos chanos* respectively. Cestodes were the least prevalent among the parasites, and were only found in *Clarias gariepinus*. As the length and weight of *Clarias gariepinus* increases, the number of parasites found in the fish increases with it. Meanwhile, the length and weight of *Chanos chanos* has no effect on the parasite count in the fish. Therefore, farmers culturing the fish species would be informed on possible treatments concerning parasitism of monogeneans and cestodes. Along with this, it would promote the awareness among fish farmers about how size could affect the extent of parasitism in their fish culture.

Recommendations. This study recommends to increase the number of fish samples and increase the number of fish farms where the samples are sourced from in order to obtain a more accurate representation of the fish population in the specific area. Also, more varied sizes of *Clarias gariepinus* and *Chanos chanos* samples could be used in future studies in order to have a more accurate analysis of the correlation of length and weight to the number of parasites present in each fish species. It is also recommended to take water and soil samples from the pond where the fish samples are collected to further relate the environmental parameters to the extent of parasitism.

Acknowledgement. The work unit extends its appreciation and thanks to the Southeast Asian Fisheries Development Center Aquaculture Department (SEAFDEC/AQD), for providing access to their facilities and equipment for the conduct of the study.

References

[1] Amare A, Alemayehu A, Aylate A. 2014. Prevalence of Internal Parasitic Helminthes Infected *Oreochromis niloticus* (Nile Tilapia), *Clarias gariepinus* (African Catfish) and *Cyprinus carpio* (Common Carp) in Lake Lugo (Hayke), Northeast Ethiopia. J Aquac Res Development. 5(3): 1-5.

[2] Echem RT, Barba HM, Li G, Peng F, Buenaventura NJC. 2018. Endoparasites in *Chanos chanos* (Forsskal, 1775) from the wetlands of Zamboanga City, Western Mindanao, Philippines. J Aquac Res Development. 9(5).

[3] Enyidi UD, Eneje UL. 2015. Parasites Of African Catfish *Clarias Gariepinus* Cultured In Homestead Ponds. J Agric Sci. 2(12): 1-9.

[4] Akoll P. Konecny R, Mwanja WW, Nattabi JK, Agoe C, Schiemer F. 2011. Parasite fauna of farmed Nile tilapia (*Oreochromis niloticus*) nd African catfish (*Clarias gariepinus*) in Uganda. J Parasitol Res. 1(1): 1-9.

[5] Iwanowicz DD. 2011. Overview on the effects of parasites on fish health. United States Geological Survey, Leetown Science Center, National Fish Health Research Laboratory; Leetown Road, Kearneysville, WV.

[6] Oscar EV, Arit ET, Philip EA. 2015. Monogenean parasites of the African catfish (*Clarias gariepinus*) from two fish farms in Calabar, Cross River State, Nigeria. J Coast Life Med, 3(6): 433-437.

[7] Bush O, Lafferty K, Lotz J, Shostak A. 1997. Parasitology Meets Ecology on Its Own Terms: Margolis et al. Revisited. J Parasitol Res. 83(4):575.

[8] Truter M, Přikrylová I, Smit NJ. 2017. Co-introduction of Ancyrocephalid Monogeneans on their Invasive Host, the Largemouth Bass, *Micropterus salmoides* (Lacepéde, 1802) in South Africa. Int J Parasitol. 6(3): 420- 429.

[9] McGill. 2016. Fish and Amphibian Euthanasia. Standard Operating Procedure #303. Available from: https://bit.ly/3cFutxH

[10] Fish Dissection. Australian Museum; [updated 2019 January 25]; Available from: https://bit.ly/3bsr0kv.

[11] Cruz-Lacierda E, Lavilla C, Lio-Po G. 2001. Health Management in Aquaculture. 56-67p.

[12] Schober P, Boer C, Schwarte L. 2018. Correlation Coefficients: Appropriate use and interpretation. Anesthesia and Analgesia. 126(5): 1763-1768.

[13] Khan MN, Aziz F, Rab A, Sahar L, Ali R, Naqvi SM. 2003. Parasitic infestation in different freshwater fish of mini dams of Potohar Region, Pakistan. PJBS. 6(13): 1092-1095.

[14] Amin B, Lee SM, Krishnasamy CC. 1986. A preliminary survey of parasites of Malaysian red jungle fowl (*Gallus gallus spadiceus*). Kajian Vetenirar. 17(2).

[15] Bichi AH, Ibrahim A. 2009. A survey of ecto and intestinal parasites of *Tilapia zillii* (Gervias) in Tiga lake, Kano, Northern Nigeria. JPAS. 2(1).

[16] Kearn GC. 2014. Some aspects of the biology of monogenean (Platyhelminth) parasites of marine and freshwater fishes. Oceanography. 2(1).

[17] Britz PJ, Hecht T. 2007. Effects of salinity on growth and survival of African sharptooth catfish (*Clarias gariepinus*). Journal of Applied Ichthyology. 5(4):194 - 202.

[18] Paperna I. 1964. The metazoan parasite fauna ofIsrael inland water fishes. Bull. Fish. Cult. Israel. 16: 3–66.

[19] Shaharom-Harrison F. 1986. The reproductive biology of *Dactylogyrus nobilis* (Monogenea: Dactylogyridae) from the gills of big head carp (*Aristichthys nobilis*). In: Maclean, J.L., Dizon, L.B. & Hosillos, L.V. (eds.), The First Asian Fisheries Forum. Asian Fisheries Society, Manila, Philippines. 265–268.

[20] El-Naggar AM, Mashaly MI, Hagras AM, Alshafei HA. 2017. Monogenean microfauna of the Nile Catfish, *Clarias gariepinus* as biomonitors of environmental degradation in aquatic ecosystems at the Nile Delta, Egypt. IOSR-JESTFT. 11(8): 45-62.

[21] Saha H, Ratan K, Saha RK, Kamilya D, Kumar P. 2013. Low pH, dissolved oxygen and high temperature induces *Thelohanellus rohita* (myxozoan) infestation in tropical fish, *Labeo rohita* (Hamilton). J Parasit Dis. 37(2): 264–270.

[22] Khalil MI, El-Shahawy IS, Abdelkader HS. 2014. Studies on some fish parasites of public health importance in the southern area of Saudi Arabia. Vet. Parasitol. 23(4): 435-442.

[23] Reed P, Francis-Floyd R, Klinger RE, Petty D. 2009. Monogenean parasites of fish. Fisheries and aquatic sciences. 4(2009): 1-4.

[24] Thomas A, Dawson MR, Ellis H, Stamper MA. 2016. Praziquantel degradation in marine aquarium water. PeerJ. 4. E1857.

[25] Francis-Floyd, R. 1996. Use of formalin to control fish parasites. University of Florida Cooperative Extension Service. Institute of Food and Agriculture Sciences. EDIS.

[26] Pandey G. 2014. Potassium permanganate for the treatment of external infections of fish. Nanaji Deshmukh Vet.Sci.Univ.Jabalpur. 1-3.

[27] Yanong RP. 2014. Use of hydrogen peroxide in finfish aquaculture. IFAS Univ.Florida. 1-6.

[28] Hauter D. 2019. Hyposalinity or Osmotic Shock Therapy Treatment for Ich. Available from: https://bit.ly/35X5PWM.

[29] Niclosamide Drug Information, Professional. Drugs. 2019 Oct 19. Available from: https://bit.ly/3fGlSMW.

Publiscience Vol. 3 Issue 1

Measurement of eye turbidity of formalin-treated *Chanos chanos* (milkfish) using image analysis

RAJO CHRISTIAN G. CADORNA, MAXINE P. CHAN, JUAN PAULO MIGUEL I. SALMON, and GERALD U. SALAZAR

Philippine Science High School - Western Visayas Campus, Brgy. Bito-on, Jaro, Iloilo City 5000, Department of Science and Technology, Philippines

Abstract

Freshness is an important factor in fish consumption. However, fish freshness is falsified by using formalin which is cancerous to humans. Fish freshness can be determined using eye color. This study aimed to determine the effect of formalin treatment on *Chanos chanos* (milkfish) through the mean saturation and value from the HSV (hue, saturation, value) color space of the eye and the pupil, and to compare the significant difference between formalin-treated and untreated fish. Sixty (60) *Chanos chanos* (milkfish) samples were documented throughout a seven-day period, segmented in GNU Image Manipulation Program 2.10.8, and processed using a program developed in Scilab 6.0.2. In both setups, the mean saturation of the eye and the value of the pupil increased over time while the mean value of the eye and the saturation of the pupil decreased. This change indicates that the eyes become cloudier as a fish loses its freshness. Formalin treatment led to a significant increase in the mean values of the eye and the pupil.

Keywords: *color, computer vision, fish freshness, formalin, image analysis*

Introduction. The Philippines is a country that primarily relies on its aquatic resources such as in the fisheries industry. In 2018, the Philippines produced a total of 4.35 million metric tons of fish, crustaceans, mollusks, and aquatic plants. The Philippines also ranked 8th among the top fish producing countries in the world in 2016 [1]. *Chanos chanos* (milkfish) is one of the three most consumed fishes in the Philippines [2]. In Region VI alone, the total number of *Chanos chanos* (milkfish) produced was 88,981.8 metric tons or 29.3% of the total country production, making Region VI the largest producer of *Chanos chanos* (milkfish) in the Philippines.

Fish is a highly perishable commodity and its freshness is an important indicator of its overall quality, as well as its fitness for human consumption. Biological and chemical changes that occur post death and during storage may result to the deterioration of fish quality. Significant changes in the appearance, odor, color, flavor, and texture of the skin, slime, eyes, gills, and belly can be used to approximate fish freshness. Color is one of the most important quality parameters in fish processing since color deterioration is a sign of decreasing freshness. However, quality evaluation performed by experts, such as sensory analysis of appearance and odor, is time-consuming and labor-intensive since humans are susceptible to fatigue, bias, and other limitations [3]. Through the developments in the field of computer vision technology, product assessment has become all the more standardized and accurate by employing automated noninvasive methods and visual evaluation [4].

Formalin is a preservative that is classified by the International Agency for Research on Cancer [5] as carcinogenic, but is used by fish traders to prevent spoilage. Formalin is a solution of 37% formaldehyde in water which is used in preservation and treatment against microorganisms that may cause fish diseases [6]. Formalin-treated fish are almost indistinguishable from untreated fish which makes them difficult to identify, leading to the accidental consumption of these fish. Considering the threat that formalin poses to consumers [7], the practice of using formalin to extend the shelf life of fish [6] in markets should be ended.

Previous studies utilized various methods for identifying the level of fish freshness. Dowlati et al. [3] evaluated the freshness of wild and farmed *Sparus aurata* (gilthead seabream) using computer vision technique by measuring lightness (L^*), redness (a^*), yellowness (b^*), chroma, and total color difference in fish eyes and gills. The results showed a strong correlation between color parameters and storage days. The L^* and b^* values increased over time, while the a^* value decreased. Similar results were reported by Unal Sengor et al. [8] whose study utilized both the Minolta color measurement method and the image analysis method to assess the freshness of *Sparus aurata* (gilthead seabream) stored without ice, with ice, and with ice and cover paper. While previous studies have utilized computer vision to determine fish freshness over time and in varying storage conditions or lighting setup, there is a scarcity of studies that use computer vision to examine the changes in the eye color of formalin-treated and untreated fish.

To overcome human limitations [3], formalin detection in fish may be automated for increased efficiency, consistency, and accuracy. However, much remains unexplored in the field, thus available training data for automation is limited. The results of this study will primarily be useful to fish quality assessment agencies, will contribute to the

How to cite this article:
CSE: Cadorna RCG, Chan MP, Salmon JPMI, Salazar GU. 2020. Measurement of eye turbidity of formalin-treated *Chanos chanos* (milkfish) using image analysis. Publiscience. 3(1):84-89.
APA: Cadorna, R.C.G., Chan M.P., Salmon J.P.M.I., & Salazar G.U. (2020). Measurement of eye turbidity of formalin-treated *Chanos chanos* (milkfish) using image analysis. *Publiscience, 3*(1):84-89.

advancement of quality assessment automation, and will be beneficial to the general public specifically, fish consumers.

The aim of this study was to determine the effect of formalin treatment on *Chanos chanos* (milkfish) through the mean saturation and value of eye and pupil of eye using computer vision. It specifically aimed to:

(i) document a timelapse of fish progression in formalin-treated and untreated samples of *Chanos chanos* (milkfish) for 7 days;

(ii) identify the mean saturation and mean value of the eye and the pupil of the eye relative to the stage of fish progression from the images using Scilab 6.0.2; and

(iii) calculate the significant difference of the mean values for the treated and untreated setups using JASP 0.9.2.

Methods. The data-gathering procedure was divided into five (5) phases: sample preparation, image acquisition, image analysis, statistical analysis, and disposal. The sample preparation was further divided into three (3) sub-phases: sample (a) collection, (b) preparation, and (c) treatment. Image acquisition was conducted over a span of 7 days where images of the samples were collected for image analysis. Image analysis consisted of image segmentation, the extraction of HSV values from the segmented images, and the calculation of the mean saturation and value of the processed images. Statistical analysis involved generating the mathematical models as visual displays of the sample progression and calculating the significant difference of values between setups. The samples used were then disposed.

Sample preparation. Fresh-caught, farmed *Chanos chanos* (milkfish) with fork lengths of 20.2 to 26.8 cm, total lengths of 26.1 to 34 cm, and weights of 123 to 252 g, were collected from the Southeast Asian Fisheries Development Center (SEAFDEC) Brackishwater Station in Dumangas, Iloilo. After capture, the fish were immersed in icy water to shock them. Euthanasia was performed shortly after capture through spiking or iki jime which physically destroys the central nervous system [9]. The fish were individually placed inside ziplock bags and immediately transported to a laboratory in Philippine Science High School - Western Visayas Campus in polystyrene boxes with 1:1 fish-to-ice volume ratio [6]. The fish were separated into two groups, one was immersed in 5% formalin for five (5) minutes [6] while the other remained untreated. The fish samples from the two groups were stored in a chest freezer at a temperature of 0°C to 5°C and observed every 24 hours for seven days.

Image acquisition. A color camera and an illumination chamber or lightbox as described by Dowlati et al. [3] were used in an image acquisition system to capture the images of fish. Two LED lamps (Natural Daylight, 240 V / 4W) with a color temperature of 6500 K were used to capture high quality images under reproducible lighting conditions. The lamps with lengths of 30 cm were installed opposite of each other on the left and right sides of a wooden lightbox of dimensions of 50 x 50 x 30 cm. The interior walls were painted matte black to minimize background light and light reflectance. The sample tray was green in color for adequate contrast with the fish sample [3]. The images of fish eyes were captured using a digital color camera (18-55mm 1:3.5-5.6G VR). Top-view images were taken at a vertical distance of 30 cm [10]. All images were taken using constant camera settings (see Table 1). The LED lamps were turned on an hour before image capturing to ensure stable lighting [3].

Table 1. Camera control settings.

Variable	Settings
Image size	6000 x 4000 pixels
Zoom	No zoom
Flash mode	No flash
Sensitivity	ISO-200
Operation mode	Manual
Aperture Av.	f/6.3
Exposure time Av.	1/15 s
Image type	JPEG
Macro	On
Focal length	18mm

Image analysis. Segmentation is the process of partitioning an image into regions that correlate strongly to features of interest in an image. The regions of interest, the eye and the pupil, were manually segmented using GNU Image Manipulation Program 2.10.8 to isolate them for color analysis [10]. The elliptical marquee tool was used to select and segment images of the eye and the pupil which appears as a black circle in the middle of the eye [11]. The RGB values of the processed images were converted to their respective HSV equivalents. Image analysis was done using Scilab 6.0.2 [12].

Statistical analysis. The analysis of results was done by calculating the statistical difference between the data points of the treated and untreated samples using the independent samples t-test through the JASP 0.9.2 software. Data was expressed using mean and standard deviation. Differences among the mean values of treated and untreated samples were examined with a significance level of α=0.05.

Safety Procedure. The proper use of splash goggles, laboratory gown, gloves, and mask was observed throughout the conduct of the study. All fish samples were buried in a vacant lot in San Miguel, Iloilo. Used and unused formalin was turned over to the science research assistant for proper storage and disposal.

Results and Discussion. Figure 1 shows the changes in the eyes of the same untreated fish over seven days. The iris became darker over time, while the pupil became cloudier. The same is true for the formalin-treated samples as seen in Figure 2. However, the iris of formalin-treated fish discolor earlier compared to untreated fish. The pupils of the formalin-treated fish became cloudier than those of the untreated samples.

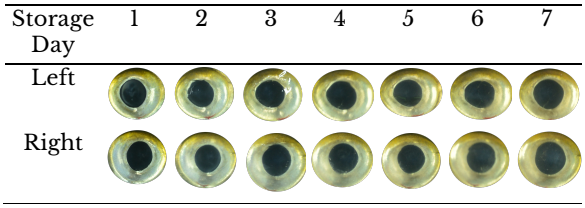

Figure 1. Typical fish eye changes during storage of untreated *Chanos chanos* (milkfish).

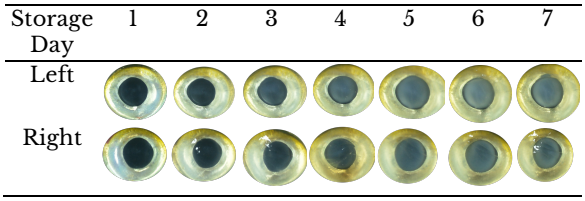

Figure 2. Typical fish eye changes during storage of formalin-treated *Chanos chanos* (milkfish).

Changes in fish freshness were determined by calculating the mean value and saturation of eye and pupil images using the Scilab 6.0.2 image processing library. Tables 2 and 3 present the mean and standard deviation of the saturation and value of the eye and pupil for untreated and formalin-treated samples, respectively.

The mean saturation of the eye increased over time in both setups, from 0.31589 to 0.36988 for untreated samples and 0.29678 to 0.39731 for formalin-treated samples. In contrast, the mean saturation of the pupil decreased over time, from 0.33927 to 0.19270 for untreated samples and 0.33872 to 0.20830 for formalin-treated samples. The mean value of the eye slightly decreased, from 0.59896 to 0.57457 in the untreated setup and from 0.63972 to 0.62432 in the formalin-treated setup. The mean value of the pupil increased, from 0.17985 to 0.24437 for the untreated setup and 0.22680 to 0.38552 in the formalin-treated setup.

Figure 3 shows the mathematical models generated to display the comparison of observable trends in the changes in saturation and values of eyes and pupil between formalin-treated and untreated *Chanos chanos* (milkfish) samples.

The graph for mean saturation of eyes as seen in Figure 3-a shows a steady increase in saturation. This is in contrast to the trend seen in the mean saturation of pupils as seen in Figure 3-b where the saturation of the pupils steadily decreases. Statistical analysis shows no significant difference for eye and pupil saturation (see Table 4).

The graph for mean value of eyes as seen in Figure 3-c shows an increase then a decrease in value halfway through. Meanwhile, the graph for mean value as seen in Figure 3-d of pupils display an increase in value over time. Statistical analysis shows a significant difference for eye and pupil value (see Table 4).

Converting an image to its HSV equivalent means separating its hue, saturation, and values into different channels. The channels produced can be converted into matrices with each pixel having an appropriate numerical value. Saturation ranges from zero to one, a saturation of zero means that the pixel is the closest to gray that it could be while one would denote that a pixel is the purest form of its respective hue. Value is the proximity of a pixel to black or white when converted into grayscale. It also ranges from zero to one, a value of zero means that the pixel is black while a value of one means that the pixel is white [13].

Table 2. Statistical parameters of the regions of interest on the basis of pixel saturation and value for untreated fish.

	Eye				Pupil of Eye			
	Saturation		Value		Saturation		Value	
Day	Mean	Std. Deviation	Mean	Std. Deviation	Mean	Std. Deviation	Mean	Std. Deviation
1	0.31589	0.04081	0.59896	0.04168	0.33927	0.04284	0.17985	0.04270
2	0.29658	0.02841	0.61924	0.03003	0.31360	0.02673	0.24334	0.04032
3	0.30757	0.03079	0.60468	0.02991	0.30239	0.03282	0.22710	0.03580
4	0.31227	0.02873	0.60815	0.02705	0.26640	0.03943	0.23290	0.02782
5	0.33848	0.03227	0.60102	0.02391	0.22886	0.02896	0.23852	0.03287
6	0.34215	0.03731	0.58334	0.02385	0.20231	0.02518	0.23912	0.02731
7	0.36988	0.04368	0.57457	0.02311	0.19270	0.02150	0.24437	0.02915

Table 3. Statistical parameters of the regions of interest on the basis of pixel saturation and value for formalin-treated fish.

	Eye				Pupil of Eye			
	Saturation		Value		Saturation		Value	
Day	Mean	Std. Deviation	Mean	Std. Deviation	Mean	Std. Deviation	Mean	Std. Deviation
1	0.29678	0.03621	0.63972	0.03854	0.33872	0.04976	0.22680	0.03693
2	0.30936	0.04304	0.64632	0.03573	0.29464	0.04322	0.27685	0.03921
3	0.32907	0.04530	0.65367	0.03731	0.24712	0.03451	0.34837	0.06162
4	0.34628	0.05262	0.65065	0.03838	0.21575	0.03088	0.38856	0.05923
5	0.34923	0.05805	0.65171	0.03828	0.21177	0.02742	0.40569	0.06166
6	0.37609	0.05936	0.63269	0.04039	0.20736	0.02696	0.39506	0.06147
7	0.39731	0.06421	0.62432	0.04345	0.20833	0.02164	0.38552	0.05602

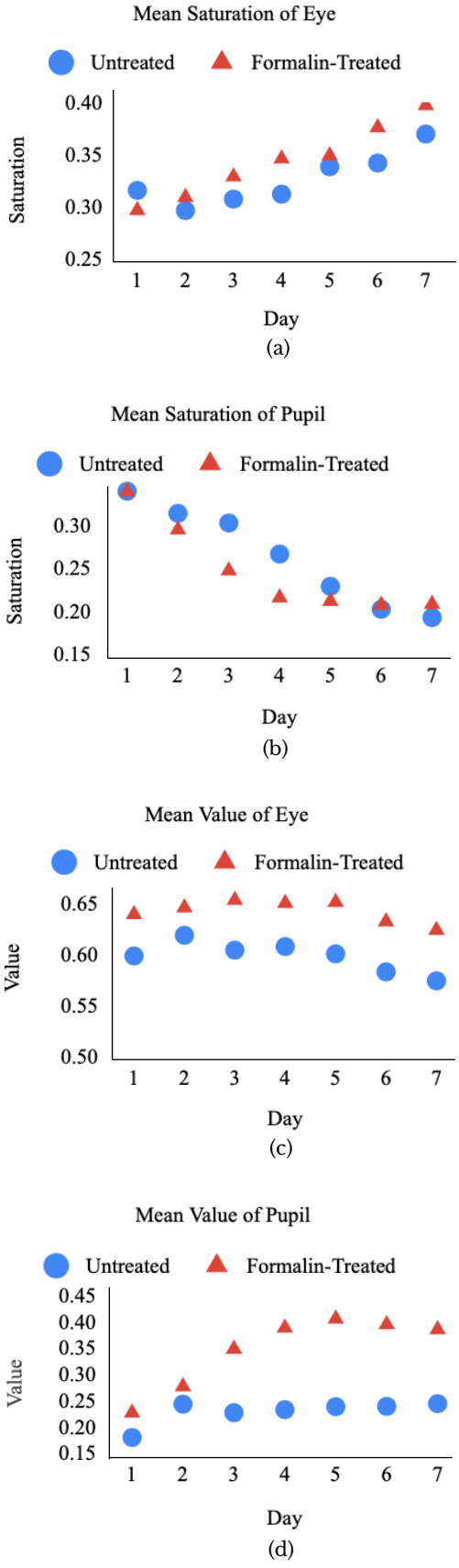

Figure 3. (a) Mean saturation of eye; (b) Mean saturation of pupil; (c) Mean value of eye; and (d) Mean value of pupil for formalin-treated and untreated samples.

Table 4. Statistical analysis of the significant difference in regions of interest parameters between treated and untreated fish.

Parameter	Significance (2-tailed, $\alpha = 0.05$)
Saturation of eye	0.313
Saturation of pupil	0.562
Value of eye	0.000
Value of pupil	0.003

The increase in saturation of the whole eye for both treated and untreated samples means that the eyes became more colored over time. This can be observed in the images acquired where the eyes gradually turns yellow or red. This change in coloration could be attributed to internal chemical changes that occur in lipids and proteins. Lipid oxidation reduces the fish's shelf life and modifies its color and texture with the formation of yellow pigment as the resulting product of reaction between protein and oxidized lipid [14]. The decrease in saturation for the pupil of the eye means that the pupil became grayer as the fish loses freshness and becomes unfit for human consumption. The pupil's grayness is an indicator of its turbidity which is a visual indicator of fish freshness [3]. However, there is no significant difference in the saturation changes in eye and pupil when the treated and untreated samples are compared, therefore it cannot be an effective indicator of formalin presence.

The increase in value of the whole eye of the untreated samples, peaking at day 2, and the formalin-treated samples, peaking at day 3, and their subsequent decrease after peaking means that the eyes gravitate towards white in the first two or three days, then proceeds towards lower value, or towards black, after. The value of the pupils displays a steady increase over time, thus indicating that the pupils become cloudier over time. This explains why for the first three days there is an observed increase in the value of the whole eye. The subsequent decrease in value is due to the yellowing of the eye starting from the fourth day, thus decreasing the total value of the whole eye. The whitening of the pupil is an indicator of turbidity in which the eyes become cloudier as a fish loses its freshness [3]. Previous studies report similar data. In the $L^*a^*b^*$ color space, lightness or L^* describes the brightness of the fish eye which is similar to value in the HSV color space. Dowlati et al. [3] found that the L^* increased during ice storage for farmed gilthead seabream while Balaban et al. [15] reported that the average L* values of the snapper and gurnard eyes increased significantly with storage time ($P < 0.05$). Contrary to the saturation of the eye and pupil, statistical analysis showed that there is a significant difference in the mean values of the eye and pupil between treated and untreated setups, suggesting that value may be a useful tool for the identification of formalin-treated fish.

Though the values of treated and untreated samples are significantly different in the eye and pupil, the resulting trend is contrary to the background literature. The study by Dowlati et al. [3] revealed that fish eyes become cloudier as a fish loses its freshness. Yeasmin et al. [6] presented the illegal use of formalin as a way to make fish appear fresher. Following this logic, the formalin-treated fish

samples should have eyes that are less cloudy than the untreated control samples, contrary to what had been observed in this study. This contradiction indicates that though formalin-treated fish may seem fresh according to several indicators of fish freshness, it does not pass as fresh when assessed through eye turbidity.

The results of the study may improve the current process of formalin presence identification in the marketplace through the development of an objective measuring standard based on value from the HSV color space instead of apparent color. This may be further enhanced through automation with the use of software development.

Limitations. Since image acquisition was manually performed, the positioning of the camera was not constant all throughout the duration of the data gathering. Slight deviations may have occurred during the conduct of the data gathering, varying the light received by the camera.

Conclusion. In this study, image processing was employed for fish freshness assessment by measuring the color parameters of the eye and pupil of formalin-treated and untreated *Chanos chanos* (milkfish). A significant difference was observed in the changes in eye and pupil value between treated and untreated samples, thus justifying the use of eye and pupil value as an indicator of formalin presence. In contrast, no significant difference was found in the changes in fish eye and pupil saturation between treated and untreated samples; hence saturation is not an effective indicator of formalin presence. Additionally, formalin immersion was found to degrade eye freshness rather than enhance it as formalin-treated fish had cloudier eyes than untreated fish.

Recommendations. The process of capturing and segmenting images is time-consuming. Automation of image segmentation removes any human biases that may be present in identifying the parts of a fish eye. However, a separate study must also be conducted for the determination of the eye and pupil of a fish using computer vision and thresholding. Automation is the potential extension of this study, thus the integration of the computer vision segmentation and image processing is recommended.

Quality assessment of the fish samples through trained experts during the conduct of the study is recommended to compare the manual and the computer-assisted process of product evaluation and to verify the precision and accuracy of the data gathered. To completely avoid light reflection in images, an image acquisition setup consisting of a light box with an external light source is also recommended.

Acknowledgement. The researchers would like to express their utmost gratitude to Mr. Victor Estilo from the SEAFDEC Brackishwater Station for providing the fish samples and for his patience and assistance in the collection and transportation of samples.

References

[1] BFAR (Bureau of Fisheries and Aquatic Resources). 2018. Philippine fisheries profile 2018 [Internet]. [Cited 13 October 2019]. Available from https://www.bfar.da.gov.ph/publication.jsp?id=2369#post

[2] Tolentino LKS, Orillo JWF, Aguacito PD, Colango EJM, Malit JRH, Marcelino JTG, Nadora AC, Odeza AJD. 2017. Fish freshness determination through support vector machine. J Telecom Elec Comp Eng. 9(2-5): 139-143.

[3] Dowlati M, Mohtasebi SS, Omid M, Razavi SH, Jamzad M, de la Guardia M. 2013. Freshness assessment of gilthead sea bream (*Sparus aurata*) by machine vision based on gill and eye color changes. J Food Eng. 119: 277-287.

[4] Misimi E, Mathiassen JR, Erikson U. 2007. Computer vision-based sorting of atlantic salmon (*Salmo salar*) fillets according to their color level. J Food Sci. 72(1): 30-35.

[5] International Agency for Research on Cancer. 2012. Formaldehyde Volume 100F [Internet]. [Cited 12 January 2019]. Available from https://monographs.iarc.fr/wp-content/uploads/2018/06/mono100F-29.pdf

[6] Yeasmin T, Reza MS, Shikha FH, Khan MNA, Kamal M. 2010. Quality changes in formalin treated rohu fish (*Labeo rohita*, Hamilton) during ice storage condition. J Bangladesh Agri U. 2(4): 158-163.

[7] Sanyal S, Sinha K, Saha S, Banerjee S. 2017. Formalin in fish trading: an inefficient practice for sustaining fish quality. Arch Pol Fish. 25: 43-50.

[8] Unal Sengor GF, Balaban MO, Topaloglu B, Ayvaz Z, Ceylan Z, Dogruyol H. 2018. Color assessment by different techniques of gilthead seabream (*Sparus aurata*) during cold storage. Food Sci Technol [Internet]. [cited 2019 Jan 22]; 1-8. doi: https://doi.org/10.1590/fst.02018

[9] Davie PS, Kopf RK. 2006. Physiology, behaviour and welfare of fish during recreational fishing and after release. New Zealand Vet J. 54(4): 161-172.

[10] Lehnert M, Balaban M, Emmel T. 2011. A new method for quantifying color of insects. Florida Entomologist. 94(2): 201-2017.

[11] Kanamori K, Shirataki Y, Quihong L, Ogawa Y, Suzuki T, Kondo N. 2017. Fish freshness estimation using eye image processing under white and UV lightings. In: Sensing for agriculture and food quality and safety IX. Proceedings of the society of photo-optical instrumentation engineers. p, 1-12.

[12] Sengar N, Dutta MK, Sarkar B. 2017. Computer vision based technique for identification of fish quality after pesticide exposure. Int J Food Prop. 20(2): 2192–2206.

[13] Bora DJ, Gupta AN, Khan FA. 2015. Comparing the performance of *L*A*B** and HSV color spaces with respect to color image segmentation. Int J Emerging Technol Adv Eng. 5(2): 192-203.

[14] Masniyom P. 2011. Deterioration and shelf-life extension of fish and fishery products by modified atmosphere packaging. Songklanakarin J. Sci. Technol. 33(2): 181-192.

[15] Balaban MO, Stewart K, Fletcher GC, Alcicek Z. 2014. Color change of the snapper (*Pagrus auratus*) and gurnard (*Chelidonichthys kumu*) skin and eyes during storage: Effect of light polarization and contact with ice. J Food Sci. 79(12): 2456-2462.

L I A D L A W

INDUSTRY, ENERGY, AND EMERGING TECHNOLOGY

LIADLAW is considered as the sun deity of the pre-colonial Visayans. Just as the sun rises day to day, so does new innovations and inventions. Technology that aims to improve our daily life and propose modern solutions to age-long problems continues to shine a bright light towards a more sustainable future. This section particularly treads towards more sustainable practices in the largely coal-based energy industry. The research proposes an alternative source of energy such as an organic waste feedstock, and improvements on existing renewable sources as in solar energy harvesting.

These studies fall under the agenda of the same name, Industry, Energy, and Emerging Technology (IEET). This agenda aims to support the growth of frontier sectors, e.g. energy, transportation, etc., with research and development, information and technology diffusion, and the development of enabling policies.

BASED ON: Harmonized National Research and Development Agenda (HNRDA)

Kinetic analysis of *Theobroma cacao* (UIT Variety) pod husks through gasification as an alternative to sub-bituminous coal

KIMBERLY SHAYNE S. TUKASIM, CHRISTIAN MARC P. BEÑOSA, MICKEL LYLE ANGELO E. PE, and FERNANDO CHRISTIAN C. JOLITO III

Philippine Science High School - Western Visayas Campus, Brgy. Bito-on, Jaro, Iloilo City 5000, Department of Science and Technology, Philippines

Abstract

Co-gasification of biomass and coal is emerging as a potential clean fuel technology as it reduces greenhouse gas emissions, lowers gross power output, and increases thermal efficiency. The present study aimed to determine the potential of *Theobroma cacao* (UIT Variety) pod husks as an alternative to coal by investigating the gasification kinetics The proximate composition of five sample blends of cacao pod husks and sub-bituminous coal (CPH-SBC): 0%-100% wt/wt, 25%-75% wt/wt, 50%-50% wt/wt, 75%-25% wt/wt, 100%-0% wt/wt, were determined using the STA 8000 in a nitrogen-enriched atmosphere at 900°C. The conversion-time data obtained were fitted using the three different kinetic models namely: Volumetric Model (VM), Shrinking Core Model (SCM), and Random Pore Model (RPM). Results showed that the blend 75%-25% CPH-SBC is the most effective in terms of the overall proximate composition. Among the three kinetic models, the RPM had the best fit, having R^2=0.964, with the data, suggesting that the growth of the pores and coalescence of the pores causes a reduction of area through a combination of overlapping of pore surfaces. The activation energy of the blends, according to the best fit model, ranged from 93.919 kJ/mol to 105.73 kJ/mol. Based on the results, it can be concluded that *Theobroma cacao* (UIT Variety) pod husks can indeed act as a substitute to sub-bituminous coal.

Keywords: *co-gasification, biomass, coal, proximate composition, kinetic modeling*

Introduction. A large percentage of the Philippines' energy demand is obtained from the use of fossil fuel - despite efforts to transition to a cleaner alternative [1,2]. To fully support the transition, an equally or even more efficient energy resource is therefore necessary. Thus, it is imperative to find alternative energy resources in order to cut the use of fossil fuel in meeting the country's energy requirements. Biomass is the cheapest and most abundant renewable energy resource in the Philippines as the country produces tons of agricultural and forestry wastes [3]. This includes in great proportion the common agricultural wastes such as rice straws, husks, and sugar bagasse [4].

Co-gasification of coal has recently gained interest as a potentially clean and efficient technology for production of energy and biofuels [5]. Gasification is the most versatile thermal conversion process in energy production [6]. In the effort to sustainably reduce the use of coal in meeting the increasing energy demands, various studies have extensively investigated the gasification of other feedstocks, especially biomass waste materials [5]. The results of these studies show that co-gasification of coal and biomass has higher overall efficiency than the separate gasification of these materials [7]. The cellulose, hemicellulose and lignin content of biomass increases the rate of gasification [8]. Moreover, gasification of biomass in ash coal can reduce the slagging and fouling problems caused by high alkali contents [9]. Coal and biomass seem to have synergistic reaction rates with lower gross power output, but higher thermal efficiency [10]. Co-gasification also has reduced greenhouse gas emissions as compared to conventional methods. It also addresses the problems associated with sulfur and ash contained in coal as biomass comparatively contains less of the two [11].

Cacao pod husk has been extensively studied as a promising biomass for gasification due to its high cellulosic and hemicellulosic content [8]. However, it lacks sufficient kinetic characterization necessary for industrial translation. Given that there is limited research on the gasification of cacao pod husk, this study aims to fill in the gap by determining the kinetic parameters: activation energy, and rate constants (k_{VM}, k_{SCM}, k_{RPM}), and the proximate analysis properties such as the moisture content, volatile matter, fixed carbon, and ash content provided by the different reaction models used [10].

Gasification is an incomplete combustion process that partially burns and converts the feed. It is often shown by using models based on the behavior of the reaction and carbon conversion. [12] These models help suggest the most probable mechanism involved in the reaction. The kinetic models that would be used in this study are the Volumetric Model (VM), Shrinking Core Model (SCM), and Random Pore Model (RPM). VM assumes the reaction to be uniform throughout the volume of the particle [13]. While the SCM assumes

How to cite this article:
CSE: Tukasim KSS, Beñosa CMP, Pe MLAE, Jolito FCC. 2020. Kinetic analysis of *Theobroma cacao* (UIT Variety) through gasification as an alternative to sub-bituminous coal. Publiscience. 3(1):91-96.
APA: Tukasim, K.S.S., Beñosa, C.M.P., Pe, M.L.A.E., & Jolito, F.C.C. (2020). Kinetic analysis of *Theobroma cacao* (UIT Variety) through gasification as an alternative to sub-bituminous coal. *Publiscience*, 3(1):91-96.

that the reaction takes place on the surface of the particle only and not throughout the particle, reducing the core radius; hence the 'shrinking' [14]. On the other hand, RPM assumes two opposing structural changes: growth and coalescence of the pores resulting in the reduction of area due to pore overlaps [15].

The kinetic study and other scientific data reported in this study can be used as a guide in designing more comprehensive and systematic studies that, in turn, would help in the design of an efficient gasifier or reactor system. Cacao pod husks are usually unutilized waste products of cacao bean production, which is a growing agricultural industry in the Philippines. The pod husk represents 70 to 75% of the whole weight of the cacao fruit [16], and thus can be promising feedstock in the co-gasification process.

The co-gasification of biomass and coal for power generation provides a real option to expand the energy supply in the Philippines and thus may reduce the country's utilization of coal and other fossil fuels, and thereby reducing the greenhouse gas and air pollutant emissions. The stated valorization of the cacao pod husk may also be economically significant as this could be a new source of income for the Filipino cacao farmers.

This study aimed to investigate the gasification kinetics of *Theobroma cacao* (UIT Variety) pod husks and coal blends as an alternative energy. It specifically aimed to:

(i) perform proximate analysis of the different ratio of cacao pod husk-sub-bituminous coal (CPH-SBC) blends: 0%-100%, 25%-75%, 50%-50%, 75%-25%, 100%-0%;

(ii) compare the different gas-solid models: Volumetric Model (VM), Shrinking Core Model (SCM), and Random Pore Model (RPM), through comparison of the coefficient of determination (R^2); and

(iii) calculate the reaction rate constant and the activation energy of the gasification reaction based on the kinetic parameters.

Methods. Five samples were analyzed in the study, this consists of CPH-SBC of 0%-100%, 25%-75%, 50%-50%, 75%-25%, 100%-0%. The blends then underwent gasification at a temperature of 900°C using a Simultaneous Thermal Analyzer 8000 (Perkin Elmer STA 8000), which undergoes the process of drying, devolatilization, gasification and combustion. The weight loss history and heat absorption of the individual blends were studied in a linearly heated environment. The char conversion obtained was then used to fit in the three kinetic models namely, Volumetric Model (2) Shrinking Core Model (3), and Random Pore Model (4).

Thermal analysis. The Thermogravimetric analyzer (PerkinElmer Simultaneous Thermal Analyzer 8000) was used in the gasification process. Thermogravimetry was used as an alternative method for obtaining the proximate analysis as it shows good correlation in results compared to the classical method [17]. For each blend, a sample weighing 20 mg was heated in a small furnace in the thermal analyzer to study its thermal degradation. The samples were heated from 20°C to 900°C at a linear heating rate of 50°C·min^{-1}. The samples were then gasified at 900°C to promote the different endothermic reactions that are occurring during gasification. Table 1 shows the summary of steps.

Table 1. Running program inputted in STA 8000.

Method	Description	Purpose
Isothermal	Heat for 2.0 min at 20°C	Mass stabilization
Temperature-Ramp	Heat for 20°C to 110°C at 50°C/min	Increase to the drying temperature
Isothermal	Hold for 4.0 min at 110°C	Moisture removal
Temperature-Ramp	Heat from 110°C to 900°C at 50°C/min	Increase to the devolatilization, gasification, and combustion temperature
Isothermal	Hold for 10.0 min at 900°C	Devolatilization, gasification, and combustion

Data Analysis. The fractional char conversion rate constant was calculated and plotted in a conversion-time graph. Then, kinetic model fitting was done by calculating for the first-order kinetic model constant with respect to the fractional char conversion.

The evaluation was carried out by determining the fractional conversion using Equation 1 (1). The fractional char conversion ratio X, at any given time t can be expressed as follows:

(1) $$X = \frac{W_0 - W}{W_0 - W_{ash}}$$

where W_0 is the initial mass of the pre-gasified char, W_{ash} is the mass of ash in the primary char sample, and W is the mass of the char at any time t [18].

After which, it was fitted into the gas-solid reaction model, namely Volumetric Model, Shrinking Core Model, and Random Pore Model given by equation 2 (2), 3 (3), and 4 (4), respectively.

(2) $$X = 1 - e^{-k_{vm}t}$$

where k_{VM} is the first-order reaction rate constant.

(3) $$3\left[1 - (1 - X)^{\frac{1}{3}}\right] = k_{SCM}t$$

where k_{SCM} is the average rate reaction constant,

(4) $$X = 1 - e^{\left[-k_{RPM}t\left(1 + \frac{\Psi k_{RPM}t}{4}\right)\right]}$$

where k_{RPM} is the reaction rate constant, $\boldsymbol{\Psi}$ is a structural parameter which describes the particle's internal structure given by

$$\Psi = \frac{2}{2ln(1 - X_{max}) + 1}$$

where X_{max} is the conversion at the maximum rate of gasification.

Using the standard deviation formula given in (5), the overall goodness of fit would then be determined.

$$SD = \sqrt{\frac{\sum(X_{exp} - X_{model})^2}{N-p}} \quad (5)$$

where X_{exp} and X_{model} are the conversion data from the experiment and each individual model and N is the number of data while p is the number of parameters fitted.

$$R^2 = 1 - \frac{\sum_1^n (X_{exp} - X_{model})^2}{\sum_1^n (X_{exp} - X)^2} \quad (6)$$

where $\bar{X}$ is the average values of char conversion.

Finally, the activation energy was calculated using the Van't hoff equation given in (7):

$$ln\frac{k_2}{k_1} = \frac{-E_a}{R}\left(\frac{1}{T_2} - \frac{1}{T_1}\right) \quad (7)$$

where k_1 is the kinetic model constant at temperature T_1 where the first change in sample mass is observed, k_2 is the kinetic model constant at temperature T_2 (900°C or 1173 K), E_a is the activation energy, and R is the gas constant 8.314 J/mol·K.

The reaction rate for the models was then graphed using a graphical and statistical analysis software to obtain the R^2 value and the graph of the predicted curve. The Root Mean Square Error (RMSE) was calculated to find the kinetic model with the lowest deviation from the predicted reaction curve.

Statistical Analysis. Analysis of Variance (ANOVA) of α=0.05 was done to determine if there is a significant difference in the R^2 and RMSE of the rate constants from the kinetic models for the five sample blends.

Safety Procedure. There was no special treatment for waste disposal of the samples, and ash content. The ash which remained in the pan after the thermal analysis was disposed of in a container as it does not contain any toxic residue.

Results and Discussion. The results and discussion were divided into four parts namely: proximate analysis, char conversion-time graph analysis, determination of kinetic parameters, and determination of Arrhenius parameters.

Proximate analysis. The desired sample blend ratio should have a low moisture content, higher amount of fixed carbon, and low ash content [8]. A lower amount of moisture would yield faster pyrolysis, while a higher amount of fixed carbon and lower ash content would help increase its rate of gas conversion. As seen in Table 2, among the five different sample blends, the ratio having 0%-100% cacao pod husks-sub-bituminous coal (CPH-SBC) contains the highest amount of moisture while 100%-0% CPH-SBC contains the lowest amount.

Table 2. Proximate composition of the samples.

Component (CPH-SBC)	Moisture (%)	Volatile Matter (%)	Fixed Carbon (%)	Ash Content (%)
0%-100%	13.02	41.56	9.25	36.16
25%-75%	12.30	46.50	11.13	29.89
50%-50%	12.00	50.49	15.43	22.08
75%-25%	11.25	64.04	19.99	4.71
100%-0%	9.39	66.15	15.34	9.11

In order to determine the most viable type of blend, these properties must be accounted for which is why in order to summarize these parameters, the following characteristics is desired: low moisture content, 40% or higher amount of fixed carbon, and less than 10% amount of ash content [10]. The blend 0%-100% CPH-SBC has the highest ash content, it was therefore arbitrarily designated as the least efficient among the blends, especially upon determination of activation energy and coefficient of determination.

Char conversion-time graph analysis. Figure 1 shows the conversion-time graph which has a direct correlation to the proximate analysis. For the moisture removal, the 100%-0% CPH-SBC has the slowest conversion rate while the 0%-100% CPH-SBC has the fastest with respect to their moisture content being the lowest and the highest among the sample blends.

The volatile matter of the sample blend increases as biomass ratio increases. This makes biomass easier to ignite than coal resulting in a faster conversion rate for the 100%-0% CPH-SBC followed by the 75%-25% CPH-SBC in the earlier parts of volatile matter removal. After 18.26 minutes, both 25%-75% CPH-SBC and 0%-100% CPH-SBC have higher conversion rates than 100%-0% CPH-SBC. At 23.89 minutes, the conversion rates are in order of higher coal ratio in the sample blend.

The fixed carbon is the carbonaceous residue when volatile matter is removed. The 75%-25% CPH-SBC has the fastest conversion rate followed by the 50%-50% CPH-SBC and the 100%-0% CPH-SBC.

After removing the fixed carbon, the 75%-25% CPH-SBC was calculated to reach 0.99 conversion after 31.02 minutes. Other sample blends were found to have reached the same conversion at 33.13, 33.11, 33.02, and 32.71 minutes for the 100%-0% CPH-SBC, 50%-50% CPH-SBC, 25%-75% CPH-SBC, and 0%-100% CPH-SBC respectively.

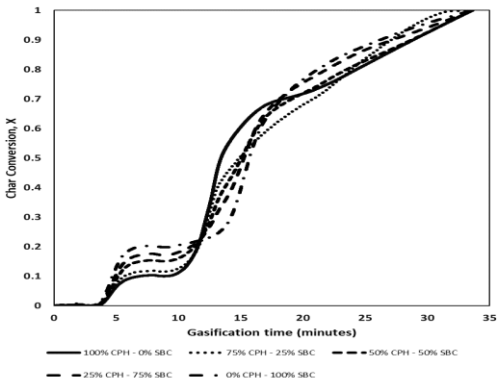

Figure 1. The graph shows char conversion (denoted by X) as a function of time (in minutes).

Determination of Kinetic parameters. Table 3 shows the different parameters of the blends obtained from the simulation of the conversion-time using the kinetic models namely: Volumetric Model (VM), Shrinking Core Model (SCM), and Random Pore Model (RPM). As well as the determination of the kinetic rate constant (k_{VM}, k_{SCM}, k_{RPM}), the coefficient of determination (R^2), and Root Mean Square (RMSE) and the standard deviation (SD).

Table 3. Kinetic parameters of the sample blends.

		0%-100%	25%-75%	50%-50%	75%-25%	100%-0%
VM	k_{VM}	0.321	0.309	0.299	0.338	0.301
	R^2	0.896	0.865	0.845	0.902	0.760
	SD	0.649	0.650	0.638	0.627	0.645
	RMSE	0.0128	0.0131	0.0125	0.0168	0.0148
SCM	k_{SCM}	0.087	0.086	0.086	0.089	0.086
	R^2	0.883	0.901	0.899	0.928	0.749
	SD	0.675	0.673	0.657	0.658	0.664
	RMSE	0.00620	0.00520	0.00483	0.00520	0.00811
RPM	ψ	2+8E-5	2+6E-5	2+6E-5	2+5E-5	2+E-5
	k_{RPM}	0.192	0.147	0.133	0.109	0.125
	R^2	0.964	0.964	0.964	0.964	0.964
	SD	0.652	0.667	0.654	0.667	0.666
	RMSE	0.0204	0.0155	0.0139	0.0116	0.0132

*All the kinetic rate constants (k_{VM}, k_{RPM}, k_{SCM}) are in the units of (1/s).

Determination of Arrhenius parameter. The activation energy (E_a) of the sample blend for the different models can be found in Table 4. The pre-exponential factors differ largely from one model to another with the lowest values from the Random Pore Model (RPM). This implies that different models result in different plots as both Arrhenius constants showed large difference of deviation from one another, thus, it is difficult to fully compare the ratios to one another.

Table 4. Activation Energy of the sample blends.

Component (cacao pod husk mass-coal mass)	Volumetric Model (E_a(kJ))	Shrinking Core Model (E_a(kJ))	Random Pore Model (E_a(kJ))
0%-100%	108.204810	104.034751	94.561378
25%-75%	109.752677	105.731682	94.096491
50%-50%	108.456908	104.5399463	93.932360
75%-25%	113.050501	108.741224	93.945847
100%-0%	106.424085	102.487189	93.919190

The RPM with R^2=0.964 was found to be the best fit model for the sample blends. The Shrinking Core Model with RMSE ranging from 0.00483-0.00811 has its experimental plot closest to the predicted model curve for all sample blends. After using ANOVA on the R^2 and RMSE of rate constants, a p-value of 0.01299 and 0.001 respectively suggests that there is no significant difference in the effect of blend ratios between cacao pod husk-sub-bituminous coal (CPH-SBC) on the gasification reaction of the sample blends.

To determine the most efficient sample blend ratio, the activation energy (E_a) and the proximate analysis must also be accounted for.

Since there is no significant difference between the blends among all models, the deciding factor would be in the proximate analysis; hence, the blend 75%-25% CPH-SBC is the most efficient. It shows great variability in terms of ash content and amount of fixed carbon having the lowest value with 4.71% and the highest with 19.99%, respectively. This suggests that the conversion from biomass to biogas is most effective in the process. It is ideal to have low ash content to avoid problems with the gasifiers which include slagging, and fouling of the equipment [19], as well as high fixed carbon as this would enable the process to fully convert the feedstock. The conversion-time graph for 75%-25% CPH-SBC also shows that 0.99 conversion is reached after 31.02 minutes, earlier than other blends which are at around 33 minutes, this suggests that char conversion for this sample blend is more efficient than others. This is followed by the blend 100%-0% CPH-SBC with the second lowest value of ash content with 9.11% making it the second most efficient. The increase in ash content may be due to the increase in the coal content of the blend.

The ash content is significantly greater when the blend contains more coal than cacao based on the proximate analysis. This causes the sample blend to have a higher heat capacity and therefore should take more time to burn and/or gasify [8].

With all parameters considered, the most efficient ratio of blends would be 75%-25% CPH-SBC, followed by 100%-0% CPH-SBC. This conclusion was made due to the (1) proximate analysis (2) and lower activation energy.

The sample blend ratio is in line with the results of Kamble et al. [8] that biomass-coal ratio should contain around 70% biomass for gasification at lower temperatures because more biomass in blends result to higher amounts of hydrocarbons enhancing the calorific value of gaseous products. It also suggests that *Theobroma cacao* (UIT variety) can be used as a substitute to coal as it has better kinetic properties than sub-bituminous coal due to its higher coefficient of determination and lower activation energy. Moreover, since slagging did not occur during the gasification process despite having ash content higher than 5%, it does not make 100%-0% CPH-SBC disadvantageous when gasified at 900°C. However, it may be disadvantageous when undergoing gasification at lower temperatures.

Limitations. The study involved *Theobroma cacao* (UIT Variety), as a biomass for gasification. Each blend was tested only once due to limited resources. Only 90 minutes of the gasification time was considered in this study. Instead of using the ASTM (American Society for Testing and Materials) standards in determining the proximate analysis, the data from the thermal analysis was used to obtain the different parameters. The experiment was carried out on a laboratory scale, so it did not involve any economic analysis for the gasification. In addition, the experiment did not include neither quantitative nor qualitative analysis of the output gas. Only SCM, RPM, and VM were used to evaluate the kinetic parameters.

Conclusion. The kinetics of *Theobroma cacao* pod husks (CPH) was investigated. Proximate

analysis and kinetic parameters suggest that the gasification of a CPH-sub-bituminous-coal (SBC) mixture is a viable alternative energy source to that of pure coal. The kinetic models that were used in this study are the Volumetric Model (VM), Shrinking Core Model (SCM), and Random Pore Model (RPM), which were chosen based on the type of feedstock used. Plots of the kinetic reaction models suggest that the RPM is the best fit model according to the coefficient of effectiveness (R^2), suggesting that the mechanism of reaction has two opposing structural changes: growth and coalescence of the pores resulting in the reduction of area due to pore overlaps. However, there was no significant difference found between the blends in RPM. Therefore, the only viable basis for efficiency is the proximate analysis which is reflective of the rate constants (k) and activation energy (E_a). Among the blends, 75%-25% CPH-SBC showed the highest efficiency in terms of its proximate analysis, specifically its amount of fixed carbon and ash content with implications of better biomass to biogas conversion of the sample blend, and its activation energy of 93.945 kJ. This can be used as a guide in the design of an efficient gasifier or reactor system.

Recommendations. Smaller interval of gasification temperature (50°C) is recommended in order to study the rate limiting behavior as it could affect the gaseous reaction of the gasification. Since great variability is shown in the ash content, it is also recommended to have the blends gasified at lower temperature, as it may yield better results. It is also recommended to run an ash analysis in order to determine the composition of the ash. As well as a gas analysis to determine the different products formed during the gasification. Determining the synergistic effect when combined with other grades of coal is also recommended because sub-bituminous coal is only a fourth-grade type of coal. There are higher grades of coal which have higher carbon and fewer moisture, volatile matter, and ash.

Acknowledgement. The authors would like to extend their gratitude to their consultant, Vergel Bungay, for sharing his knowledge and expertise. Their gratitude is also extended to the University of the Philippines Visayas: Miag-ao Campus for allowing them to run the thermal analysis for the samples.

References

[1] Department of Energy, Philippines. 2016. [cited 2019 Jan]

[2] Brahim S. 2015.Renewable energy and energy security in the Philippines in Energy Procedia.

[3] PSA. 2016. Highlight of Philippine Population 2015 Census of Population.

[4] Foong S, Liew R, Yang Y, Cheng Y, YuhYek P, Mahari W, Lee X, Han C, Vo D, Le Q, Aghbashlo M, Tabatabaei M, Sonne C, Peng W, Lam S. 2020. Valorization of biomass waste to engineered activated biochar by microwave pyrolysis: Progress, challenges, and future directions. Elsevier. Chemical Engineering Journal. Volume 389:124401

[5] Emami-Taba L, Irfan MF, Wan Daud WAM, Chakrabarti MH. 2012. The effect of temperature on various parameters in coal, biomass and CO-gasification: A review. Renewable and Sustainable Energy Reviews, 16(8): 5584-5596.

[6] Wu Y, Wu S, Gao J. 2009. A Study on the Applicability of Kinetic Models for Shenfu Coal Char Gasification with CO_2 at Elevated Temperatures. Energies. 2(3):545.

[7] Manzanares-Papayanopoulos E, Herrera-Velarde JR, Arriola-Medellín A, Alcaraz-Calderón AM, Altamirano-Bedolla JA, Fernández-Montiel M. 2014. The co- gasification of coal-biomass mixtures for power generation: a comparative study for solid fuels available in Mexico. Energy Sources Part A. 36 (1):104–11.

[8] Kamble AD, Saxena VK, Chavan PD, Mendhe VA. 2018. Co-gasification of coal and biomass: Status and prospects of development in Indian context. Int J Min Sci Technol. (2018): 1-16.

[9] Henry A, Long III, Wang T. 2011. Case studies for biomass/coal co-gasification in IGCC applications. Proceedings of ASME Turbo Expo.

[10] Cormos CC. 2012. Hydrogen and power co-generation based on coal and biomass/solid wastes co-gasification with carbon capture and storage. International Journal of Hydrogen Energy. 37(7):5637-5648.

[11] Kumabe K, Hanaoka T, Fujimoto S, Minowa T, Sakanishi K. 2006. Co-gasification of woody biomass and coal with air and steam. Fuel. 86(2007):684-689.

[12] Wu Y, Wu S, Gao J. 2009. A Study on the Applicability of Kinetic Models for Shenfu Coal Char Gasification with CO_2 at Elevated Temperatures. Energies. 2(3): 545.

[13] Jayaraman K, Gokalp I, Bonifaci E, Merlo N. 2015. Kinetics of steam and CO2 gasification of high ash coal–char produced under various heating rates. Fuel. 154: 370-379. doi: 10.1016/j.fuel.2015.02.091

[14] Yagi, S and Kunii D. 1961. Fluidized solids reactors with continuous solids feed-I Residence time of particles in fluidized bed. Chemical Engineering Science. 16: 364-371.

[15] Bhatia S and Perlmutter D. 1979. A random pore model for fluid-solid reactions, i. isothermal, kinetic control.

[16] Cruz G, Pirilä M, Huuhtanen M, Carrión L, Alvarenga E, Keiski R. 2012. Production of Activated Carbon from cacao (*Theobroma cacao*) Pod Husk. J Civil Environment Engg. 2(2): 1-6.

[17] Ottaway M. 1982. Use of thermogravimetry for proximate analysis of coals and cokes. Fuel, 61.

[18] Massoudi Farid M, Jeong HJ, Hwang J. 2016. Kinetic study on coal–biomass mixed char co-gasification with H_2O in the presence of H_2. Fuel. 181:1066-1073. doi: http://dx.doi.org/10.1016/j.fuel.2016.04.130

[19] Demirbas A. 2009. Biomass feedstocks Biofuels: Springer.

A novel application of a double convex-hemispherical lens configuration for a III-V tandem InGaP/GaAs/Ge multi-junction solar cell

ADONIS F. EBOJO JR., JESTER L. MAGAN, RYAN JAMES M. DUMALAG, ARIS C. LARRODER and ATHENES JOY P. ABAN

Philippine Science High School - Western Visayas Campus, Brgy. Bito-on, Jaro, Iloilo City 5000, Department of Science and Technology, Philippines

Abstract

Concentrator photovoltaics require solar trackers to maximize sunlight capture. However, solar trackers are expensive both in components and utility. In this study, the lens configuration was modified to eliminate the need for solar trackers, as well as improve power output. This configuration consisted of a double convex, hemispherical lens, and a Fresnel lens all positioned on top of the multi-junction solar cell. The double convex-hemispherical lens (DCX-HSL) setup was based on the Fresnel lens setup which is composed of a Fresnel lens placed on top of the multi-junction solar cell. To test the merits of the DCX-HSL setup, it was tested against a signal Fresnel lens concentrator over the course of one photoperiod. The results showed that there is a significant difference in the power output of the DCX-HSL to the Fresnel lens setup from 10:15 to 14:15. The improvement of the power output from 10:15 to 14:15 is due to the added convex lens and hemispherical lens that focuses more light to the solar cell.

Keywords: *three-lens system, concentrator photovoltaic, hemispherical lens, convex lens*

Introduction. The lenses concentrate the sun's rays to the solar cell. Photovoltaics (PV) systems are known to convert sunlight into electricity at an estimated amount of one sun (1368 W/m^2) under favorable weather conditions [1]. The manufacturing of PV systems is expensive due to the components used in the system. There are different kinds of PV systems, ranging from conventional PV to Concentrator PV (CPV). CPVs were developed to utilize concentrating lenses and mini-reflecting mirrors to increase the power efficiency of the device. The introduction of concentrator lenses and mirrors in a PV system increases the power output per unit cost. CPV technology is relatively new when compared to conventional PV systems, requiring further optimization and research in comparison to them. One such consideration is the dispersion of light caused by the concentrating lenses. This is due to the optical properties and design of the lens being used [2]. The angle of the CPV relative to the sun is an important factor in optimizing sunlight collection, and therefore power production [3]. To achieve maximum efficiency, the sun must be perpendicular to the CPV for the concentrated light to be focused unto the solar cell [1].

To improve the CPV's ability to concentrate light, there were various designs and modifications that have been investigated. One study involved the use of a compound convex lens set up to improve the concentration of light and the concentration ratio [3]. Additionally, Jing et al. [4] developed a cost-effective compound setup using a three-dimensional lens. The setup also increases the acceptance angle and improves the irradiance distribution. This increases the performance of the solar cell as sunlight is directed to the solar cell longer due to the increase in acceptance angle. If a three-lens system CPV with a convex lens and a three-dimensional lens or similar were added to a Fresnel lens-based CPV, then the modified CPV may gain both benefits from the two studies.

The lenses concentrate the sun's rays to the solar cells; thus, it produces more electrical energy per cell and decreases the need for several solar cells, making CPVs more efficient than PVs [5]. The drawback is the increase in the cost for each individual solar panel or module [6]. To further improve the CPV, studies by Jing et al. [4], Huang et al. [7], and Barrios et al. [3] attempted different designs and modifications to improve the collection efficiency of the lens system, conversion efficiency of the solar cell [8], and many more aspects. As a result of these different studies, cost-effective CPVs were developed with capabilities of the costlier variants.

The Fresnel lens has been the lens of interest in these studies due to its properties such as being lightweight, cost-efficient, and smaller in volume compared to other concentrating lenses [7]. Fresnel lenses were used as a circular spot concentrating lens, which increased the conversion efficiency of the solar cell from 6.4% to 7%.

This study aimed to design a three-lens system to improve the range of the acceptance angle and the overall power output of a Fresnel lens CPV. The three-lens setup is referred to as the double convex-hemispherical lens (DCX-HSL), which was the modified setup while the Fresnel lens setup was the control setup. It specifically aimed to:

How to cite this article:

CSE: Ebojo Jr. AF, Magan JL, Dumalag RJM, Larroder AC, Aban AJP. 2020. A novel application of a compound convex-hemispherical lens configuration for a III-V tandem InGaP/GaAs/Ge multi-junction solar cell. Publiscience. 3(1):97-100.

APA: Ebojo Jr., A.F., Magan, J.L, Dumalag, R.J.M., Larroder AC, & Aban AJP. (2020). A novel application of a compound convex-hemispherical lens configuration for a III-V tandem InGaP/GaAs/Ge multi-junction solar cell. *Publiscience*, 3(1):97-100.

(i) measure the voltage and current of the DCX-HSL setup and the Fresnel lens setup; and

(ii) compute and compare the power output of the DCX-HSL setup and the Fresnel lens setup.

Methods. The software Ray Optics Simulation™ v1.0.0 was utilized to create a light ray diagram for the theoretical modeling of the DCX-HSL setup and the Fresnel lens setup. A diagram was created to simulate how the ray dispersion differs between the DCX-HSL setup and the Fresnel lens setup. The acceptance angles of the DCX-HSL setup and the Fresnel lens setup were theoretically modeled.

Assembly of the Fresnel lens setup. Figure 1 shows the structure of the Fresnel lens setup. The setup was composed of one 5 cm x 5 cm Fresnel lens with a focal point of 5 cm and a multi-junction solar cell. The Fresnel lens, which served as the primary lens in this setup, was situated 5 cm above the multi-junction solar cell.

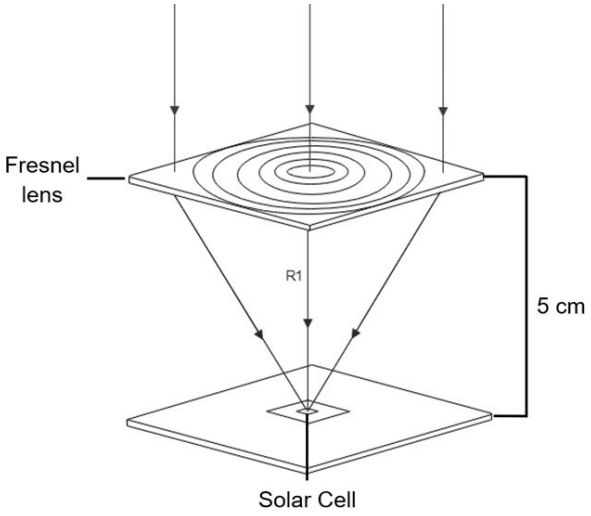

Figure 1. 3D image of the Fresnel lens setup.

Assembly of the DCX-HSL setup. A double convex lens and a hemispherical lens (HSL) with a radius of 2.5 cm and 0.5 cm, respectively, were attached to a Fresnel lens setup as shown in Figure 2. The hemispherical lens with a focal point of 0.5 cm was attached above the solar cell. The Fresnel lens was adjusted 5 cm above the hemispherical lens while the convex lens with a focal point of 10 cm was situated 5 cm above the Fresnel lens.

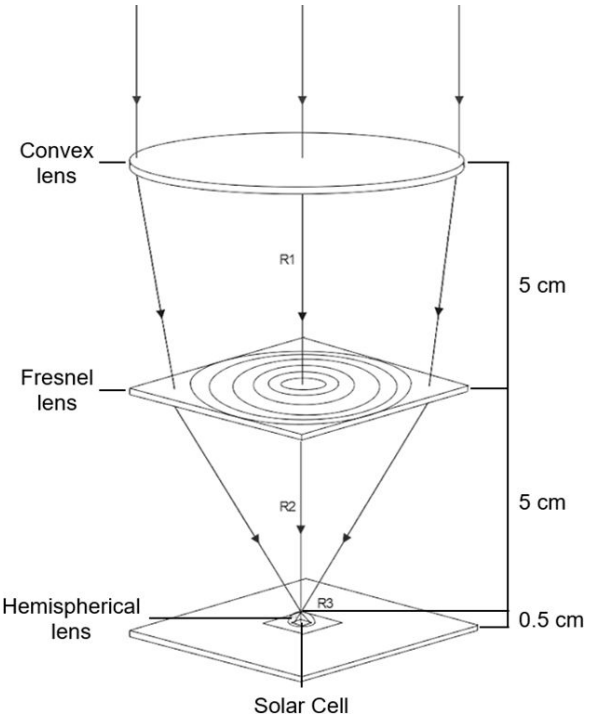

Figure 2. 3D image of the DCX-HSL lens setup.

The control setup consisted of a solar cell with a Fresnel lens functioning as its primary concentrator whereas the DCX-HSL setup was comprised of the same solar cell with convex, Fresnel, and hemispherical lenses acting as its primary, secondary, and tertiary concentrators respectively

Field testing of the Compound Fresnel-3D lens setup and Fresnel lens setup. The setups were tested on the rooftop of the Student Learning Resource Center Building located at Philippine Science High School - Western Visayas (10°45'10.7"N 122°35'15.8"E). The DCX-HSL setup and Fresnel lens setup were placed flat on a table and were adjusted to 0° with reference to the ground using a surface leveling application. Voltage, current, and solar irradiance were measured hourly with the time of data gathering recorded. A multimeter was used to measure the voltage and the current ,while a solar irradiance meter was used to measure the solar irradiance. Multiple trials were done until the value of three consecutive trials for each data had a difference of 0.001 volts for the voltage, 0.01 mA for the current, and 1 W/m² for the solar irradiance, which were the lowest precisions of the measuring devices used. The testing was conducted hourly from 6:15 am to 5:15 pm. Weather conditions such as the cloud cover were recorded as it may affect the data gathered.

Data Analysis. The hourly mean of the voltage and current was calculated and was used for the calculation of the hourly power output. The power output of the DCX-HSL setup and Fresnel lens setup was calculated using the formula

$$P = I \times V \quad (1)$$

where P is the calculated power output in watts, I is the measured current in amperes, and V is the measured voltage in volts. The values, however, of

the power and current in this paper were expressed in milliwatts and milliamperes, consistent with the precision of the tools used.

For the statistical analysis, the Wilcoxon Signed Ranks Test was used to compare the power output of the DCX-HSL setup and the Fresnel lens setup.

Results and Discussion. The findings and discussion were separated into four parts: voltage and irradiance, current and irradiance, power and irradiance, and data analysis.

Voltage and Irradiance. The Double Convex-Hemispherical Lens (DCX-HSL) setup had a lower voltage output compared to the Fresnel lens throughout the photoperiod, except from 10:15 to 14:15 (midday) as shown in Figure 3. The lower output of the DCX-HSL setup may have been due to the refraction caused by the HSL. Sunlight during 6:15 to 8:15 and 15:15 to 17:15 can reach the solar cell of the Fresnel lens setup without going through the Fresnel lens. The DCX-HSL, on the other hand, has an HSL that may have refracted some sunlight away from the solar cell. During midday, it was expected for both setups to have the highest output but only the DCX-HSL setup reached its peak, while the Fresnel lens setup dropped. This may have been due to the offset of the sun and the acceptance angle of the two setups. The setups were stationary and adjusted to be perpendicular with respect to the horizon. Therefore, the conditions do not meet the requirements for the CPV to produce the maximum power. Since the DCX-HSL has a higher acceptance angle compared to the Fresnel lens setup, light rays were still redirected to the solar cell. This may be why the DCX-HSL setup increased in voltage and current output during midday, as expected while the Fresnel lens setup's dropped. The mean voltage of the DCX-HSL setup and Fresnel lens setup during 05:15 to 17:15 (whole day) was 2.1512 V and 2.1649 V, respectively.

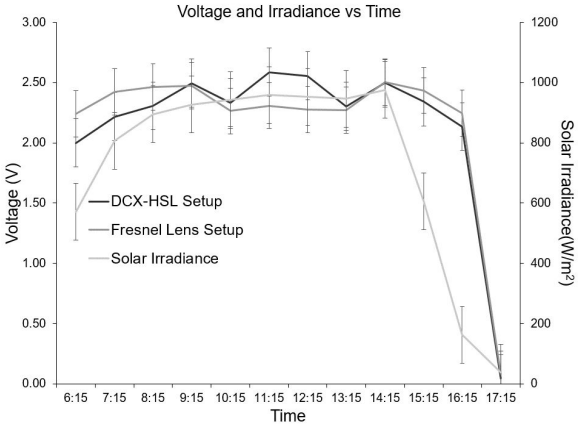

Figure 3. Average voltage of the DCX-HSL and Fresnel lens setup vs time during the photoperiod.

Current and Irradiance. The current of the two setups has a similar pattern to Figure 3 as shown in Figure 4. Since the current is proportional to the voltage, the current of the DCX-HSL setup is lower to the current of the Fresnel lens setup except during midday just like Figure 3. It is notable that during midday the Fresnel lens setup had a constant output. Other than the offset of the sun, this may also be due to the limit in the precision of the measuring tools. The same may be said when the two setups had a zero current output where they may have had an output between 0.01 mA and 0.00 mA. The mean current of the DCX-HSL in the whole day setup was 0.0242 mA while the Fresnel lens setup was 0.0142 mA.

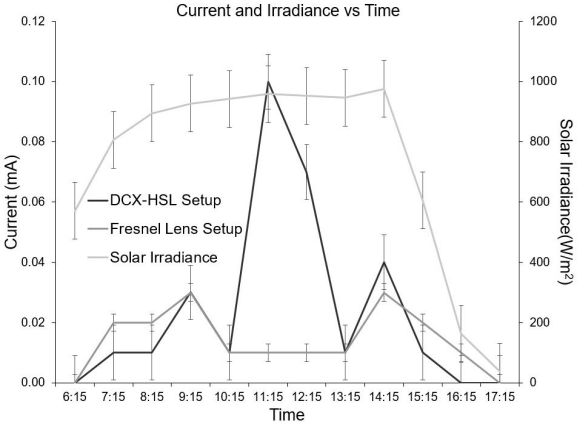

Figure 4. Average current of the DCX-HSL and Fresnel lens setup vs time during the photoperiod.

Power and Irradiance. After calculating the power output of the DCX-HSL and Fresnel lens setup, the results show a similar trend to that of Figures 3 and 4. The mean power output throughout the day of the DCX-HSL setup was 0.0606 mW, while for the Fresnel lens setup, it was 0.0341 mW.

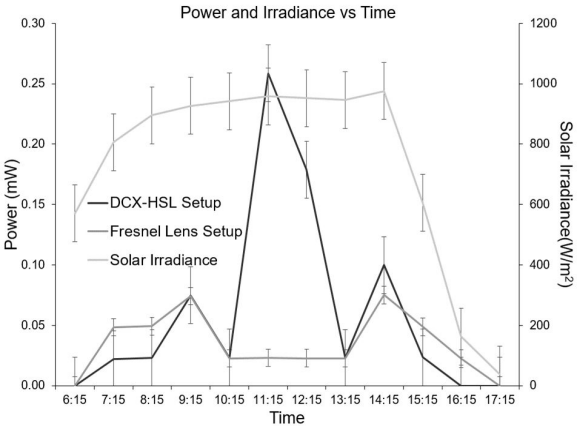

Figure 5. Average power output of the DCX-HSL and Fresnel lens setup vs time during the photoperiod.

The mean irradiance throughout the day was 732 W/m^2. Irradiance gradually increased until 11:15, upon which it gradually decreased. At 13:15 to 14:15, the irradiance had a slight increase before rapidly decreasing until 17:15.

The DCX-HSL setup yielded a higher power output than the Fresnel lens setup for both the whole day and midday by 77.65% and 251.05%, respectively.

Data Analysis. The p-value of the data was calculated using the Wilcoxon Signed Ranks Test with a confidence value (α) of 0.05 for a 95% confidence level. The test showed a significant difference from 10:15 to 14:15 (midday) in the output of the DCX-HSL setup and the Fresnel lens setup, as shown in Table 1. As for the whole photoperiod,

there is no significant difference between the output of the DCX-HSL setup and the Fresnel lens setup.

Table 1. The p-value for the difference in the power outputs between the DCX-HSL and Fresnel setups at midday and the whole day.

Time of the day	Z	p-value Asymp. Sig. (2-tailed)
Midday	-2.023	0.043
Whole Day	-0.255	0.799

The addition of a convex lens as a primary lens and a hemispherical lens as another secondary lens in the optical system of a Fresnel lens setup increased its overall power output. The increase in power output was calculated to be 77.65% by the whole day while the calculated increase during midday was 251.05%. This may be due to the addition of lenses which increased the acceptance angle of the system [3].

At 10:15, cloud covers were observed; therefore, a lower output is expected for both setups. The power output of the DCX-HSL and Fresnel lens setup from 9:15 to 10:15 dropped from 0.0749 and 0.0742 to 0.0233 and 0.0226, respectively.

The data shows a similar trend to Barrios et al. [3] wherein the irradiance rose from 6:15 to 12:15, where the sun rises to its peak, resulting in an increase in the voltage and current output throughout the said duration. As the irradiance decreased from 13:15 to 17:15, the voltage and current output also decreased. Weather conditions may explain the similarities observed between the results of this study and of Barrios et al. [3]. Furthermore, cloud covers noted in the study caused a sudden decrease in the voltage and current output; resulting in a lower power output. The standard deviation of the power of the DCX-HSL setup was ±0.0815 whereas the Fresnel lens setup was ±0.0251. This shows a large standard deviation in the power of both setups. The large standard deviation may be caused by the intermittent cloud covers during the conduct of the data gathering.

Limitations. External factors such as the sudden cloud covers cannot be controlled during the data gathering. This may have affected the voltage and current output of the CPV. Precision in measurements was limited to the precision of the tools used. The schedule of the data gathering was affected by time constraints, thus, it was only performed in under one day.

Conclusion. It was determined that the power output of the CPV increased with the addition of a convex and hemispherical lens for the entire photoperiod. The DCX-HSL had a higher power output than that of the Fresnel lens setup. The DCX-HSL setup yielded a significant power output relative to the Fresnel setup from 10:15-14:15. The mean power output of the DCX-HSL setup and Fresnel lens setup during the photoperiod was 0.0606 mW and 0.0341 mW, respectively. Highest power output increase of DCX-HSL setup was recorded at midday at 251.05%, while on average, the DCX-HSL setup reported a 77.65% increase for the whole day. Although it is worth noting, that there is a large calculated standard deviation of the power for the DCX-HSL and the Fresnel lens setup. This shows similar results with Barrios et al. regarding the increase in power output and a significant difference during midday only.

Since the data gathering was conducted for only one day, the effects of the atmospheric condition were not minimized. Therefore, the results may vary during other days where the weather conditions are different. Further research regarding the three-lens CPV system should be done with at least a three day data gathering period for more accurate data. The type, design, or number of lenses may also be altered to learn its effects on the CPV.

Acknowledgment. The researchers of this study would like to thank the Okada Laboratory University of Tokyo, Japan for providing the concentrator photovoltaic setup and for aiding the course of the study.

References

[1] Hersch P, Zweibel K. Basic photovoltaic principles and methods. 1982 Jan:34–34. doi:10.2172/5191389

[2] Jing L, Liu H, Wang Y, Xu W, Zhang H, Lu Z. 2014. Design and optimization of Fresnel lens for high concentration photovoltaic system. Int J of Photoenergy. 2014(539891):1-7.

[3] Barrios JPLG, Cortez JR, Herman GM, Larroder A, Yu Jeco BM, Watanabe K, Okada Y. (2018). The use of convex lens as primary concentrator for multi-junction solar cells. Emergent Scientist 2(5):1-7

[4] Jing L, Liu H, Zhao H, Lu Z, Wu H, Wang H, Xu J. 2012. Design of Novel Compound Fresnel Lens for High-Performance Photovoltaic Concentrator. International Journal of Photoenergy. 2012(1):1-7

[5] Anderson W, Tamanna S, Sarraf D, Dussinger P, Hoffman R. Heat Pipe Cooling of Concentrating Photovoltaic (CPV) Systems. 6th International Energy Conversion Engineering Conference (IECEC). 2008. doi:10.2514/6.2008-5672

[6] Kurtz S. Opportunities and Challenges for Development of a Mature Concentrating Photovoltaic Power Industry (Revision). 2012 Jan. doi:10.2172/935595

[7] Huang H, Su Y, Gao Y, Riffat S. 2011. Design analysis of a Fresnel lens concentrating PV cell. Low-Carbon Technology. 6(3):165-170

[8] Singh P, Ravindra N. Temperature dependence of solar cell performance—an analysis. Solar Energy Materials and Solar Cells. 2012;101:36–45. doi:10.1016/j.solmat.2012.02.019

Use of 1:7 rice bran wax to rice bran oil mixture as phase change material in increasing the efficiency of photovoltaic cells

CYRUS JEHU R. BARRERA, MANDY D. UMADHAY, JASPER C. CANSON, and ARIS C. LARRODER

Philippine Science High School - Western Visayas Campus, Brgy. Bito-on, Jaro, Iloilo City 5000, Department of Science and Technology, Philippines

Abstract

The efficiency of photovoltaic (PV) panels decreases as their operating temperature increases. To address this, phase-change materials (PCMs) are attached to the panel to absorb heat. PCMs are used to cool PV panels since they have the desired thermodynamic properties for heat storage such as high latent heat. The study focuses on determining the conversion efficiency of PV cells with rice bran wax in rice bran oil (RBW/RBO) mixture as PCM. Rice bran wax was added to rice bran oil in 1:7 by volume ratio. Three setups were compared in this study: PV cell without PCM, with paraffin wax, and with the RBW/RBO mixture. The paraffin wax was used because it is a commonly-used PCM for PV cells. The RBW/RBO mixture was used because it is a renewable resource and considered a waste product. The voltage and current of the PV cells were measured every 15 minutes for 45 minutes to compute the conversion efficiency. The RBW/RBO mixture increased the conversion efficiency of the PV cell by 0.232%. This may be attributed to its melting point being within the PV cell's operating temperature. The RBW/RBO mixture can be used and improved to further increase the efficiency of PV cells for household use.

Keywords: *phase change materials (PCM), photovoltaic cells, rice bran, solar energy, bio-based*

Introduction. PV cells generate electricity by creating a potential difference in PV panels using light energy from the sun [1]. The sudden decrease in the efficiency of PV panels is due to the radiation losses when the operating temperature is above ambient temperature [2]. Since much of the sunlight that is shining on the PV cells becomes heat, proper thermal management improves its conversion efficiency or the amount of the solar energy that can be converted into electricity. Thus, operating temperatures above the ambient temperatures will always mean less output for PV cells [3]. Researchers are seeking to mitigate the influence of high temperature on PV conversion efficiency by rapidly removing heat from PV module surfaces to maintain as good a performance as possible, and hence better meet performance expectations [4]. Gondora et al. [5] suggested the use of phase change materials (PCM). It is an example of a passive cooling system that can function as energy storage mediums, whereby energy is stored during the melting process and is released during solidification [6]. It is the best option in maintaining ideal operating temperature of the PV cells as it absorbs a significant amount of heat without raising the temperature of the PV panel, and offers more energy storage capacity and less temperature fluctuation with respect to traditionally used materials due to their having a high latent heat capacity [6].

Paraffin wax is the most common type of PCM as it possesses a melting temperature within the thermal comfort range of PV cells, a high latent heat capacity, and exhibits small volume changes during the transition phase [7]. However, paraffin wax is unsustainable in the long term [8]. It is a non-renewable resource created as a by-product of petroleum, coal, or oil shale [8]. Schukina et al. [9] used bio-based PV cell with attached bio-based PCMs that are derived from fatty acids have higher efficiencies than those attached with salt hydrates and petroleum-based PCMs.

The food and agricultural industry produce numerous by-products that is considered by most as waste. Rice bran is a by-product of rice milling and is considered as bio waste [10]. Fatty acids from the rice bran can be extracted into rice bran oil or rice bran wax, which are organic bio-based materials. Zaccheria et al. [11] conducted a study about potential bio based PCM. The results showed that the rice bran can be used to produce an oil with a very high free fatty acids (FFA) content. Muthuvel et al. [12] checked the thermophysical properties of the rice bran oil distilled fatty acid (RBDFA); his study showed that the melting point of RBDFA ranges from 29°C to 30°C, heat of fusion value is 140.3 kJ/kgK and the value of the specific heat which is 2303 J/kgK. The high value of specific heat indicates its capacity to absorb higher amounts of heat energy, making it a viable PCM in building applications [12].

This study aimed to determine the potential of rice bran wax and rice bran oil (RBW/RBO) mixture as a bio-based PCMin determining the conversion efficiency of PV cells. It specifically aimed to:

(i) determine the thermophysical properties of the rice bran oil;

How to cite this article:
CSE: Barrera CJR, Umadhay MD, Canson JC, Larroder AC. 2020. Use of 1:7 rice bran wax to rice bran oil mixture as phase change material in increasing the efficiency of photovoltaic cells. Publiscience. 3(1):101-104.
APA: Barrera, C.J.R., Umadhay, M. D., Canson, J.C. & Larroder, A.C.. (2020). Use of 1:7 rice bran wax to rice bran oil mixture as phase change material in increasing the efficiency of photovoltaic cells. *Publiscience, 3*(1):101-104.

(ii) measure the temperature, voltage, and current of the PV cells with and without attached phase-change material; and

(iii) compute the conversion efficiency of the PV/PCM systems.

Results of the conversion efficiency of the PV cells using RBW/RBO mixture from the study can be compared to the conversion efficiency of the PV cells without PCM and with paraffin wax to determine which of the following PV systems generated the highest conversion efficiency.

Methods. The study was done in three phases. The thermophysical properties of the rice bran wax and rice bran oil (RBW/RBO) mixture were analyzed using Differential Scanning Calorimetry (DSC). The second phase was the assembly of the set-up of PV cells with the PCM (PV/PCM) systems. Three PV setups were used in this study. One PV cell without PCM attached was used as a control setup. Then, the same PV cell was subjected to two kinds of PCM: paraffin wax, and the 1:7 rice bran wax in rice bran oil mixture. The last phase was the measurement of the values of the voltages and currents in order to compute and compare the conversion efficiencies of the PV/PCM set-ups.

Finding a potential bio-based PCM. For thermal storage applications of solar energy, the PCM must have a melting point of 16°C to 65°C [2]. A certificate of analysis was issued upon purchase of rice bran oil from a local oil company. According to the result of the analysis, the melting point of the rice bran oil is 15°C. To increase the melting point to be within the accepted range, rice bran oil was mixed with rice bran wax, which has a melting point of 79° C [8]. The rice bran wax was melted first using a hot plate and rice bran oil was added to it while it was being heated. It was then mixed and stirred. Several ratios were tested, and it was found that the 1:7 ratio in terms of volume was the most suitable; since, its melting temperature is in line with the operating temperature of the PV cell of between 15°C to 35° C [13].

Measuring the thermophysical properties using DSC. The melting point and latent heat of fusion were measured using DSC which was done at the University of the Philippines Miag-ao. One gram of the rice bran mixture sample was heated and the changes in its heat capacity were tracked as changes in the heat flow. This allowed the detection of changes in the physical properties of the PCM. In DSC, the 1:7 ratio of the RBW/RBO mixture was heated at a constant rate. The samples were held for 1 minute at 15 °C. It was heated at a linear rate of 10°C/min from 15 °C to 36 °C in a nitrogen atmosphere. This was to determine if the sample was starting to melt. It was held again for 2 minutes at 36 °C and was heated from 36°C to 40°C at 1°C/min before it was held for 2 minutes to determine if the samples were completely melted. It was heated again at 40°C to 500 °C with a heating rate of 10°C/min before it was cooled from 500 °C to 40 °C at 20°C/min. The latent heat of fusion of the material was determined by taking the area under the peak of the curve and the melting point was determined by taking the slope of the point tangent to the peak. Data on the thermophysical properties of RBW/RBO mixture were compared to the established thermophysical properties of paraffin wax as it is the most common type of PCM that is being attached to PV cells for cooling. The basis of the thermophysical properties of paraffin wax was acquired from the research of Kavitha and Arumugam [7].

Testing of PV set-ups. The testing of the PV cell with and without attached phase change materials was performed in Philippine Science High School-Western Visayas Campus. A box made of illustration board 21 cm high, 9 cm wide and 15 cm long was constructed to act as a dark room for the PV cell and to hold in place the xenon lamp. The container was placed under the PV module to create the PV/PCM system. K-type thermocouples were attached to the back of the PV cell and to the PCM to monitor temperature changes. The temperature, current, and voltage were measured every 15 minutes using thermocouples and multimeter. The open-circuit voltage (V_{OC}) and short circuit current (I_{SC}) were first measured by connecting the PV cell to an equivalent circuit with a single diode and series resistance mode, under illuminated light of a xenon lamp. The V_{OC} was measured when the current in the circuit was zero, while the I_{SC} was measured when the voltage is zero. Only V_{OC} and I_{SC} were measured due to the unavailability of specialized equipment for voltage sweep analysis, used in determining the actual measurement of maximum power output (P_{MAX}) in the PV cell. Instead, the actual values of the two were used in a derived equation to calculate the efficiency, together with its underlying parameters-fill factor (FF) and maximum power output (P_{MAX}). The voltage and current of the PV cells were simultaneously measured using a multimeter. The temperature of the PCM and the back surface of the PV cell were also measured simultaneously. The value of the solar irradiance was also measured every 15 minutes using the solar irradiance meter.

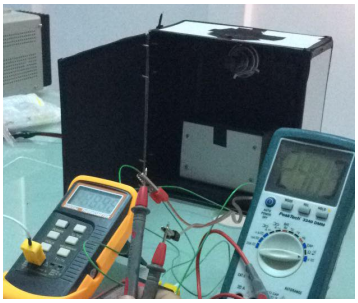

Figure 1. Photo of the setup with the PV cell, PCM inside the aluminum container, xenon lamp inside a dark box, multimeter for the measuring of the voltage and k-type thermocouple thermometer for measuring the temperatures.

Calculation of the Conversion Efficiency. To calculate the conversion efficiency, the fill factor (FF) of the PV cell is needed. Fill Factor (FF) was essentially a measure of the quality of the solar cell. It is solved using the equation:

$$FF = \frac{P_{MAX}}{P_T} = \frac{I_{MP} \times V_{MP}}{I\,sc \times Voc}$$

where P_{MAX} was the measured power of the PV cell, P_T was the theoretical power of the PV cell using LTSpice software simulation, I_{MP} was the current of the maximum power of the PV cell, V_{MP} was the voltage of the maximum power of the PV cell, V_{OC} was the open-circuit voltage, and I_{SC} was the short-circuit current.

The conversion efficiency of the PV/PCM systems can then be calculated using the equation:

$$\eta = \frac{FF \times Isc \times Voc}{P_{in}}$$

where V_{OC} was the open-circuit voltage, I_{SC} was the short-circuit current, FF was the fill factor, P_{in} was the power input and η was the efficiency. The gathered data was compared to the PV cell without PCM attached, and to the PV cell with paraffin wax.

Safety Procedure. Proper laboratory attire was worn, such as laboratory gown, with respect to the laboratory's rules and regulations Proper precaution during data gathering was practiced while handling the PCMs and the set-up to avoid burns. After handling the phase change materials, hands were washed to avoid accidental ingestion.

Results and Discussion. The temperatures of the PV cells and PCMs were measured and results showed that the PV cell with RBW/RBO mixture had the lowest average change in temperature of 0.050 °C/min. The conversion efficiencies of the different set-ups were calculated and the results showed that the PV cell with RBW/RBO mixture had the highest efficiency with 18.776%.

Thermophysical properties of 1:7 RBW/RBO mixture. Results of the DSC analysis show that the melting point of paraffin wax is 58.75°C, while the melting point of the RBW/RBO mixture is 30.06 °C. A PCM with melting points in the temperature range of the operating temperature of the PV cells, which is between 15 to 35° C [13], may have the advantage of not melting at most ambient temperatures and being melted solely by incident solar radiation [2]. Consequently, they may continue melting and absorbing heat for a longer period providing a longer duration of PV temperature regulation [8]. The latent heat of fusion is the amount of energy that the PCM must absorb to change from solid to liquid phase. Latent heat can play a significant role in storing greater amounts of energy [14]. Table 1 shows that one gram of PCM needs 34.945 Joules (J) to change its phase. Especially, the melting point of the material must be equal or close to the operating temperature on some applications. The latent heat should be as high as possible on a volumetric basis to minimize the size of the thermal energy storage device [15]. In this case, RBW/RBO mixture starts melting above the ambient temperature of 25° C at 30° C, in contrast with the paraffin wax which starts melting at 58° C.; hence, the RBW/RBO mixture provides better thermal regulation than the traditional paraffin wax, which is the commonly-used PCM.

Table 1. The values of the thermophysical properties of the different phase change materials.

Parameters	RBW/RBO mixture	Paraffin wax
Melting point (°C)	30.06	58.75
Latent heat (J/g)	34.95	193.9

Values of the temperature, voltage, and current of PV cells with and without phase-change materials. The PV cell with the attached RBW/RBO mixture had the highest voltage of 4.530 V followed by the PV cell with paraffin wax with 4.526 V, then lastly the PV cell without PCM with 4.500 V. As for the current, it remains constant at 0.006 A in all setups. The temperature of the PV cell with RBW/RBO rises by 1.5 °C from 34.3 °C during the first trial up to 35.8 °C during the 3rd trial. The PV cell with paraffin wax increased by 1.7 °C from 33.3 °C to 35.0 °C. The PV cell without PCM rises by 2.4 °C from 35.9 to 38.3 °C. The temperature of the PV cell in the setup without the PCM is higher than that of those with attached PCMs. The average change in temperature for the 45 -minute duration of the PV cell with RBW/RBO mixture was found to be 0.050 °C/min, the paraffin's was 0.056 °C/min and the PV cell without PCM was 0.080 °C/min. As in Figure 2, the temperature of PV cells with PCMs is lower than the PV cell without the PCM in the 45-minute duration. This implies that PCMs absorbed the heat during the period. Results show that the PV without PCM attached has a low voltage output compared to those with PCMs attached. This may be due to the elevated temperatures with which the PV cell without PCM operated in.

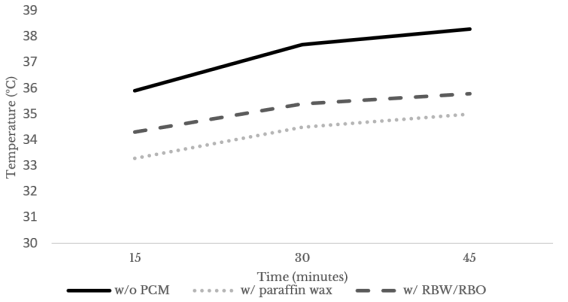

Figure 2. Graph of temperature vs time of the PV cell with and without PCM.

Computed power and efficiency of the different set-ups of PV cell. It can be seen in Figure 1 that PCM reduced the PV's temperature. As the temperature of the PV cell decreased, its voltage output increased. Therefore, attaching a PCM to a PV cell can increase the power of PV cell and conversion efficiency. The value of the efficiency of photovoltaic cells with the rice bran wax and oil (RBW/RBO) mixture was the highest among the three with 18.776% for the three trials, followed by the PV cell without paraffin wax which has a conversion efficiency of 18.750% then lastly the PV cell without PCM which has 18.544% . RBW/RBO has the highest conversion efficiency since it absorbs and discharges a large amount of energy during its phase change. Its melting temperature, which is

30.06 °C is within operating temperature of the PV cell that ranges between 15 °C and 35 °C, within which it will produce energy at maximum efficiency [13]. This contributes to the efficiency of the PV cell as the PCM absorbs the heat. This is evident in the results that the PV cell with RBW/RBO mixture has the highest efficiency value of 18.776%.

Limitations. The solar simulator was improvised using a xenon lamp as it emits the same irradiance value of 1000 W/m^2 as the solar simulator.

Conclusion. Rice bran oil in wax mixture was investigated as a possible PCM for PV panels. Comparing PV cell with and without PCM showed that the rice bran oil and wax (RBW/RBO) mixture as PCM was effective in reducing temperature and improving the efficiency of the PV cell. The reason was that the melting point of RBW/RBO mixture was around the operating temperature of the PV cell, which contributes to the heat removal from the panel by phase change. Results showed that the PCM with rice bran mixture had the lowest temperature of the PV cell among the three. Among PCMs that were evaluated, the RBW/RBO mixture showed a potential for the desired application of the photovoltaic cells. Based on the presented results, it can be concluded that the incorporation of RBO/RBW on the back surface of the PV cell had a positive impact on lowering the temperature of the PV cell and on increasing its power and conversion efficiency.

Recommendations. Considering the findings and the conclusions drawn from the results, it is recommended that further studies should explore other bio-based phase change materials. Rice bran oil has a low melting point of only 15°C and it would not suit as a PCM if put under the operating temperature of a PV cell. Hydrogenation of the PCM can increase its melting temperature, but the lack of time and complexity of the process made mixing of two PCMs a better option. The setup was an improvised solar simulator to have a controlled condition. It would have been better if a real solar simulator was used. Testing the PV/PCM systems in practical conditions, e.g. under the sun, is also recommended.

Acknowledgment. The authors would like to extend their gratitude to the University of the Philippines - Visayas Miag-ao Campus for allowing us to perform the Differential Scanning Calorimetry (DSC) for the samples.

References

[1] Gafford A, Minor R, Allen A, Cronin A, Brooks E, Pavao-Zuckerman M. 2016. The Photovoltaic Heat Island Effect: Larger solar power plants increase local temperatures. Scientific Reports volume6, Article number: 35070 (2016).

[2] Biwole PH, Eclache P, Kuznik F. 2013. Phase-change materials to improve solar panel's performance. Energy and Buildings. 62: 59-67.

[3] Dincer I, Rosen MA. 2007. Exergy: Energy, Environment and Sustainable Development. Elsevier Science Publishers.

[4] Thaib R, Rizal S, Rizal M, Manila TM, Rizal TA. 2018. Beeswax as phase change material to improve solar panel performance. Mater. Sci. Eng. C. 30: 012024.

[5] Gondora W, Doudin K, Nowakoski DJ, Xiao B, Ding Y, Bridgwater T, Yuan Q. 2016. Encapsulation of phase change materials using rice-husk-char. Applied Energy. 182, 274-281. https://doi.org/10.1016/j.apenergy.2016.08.102

[6] Paria S, Sarhan, A, Goodarzi, MS, Baradaran S, Yarmand H, Alavi, MA, Kazi, SN, Metselaar HSC. 2015. Indoor solar thermal energy saving time with phase change material in a horizontal shell and finned-tube heat exchanger. Sci. World J. 2015: 1-7.

[7] Kavitha K, Arumugam S. 2013. Performance of paraffin as a PCM solar thermal energy storage. International Journal of Renewable Energy Resources 3 (2013) 1- 5.

[8] Hassan, A. (2010) Phase Change Materials for Thermal Regulation of Building Integrated Photovoltaics. Doctoral Thesis. Dublin Institute of Technology. doi:10.21427/D7461W.

[9] Shchukina EM, Graham A, Zheng Z, Shchukin DA. 2018. Nanoencapsulation of phase change materials for advanced thermal energy storage systems. RSC. 47(11): 4156–4175.

[10] Sharif MK, Butt MS, Anjum FM, Khan SH. 2014. Rice bran: a novel functional ingredient. Critical Reviews in Food Science and Nutrition. 54(6): 807-816. DOI:10.1080/10408398.2011.608586.

[11] Zaccheria F, Mariani M, Ravasio N. 2015. The use of rice bran oil within a biorefinery concept. Chem. Biol. Technol. Agric. (2): 1.

[12] Muthuvel S, Saravanasankar S, Sudhakarapandian R, Muthukannan M. 2014. Passive cooling by phase change material usage in construction. BUILD SERV ENG RES T. 3 (64): 411-421.

[13] Tan Jian Wei N, Jian Nan W, Guiping C. Experimental study of efficiency of solar panel by phase change material cooling. IOP Conf. Series: Materials Science and Engineering 217 (2017) 012011 doi:10.1088/1757-899X/217/1/012011

[14] Tan L, Datea A, Fernandesa G, Signhb B, Ganguly S. 2019. Efficiency gains of photovoltaic system using latent heat thermal energy storage. Energy Procedia. 110(2017): 83-88.

YNAGUINID

MATERIAL SCIENCE

YNAGUINID is the war deity of the Visayan pantheon, whom the natives prayed to for success in the battlefield. In order to gain an upper hand in any warfare – intellectual, scientific, economic, etc. – it is necessary to have access to the best materials at minimal costs. Many of the most pressing scientific problems faced by humans are due to the limits and management of resources. This section contains studies that exploit the various properties of matter to offer solution to real-world problems as well as provide insight as to the effects of the mismanagement of such resources.

These studies fall under Industry, Energy, and Emerging Technology (IEET) Research and Development Agenda particularly in the management of industries and the use of technology towards the improvement of communities.

BASED ON: Harmonized National Research and Development Agenda (HNRDA)

The extraction and isolation of polyethylene-based plastic-degrading bacteria from Iloilo City Engineered Sanitary Landfill, Mandurriao, Iloilo City

JEREMY SEAN O. CANJA, REX S. HILIS, JV C. GALAN, and FERNANDO CHRISTIAN JOLITO III

Philippine Science High School - Western Visayas Campus, Brgy. Bito-on, Jaro, Iloilo City 5000, Department of Science and Technology, Philippines

Abstract

Plastics are known for being a durable material while still maintaining a low cost of production. It is an important material for commercial use all over the world. However, due to the lack of a reliable method of disposal, the risk of plastic pollution is steadily increasing throughout the years. Bioremediation is a promising method in this aspect as it is an eco-friendly way of dealing with this problem. Thus, this study aimed to extract and isolate bacteria from Iloilo City Engineered Sanitary Landfill and determine their biodegradation capability on low density polyethylene, high density polyethyelene, and polyethylene terephthalate. Bacteria were extracted from randomly chosen sites and two strains were identified, EMBP2A and MSAP2A. There were three set-ups done in triplicates: EMBP2A cultivated with LDPE, HDPE, and PET, MSAP2A cultivated with the same plastics, and the control set-up with the bacteria-free medium. After 10 days of incubation, Strain EMBP2A had decreased the weight of an HDPE plastic to a high percentage of 0.437% and PET to 0.147%. Strain MSAP2A had achieved the highest dry weight loss of 0.495% for PET.

Keywords: *bioremediation, strain, LDPE, PET, HDPE*

Introduction. Plastic has been widely used in many of the products present today due to the low cost of production and high durability of this material. However, due to the uncontrolled increase in the production rate [1], it slowly became a problem which led to pollution on water and land [2]. Several methods of disposal are currently being utilized such as landfilling and incineration; however, due to the environmental problems posed by these methods, it is necessary to look for an alternative method which is both environmentally friendly and still is efficient in the disposal of plastics. One promising field currently being studied is bioremediation [3].

To be able to understand bioremediation more, it is necessary to define the terms that were commonly used in this study. The terms are plastic and biodegradation. Based on the study by Andrady and Neal [4], plastic is a versatile material made up of polymers that is usually utilized for commercial use. Plastics can be categorized into different types using a code. Based on the system established by the Society of the Plastics Industry [5], there are seven codes in classifying plastic: 1 for Polyethylene Terephthalate (PET), 2 for High Density Polyethylene (HDPE), 3 for Polyvinyl Chloride (V), 4 for Low Density Polyethylene (LDPE), 5 for Polypropylene (PP), 6 for Polystyrene (PS), and 7 for others. This system is usually used by consumers and recyclers for identification and segregation. Biodegradation is a method of degradation that uses microorganisms to breakdown polymers in the plastic either through metabolic or enzymatic action [6]. There is a study done to assess the biodegradation capability of microbes extracted from a dumpsite. Bolo et al. [7] extracted bacteria from the Payatas Dumpsite, Quezon City, Philippines, and out of the four isolates, *Pseudomonas stutzeri* is the most well-known plastic degrader and has the highest efficiency among them.

There are studies that identified the microbes associated with dumpsites. Based on the study by Williams and Hakam [8], the species isolated from four dumpsites in Port Harcourt Metropolis, Nigeria, were *Bacillus spp., E. coli, Klebsiella spp., Proteus spp., Pseudomonas spp., Staphylococcus aureus,* and *Streptococcus spp.* There are studies that identified the microbes that have the capability to degrade polymers. Bhardwaj et al. [9] researched about the microbial populations that are associated with plastic degradation. Based on their findings, the microbes that are known for their biodegradation capability are *Rhizopus delemar, Firmicutes, Protobacteria, Penicillium, Rhizopus arrizus,* and *Pseudomonas stutzeri.*

There are several methods available for the assessment of the biodegradation capability of the microbes. The study by Bolo et al. [7] used two methods, namely the Fyrite gas analyzer and scanning electron microscopy. Shovitri et al. [10] used a different method wherein the dry weight loss of the plastic is used to confirm plastic degradation. There are also methods for the incubation of bacteria with the plastic samples. Singh et al. [11], Kathiresan [12], and Sowmya et al. [13] used the conical flask method, while Mahdiyah et al. [3] and Shovitri et al. [10] used the soil burial method. Although the field has been studied extensively, there is a lack of research regarding this field here in the Philippines, a

How to cite this article:
CSE: Canja, JSO, Galan, JC, Hilis, RS, Jolito, FC, III. 2020. The extraction and isolation of polyethylene-based plastic-degrading bacteria from Iloilo City Engineered Sanitary Landfill, Mandurriao, Iloilo City. Publiscience. 3(1):106-110.
APA: Canja, J.S.O., Galan, J.C., Hilis, R.S., & Jolito, F.C. III. (2020). The extraction and isolation of polyethylene-based plastic-degrading bacteria from Iloilo City Engineered Sanitary Landfill, Mandurriao, Iloilo City. *Publiscience,* 3(1):106-110.

country that ranks third among other countries of the world in producing plastic waste dumped into the oceans [14]. It is also necessary to note that the existing studies might have overlooked the use of the plastic swab as a method of collecting bacterial samples. This study aimed to extract and isolate bacteria from Iloilo City Engineered Sanitary Landfill, Mandurriao, Iloilo City, and assess their biodegradation potential on LDPE, HDPE, and PET. It specifically aimed to:

(i) extract plastic swab and soil samples from five randomly selected areas in the dumpsite;

(ii) isolate bacteria from the swab and soil samples extracted from the dumpsite; and

(iii) determine which isolated bacteria has the best bioremediating capability using a formula to compute for the plastic chips' dry weight losses.

Methods. The methods were divided into five main steps namely sample collection, plastic preparation, bacteria culture cultivation, plastic degradation, and data analysis. The steps were done for all nine setups, and the data were collected after 10 days upon the placement of the plastic films in the medium.

Sample collection. The bacteria were extracted from plastic waste, using swab sampling, and from soil samples taken from the dumpsite. The plastic wastes were randomly selected, and a total of five swab samples were collected and sealed inside test tubes. They were then transported to a laboratory in Philippine Science High School - Western Visayas Campus (PSHS-WVC). For the soil, five samples were collected from a depth of 10 - 20 cm, then placed inside sterile containers and kept at a temperature of 4°C [7].

Random sampling was done by having an aerial view of the area (Coordinates: 10°42'34.7"N 122°31'25.8"E) and sectioning it equally into 25 sites. Five randomly selected sites were chosen using a random number generator. Site 1 was located in area 7, site 2 in area 6, site 3 in area 13, site 4 in area 18, and site 5 in area 9.

Plastic preparation. Three different types of plastics (PET, HDPE, LDPE) were cut into strips having dimension of 2cm x 2cm with three replicates for each plastic in each set-up. They were sterilized in 70% ethanol for approximately 30 minutes, washed with distilled water and subsequently dried in an incubator at 60°C for 24 hours. Afterwards, plastics were put into a silica gel-containing desiccator for 24 hours for total water evaporation. Initial dry weight of plastic was measured with an analytical balance [11].

Bacteria culture cultivation. The bacterial samples in the swabs were plated on nutrient agar (NA) medium using streak method of inoculation. Three plates of NA media were utilized for the growth of the bacteria. The plates were incubated at 30°C for 24-48 hours. Colonies with different morphological appearance was subcultured onto fresh NA for the purpose of identification.

As for the soil samples, four grams of each were suspended in 96 ml of sterile distilled water and shaken vigorously for two minutes. These were then heated at 60°C for 60 minutes in a water bath. The mixture was then put to rest to allow the soil particles to settle. It was then plated on nutrient agar using streak method. Incubation was done at 30°C for 24-48 hours. Identification was done using morphological observation and Gram staining, then selective media were used to allow the specific bacteria to grow [12].

Samples were then plated in selective media, eosin methylene blue (EMB) agar and mannitol salt agar (MSA), to further categorize the bacteria. Out of the ten plates, two were selected for incubation based on their morphological properties, one from EMB and the other from MSA.T The strains were given codes for identification.

Plastic degradation. Three set-ups were made, the first being the medium inside the Petri dish where Bacteria 1 was cultivated with the three types of plastic strips (HDPE, LDPE, and PET) having each type of test plastics in triplicates. The second setup was the medium with Bacteria 2, and the same was done for this set-up. The last set-up is the control, which was maintained with polyethylene strips in the microbe-free medium. Pre-weighed strips of sterilized plastics of each type were aseptically transferred to the Petri dish containing mineral salt medium (MSM) and inoculated with the bacteria to be tested.

Triplicates were maintained for each type of plastic and were left on the incubator. After 10 days, the plastic discs were collected and washed thoroughly using distilled water. They were then dried in a hot air oven at 50°C overnight for at least 10 hours and were weighed for final dry weight.

Data Analysis. Dry weight loss percentage is used to indicate the biodegradation rate of plastic during the incubation process. The percentage weight loss was calculated using the formula below

$$Weight\ loss\ \% = \frac{I.W. - F.W.}{I.W.} \times 100$$

where I.W. is the initial dry weight of the plastic strips pre-degradation and F.W. is the final dry weight of the plastic strips post-degradation [13]. The dry weights of the plastic strips after degradation were also subjected to statistical analysis using one-way analysis of variance (ANOVA).

Safety Procedure. The researchers underwent biosafety training before the conduct of the study. Proper personal protective equipment was used during the whole conduct of the study. During the sample collection, boots, gloves, and masks were used to protect the researchers. During the laboratory work, lab gowns, gloves, and masks were used. Proper tools were also used during the inoculation and preparation of the bacteria. Samples were sterilized and dried before being disposed of in the biohazard bin, while excess chemicals, which were unused, were stored in the laboratory.

Results and Discussion. Degradation of plastics by microorganisms has been studied for several years. The present investigation was performed to provide an analysis on the biodegradation potential of bacteria from a local dumpsite using the three commonly used plastics:

PET, HDPE, and LDPE. Biological decomposition of synthetic materials such as plastics can be facilitated by microorganisms in natural environments.

A total of 28 colonies were isolated from plastic waste swab and soil samples taken from Iloilo City Engineered Sanitary Landfill using NA and TSB media. This was done by identifying the morphological appearance of colonies. After facilitating growth in selective media, strains of bacteria were identified. Bacterial strains EMBP2A and MSAP2A as shown in the plates below were subjected to the three types of plastics. These were the bacterial codes used that would indicate the nature of the bacterial strain. Strain EMBP2A signifies that the bacterial sample was collected from plastic swab in site 2 of the sampling area and was cultivated in EMB media. Strain MSAP2A signifies that the bacterial sample was collected from plastic swab in site 2 of the sampling area and was cultivated in MSA media.

Plate 1. Identified bacterial strains EMBP2A and MSAP2A for incubation.

Dry weight loss percentage is used to indicate the biodegradation rate of plastic during the incubation process. The percentages for the three types of plastics are shown below (Figure 1) for the entire biodegradation period of 10 days. It showed that the plastics used have decreased the weight of some plastic strips. A minimal increase in the weight of other plastic strips can also be observed. Mean weight changes were computed and used to compare the effectiveness of biodegradation between the two strains of bacteria. A negative mean indicates that there was a gain in weight instead of a loss. These plastic strips that have been found to increase their weight were undegraded in the incubation time period of 10 days. Strain EMBP2A had decreased the weight of an HDPE plastic to a highest percentage of 0.437% and PET to 0.147%. Strain MSAP2A had achieved a highest dry weight loss of 0.495% for PET.

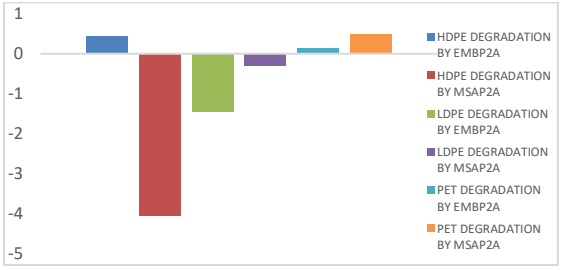

Figure 1. The comparison of the dry weights of HDPE, LDPE, and PET after bacterial degradation by strains EMBP2A and MSAP2A.

Using one-way analysis of variance (ANOVA) with α value set to 0.05, it was found that there was no significant statistical difference between the dry weights as presented in Table 1. Given the two bacterial strains, EMBP2A and MSAP2A, none of them have shown a significant effect on the degradation of any type of plastic used as shown below:

Table 1. P-values of HDPE, LDPE, and PET plastic chips.

	HDPE	LDPE	PET
P-value	0.0631	0.853511	0.9077

Microorganisms play an important role in the biodegradation of materials, including synthetic polymers, such as plastic, in natural environments. During degradation, enzymes from the microorganisms break down the polymers into smaller molecules of short chains that can pass through the microbes' semi-permeable outer membranes, allowing the plastics to be used as carbon and energy sources [6].

In the current study, three types of plastics were used to measure the degradation percentage, which were high density polyethylene, low density polyethylene, and polyethylene terephthalate. These were chosen because they are the most commonly used plastics, and they degrade at a slow rate in the natural environment, estimated in decades, which causes serious environmental problems [14]. A decrease in the mean weight of some plastics indicates that the bacteria can have the potential to use plastic as an alternative carbon and energy source. Strain EMBP2A had decreased the weight of an HDPE plastic to a high percentage of 0.437% and PET to 0.147%. Strain MSAP2A had achieved the highest dry weight loss of 0.495% for PET. Kathiresan and Bingham [15], which have reported in their study that biodegradation using bacteria is ranging from 0.56 to 8.16% for plastics. Their study, however, performed the degradation process in a duration of 90 days. An increase with the weight for some plastic strips could be correlated with its exposure to external factors that could possibly influence the weight. According to Gajendiran et al. [16], due to the adherence of microbes utilizing the polymers, plastic samples could increase in weight.

There was no significant statistical difference found between the dry weights of the plastic strips before and after they were subjected to degradation. Degradation is a naturally occurring phenomena and it could take hundreds of years for a plastic to break down completely. Biodegradation utilizes the capability of microorganisms with the enzymes they produce to enhance the biodegradation process. It would require a considerable amount of time for the bacteria to consume the plastics to achieve a significant decrease in the weight of plastics after they are consumed. This can be observed in studies like that of Singh et al. [6] where they tested the biodegradation capability of bacteria isolated in soil for 40 days; Kathiresan and Bingham [14] where they performed this process in a duration of 90 days; and lastly, Usha et al. [13], where they found out that *Pseudomonas sp.* was able to degrade 28.42% of plastics in a period of six months.

The results of this work were also in accordance with earlier research studies done by Sowmya et al. [1], in which they reported that some bacteria were able to grow on minimal medium containing polyethylene as sole carbon source. This showed its capability to utilize

plastic as a carbon source and to degrade polyethylene. Degradation of plastic was carried out between the two bacterial strains, EMBP2A and MSAP2A. The bacteria were able to degrade PET the most among the three types of plastics. But because of a limited period, in a 10-day course, results showed a nonsignificant biodegradation of the three types of plastic using the two bacterial strains.

Limitations. The study only covers the testing of dry weight loss to confirm degradation without the support of visual testing using scanning electron microscope (SEM). Bacteria were also tested only up to the morphological level based on the growth of the colony. The incubation of the plastic with bacteria only lasted for 10 days due to the time constraint.

Conclusion. Bacteria capable of degrading plastics were isolated from Iloilo City Engineered Sanitary Landfill. In a course of 10 days, in some setups, the bacteria used were able to utilize the plastics as their sole carbon source during the incubation period. Some could degrade the plastics; however, the dry weight loss percentage among all the setups was not significant. The nature of the degradation process also played a major role for the minimal dry weight loss percentage.

Recommendations. It is recommended to replicate the study with focus on reducing external factors that may affect the degradation process of the plastic (e.g. temperature, humidity, etc.). Extending the duration of the experiment and observing the intervals are also recommended to further improve the study. Addition of parameters to be observed to confirm degradation is also advised to further improve the quality of the study. It is also recommended to extend the incubation time for future studies because the biodegradation process could be more extensive the longer the bacteria could feed on the plastics. Future researchers of similar fields can also utilize a scanning electron microscope to observe the surface of the plastics and to see if there is significant physical change on the microscopic level. Implementation of the project on a larger scale can also improve the quality of the data gathered as more accurate representation of the data can be observed.

Acknowledgement. The researchers would like to acknowledge the help of the guards and workers especially to the head of operations, Engr. Ernest Navida from the Iloilo City Engineered Sanitary Landfill for their guidance during the conduct of the data gathering.

References

[1] Sowmya, HV, Ramalingappa, MK, Krishnappa, M, Thippeswamy, B. 2014. Biodegradation of polyethylene by *Bacillus cereus.*

[2] Bolo, NR, Diamos, MJC, Sia Su, GL, Ocampo, MAB, Suyom, LM. Isolation, identification, and evaluation of polyethylene glycol and low-density polyethylene-degrading bacteria from Payatas dumpsite, Quezon City, Philippines. Philipp J Health Res Dev. 19(1): 50-59.

[3] Mahdiyah, D, Mukti, BH. 2013. Isolation of polyethylene plastic-degrading bacteria. Biosci Int.

[4] Andrady, AL, Neal, MA. 2009. Applications and societal benefits of plastics. Phil Trans R Soc B. 364: 1977-1984.

[5] Society of the Plastics Industry. 1988. Different types of plastics and their classification.

[6] Singh, G, Singh, AK, Bhatt, K. 2016. Biodegradation of polythenes by bacteria isolated from soil. Int J Res Dev Pharm Life Sci. 5(2): 2056-2062

[7] Williams, JO, Hakam, K. 2016. Microorganisms associated with dump sites in Port Harcourt Metropolis, Nigeria. J Eco Nat Envi. 8(2): 9-12.

[8] Bhardwaj, H, Gupta, R, Tiwari, A. 2012. Microbial population associated with plastic degradation. Open Acc Sci Rep. 1(5).

[9] Shovitri, M, Nafi'ah R, Antika, TR, Alami, NH, Kuswytasari, ND, Zulaikha, E. 2016. Soil burial method for plastic degradation performed by *Pseudomonas* PL-01, *Bacillus* PL-01, and indigenous bacteria. AIP Conf Proc. 1854: 020035-1-020035-9.

[10] Kathiresan, K. 2003. Polythene and plastics-degrading microbes from mangrove soil. Rev Biol Trop. 51(3): 629-634.

[11] Kyaw, BM, Sakharkar, M. 2012. Biodegradation of low density polyethylene (LDPE) by *Pseudomonas* species. Indian J Microbiol. 52(3): 411-419.

[12] Al-Humam, NA. 2016. Heat-shock technique for isolation of soil *Bacillus* species with potential of antibiotics secretion in Saudi Arabia. British Microbiol Res J. 17(3): 1-6.

[13] Usha, R, Sangeetha, T, Palaniswamy, M. Screening of polyethylene degrading microorganisms from garbage soil. Libyan Agri Res Cen J Intl. 2(4): 200-204.

[14] Jambeck, JR, Geyer, R, Wilcox, C, Siegler TR, Perryman M, Andrady A, Narayan R, Law KL. 2015. Plastic waste inputs from land into the ocean. Marine Pollution. 347(6223): 768-771.

[15] Gu, JD. 2003. Microbiological deterioration and degradation of synthetic polymeric materials. Recent Res Adv Int Biodeter Biodegrad. 52: 69-91.

[16] Kathiresan, K, Bingham, BL. 2001. Biology of mangroves and mangrove ecosystems. Advances Mar Bio. 40: 81-251.

[17] Gajendiran, A, Krishnamoorthy, S, Abraham, J. 2016. Microbial degradation of low-density polyethylene (LDPE) by *Aspergillus clavatus* strain JASK1 isolated from landfill soil. 3 Biotech. 6: 52.

Optimization of reaction parameters for the synthesis of silver nanoparticles using ascorbic acid and trisodium citrate

LUKE DANIEL G. SOCRATES, MARY JANE O. TANG, SETH WILLIAM C. TIONKO, MIALO L. BAUTISTA, and MICHAEL PATRICK M. PADERNAL

Philippine Science High School - Western Visayas Campus, Brgy. Bito-on, Jaro, Iloilo City 5000, Department of Science and Technology, Philippines

Abstract

Silver nanoparticles (AgNPs) have excellent properties and various applications in several scientific fields. The present study aimed to optimize the reaction parameters for AgNP synthesis using ascorbic acid and trisodium citrate, through response surface methodology (RSM). Three parameters were evaluated - initial pH of silver nitrate ($AgNO_3$) solution, digestion time, and $AgNO_3$ concentration. Absorbances at peak wavelength of the resulting solutions were analyzed using an ultraviolet-visible (UV-vis) spectrophotometer and was taken as a measure of yield. The effects and combined interactions of the parameters to the yield, and the optimal conditions for synthesis were determined using RSM. $AgNO_3$ concentration was found to be the most significant determinant of the yield. Atomic Force Microscopy (AFM) showed that the synthesized AgNPs at optimal conditions were spherical and about 30 nm in diameter. It is believed that these parameters are suitable for bulk production of AgNPs for various applications in several scientific fields.

Keywords: *absorbance, yield, response surface methodology (RSM), UV-visible (UV-vis) spectrophotometry, atomic force microscopy (AFM)*

Introduction. Nanoparticles are structures with dimensions under 100 nm. Silver nanoparticles (AgNPs) have been widely explored due to their excellent physical, chemical, and optical properties that depend on their size, shape, and structure that can be vastly different from their bulk forms. AgNPs have also been widely used in several scientific fields from chemistry to medicine [1,2].

One cost-effective method of synthesizing AgNPs with high yield and without agglomeration is through the chemical reduction method using chemical reductants. Examples of reductants used to reduce the precursor salt, silver nitrate ($AgNO_3$), are hydrazine hydrate, ascorbic acid, and the combination of ascorbic acid and trisodium citrate [3,4,5]. Studies of Guzman et al. [3], Malassis et al. [4], and Qin et al. [5], have used these reductants to synthesize AgNPs. Furthermore, this method is widely investigated due to the ease and accuracy of the process and its potential for the bulk production of AgNPs [6].

Published work regarding optimization mostly utilized the one-factor-at-a-time (OFAT) method. This method, however, overlooks the interaction between the different variables involved in the system. In order to precisely determine the interaction of these variables, the design of experiment (DoE) method needs to be employed, in which face-centered central composite design (FCCCD) under RSM is a utilizable tool. Response Surface Methodology (RSM) is a statistical tool that can define the effect of independent variables, alone or in combination, on the process. A mathematical model is also produced from the analysis of the effect of the independent variables [7].

Chowdhury et al. [8] were able to optimize the synthesis of AgNPs using RSM. Their study used trisodium citrate as the reductant and $AgNO_3$ as the precursor salt. The variables that were tested were the concentrations of silver nitrate (0.5 mM, 1.0 mM, 1.5 mM), trisodium citrate (0.5 %, 1.0 %, 1.5 %), and the stirring time (10 minutes, 15 minutes, 20 minutes). Design-Expert 11, a software which can be used for constructing design of experiments under RSM and can be used for the statistical, regression, and graphical analysis of the results, suggested a total of 17 experimental runs. In addition, Design-Expert 11 also includes the interpretation and graphics for the analyses and the optimization process [9]. This study applies the same methods but on different manipulated variables such as those used in an OFAT study conducted by Yusof et al. [10] that established the importance of initial pH of the $AgNO_3$ solution, digestion time (or the reaction time of the synthesis where $AgNO_3$ was used as precursor salt, ascorbic acid as reductant, and trisodium citrate as stabilizer) and $AgNO_3$ concentration as variables that affect the synthesis of AgNPs.

There is a lack of studies optimizing AgNPs by manipulating the initial pH of the $AgNO_3$ solution, digestion time, and $AgNO_3$ concentration through RSM; therefore, this study wanted to tackle this. It specifically aimed to:

(i) obtain the absorption spectra and the absorbance at peak wavelength (λ_{max}) of the AgNPs using a UV-visible spectrophotometer synthesized by varying the following variables: initial pH of the $AgNO_3$ solution, digestion time, and $AgNO_3$ concentration;

How to cite this article:
CSE: Socrates LDG, Tang MJO, Tionko SWC, Bautista ML, Padernal MPM. 2020. Optimization of reaction parameters for the synthesis of silver nanoparticles using ascorbic acid and trisodium citrate. Publiscience. 3(1):111-116.
APA: Socrates, L.D.G., Tang, M.J.O., Tionko, S.W.C., Bautista, M.L., Padernal, M.P.M. (2020). Optimization of reaction parameters for the synthesis of silver nanoparticles using ascorbic acid and trisodium citrate. *Publiscience,* 3(1):111-116.

(ii) determine the optimal values of the three variables varied simultaneously at three levels each in a central composite design;

(iii) estimate the yield of the synthesized AgNPs under predicted optimal conditions; and

(iv) evaluate the accuracy of the prediction model by comparing the yield/absorbance predicted by the model to the experimental yield/absorbance of AgNPs at optimum conditions.

The optimal conditions may then be used to efficiently synthesize AgNPs for bulk production in the future.

Methods. A total of 17 AgNP aqueous solutions were prepared varying the three parameters. The respective absorbances at λ_{max} for each setup was determined using UV-vis spectrophotometry. Optimal conditions for the synthesis of AgNPs were determined through RSM using the software Design-Expert 11. Actual yield of the AgNPs synthesized with the optimal conditions of the variables was then compared to the predicted yield given by the software. Atomic Force Microscopy (AFM) was then performed to determine the size of the synthesized AgNPs at optimal conditions.

Materials. All chemicals were of analytical grade and were either provided by PSHS-WVC or bought from D'Malt Enterprises.

Synthesis of AgNPs. An 80-mL solution of 6.0 x 10^{-4} M ascorbic acid and 3.0 x 10^{-3} M trisodium citrate solution was stirred for five minutes at 100°C. Then, 15 mL of the $AgNO_3$ solution of desired concentration was poured into the solution. The resulting solution was kept heated and stirred at 900 rpm using a magnetic stirrer. All experiments utilized the same process; however, variables were varied according to the values presented in Table 1. The pH, time, and concentration values were converted to their coded factors (-1, 0, +1). Coding reduces the range of each factor to a common scale, -1 to +1, regardless of its relative magnitude. Coded factors could then be used for the design description and analyses in RSM [9].

Table 1. Coded factors and the corresponding values for each variable.

Variables	-1	0	+1
pH	6	7	8
Digestion time (minutes)	2.5	3.5	4.5
$AgNO_3$ concentration (M)	0.005	0.010	0.015

Determination of Absorbance/Yield. The reaction mixture samples were studied at a wavelength of 300 to 500 nm using a Shimadzu UV-1800 Ultraviolet-visible spectrophotometer. The absorbance at λ_{max} (~400-420 nm) for each sample were obtained from the spectra. The yield or concentration of NPs in the NP solution is proportional to the absorbance at λ_{max} following Beer-Lambert's Law [11]:

$$Yield\ (in\ M) = A/L\varepsilon \quad (1)$$

where A is the absorbance at λ_{max}, L is the path length = 1 cm and ε is the extinction coefficient expressed in $M^{-1}\,cm^{-1}$.

This yield can also be expressed in number of particles per unit volume by multiplying the yield (in M) to the Avogadro's number (N_A):

$$Yield\ (in\ particles/L) = Yield\ (in\ M)\ x\ N_A \quad (2)$$

This estimation is based on the premise that the size distribution and shape of particles are uniform [11]. From the spectra and AFM images, this appears to be relatively satisfied; hence, the obtained absorbances can still be a fair estimate of the yield.

Statistical analysis. A multiple regression analysis was performed after obtaining the absorbances of all the samples. The absorbances were taken as the response since they are proportional to the yield. Then, a mathematical equation can be determined which best describes the relationship of the response to each variable and the relationship of each variable to one another. Analysis of Variance (ANOVA) for the response surface model was conducted and the mathematical model was validated using the p-value at 95% confidence level. The optimal pH, digestion time, and $AgNO_3$ concentration can be determined through the response surface plot generated by the software [7].

Testing of optimal conditions. AgNPs were synthesized using the calculated optimal conditions provided by the software to validate the predicted absorbance.

The percent error was computed by dividing the difference of the actual absorbance and the predicted absorbance by the actual absorbance multiplied by 100 and was used as a measure of the accuracy of the model or simply, how far the derived values are compared to the values obtained from the experiment:

$$\%\ error = \left|\frac{(actual\ absorbance - predicted\ absorbance)}{actual\ absorbance}\right| x\ 100 \quad (3)$$

AFM. Images of AgNPs deposited on a mica surface were taken to determine the size and observe the size distribution of the synthesized AgNPs at optimal conditions. For this purpose, a Shimadzu SPM-9700HT AFM was used in contact mode.

Safety procedure. Personal protective equipment was worn during the preparation of several chemical solutions and in the synthesis of AgNPs. All excess chemicals were stored and labelled in waste bottles and were handed over to the PSHS-WVC Science Research Specialist (SRS) for proper storage and disposal.

Results and Discussion. This section presents the results and discusses first, the synthesis process which includes the mechanism and the UV-vis characterization technique, followed by the statistical analysis and determination of optimum conditions through RSM, and finally, the accuracy of the

statistical model through characterization of a sample synthesized using optimal parameters through UV-vis and AFM.

Synthesis. The preliminary confirmation of the formation of silver nanoparticles is the change in color of the solution from colorless into a specific color depending on the resulting particle size and shape. Presence of surface plasmon resonance (SPR), the frequency in which conducting electrons on the particle oscillate in response to the incident electromagnetic radiation, gives rise to the different colors of silver colloids due to light absorption and scattering in the visible region. Metals with free electrons possess plasmon resonance. For AgNPs, this is characterized by a peak at 400-420 nm in the visible spectrum which provides specific colors to the aqueous solution [12]. In the study, the solutions were observed to change color from colorless to green during the synthesis (Figure 1). The resulting solutions also had an absorption peak within 400-420 nm (Figure 2) which is indicative of the presence of spherical AgNPs of ~30 nm in diameter [11,12,13]. This was also in accordance with the study of Zielinska et al. [12] in which silver nanoparticles were synthesized by reducing silver nitrate using ascorbic acid, and a green color of the aqueous solution was obtained.

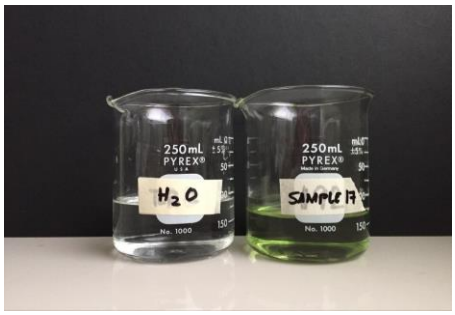

Figure 1. Presence of AgNPs is denoted by the color change from colorless (left beaker) to green (right beaker) after synthesis.

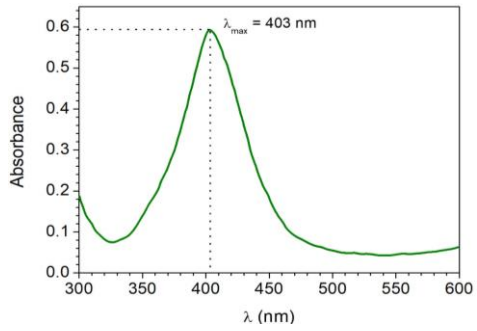

Figure 2. UV-vis spectrophotometry absorbance spectrum of a sample prepared using 0.015 M $AgNO_3$ (pH=8).

Mechanism. The mechanism behind the synthesis of silver nanoparticles was the reduction of silver ions (Ag^+) to metallic silver (Ag^0). Ascorbic acid having a higher redox potential than silver, reduced the silver ion to metallic silver according to the following reaction [14]:

$$C_6H_8O_6 + 2\,Ag^+ + \rightarrow 2\,Ag^0 + C_6H_6O_6 + 2\,H^+$$

During the initial stages of the reaction, the Ag^+ reduced to Ag^0 acted as nucleation centers and eventually became catalysts for the reduction of the remaining metal ions [15]. Metal clusters were formed due to coalescence of atoms and are then stabilized by capping agents which can be in the form of ligands, surfactants, or polymers. In this study, trisodium citrate acted as a capping agent and adsorbed into the surface of Ag atoms, preventing them from agglomerating. Growth of AgNPs were observed through the color change from light yellow to yellow to green into which it finally stabilized.

Yield determination. UV-vis spectrophotometry was conducted to obtain the respective absorbances at λ_{max} for each setup. After the acquisition of the data for all 17 samples, RSM was used to analyze the data and determine the optimal conditions. RSM is a combination of mathematical and statistical techniques that could be used to approximate and optimize a system from several responses and different types of experimental runs [7]. A face-centered central composite design (FCCCD) under RSM was employed to identify the interaction between the variables for high absorbance and AgNP yield and to develop a statistical model that describes the synergistic or antagonistic effects of each variable to one another within a minimum number of experimental runs. Table 2 shows the FCCCD of three variables along with absorbance at λ_{max} (E) as the response. The highest response, 0.611, was found at run 12, whereas the lowest response, 0.020, was found at run 17.

Legend: A = Run, B = Initial pH of $AgNO_3$ solution, C = Digestion time (in minutes), D = $AgNO_3$ concentration, E = Absorbance

Table 2. Face-centered central composite design (FCCCD) of three variables along with absorbance at peak wavelength as response.

A*	B	C	D	E
1	1	0	0	0.160
2	-1	-1	1	0.534
3	0	1	0	0.300
4	0	0	0	0.279
5	1	-1	1	0.510
6	0	0	0	0.227
7	1	-1	-1	0.108
8	0	0	-1	0.016
9	0	-1	0	0.125
10	-1	0	0	0.262
11	-1	1	1	0.426
12	0	0	1	0.611
13	1	1	1	0.592
14	0	0	0	0.255
15	1	1	-1	0.101
16	-1	-1	-1	0.131
17	-1	1	-1	0.020

** arranged based on standard order given by the software*

There was a total of fifteen (15) experiments which had unique variable combinations and two (2) more experiments replicating the center-point (middle point of all variables). The center-point provides a measure of process stability and inherent variability and a way to check for the curvature of the response surface model [7].

Table 3 shows that the established model and model terms are significant at $p < 0.05$ and can thus represent the system accurately. Model terms A, B,

and AB were added nevertheless to increase the measure of fit (R^2) of the system albeit insignificant. In addition, an insignificant lack-of-fit indicates that the model is an accurate representation of the system. Table 4 shows the fit statistics of the response surface model. An R^2 value equal to 1 implies a perfect correlation between the actual system and the established model that represents the system. Adjusted R^2 was determined to be 0.8902, and the predicted R^2 was determined to be 0.8262. This was in reasonable agreement with the adjusted R^2 in terms of a high significance value of a model as the difference of adjusted R^2 and predicted R^2 is less than 0.2 [9]. The lack-of-fit F-value, adjusted R^2 and predicted R^2 values indicate that the model fits the trend for synthesis of AgNPs using ascorbic acid and trisodium citrate as far as the chosen parameters are concerned.

Table 3. ANOVA for response surface model.

ANOVA for Reduced Quadratic Model

Source	Sum of Squares	df	Mean Square	F-value	p-value	
Model	0.5628	5	0.1126	26.94	< 0.0001	significant
A-pH	0.0010	1	0.0010	0.2299	0.6410	
B-Digestion time	0.0001	1	0.0001	0.0230	0.8822	
C-$AgNO_3$ concentration	0.5276	1	0.5276	126.28	< 0.0001	
AB	0.0108	1	0.0108	2.59	0.1361	
C^2	0.0233	1	0.0233	5.57	0.0378	
Residual	0.0460	11	0.0042			
Lack of Fit	0.0446	9	0.0050	7.32	0.1260	not significant
Pure Error	0.0014	2	0.0007			
Cor Total	0.6087	16				

Table 4. Fit statistics for response surface model.

Fit Statistics			
Std. Dev.	0.0646	**R^2**	0.9245
Mean	0.2739	**Adjusted R^2**	0.8902
C.V. %	23.60	**Predicted R^2**	0.8262
		Adequate Precision	14.3875

Determination of second order polynomial equation. A three-level factorial design in FCCCD was used to calculate all possible combinations of input variables that are able to optimize the response within the region of 3-D space. The general equation for response surface methodology is a full quadratic equation. Using Design-Expert 11, the equation was found to be:

$$Absorbance = +0.22 + 0.0098A + 0.0031B + 0.22C + 0.0368AB + 0.0752C^2 \quad (4)$$

where A = pH, B = digestion time, C = $AgNO_3$ concentration

The reduced quadratic equation indicated how a high absorbance of AgNP sample was affected slightly by initial pH of $AgNO_3$ solution and digestion time, but significantly by the $AgNO_3$ concentration during reaction. Positive coefficients signified a synergistic effect on the response. The reduced quadratic equation can be used to make predictions about the response (absorbance) for given values of each factor. However, the values for each factor must be specified in the original units consistent to each factor.

From the results, as pH was increased from 6 to 8, the yield increased to some extent. A study by Deepak et al. [16] has stated that synthesis of AgNPs in the alkaline conditions proceeds faster than in acidic conditions. In acidic conditions, there is less nucleation for silver crystal formation in which new silver atoms deposit to form silver nanoparticles. As pH increases, dynamics of Ag^+ ions increase, and more nucleation regions are formed due to the presence of hydroxyl (OH^-) ions which are very much needed for the reduction of metal ions. The results of the study also coincide with the results of Chitra and Annadurai [17] in which their synthesis of AgNPs was found to be more favorable at alkaline conditions.

Digestion time is also important in synthesis of AgNPs as you allow more time for the reaction to proceed. The RSM results show that increasing the digestion time subtly increases the yield.

Albeit statistically insignificant, AB (pH and digestion time interaction) had lower p-value than AC (pH and $AgNO_3$ concentration interaction) and BC (digestion time and $AgNO_3$ concentration interaction); the values of the latter two are not shown. This may indicate that the interaction of the two parameters only affect slightly the absorbance and subsequently, the yield of AgNP. However, it is ultimately the $AgNO_3$ concentration which had the most intense effect on the response and is in line with the study of Chowdhury et al. [8].

The chosen range for the pH and digestion time happened to be already close to the optimum values and appears to be only slight changes; thus, the effect of these two parameters (and even their combined interaction) are not observed significantly. In the cases where the pH and digestion times are favorable, the parameter that matters more is the concentration of $AgNO_3$ which determines the amount of available Ag^+ for reduction to Ag^0 and eventually, the formation of NPs. This is expected as the high concentration of the reactant drives the reaction forward in the initial stages of the equilibrium reaction. This effect is also consistent with the RSM analysis where the factor corresponding to the $AgNO_3$ concentration (C) had a statistically significant weight in the derived quadratic model.

Determination of surface response plot. A 3D surface response plot is a graphical representation of the statistical equation obtained from the established model. This is used to visualize the interaction among the variables and to define the optimal condition of each variable for maximum AgNPs yield production. The plot is based on the function of two variables while the third variable is at its optimum condition. Furthermore, the elliptical or saddle shape of the contour plot specifies the level of the interaction significance. It also indicates when there is a perfect interaction among independent variables [18]. Figures 3 and 4 demonstrate the 3D plot of AgNPs yield using

the interaction of $AgNO_3$ concentration with the other two parameters.

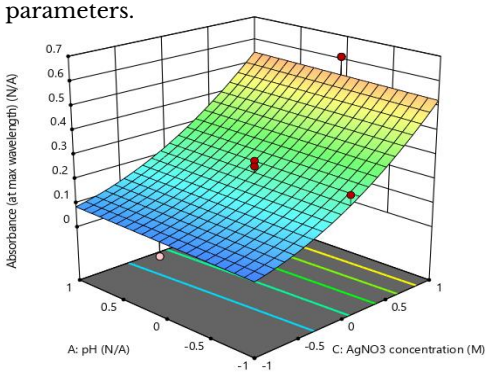

Figure 3. 3D interaction plot of AgNPs yield, initial pH and $AgNO_3$ concentration.

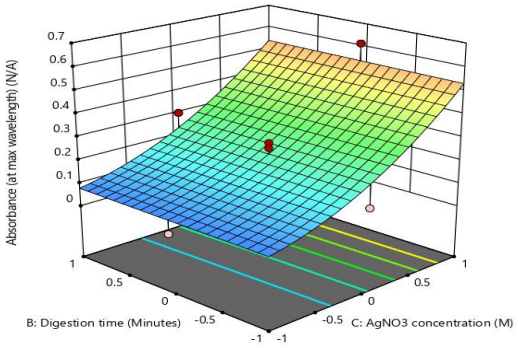

Figure 4. 3D interaction plot of AgNPs yield, digestion time, and $AgNO_3$ concentration.

These surface plots further establish the idea that the optimal condition of high yield AgNPs depends on the $AgNO_3$ concentration.

Determination of optimal conditions. Optimal values of each parameter were determined after the mathematical model was deemed fit to represent the whole system. Optimization of reaction parameters was performed using the software and 87 solutions were presented. The solution with the highest desirability (desirability = 0.955) was chosen which was pH = 8, digestion time = 4.5 minutes, and $AgNO_3$ concentration = 0.015 M. The predicted absorbance value using these conditions is 0.582. Comparing this to the actual measured absorbance of 0.592, the model is accurate by 98.28% (1.72% error).

The yield in concentration units can be calculated using Equation 1 and the approximate value of the extinction coefficient (ε=235 x 10^8 M^{-1} cm^{-1}) for the size and wavelength of the nanoparticles synthesized [11]. Thus, at the optimum condition within the range studied, the yield is about 1.5 x 10^{10} particles/mL (using Equation 2). The findings of the study aligned with that of Soni and Prakash [19] and Baker et al. [20] which stated that the concentration of raw materials ($AgNO_3$), initial pH of the $AgNO_3$ solution, and digestion time affect the yield of AgNPs produced.

Atomic force microscopy analysis. Figure 5 shows the image obtained through atomic force microscopy of the AgNPs synthesized using optimum conditions. The dark sections show imperfections in the substrate used. The particles are roughly homogenous, spherical in shape, and are ~30 nm in diameter.

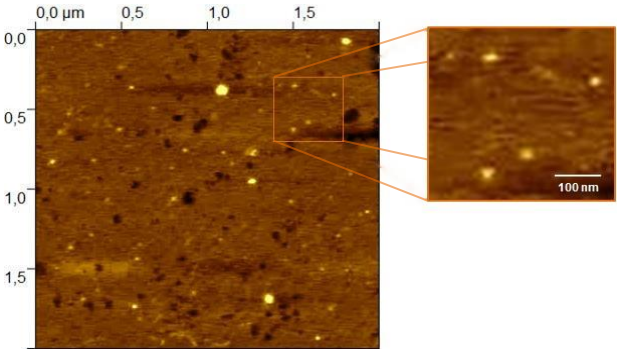

Figure 5. AFM photograph of synthesized AgNPs at optimal conditions.

The use of FCCCD, using RSM, is a relatively efficient method to determine optimal conditions especially in the synthesis of NPs. The study showed that the optimization of three process parameters namely initial pH of the $AgNO_3$ solution, digestion time between $AgNO_3$ solution, ascorbic acid and trisodium citrate solution, and $AgNO_3$ concentration to yield of AgNPs was possible. Previous studies such as that of Chowdhury et al. [8] and of Quintero-Quiroz et al. [21] both optimized synthesis of AgNPs using RSM with three and four variables, respectively. The findings of the study supported the idea from the aforementioned studies that the synthesis of AgNPs by altering process parameters can be optimized through FCCCD using RSM.

Limitations. The factorial design (three-level) was limited to three variables only namely initial pH of the $AgNO_3$ solution, digestion time, and $AgNO_3$ concentration. Other variables such as temperature, stirring speed, reductant concentration, and stabilizer concentration were all held constant. It is also worth noting that the optimum condition only applies within the range of values used for each parameter. Lastly, the yields are also estimated based on the assumption that the particles are monodispersed as seen in the AFM image, and the relative uniformity in color (λ_{max}) but should nonetheless be confirmed by other more accurate particle characterization techniques.

Conclusion. This study aimed to optimize reaction parameters for the synthesis of AgNPs using ascorbic acid and trisodium citrate through RSM. Optimal conditions for the synthesis of AgNPs resulted in a yield of 1.5 x 10^{10} particles/mL. This was achieved at pH 8 for the initial $AgNO_3$ solution, 4.5 minutes of digestion time, and 0.015 M of $AgNO_3$ concentration. $AgNO_3$ concentration had the most pronounced effect on the absorbance within the specified range of values used in the experiments. It is believed that the three parameters are highly suitable for the bulk production of spherical-shaped AgNPs with sizes of about 30 nm to be used in several scientific fields.

Recommendations. Dynamic Light Scattering (DLS) characterization technique should be performed to determine particle distribution and to correct for the absorbance values so that more accurate yield estimations can be achieved. The chosen range of the parameters was also still not at the saturation point which will probably be determined

by the amount of reducing or stabilizing agent. This is because the latter two will eventually become the limiting reagents once $AgNO_3$ is already present in excess. However, the effect of other parameters at elevated concentrations should not be ruled out and still needs to be explored. The proponents of the study also recommend accounting other factors such as stirring speed, heating temperature, and reductant and stabilizer concentration among others as factors to be altered simultaneously and tested using RSM. A six-level factorial design is recommended so that all the interactions of these variables will be accounted for. This will be done in order to further optimize the synthesis process of silver nanoparticles, particularly for bulk production.

Acknowledgement. First and foremost, the proponents of the study would like to thank their families for their never-ending support in their research work. The proponents of the study are also very much grateful to Mr. Norwell Bautista, Prof. Sherwin Escayo, and Prof. Steve Janagap for helping them to understand the necessary concepts regarding synthesis of silver nanoparticles and the use of Response Surface Methodology. Extended thanks are also given to Ms. Jessebel Gadot of UPV Miag-ao for her help and assistance in the characterization of the AgNP sample using an Atomic Force Microscope. Lastly, thanks are given to God Almighty. Without His blessings, this study would not have been successful.

References

[1] Krishnaraj C, Ramachandran R, Mohan K, Kalaichelvan PT. 2012. Optimization for rapid synthesis of silver nanoparticles and its effect on phytopathogenic fungi. Spectrochimica Acta Part A: Mol & Biomol Spectroscopy. 93(2012):95-99.

[2] Lee S, Jun B. 2019. Silver nanoparticles: synthesis and application for nanomedicine. Int J Mol Sci. 20(865):1-24.

[3] Guzman M, Dille J, Godet S. 2008. Synthesis of silver nanoparticles by chemical reduction method and their antibacterial activity. Int J Mat & Met Eng. 2(7):1-8.

[4] Malassis L, Dreyfus R, Murphy R, Hough L, Donnio B, Murray C. 2016. One-step green synthesis of gold and silver nanoparticles with ascorbic acid and their versatile surface post-functionalization. RSC Adv. 6(2016):33092-33100.

[5] Qin Y, Ji X, Jing J, Liu H, Wu H, Yang W. 2010. Size control over spherical silver nanoparticles by ascorbic acid reduction. Colloids and Surfaces: A Physicochem and Engg Aspects. 372(2010):172-176.

[6] Khatoon U, Rao K, Rao J, Aparna Y. 2011. Synthesis and characterization of silver nanoparticles by chemical reduction method. Intl Conf on Nanosci, Engg, & Tech. (2011):97-99.

[7] Bas D, Boyaci I. 2007. Modelling and optimization: Usability of Response Surface Methodology. J. Food Engg. 78(3):836-845.

[8] Chowdhury S, Yusof F, Faruck M, Sulaiman N. 2016. Process optimization of silver nanoparticles using Response Surface Methodology. Procedia Engg. 148(2016):992-999.

[9] Farahi AG, Najafpour G, Ghoreyshi A, Mohammadi M, Esfahanian M. 2012. Enzymatic production of reducing sugars from broomcorn seed (*Sorghum vulgare)*: Process optimization and kinetic studies. World App. Sci. Journ. 18(4):568-574.

[10] Yusof F, Chowdhury S, Sulaiman N, Faruck M. 2018. Effect of process parameters on the synthesis of silver nanoparticles and its effects on microbes. Jurnal Teknologi (Sci & Eng.). 80(3):115-121.

[11] Paramelle D, Sadovoy A, Gorelik S, Free P, Hobley J, Fernig DG. 2014. A rapid method to estimate the concentration of citrate capped silver nanoparticles from UV-visible light spectra. Analyst. 139(2014):4855-4861.

[12] Zielinska A, Skwarek E, Zaleska A, Gazda M, Hupka J. 2009. Preparation of silver nanoparticles with controlled particle size. Procedia Chemistry. 1(2009):1560-1566.

[13] Huang T, Xu XHN. 2010. Synthesis and characterization of tunable rainbow-colored colloidal silver nanoparticles using single nanoparticle plasmonic microscopy and spectroscopy. J Mater Chem. 20(44):9867-9876.

[14] Velikov K, Zegers G, Blaaderen A. 2003. Synthesis and characterization of large colloidal silver particles. Langmuir. 19(2003):1384-1389.

[15] Suriati G, Mariatti M, Azizan A. 2014. Synthesis of silver nanoparticles by chemical reduction method: Effect of reducing agent and surfactant concentration. Int J Automotive and Mech Engg. 10(2014):1920-1927.

[16] Deepak V, Kalishwaralal K, Pandian S, Gurunathan S. 2011. An insight into the bacterial biogenesis of silver nanoparticles, industrial production and scale-up. Metal Nano in Microbio. (2014):17-35.

[17] Chitra K, Annadurai G. 2014. Antibacterial activity of pH-dependent biosynthesized silver nanoparticles against clinical pathogen. Biomed Res Int. 2014(725165):1-6.

[18] Muralidhar R. 2001. A response surface approach for the comparison of lipase production by *Candida cylindracea* using two different carbon sources. Biochem Eng J. 9(1):17-23.

[19] Soni N, Prakash S. 2011. Factors affecting the geometry of silver nanoparticles synthesis in *Chrysosporium tropicum* and *Fusarium oxysporum.* American J of Nanotech. 2(1):112-121.

[20] Baker S, Rakshith D, Kavitha KS. 2013. Plants: emerging as nanofactories towards facile route in the synthesis of nanoparticles. BioImpacts. 3(3):111-117.

[21] Quintero-Quiroz C, Acevedo N, Zapata-Giraldo J, Botero L, Quintero J, Zarate-Triviño D, Saldarriaga J, Perez V. 2019. Optimization of silver nanoparticle synthesis by chemical reduction and evaluation of its antimicrobial and toxic activity. Biomater Res. 23(27):1-15.

Evaluation of the ultraviolet and visible light photocatalytic activity of undoped and nitrogen-doped titanium dioxide nanoparticles (N-TNPs) against low-density polyethylene (LDPE)

CYRA MARIE P. AGNO, PAULINE YSABELLE A. GILONGOS, YANI ANGELINE D. JALANDONI, and RAMON ANGELO N. SINCO

Philippine Science High School - Western Visayas Campus, Brgy. Bito-on, Jaro, Iloilo City 5000, Department of Science and Technology, Philippines

Abstract

Plastics have become a major environmental concern due to its persistence in ecosystems. Plastic degradation processes nowadays are centered on photocatalysis because of its potential as a clean energy source. This study used undoped and nitrogen-doped titanium dioxide nanoparticles (TNPs/N-TNPs) as photocatalysts. TNPs were reported effective in polyethylene degradation due to its high surface-area-to-volume ratio, and nitrogen doping can shift its absorption spectrum to the visible region. To test photocatalytic activity, LDPE films were irradiated in aqueous nanoparticle suspensions under ultraviolet and visible light. FTIR and microscope characterization were conducted before and after irradiation. Photodegradation was then quantified by solving for carbonyl and vinyl indices. N-TNP treated films under visible light showed the most observable difference in the number of spots and scratches and the greatest increase in carbonyl index. This confirms that nitrogen doping extended the photocatalytic activity of TNPs into the visible spectrum for more efficient photodegradation.

Keywords: *carbonyl index, irradiation, nitrogen-doping, photocatalysis, vinyl index*

Introduction. Polyethylene is a type of plastic that is usually discarded after being used for a short period of time [1]. Low-density polyethylene (LDPE) is commonly used for household and industrial purposes due to its resistance from being dissolved in concentrated acids, ketones, and vegetable oils [2]. However, its accumulation made it a major cause of pollution and a threat to all types of biomes, especially the aquatic environment. Plastic particles are being consumed by marine life that confuse them with food sources [3]. Different ways have been proposed for the conversion of plastic waste, but none is considered as a sustainable solution that can significantly reduce the pollution it causes. Thus, there is an urgent need to develop methods on how to properly degrade LDPE plastics.

Recent studies on plastic degradation are centered on photocatalysis which uses solar or other forms of energy to degrade plastics. Heterogeneous photocatalysis was proven efficient for polymer degradation. It uses semiconductors as catalysts to generate reactive species like superoxides and hydroxyl radicals when exposed to light [4].

Titanium dioxide (TiO_2) has the most potential as a semiconductor catalyst due to its high efficiency, low cost, chemical inertness, long-term stability, and nontoxicity [5,6]. TiO_2 nanoparticles (TNPs) have been reported to be effective in polyethylene degradation due to its high surface-area-to-volume ratio, particularly with the tube-shaped TNPs, creating a larger surface area with more active sites for reactions to occur [7]. However, the TNP's wide band gap (3.0-3.2 eV) and high recombination of electrons and holes limit its practical applications [8]. It can only absorb light from the ultraviolet (UV) spectrum, which is ~4% of the solar energy reaching the earth's surface [10]. By shifting the absorption threshold towards the visible region which is ~43% of the solar energy, its photocatalytic functions can be maximized [9].

Doping or the substitution of a dopant for an ion in the precursor material is a method used to shift the absorption threshold of a nanoparticle and further enhance its photocatalytic abilities [9]. Doping using nonmetals produces localized states within the band gap. Thus, when TiO_2 is exposed to visible light, electrons are promoted from these localized states to the conduction band [9]. TNPs that have been doped at the Oxygen (O) sites with nonmetals showed significant improvement in photocatalytic abilities [11,12,13]. However, nitrogen doping was found to be the most effective compared to other nonmetal doping such as Sulphur (S), Phosphorus (P), and Carbon (C), due to the efficient mixing of 2p orbitals of N and O [9,14].

Nitrogen-doped TNPs (N-TNPs) were already used to degrade other organic pollutants including benzenes [15], rhodamine B [16], and organic dyes [17]. Hence, N-doping of the TNPs can notably enhance the photocatalytic degradation of LDPE.

How to cite this article:

CSE: Agno CM, Gilongos PY, Jalandoni YA, Sinco RA. 2020. Evaluation of the ultraviolet and visible light photocatalytic activity of undoped (TNPs) and nitrogen (N) doped titanium dioxide nanoparticles (N-TNPs) against low-density polyethylene (LDPE). Publiscience. 3(1): 117-121.

APA: Agno, C.M., Gilongos, P.Y., Jalandoni, Y.A, Sinco, R.A. (2020). Evaluation of the ultraviolet and visible light photocatalytic activity of undoped (TNPs) and nitrogen (N) doped titanium dioxide nanoparticles (N-TNPs) against low-density polyethylene (LDPE). *Publiscience*. 3(1): 117-121.

The aim of this study was to compare the efficiency of undoped with nitrogen-doped titanium dioxide nanoparticles in degrading low-density polyethylene when irradiated under ultraviolet and visible light. It specifically aimed to:

(i) describe the degree of morphological changes on LDPE films through microscope images; and

(ii) determine the chemical changes in the LDPE films in terms of its carbonyl and vinyl indices using Fourier Transform Infrared (FTIR) Spectroscopy.

Methods. This experimental research aimed to evaluate the photocatalytic activity of undoped (TNPs) and nitrogen-doped titanium dioxide nanoparticles (N-TNPs) against low-density polyethylene (LDPE).

Reagents. Commercially available LDPE were purchased from the local market. Undoped, tube-shaped, titanium dioxide nanoparticles (TNPs) with 99.9% purity and, <50nm APS and nitrogen-doped, tube-shaped, titanium dioxide nanoparticles (N-TNPs) with 99.9% purity and, <80nm APS were purchased at Nano Research Inc.

Preparation of nanoparticle suspension and LDPE films. TNPs and N-TNPs aqueous suspensions at 20mM concentration were prepared by mixing 1.599g of TNPs and 1.878g of N-TNPs each with 1L of distilled water in separate beakers. The mixtures were then ultrasonicated for 30 minutes.

Twelve pieces of LDPE films were cut into 4cm by 26cm strips prior to the exposure to light [4]. Only the 4cm by 4cm at the center of the films were analyzed leaving the remaining area touchable.

Irradiation. Photodegradation of LDPE films were carried out for 336 hours in 250mL beakers containing 150mL of the 20mM TNP and N-TNP aqueous suspensions enclosed in two 24" x 8" x 6" wooden boxes containing either an 18W UV lamp or a 9W visible lamp [7]. After irradiation, LDPE films were thoroughly rinsed with distilled water.

Characterization. LDPE films were observed under a compound light microscope at 40x total magnification for scratches and spots that may be caused by photodegradation [4]. The films were also characterized using Fourier Transform Infrared (FTIR) Spectroscopy before and after irradiation. Vibration peaks were recorded and analyzed for the chemical transformation of the films [18].

Data analysis. The carbonyl index (C.I) was solved using the following formula:

$$Carbonyl\ index\ (C.I.) = A1710/A1380$$

The peak at 1710 cm^{-1} from the FTIR corresponds to the absorption from the presence of carbonyl group (C=O). The peak absorbance of 1380 cm^{-1} was taken as reference peak [7,19].

The vinyl index was determined using the following formula:

$$Vinyl\ Index\ (V.I.) = A909/A2020$$

The peak at 909 cm^{-1} corresponds to the stretching vibration of the vinyl group (CH_2=CH). The peak absorbance of 2020 cm^{-1} was taken as the reference peak [20].

Paired t-test was the statistical tool used to determine if there was a significant difference in the indices before and after irradiation.

Safety Procedure. The sonication process of the nanoparticles was made under the fume hood to reduce the smell. Used nanoparticles were placed in separate waste bottles and were turned over to the unit that disposes chemicals.

Results and Discussion. After irradiation, scratches and spots were seen on the surface of the LDPE. Figure 1 shows microscopic images of the surface of LDPE films before and after 336 hours of irradiation. There is an observable difference in the scratches observed on the surface of TNP-UV films before and after irradiation. However, the scratches on the surface of TNP-VL after irradiation were consistent with the image before. N-TNP-UV set-up showed additional spots and two highlighted scratches after the treatment. The set-up N-TNP-VL formed larger and longer scratches with additional spots on the surface of the LDPE.

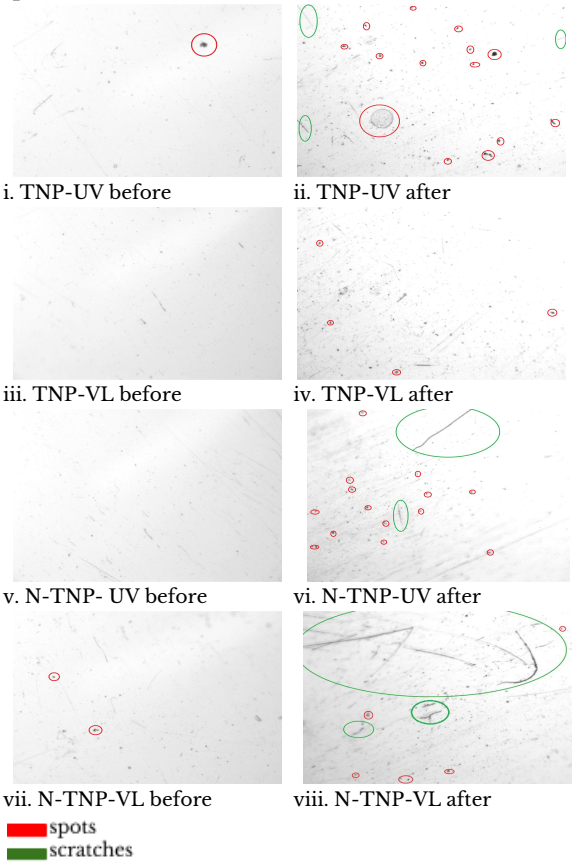

Figure 1. Microscopic images at 40x total magnification of LDPE films before and after 336 hours of irradiation under ultraviolet and visible light.

Chromophoric groups, factory defects, and weak links within the LDPE surface can be initiation sites for photocatalytic reactions, leading to the degradation of the plastics upon prolonged exposure to TNP or N-TNP suspension with UV and visible light irradiation [4]. Hence, scratches seen on the surface of LDPE films indicate photocatalytic degradation. These visual changes on the surface of LDPE films due to photodegradation were also confirmed by the results from the FTIR analysis.

FTIR analysis was used to describe the structural changes made in the surface of LDPE. Figure 2 shows the infrared spectra of the LDPE irradiated under visible and ultraviolet light before and after 336 hours of irradiation. The increase in the absorbance values around 2850cm^{-1} to 3000cm^{-1} means that there is a formation of carbonyl and vinyl compounds. The increase in the absorbance values around 3584cm^{-1} to 3700cm^{-1} implies the formation of hydroperoxides and -OH stretching. Hydroperoxides are reactive species generated after the exposure to light of nanoparticles [4]. Among all the set-ups, only TNP-VL treated films showed a consistent graph before and after treatment and irradiation. These results from the FTIR analysis were used to calculate the carbonyl and vinyl indices which are indicators of photodegradation.

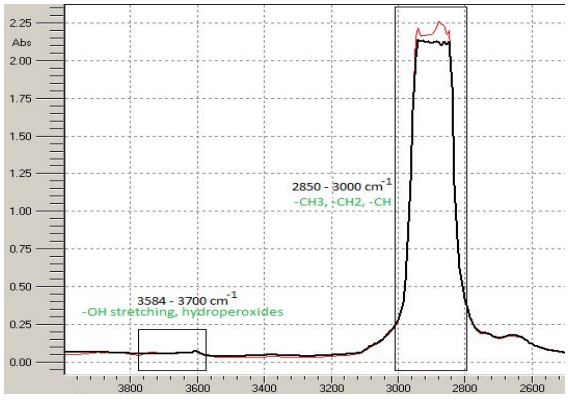

i. TNP-UV

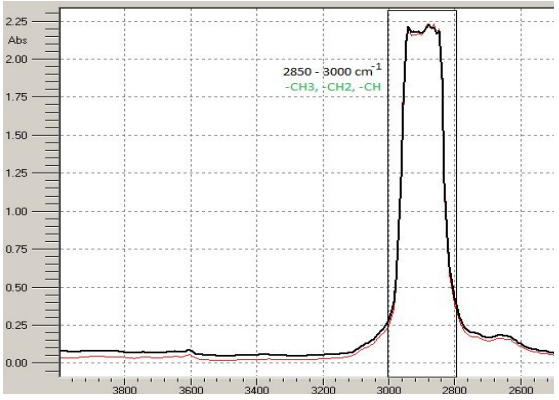

ii. TNP-VL

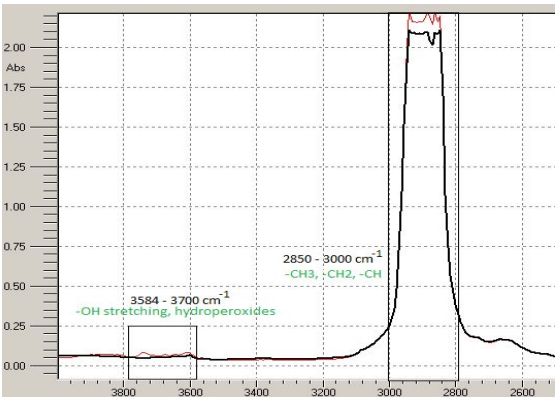

iii. N-TNP-UV

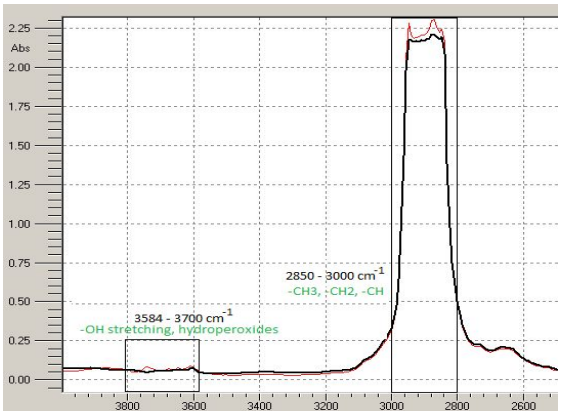

iv. N-TNP-VL

Before After

Figure 2. FTIR graphs of LDPE films before and after treatment and 336 hours of irradiation under ultraviolet and visible light.

Table 1 shows the computed mean, standard deviation, t-values, and P-values of the CIs of each treatment. TNP-UV and N-TNP-VL treatments showed P-values lower than 0.05 and t-values higher than the t_{crit} (t_{crit} = 4.30) which indicates a significant difference in the CIs of the films before and after 336 hours of irradiation. The highest mean value was observed in N-TNP-VL treated films while TNP-VL showed the lowest.

Table 1. Paired t-test of the carbonyl indices (CI) of LDPE films at 95% confidence level.

	Paired Differences		t	Sig. (2-tailed)
	Mean	Standard Deviation		
TNP-UV	0.09443	0.02152	7.601	0.017
TNP-VL	0.00234	0.01953	0.208	0.855
N-TNP-UV	0.09893	0.06673	2.568	0.124
N-TNP-VL	0.12290	0.02200	9.673	0.011

Based on the results of the statistical test, CIs of set-ups TNP-UV and N-TNP-VL after irradiation are significantly different with the value before irradiation, thus, photodegradation occurred [4]. The

set-up for N-TNP-UV showed no significant difference. However, the mean difference is as high as TNP-UV and N-TNP-VL set-ups. This might be caused by a low precision of data as reflected by the high standard deviation. TNP-VL has a P-value higher than 0.05 and t-value lower than 4.30. This suggests that low to no photodegradation occurred and that TNPs do not react with visible light [15].

Table 2 shows the computed mean, standard deviation, t-values, and P-values of the VIs of each treatment. All showed P-values higher than 0.05 and t-values lower than the t_{crit} (t_{crit} = 4.30). This means that the difference in the VIs of the films before and after 336 hours of irradiation is not significant.

Table 2. Paired t-test of the vinyl indices (VI) of LDPE films at 95% confidence level.

	Paired Differences		t	Sig. (2-tailed)
	Mean	Standard Deviation		
TNP-UV	0.09576	0.12083	1.373	0.304
TNP-VL	0.04416	0.14890	0.514	0.659
N-TNP-UV	-0.00367	0.19312	-0.033	0.977
N-TNP-VL	0.02253	0.07852	0.497	0.669

The formation of vinyl groups from the photocatalytic degradation of LDPE films was not as intense as that of the carbonyl groups, due to the vinyl groups being typical of chain terminations, while the carbonyl groups appear throughout the polymeric chain. The formation of vinyl groups occurred in the latter parts of the degradation process [21]; thus, the results for the vinyl index were inconclusive.

Limitations. The use of FTIR was not maximized. The options *peak search* and *spectrum search* could have been used to easily identify the peaks and its corresponding functional groups. However, due to some defects in the equipment, it was impossible to do so. Also, set-ups for nanoparticle treatment only and irradiation only were not included. Thus, results might be due to the irradiation only or the nanoparticle treatment only.

Conclusion. Based on carbonyl index values, nitrogen doping of TNPs was able to enhance its ability by utilizing both UV and visible light in the photocatalytic degradation of LDPE films. It can use solar energy more efficiently to produce reactive species, such as hydroxyl radicals and superoxides, and accelerate the degradation of LDPE films. While TNPs are effective in utilizing UV light for the photodegradation of LDPE films, they are inefficient in absorbing light from the visible spectrum.

Recommendations. The results obtained can be further improved with the use of ImageJ software by quantifying the length, depth, and the area of scratches and spots made on the surface of the LDPE. Additionally, the use of the FTIR spectrophotometer can be maximized by using the peak search option, which was not available during the data gathering process. It is recommended to allot a longer time of irradiation to light to clearly observe the degradation progress of plastics. As the time of irradiation is increased, the amount of nanoparticle suspension must also be increased for the reaction to continue. Also, a negative control can also be added in the research design.

Acknowledgement. The researchers would like to thank the external consultant, Mr. Ryan Sherwin D. Jalandoni, for imparting his knowledge and giving out suggestions and comments for the improvement of this paper.

References

[1] Koutny M, Lemaire J, Delort A. 2006. Biodegradation of polyethylene films with prooxidant additives. Chemosphere 64, p.1243.

[2] Grover A, Gupta A, Chandra S, Kumari A, Khurana SMP. 2015. Polythene and environment. Int J Environ Sci. 5(6): 1091-1105.

[3] Haward M. 2018. Plastic pollution of the world's seas and oceans as a contemporary challenge in ocean governance. Nat Commun, 9:667.

[4] Tofa TS, Kunjali KL, Paul S, Dutta J. 2019. Visible light photocatalytic degradation of microplastic residues with zinc oxide nanorods. Environ Chem Lett.

[5] Chen HW, Su SF, Chien CT, Lin WH, Yu SL, Chou CC, Chen JJ, Yang PC. 2006. Titanium dioxide nanoparticles induce emphysema-like lung injury in mice. FASEB J. 20(13):2393-5.

[6] Kamrannejad MM, Hasanzadeha A, Nosoudib N, Maic L, Babaluo AA. 2014. Photocatalytic degradation of polypropylene/TiO_2 Nano-composites. Mat Res. 17(4): 1039-1046.

[7] Ali SS. Qazi IA Arshad M, Khan Z, Voice T, Mehmood CT. 2016. Photocatalytic degradation of low-density polyethylene (LDPE) films using titania nanotubes. Environ Nanotech Monitor Manage. 5(2016):44-53.

[8] Lin X, Rong F, Fu D, Yuan C. 2012. Enhanced photocatalytic activity of fluorine doped TiO_2 loaded with Ag for degradation of organic pollutants. Powder Techno. 219: 173–178.

[9] Senthilnathan J, Philip L. 2010. Photocatalytic degradation of lindane under UV and visible light using N-doped TiO_2. Chem Eng J. 161: 83-92.

[10] Kumar SG, Devi LG. 2011. Review on Modified TiO_2 photocatalysis under UV/Visible light: Selected results and related mechanisms on interfacial charge carrier transfer dynamics. J Phys Chem A. 115(46): 13211-13241.

[11] Ji L, Zhang Y, Miao S, Gong M, Liu X. In situ synthesis of carbon doped TiO_2 nanotubes with an enhanced photocatalytic performance under UV and visible light. Carbon. 2017;125:544-550.

[12] He Z, Zhan L, Hong F Song Shuang, Lin Z, Chen J, Jin M. 2010. A visible light-responsive iodine-doped titanium dioxide nanosphere. J Environ Sci. 23(1):166-170.

[13] Yu W, Liu X, Pan L, Li J, Liu J, Zhang J, et al. Enhanced visible light photocatalytic degradation of methylene blue by F-doped TiO_2. Applied Surface Science. 2014;319:107-112.

[14] Morikawa T, Asahi R, Ohwaki T, Aoki K, Taga Y. 2001. Band gap narrowing of titanium dioxide by nitrogen doping. Jpn J Appl Phys. 40: 561-563.

[15] Nassoko D, Li Y-F, Wang H, Li J-L, Li Y-Z, Yu Y. 2012. Nitrogen-doped TiO_2 nanoparticles by using EDTA as nitrogen source and soft template: Simple preparation, mesoporous structure, and photocatalytic activity under visible light. J Alloy Comp. 540: 228-235.

[16] Gautam A, Kshirsagar A, Biswas R, Banerjee S, Khana PK. 2015. Photodegradation of organic dyes based on anatase and rutile TiO2 nanoparticles. RSC Advances. 47(10) 1772-1782.

[17] Kim SH, Kwak SY, Suzuki T. 2006. Photocatalytic degradation of flexible PVC/TiO_2 nanohybrid as an eco-friendly alternative to the current waste landfill and dioxin-emitting incineration of post-use PVC. Polymer. 47(9):3005–3016. doi:10.1016/j.polymer.2006.03.015.

[18] Ashraf A. (2014). FTIR & UV-Vis analysis of Polymer (Polystyrene, LDPE) samples. doi: 10.13140/2.1.3819.0880.

[19] Salem, M. & Farouk, Habibu & Kashif, Ismail. (2002). Physicochemical changes in UV exposed low-density polyethylene films. Macromol Res. 10:168-173.

[20] Martínez-Romo A, González-Mota R, Soto-Bernal J, Rosales-Candelas I. 2015. Investigating the Degradability of HDPE, LDPE, PE-BIO, and PE-OXO Films under UV-B Radiation. J Spec. 2015. 1-6. 10.

[21] Klein JM, Ramos GR, Grisa AMC, Brandaise RN, Zeni M. 2013. Thermogravimetric and morphologic analysis of oxo-degradable polyethylene films after accelerated weathering. Prog Rubber Plast Re, 29(1): 39-54.

Publiscience Vol. 3 Issue 1

Microplastic occurrence in the coastal sediments of selected barangays of Anilao, Iloilo, Philippines

DANIELLE ANLEIGH B. COLACION, ELOISA MARIE M. SAN DIEGO, JUSTIN REY P. SECONDES, and ZENNIFER L. OBERIO

Philippine Science High School - Western Visayas Campus, Brgy. Bito-on, Jaro, Iloilo City 5000, Department of Science and Technology, Philippines

Abstract

Microplastics have been identified as a significant threat towards aquatic ecosystems and human life as they can easily be ingested due to their microscopic size. Due to this, there has been a demand to conduct research on the occurrence of the material. However, there is currently a lack of studies pertaining to the problem in the Philippines despite it being an archipelago. This paper presents the investigation of microplastic occurrence in the coastal sediments of Anilao, Iloilo, Philippines. Sediment samples were collected and were subjected to sieving, density separation, and wet peroxide oxidation for microplastic extraction. The acquired microplastics were observed under a compound inverted microscope for quantification and classification, and analyzed using ATR-FTIR spectroscopy for the identification of their chemical compositions. The study found that fibers and fragments comprise the majority of the extracted microplastics. It was also determined that a total of approximately 1 particle/g d.w., 5 particles/g d.w., and 2 particles/g d.w. constitute the sediments collected from Barangays Dangula-an, Pantalan, and San Carlos, respectively. Only two microplastic particles were successfully analyzed by FTIR and both were identified to be polyethylene.

Keywords: *microplastics, abundance, composition, fibers, fishing*

Introduction. **S**ince the introduction of plastics in the 1860s, there has been a rapid increase in its annual production, from 1.5 million tonnes in the 1950s to an estimate of 320 million tonnes in the year 2015 [1]. Furthermore, it was discovered that approximately 8% of these materials end up in marine systems every year, leading to marine plastic pollution [2]. This is mainly attributed to the poor waste management of industrial factories, fishing activities, and discharges from residential areas transported through sewage systems and natural waterways [3].

Aside from large plastic materials, however, plastics also come in the form of small particles called microplastics, defined as plastics of size 5 mm and below [4]. Compared to plastics of larger sizes, microplastics can be ingested by a wider range of organisms, obstructing their digestive tracts, and accumulating during digestion [5]. This may then facilitate the release of toxic chemicals that they have previously acquired during their manufacture and other contaminants that may have adsorbed onto their surfaces during their stay in the environment [6].

This phenomenon may also pose great risks to humans due to their regular seafood consumption. Furthermore, the toxins that these plastics contain may include those which are fatal to human health such as carcinogens, endocrine disruptors, and neurotoxic chemicals [7].

Studies have been conducted investigating the occurrence of microplastics in various coastal areas of the world. Stolte et al. [8] examined the microplastic concentrations along the beach sediments of the German Baltic Coast, while Vianello et al. [9] observed the occurrence and spatial patterns of microplastics in the lagoon sediments of Venice, Italy. Evidence suggests that shore sediments may be considered as a representative of aquatic ecosystems as they reflect the interactions between the water and land surface, thus providing information on the transportation of pollutants in the environment [10].

Despite microplastics being one of the most persistent pollutants in coastal environments today, studies pertaining to the topic have only emerged in the last few years [3]. At present, only a few studies tackling microplastic pollution have been published in the Philippines, including that of Kalnasa et al. [11] wherein the surface sand of Macajalar Bay, Bohol, Philippines was assessed for microplastic occurrence.

According to DENR and DILG [12], 54% of all Philippine municipalities are coastal, leading to the emergence of fishing and mariculture as one of the primary sources of food and livelihood in the country. Included in these coastal municipalities is Anilao, Iloilo, a community known for its large-scale cultivation and production of various seafood such as shrimp paste, mussels, and oysters which are widely distributed to different parts of the province. Despite playing a significant role in the local seafood industry, there is still a lack of information concerning microplastic pollution in the area.

Thus, this study aimed to acquire further information on the topic by investigating three barangays of Anilao, Iloilo based on the occurrence

How to cite this article:
CSE: Colacion DAB, San Diego EMM, Secondes JRP, Oberio ZL. 2020. Microplastic occurrence in the coastal sediments of selected barangays of Anilao, Iloilo, Philippines. Publiscience. 3(1):122-126.
APA: Colacion, D.A.B., San Diego, E.M.M., Secondes, J.R.P., & Oberio, Z.L. (2020). Microplastic occurrence in the coastal sediments of selected barangays of Anilao, Iloilo, Philippines. *Publiscience,* 3(1):122-126.

of microplastics in their coastal sediments. It specifically aimed to:

(i) determine the relative abundance in percent of microplastics of each morphological type – fiber, film, fragment, and pellet;

(ii) determine the total abundance in particles/g dry weight (d.w.) of microplastics contained in the collected sediment samples;

(iii) compare the relative and total abundances of microplastics in the three barangays; and

(iv) identify the chemical composition of the extracted microplastics through Attenuated Total Reflection - Fourier Transformed Infrared (ATR-FTIR) spectroscopy.

Methods. The data gathering procedure was divided into four general steps. These include the sample collection, microplastic extraction, visual inspection, and the FTIR analysis.

Sample Collection. Anilao, Iloilo was selected as the coastal community to investigate due to its large impact on the province's seafood industry, as well as its accessibility to the researchers. Three coastal areas in the municipality, specifically Barangays Dangula-an (10°58'58.2" N 122°46'44.2" E), Pantalan (10°57'5" N 122°45'52" E), and San Carlos (10°58"48" N 122°46'42" E), were selected as sampling sites based on the fishing and mariculture activities in the areas. Three quadrats were randomly positioned along a stretch of 100 m on the high tide line of each site. Coastal sediments were collected to a depth of approximately 2 cm from the surface. The samples were properly stored and transported to the Philippine Science High School – Western Visayas Campus' (PSHS-WVC) research laboratory immediately after collection.

Extraction. The sediment samples were oven-dried at 60°C for 48 h. They were then passed through a stack of 4 mm and 2 mm sieves. The retained fraction on both sieves were properly disposed while those which passed through were temporarily stored for further processing.

Sieved samples of mass 500 g were mixed with 2000 mL of saturated NaCl solution. The mixture was stirred for five minutes and was allowed to stand for an hour. The top layer of the mixture was filtered with Whatman No. 41 filter paper and was then oven-dried at 50°C for 48 h.

The dried particles were then treated with 20 mL of 30% hydrogen peroxide and incubated at 60°C for 24 h. The treatment setup was filtered, and the acquired particles were oven-dried at 50°C for 48 h. The dried samples were transferred into a glass petri dish for storage.

Visual Inspection. The microplastics of size ≤2 mm acquired after the extraction process were inspected using a compound inverted microscope at 40x magnification. Microplastics were identified based on the criteria presented by Norén [13]. They were also classified into four types namely fiber, film, fragment, and pellet based on the criteria provided by Free et al. [14] and Frias et al. [15]. The microplastics were manually counted to determine their total and relative abundances.

FTIR Analysis. Petri dishes containing the obtained microplastics of size ≤2 mm from each sampling location were sent to Advanced Device and Materials Testing Laboratory (ADMATEL) in Taguig City, Metro Manila for analysis. The Perkin Elmer FTIR Spectrometer Frontier ATR-FTIR model was used to determine the chemical composition of the identified microplastics. One representative microplastic piece from each sample was selected and subjected to the analysis. The instrument was set to reflection mode with a 4000-600 cm^{-1} range with 20 scans at 8 cm^{-1} resolution. A spectra library linked to the ATR-FTIR was used to determine the identity of the acquired sample spectra.

Calculations. Relative abundance is defined as the amount of microplastics for each morphological type relative to the total amount of microplastics present in each sediment sample in percent. The relative abundance of microplastics per morphological type was computed using the equation below.

$$Abundance_{Relative} = \frac{no.\,of\ microplastics\ (based\ on\ type)}{total\ no.\,of\ microplastics} \times 100\%$$

Total abundance refers to the total amount of microplastics extracted from each sampling site. The total abundance of microplastics per sample was computed using the following equation.

$$Abundance_{Total} = \frac{no.\,of\ microplastics\ (particles)}{mass\ of\ treated\ sediment\ sample\ (g\ d.w.)}$$

Results and Discussion. The results and discussion of the study is divided into three sections, specifically relative abundance, total abundance, and chemical composition.

Relative Abundance. In Barangays Dangula-an and San Carlos, fiber was found to be the most abundant type of microplastic, followed by fragments, and lastly, films. Meanwhile, fragments constitute the highest percentage of the total abundance in Barangay Pantalan, as shown in Figure 1. This is then followed by fibers and films, respectively. Little to no amount of pellets was found from all sampling locations.

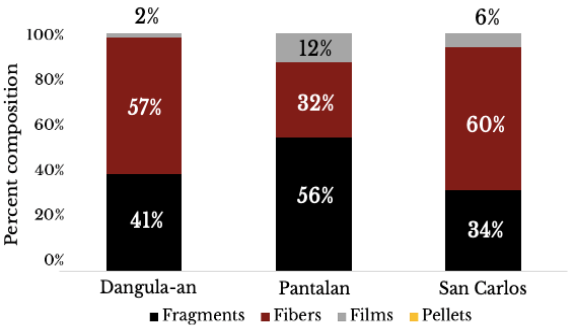

Figure 1. The relative abundances (%) of microplastics in the barangays.

Microfibers in marine ecosystems may come from various sources such as the breakdown of fishing ropes and/or nets caused by ocean currents and exposure to UV-B light, and frequent anthropogenic

activities such as the washing of textiles [16,17]. Meanwhile, fragments may result from the degradation of plastic bottles and other sturdy plastics from nearby households [18]. The presence of films is mainly attributed to the breakdown of plastic bags, wrappers, and sheeting carried off from residences near the coastal areas [14]. Unlike fibers, fragments, and films, micro-pellets are directly manufactured in microscopic sizes. They are usually found in cleaning and cosmetic products [19].

From these information, it is deduced that the active fishing and mariculture activities in the coastal areas may have resulted to the detected high microfiber abundance. Meanwhile, as fragments and films mostly originate from plastics used in households, the large number of residences in Barangay Pantalan may have attributed to fibers and films comprising a higher percentage of the total microplastic abundance in the area compared to that of the other two sampling sites. Additionally, the data also suggests that plastics carried off from these households constitute more of hard, sturdy plastics compared to thin, flimsy ones as films account for a smaller portion of the total abundance than fragments. Lastly, the trace amount of pellets in all sampling sites suggests that only a small portion of the microplastics originated from cleaning and cosmetic products.

Total Abundance. The study shows that Barangay Pantalan has the greatest number of microplastics with 5 particles/g d.w., followed by Barangay San Carlos with 2 particles/g d.w., and Barangay Dangula-an with 1 particle/g d.w., as shown in Figure 2.

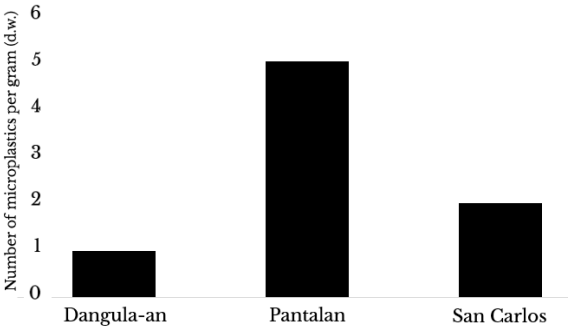

Figure 2. The total abundance (particles/g d.w.) of microplastics in the barangays.

Barangay Pantalan was determined to have the most number of microplastics among the three sampling sites. In accordance with the study of Brown et al. [18], wherein it was stated that population density may be a potential factor affecting microplastic abundance, Barangay Pantalan also has the largest population residing near its coastal area, with a total of 22 households compared to only 3-4 households each in Barangays Dangula-an and San Carlos. This may be attributed to the carrying off of plastics wastes from the residences.

Based on the coastal activity survey conducted by the researchers, all three sampling sites are in close proximity with rivers and fishing facilities, but only Barangays Pantalan and San Carlos are located near sewage inputs. The study by Brown et al. [2018] states that sewage is one of the most prevalent sources of microplastic pollution, thus supporting the detection of larger amounts of microplastics in the two sites compared to Barangay Dangula-an.

Aside from these, the large amount of microplastics may have also resulted from the transport of plastic waste to the sampling sites from different areas through water circulation [20]. According to the barangay officials, the sites serve as "catch basins" of interconnecting rivers, serving as transport pathways of debris from a nearby municipality, Banate, Iloilo, and three other provinces, Negros, Guimaras, and Cebu. In relation to this, Claessens et al. [21] and Faure et al. [22] also reported that high microplastic concentrations are attributed to the discharge of rivers potentially containing microplastics to larger bodies of water.

Another notable mechanism for the transport of microplastics to the coastal environment are the monsoons. Frequent heavy and prolonged downpour during the monsoon season in urban areas causes plastic litter to be washed down in storm drains, flowing into the rivers and seas [23]. In this study, the sediment samples were collected outside the monsoon season of the particular area of study. However, it is still possible that the microplastics found in the coastal sediments of the barangays were previously transported through this natural phenomenon.

Chemical composition. The chemical composition of two microplastic particles, with one acquired from Barangay San Carlos and one from Barangay Pantalan, were determined through analysis using an ATR-FTIR spectrophotometer. The infrared vibration spectra acquired from the spectroscopy presented the peaks exhibited by both materials. Five peak assignments of the analyzed sample from both locations matched with the polyethylene standard supported by Table 1, as shown below.

Table 1. Peak assignments in the infrared spectrum of microplastic samples from Barangay San Carlos (Sample 1) and Barangay Pantalan (Sample 3).

Wavenumber (cm^{-1})			
Polyethylene Standard	SAMPLE 1	SAMPLE 3	Bonds*
2916	2916.61	2916.06	C – H Anti-symmetric Stretching
2849	2849.52	2848.61	C – H Symmetric Stretching
1472 -	1471.57 -	1470.31 1375.79	C – H Deformation/ Bending
730 719	730.24 717.27	730.23 716.98	C – C Skeletal Bending

* References: [1] Spectrum Search Plus Library, Perkin Elmer. [2] Pretsch, E., et al. (2009), Structure Determination of Organic Compounds, 4th Ed., Springer – Verlag Berlin Heidelberg.

Polyethylene can be further classified into two structural isomeric polymers namely low-density polyethylene (LDPE) and high-density polyethylene (HDPE) [24]. According to the criteria proposed by Jung et al. [24], an LDPE infrared spectrum can be differentiated from that of an HDPE with the peak it exhibits at 1377 cm^{-1}. Thus, from the provided peaks in Table 1, sample 3 from Barangay Pantalan can be classified as LDPE with the distinct peak it forms at

1375.79 cm^{-1}. Sample 1, on the other hand, is identified as HDPE due to the absence of the said peak.

Globally, polyethylene is one of the most common polymer types found in coastal environments [25]. Potential sources of LDPE microplastics include plastic bags, plastic bottles, and fishing nets while HDPE ones may be sourced from milk jugs [19]. Additionally, Andrady [19] reported that 18% of marine debris comes from fishing ropes and nets commonly composed of polyethylene, polypropylene, and nylon. Thus, the analyzed microplastics may be primarily attributed to the fishing ropes and nets used in the mariculture activities in the coastal areas, as well as plastic containers utilized in nearby residences.

Limitations. The microplastics included in the study were limited to those of size ranging from 20 µm to 2 mm which are the grid sizes of the utilized filter paper and sieve, respectively. Additionally, only microplastics of density lesser than 1.2 g/cm^3, the density of the saturated salt solution used in the density separation method, were included in the scope of the study. It should also be considered that the possible sticking of microplastics onto the filter papers might have caused some particles to not be taken into account.

Furthermore, only an ATR-FTIR equipment, an apparatus that requires the manual handling of samples, was utilized for the chemical composition analysis of the microplastics. Hence, due to the absence of a microplastic particle from the Barangay Dangula-an sample that can be manually handled, no microplastic piece from its coastal area was analyzed for chemical composition.

As the researchers were unable to conduct an in-depth study on the water circulation flow in the areas, no concrete report can be made with regards to the different areas contributing to the microplastic abundance in the sampling sites. The study is also unable to conclude whether the total abundance values for each barangay can be considered as pollution as no standard criteria are available regarding this matter.

Conclusion. Microplastics were confirmed to be present in the coastal areas of the three barangays. They were found to be abundant in various morphological types, with fibers and fragments accounting for the majority of the total abundances. Among the three sampling sites, Barangay Pantalan was determined to have the most number of microplastics. Due to resource limitations, only two microplastic pieces were analyzed through FTIR analysis, and both were identified to be polyethylene. The results of this study may be used in the making of policies for the protection of seafood consumers and as a baseline for more in-depth research on microplastics.

Recommendations. In order to improve the entirety of the study and provide more accurate results, it is recommended that a more appropriate tool, specifically corers, will be utilized in the collection of coastal sediments. It is also suggested that a more appropriate equipment, specifically the micro-FTIR, will be utilized for the visual identification and chemical composition analysis of microplastics. Furthermore, subjecting a greater amount of sediments with sizes less than 2 mm to density separation is also recommended. Utilizing a saturated NaCl solution of higher purity for the density separation process may also help in improving the results of the study. Lastly, in order to assure the digestion of most or all biological matter in the samples, it is also suggested that wet peroxide oxidation will be conducted twice or will be replaced with a more efficient method.

Acknowledgment. The authors would like to thank Mayor Nathalie Ann Debuque of the municipality of Anilao, as well as the barangay captains of Barangays Dangula-an, Pantalan, and San Carlos, for permitting the conduct of the sample collection in their coastal areas. The authors would also like to acknowledge the efforts of Mrs. Emie Bragancia, the head of the Fisheries Department - Office of the Agriculturist, in guiding them to the sampling locations and facilitating arrangements with the barangay offices for the conduct of the sample collection. Furthermore, the authors would like to express their gratitude to Barangay Captain Junalyn Provido of Barangay Bito-on for permitting the conduct of the preliminary sample collection in their coastal area.

References

[1] Europe P. 2016. Plastics—The Facts 2016. An analysis of European latest plastics production, demand and waste data. Available from: bit.ly/PlasticsEur2016.

[2] Van Sebille E, Wilcox C, Lebreton L, Maximenko N, Hardesty BD, Van Franeker JA, Eriksen M, Siegel D, Galgani F, Law KL. 2015. A global inventory of small floating plastic debris. Environ Res Lett. 10(12): 124006. DOI: 10.1088/1748-9326/10/12/124006.

[3] De Jesus Piñon-Colin T, Rodriguez-Jimenez R, Pastrana-Corral M, Rogel-Hernandez E, Wakida F. 2018. Microplastics on sandy beaches of the Baja California Peninsula, Mexico. Mar Pollut Bull. 131(2018): 63-71. DOI: 10.1016/j.marpolbul.2018.03.055.

[4] Carr S, Liu J, Tesoro A. 2016. Transport and fate of microplastics marine particles in wastewater treatment. Water Res. (2016): 1-25. DOI: 10.1016/j.watres.2016.01.002.

[5] Cozar A, Echevarria F, Gonzalez-Gordillo J, Irogoien X, Ubeda B, Hernandez-Leon S, Palma Am Navarro S, Garcia-de-Lomas J, et al. 2014. Plastic debris in the open ocean. PNAS. 111(28): 10239-10244. DOI: 10.1073/pnas.1314705111.

[6] Barboza LG, Vethaak AD, Lavorante BR, Lundebye AK, Guilhermino L. 2018. Marine microplastic debris: An emerging issue for

food security, food safety and human health. Mar Pollut Bull. 133: 336-348. DOI: 10.1016/j.marpolbul.2018.05.047.

[7] Hahladakis JN, Velis CA, Weber R, Iacovidou E, Purnell P. 2018. An overview of chemical additives present in plastics: migration, release, fate and environmental impact during their use, disposal and recycling. J Hazard Mater. 344: 179-99. DOI: 10.1016/j.jhazmat.2017.10.014.

[8] Stolte A, Forster S, Gerdts G, Schubert H. 2015. Microplastic concentrations in beach sediments along the German Baltic coast. Mar Pollut Bull. 99(1-2): 216-229. DOI: 10.1016/j.marpolbul.2015.07.022.

[9] Vianello A, Boldrin A, Guerriero P, Moschino V, Rella R, Sturaro A, Da Ros L. 2013. Microplastic particles in sediments of lagoon of Venice, Italy: First observations on occurrence, spatial patterns and identification. Estuary Coast Shelf S. 130: 54-61. DOI: 10.1016/j.ecss.2013.03.022.

[10] Yu X, Peng J, Wang J, Wang K, Bao S. 2016. Occurrence of microplastics in the beach sand of the Chinese inner sea: the Bohai Sea. Environ Pollut. 214: 722-730. DOI: 10.1016/j.envpol.2016.04.080.

[11] Kalnasa ML, Lantaca SM, Boter LC, Flores GJ, Van Ryan Kristopher RG. 2019. Occurrence of surface sand microplastic and litter in Macajalar Bay, Philippines. Mar Pollut Bull. 149: 110521. DOI: 10.1016/j.marpolbul.2019.110521.

[12] DENR DB, DILG C. 2001. Philippine coastal management guidebook series no. 8: Coastal law enforcement. Coastal Resource Management Project of DENR, Cebu City, Philippines. 8(5): 106. Available from: bit.ly/DENR2001.

[13] Norén FR. 2007. Small plastic particles in coastal Swedish waters. KIMO Sweden. 2007:1-11. Available from: bit.ly/Noren2007

[14] Free C, Jensen O, Mason S, Eriksen M, Williamson N, Boldgiv B. 2014. High-levels of microplastic pollution in a large, remote, mountain lake. Mar Pollut Bull. 85(2014): 156-163. DOI: 10.1016/j.marpolbul.2014.06.001.

[15] Frias J, Gago J, Otero V, Sobral P. 2016. Microplastics in coastal sediments from Southern Portuguese shelf waters. Mar Environ Res. 144(2016): 24-30. DOI: 10.1016/j.marenvres.2015.12.006

[16] Zhang C, Zhou H, Cui Y, Wang C, Li Y, Zhang D. 2019. Microplastics in offshore sediment in the Yellow Sea and East China Sea, China. Environ Pollut. 244(2019): 827-833. DOI: 10.1016/j.envpol.2018.10.102.

[17] Santos IR, Friedrich AC, Do Sul JA. 2009. Marine debris contamination along undeveloped tropical beaches from northeast Brazil. Environ Monit Assess. 148(1-4): 455-462. DOI: 10.1007/s10661-008-0175-z.

[18] Brown M, Crump P, Niven S, Teuten E, Tonkin A, Galloway T, Thompson R. 2011. Accumulations of microplastic on shorelines worldwide: Sources and sinks. Environ Sci Technol, 45(2011): 9175-9179. DOI: 10.1021/es201811s.

[19] Andrady A. 2011. Microplastics in the marine environment. Mar Pollut Bull. 62(2011): 1596-1605. DOI: 10.1016/j.marpolbul.2011.05.030.

[20] Nel A, Froneman P. 2015. A quantitative analysis of microplastic pollution along the south-eastern coastline of South Africa. Mar Pollut Bull. 101(2015): 274-279. DOI: 10.1016/j.marpolbul.2015.09.043.

[21] Claessens M, Meester S, Landuyt L, Clerck K, Janssen C. 2011. Occurrence and distribution of microplastics in marine sediments along the Belgian coats. Mar Pollut Bull. 62(2011): 2199-2204. DOI: 10.1016/j.marpolbul.2011.06.030.

[22] Faure F, Demars C, Wieser O, Kunz M, De Alencastro L. 2015. Plastic pollution in Swiss surface waters: Nature and concentrations, interaction with pollutants. Environ Chem. 12(5): 582-591. DOI: 10.1071/EN14218.

[23] Browne M, Galloway T, Thompson R. 2010. Spatial patterns of plastic debris along estuarine shorelines. Environ Sci Technol. 44(2010): 3404-3409. DOI: 10.1021/es903784e.

[24] Jung MR, Horgen FD, Orski SV, Rodriguez V, Beers KL, Balazs GH, Jones TT, Work TM, Brignac KC, Royer SJ, Hyrenbach KD, et al. 2018. Validation of ATR DT-IR to identify polymers of plastic marine debris, including those ingested by marine organisms. Mar Pollut Bull. 127: 704-716. DOI: 10.1016/j.marpolbul.2017.12.061.

[25] Hidalgo-Ruz V, Gutow L, Thompson R, Thiel M. 2012. microplastic in the marine environment: A review of the methods used for identification and quantification. Environ Sci Technol. 46(2012): 3060-3075. DOI: 10.1021/es2031505.

SARAGNAYAN

COMPUTER SCIENCE

SARAGNAYAN is known as the Keeper of Light in Visayan folklore. Like light, technology is used in daily life. With the world essentially running on data, it is essential to maximize the use of technology to ensure that information is used properly. This section contains a study that centers on the application of computer technology in data management.

The study in this section falls under the Industry, Energy, and Emerging Technology (IEET) Research Development Agenda particularly towards the goal of using information and communication technology (ICT) for data analytics.

BASED ON: Harmonized National Research and Development Agenda (HNRDA)

Determining the maximum number of transaction records that the Apriori algorithm can scan in 90 seconds

CHRISTIAN DALE P. CELESTIAL, BASSY LEIAH V. IBARRETA, RUTH SP G. TIRON, MARIA MILAGROSA A. NULLA, and ZENNIFER L. OBERIO

Philippine Science High School - Western Visayas Campus, Brgy. Bito-on, Jaro, Iloilo City 5000, Department of Science and Technology, Philippines

Abstract

The Apriori algorithm is a data mining algorithm used for frequent itemsets. It is easy and simple to use, but its main disadvantage is its inefficiency in scanning large databases. Studies about the algorithm focus on improving its efficiency in large databases, but there is no definite value yet as to the maximum number of transactions that the Apriori algorithm can process in 90 seconds, the tolerable offline waiting time for the human attention span. The methods of this study consist of the hardware and database acquisition, program implementation, data collection, and data analysis. Five hundred transactions were first scanned using the algorithm. It was determined that the classic Apriori algorithm can process 1,310 transaction records in 90 seconds, with a percentage prediction error of 0%. The percentage prediction error was computed using the actual and outputted frequencies.

Keywords: *Apriori algorithm, data mining, frequent itemsets, percentage prediction error, accuracy*

Introduction. Data mining is a process that analyses large databases in order to discover meaningful patterns [1]. The Apriori algorithm is a classic data mining algorithm for frequent itemset mining. It is under the association rule technique of data mining which was initially introduced by Rakesh Agrawal [2]. It enumerates all of the frequent itemsets in a database [3] and is considered best to be used for closed itemsets [2].

Although the algorithm is easy and simple to use, its main disadvantage is that it is not suitable for large databases because its performance declines as the number of transaction records increase. When the database contains a large number of transaction records, scanning the database for frequent itemsets becomes time-consuming [4]. Previous studies pointed out that the algorithm needs to scan the database several times [5], that it is limited to only a small database [6], and that the time that it takes for the algorithm to scan the database increases as its size increases [7]. The performance of the algorithm in dense data is also shown to decline due to the large number of long patterns [8]. Aggarwal and Sindhu [9] discovered that the Apriori algorithm works inefficiently in terms of memory requirement when large numbers of transaction records are considered.

According to the study by Al-Maolegi and Arkok [10], the Apriori algorithm has two parameters to consider, namely the minimum support and confidence level, which are both set by the user. The scanning time of the algorithm is affected by the minimum support because it indicates the number of itemsets to be scanned by the algorithm. The minimum support is used to exclude itemsets in the results which have a support less than the set minimum support. The support of an itemset is the number of transactions that contain all the items of that itemset. A small minimum support would mean that a large number of itemsets will be considered in the scanning process whereas, a large minimum support would mean that the algorithm would be considering only few itemsets.

Studies about improving the algorithm's performance focus on improving its scanning time and accuracy. Different solutions and improvements such as the Bit Array Matrix by Vijayalakshmi and Pethalakshmi [7] improved the algorithm's scanning time and accuracy in large databases. Other solutions are those by Kaur [8] which based the improvement of the algorithm on the accuracy alone, and the studies by Rehab *et al.* [4], Singh *et al.* [11], and Najadat *et al.* [12] which improved the algorithm's scanning time only.

Although some studies have already described the number of transaction records scanned by the algorithm and the algorithm's scanning time [6,12], there is no definite maximum value yet as to the number of transaction records that can be scanned in 90 seconds, the tolerable offline waiting time for the human attention span. [13].

This study aimed to determine the size of the database which Apriori can process accurately at a tolerable waiting time, which is 90 seconds, given that the complexity of the database and the hardware used are constant. Specifically, it aimed to:

(i) determine the algorithm's scanning time and accuracy in a database with an increasing number of transaction records; and

(ii) determine the maximum number of transaction records that the algorithm can process within the tolerable waiting time of 90 seconds, with a percent error of 0%.

How to cite this article:
CSE: Celestial CDP, Ibarreta BLV, Tiron RSG, Nulla MMA, Oberio ZL. 2020. Determining the maximum number of transaction records that the Apriori algorithm can scan in 90 seconds. Publiscience. 3(1):128-131.
APA: Celestial, C.D.P., Ibarreta, B.L.V., Tiron, R.S.P., Nulla, M.M.A., & Oberio, Z.L. (2020). Determining the maximum number of transaction records that the Apriori algorithm can scan in 90 seconds. *Publiscience, 3*(1):128-131.

The results of this study will benefit researchers who aim to further enhance the performance of the Apriori algorithm. The number of transactions scanned by the enhanced algorithm can be compared with the quantified results from this study.

Methods. This study aimed to determine the size of the database which Apriori can process accurately in 90 seconds, given that the complexity of the database and the hardware used are constant. Specifically, it aims to determine the algorithm's scanning time and accuracy in a database with an increasing number of transaction records. It also aims to determine the maximum number of transaction records that the algorithm can process within 90 seconds [13], with a percent error of 0%.

Hardware and Database Procurement. A laptop with an Intel Core i5 3.4GHz Processor with 4GB RAM was used in the testing process. A grocery database having 9,835 transaction records in total was acquired from the website of Salem Marafi [14]. It contained a collection of receipts with each line representing one (1) receipt and the items purchased. The database was converted from a comma-separated values (.csv) file to a text (.txt) file by replacing the commas with spaces, since the source code used required plain text for its input.

Program Implementation. The Java source code of Apriori was acquired from Github [15] and was modified to output the execution time of the algorithm and the frequency of the frequent itemsets. The modified source code was then checked by two consultants who had a background on data mining.

Data Collection. The testing process had three trials for each set of transactions, with the execution time and frequency tabulated after each set of trials. Five hundred transaction records were initially used during the testing process, based on the study of Najadat *et al.* [12], with an increment of 200 transaction records added after each set of trials, following the methods of Sahu *et al.* [6]. The process was repeated until the average scanning time of the algorithm exceeded 90 seconds [13], after which the transaction records added were reduced by half until the scanning time reached 90 seconds.

A minimum support of five was used throughout the whole testing process.

It must be noted that the Java IDE used in the study was closed after each trial to ensure that the program's memory consumption did not interfere with the algorithm's scanning time.

Data Analysis. The average scanning time of the algorithm was first graphed using a scatter chart in Microsoft Excel. A trendline was then added.

The percentage prediction error (PPE) was analyzed using the outputted frequency (OF) and actual frequency (AF). It was computed using the equation below [16],

$$PPE = \frac{(OF - AF)}{OF} \; x \; 100$$

Using the frequency displayed by the program, which served as the outputted frequency, and the actual frequency of the frequent itemsets, the percentage prediction error was determined.

In order to determine the actual frequency of each itemset, the transaction records from the database were transferred to a word document. Next, the itemsets that were displayed by the program were used as a guide for the manual searching of each item contained in the frequent itemset. The items contained in the itemset were searched individually to remove the transaction records which did not contain the items. This was repeated until all the items in the frequent itemset were located in the database. The remaining transaction records contained all the items in the frequent itemset, and these transaction records were counted manually. The same process was repeated for all the frequent items displayed by the program. The number obtained served as the actual frequency, which was used in the calculation for the percentage prediction error of the algorithm.

Safety Procedure. Ensuring the privacy of users' data and the integrity of the data was a key ethical issue which the group took into account. The code used and modified for the purpose of this study was cited, acknowledging the creator of the said code. Proper credit was also given to the source of the database used in the study.

Results and Discussion. Table 1 shows the average scanning time for each set of transaction records. It can be observed that the scanning time of the algorithm increased between 1,100 and 1,300 transaction records, where the scanning time rose from 15.25 seconds to 77.121 seconds. The maximum number of transaction records that the algorithm processed under 90 seconds can also be seen in Table 1 – in this case, the algorithm was able to process 1,310 transaction records. The average scanning time of the algorithm for 1,310 transaction records was 82.53 seconds.

Table 1. The average scanning time of each set of transaction records.

Number of Transaction Records	Average Scanning Time (s)
500	0.536
700	1.756
900	4.953
1100	15.25
1300	77.121
1310	82.53
1311	91.57
1350	103.238
1400	117.551
1500	148.69

This increase in the scanning time of the algorithm can also be seen in the graph in Figure 1, where it can be observed the increase was between 1,100 to 1,300 transaction records. This is also seen in the trendline of the graph in Figure 1, as the average scanning time is seen to rise exponentially as the number of transaction records increase.

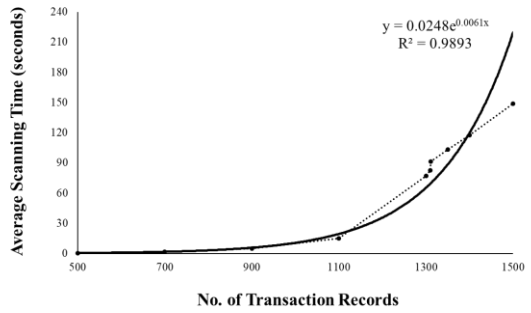

Figure 1. The average scanning time of the algorithm and the corresponding number of transaction records.

The accuracy of the algorithm was computed using the equation for percentage prediction error. The percentage prediction error of the first itemsets in every set of transaction records was 0% as shown in Table 2.

Table 2. Percent error of the algorithm computed using the actual and outputted frequency.

Number of Transaction Records	Actual Frequency	Outputted Frequency	Percent Error (%)
500	5	5	0
700	5	5	0
900	5	5	0
1100	6	6	0
1300	5	5	0
1310	5	5	0
1311	5	5	0

The results show that the highest number of transaction records that the classic Apriori algorithm can process under 90 seconds is 1,310 transaction records. The average scanning time of the algorithm in scanning 1,310 transaction records was 82.53 seconds.

The time complexity of the classic Apriori algorithm is $O(2^n)$ [17]. Exponential (base 2) running time means that the calculations performed by an algorithm double every time as the input grows. This can be supported by Figure 1 due to the exponential trendline having an $R^2 = 0.9893$ as compared to other types of trendlines which have a lesser R^2 value.

In the study by Vijayalakshmi and Pethalakshmi [18], the classic Apriori algorithm was able to scan about 1,750 transactions in under 0.12 seconds. In the current study, it can be observed that the algorithm scanned 1,100 transaction records in 15.25 seconds, which shows that the algorithm was able to scan less transaction records in a greater amount of time. The difference in the number of transaction records scanned by the algorithm may have been due to the difference of the databases used by the researchers. A numerical database with 1's and 0's was used in the study by Vijayalakshmi and Pethalakshmi [18], while a grocery database, composed of strings, was used in this study.

Another variable that may have caused the differences between the studies would be the minimum support. The performance of the algorithm is strongly dependent on its minimum support [19], since having a lesser minimum support would make the algorithm more flexible in accepting associations, requiring more time for it to process.

In relation to this, the database had varying number of items in the itemsets, which could have affected the scanning process of the algorithm. This is because having lesser number of items in an itemset would reduce the number of transaction records for an association. Thus, fewer associations will be considered, due to having a support less than the minimum support [8].

The results of this study could be used as a basis for researchers who aim to study the same algorithm in the future. Since the classic Apriori algorithm is still being improved [7], researchers may use the results of this study to compare the scanning time of the classic Apriori algorithm with their improved version of the algorithm. For example, if the number of transaction records scanned by their improved algorithm surpasses 1,310 records, then it can be determined that the improved Apriori algorithm is effective. The trendline acquired in the study could be used to predict the increase of the scanning time of the algorithm during the testing process, given the same parameters.

The methods of this study could be adopted by researchers and compare their results with this study to aid in the improvement of the classic Apriori algorithm, provided that the database, minimum support, and processor used will be similar to those used in this study.

Limitations. The limitations of this study include its applicability to the Java source code of the classic Apriori algorithm. the varying number of items in each itemset of the database and the inefficiency of the testing process.

If the number of items in the itemset is lesser, the number of transaction records for an association would be lesser as well. This leads to fewer associations being considered, due to having support less than the minimum support [8].

The hardware used in the testing process could have also limited the number of transaction records scanned because better hardware would be able to scan more transaction records in a short amount of time according to Aho et al. [20].

The inefficiency of the testing process is a also a limitation since the source code used could not read text files automatically. The contents of the database had to be copied and pasted to the source code, which consumed an additional two minutes for each trial.

Conclusion. Although the Apriori algorithm is easy and simple to use, its main disadvantage is its inefficiency in scanning large databases. Studies performed on the algorithm have focused on improving it, and some studies have already described the number of transaction records scanned by the algorithm and the algorithm's scanning time. There is, however, no definite maximum value yet as to the number of transaction records that can be

scanned in a tolerable amount of time, which is 90 seconds. The results of the study showed that this value is 1,310 transaction records with a percentage prediction error of 0% throughout the whole process. The factors that affect the scanning time of the classic Apriori algorithm are the processor of the hardware and the minimum support. These variables were kept constant throughout the whole study. This study can aid the improvement of the algorithm by using the results as a basis for future studies.

Recommendations. In order to improve this study, it can be performed using other types of Apriori algorithms. It can also be tested using the source code of a different programming language such as C++ and Python. Other types of hardware can be used in the testing process to determine the hardware's effect on the scanning time of the algorithm. It is also recommended to redesign the used source code to be able to process a database in a text file rather than manually copying and pasting items from the database to the source code. For future studies, the columns of the database must be filled out when testing the algorithm. There must be no null value in any column of the database so that the number of items in each transaction record will be consistent. Through this, the minimum support will be applicable to all the transaction records.

Acknowledgement. The group would like to extend their gratitude to Mr. Christian Chiu and Mr. Marc San Pedro for taking the time to evaluate the group's modified source code.

References

[1] Neha D and Vidyavathi BM. 2015. A survey on applications of data mining using clustering techniques. Int J Comput Appl. 126(2): 7-12.

[2] Prithiviraj P and Porkodi R. 2015. A comparative analysis of association rule mining algorithms in data mining: A study. Am J Comput Sci Eng Surv. 3(1): 98-119.

[3] Yabing J. 2013. Research of an improved Apriori algorithm in data mining association rules. Int J Comput Comm Eng. 2(1): 25-27.

[4] Rehab A, Alwa H, Patil AV. 2013. New matrix approach to improve Apriori Algorithm. Int J Comput Sci Netw Soln. 1(4): 102 -109.

[5] Wei Y, Yang R, Liu P. 2009. An improved Apriori algorithm for association rules mining. Proceedings of a symposium held at the 2009 Institute of Electrical and Electronics Engineers International Symposium on IT in Medicine an Education; Jinan, China.

[6] Sahu A, Dhakar M, Rani P. 2015. Comparative analysis of Apriori algorithm based on association rule. Int J Comp Sci Comm. 6(2):18-21.

[7] Vijayalakshmi V and Pethalakshmi A. 2013. Mining of frequent itemsets with an enhanced Apriori algorithm. Int J Comput Appl. 81(4): 1-4.

[8] Kaur G. 2014. Improving the efficiency of Apriori algorithm in data mining. Int J Sci Eng Tech. 2(5): 315-326.

[9] Aggarwal S and Sindhu R. 2015. An approach to improve the efficiency of the Apriori algorithm. PeerJ PrePrints [Internet]. [cited 2018 Nov 21]; 1-13. Available from: https://doi.org/10.7287/peerj.preprints.1159v

[10] Al-Maolegi M and Arkok B. 2014. An improved Apriori algorithm for association rules. Int J Nat Lang Comp. 3(1): 21-29.

[11] Singh J, Ram H, Sodhi JS. 2013. Improving efficiency of Apriori algorithm using transaction reduction. Int J Sci Res Pub. 3(1): 1-4.

[12] Najadat HM, Al-Maolegi M, Arkok B. 2013. An improved Apriori algorithm for association rules. Int Res J Comput Sci Appl. 1(1): 1-8.

[13] Antonides G, Verhoef PC, van Aalst M. 2002. Consumer perception and evaluation of waiting time: A field experiment. J Consum Psychol. 12(3): 193–202.

[14] Salem. 2014. Market basket analysis with R [Internet]. Salem Marafi [cited 2019 Sept 13]. Available from: http://www.salemmarafi.com/code/market-basket-analysis-with-r/

[15] Umanghome. 2016. Apriori implementation in Java [Internet]. Github Gist [cited 2019 Sept 9]. Available from: https://gist.github.com/umanghome/2c1ee7f03eb99dc9fde2512be3fd36fd

[16] Wu G, Baraldo M, Furlanut M. 1995. Calculating percentage prediction error: A user's note. Pharmacological Res. 32(4): 241-248.

[17] Pai GAV. 2008. Data structures and algorithms: Concepts, techniques, and applications. India: McGraw Hill Education, 12-19 p.

[18] Vijayalakshmi V and Pethalakshmi A. 2015. An efficient count based transaction reduction approach for mining frequent patterns. 47(2015):52-61.

[19] Mehta D and Samvastar M. 2017. Implementation of improved Apriori algorithm on large dataset using Hadoop. Asian J Comput Sci Eng. 2(6): 10-13

[20] Aho AV, Hopcroft JE, Ullman JD. 1974. The design and analysis of computer algorithms. Reading (MA): Addison-Wesley. 2

RESEARCH EVENTS

The Research Events circuit is the series of research-related activities prepared by the Research Unit and/or the scholars with the aim of bringing their studies to the community. The logo to the right is the overarching symbol of the events circuit. The multicolored flame representing the multitude of activities the scholars undertake as embodied in each of the event logos. The interwoven circles represent the infinite possibilities in research. The logo itself is reminiscent of the PSHS logo, representing the values of truth, excellence, and service.

START OF SCHOOL YEAR

BANTALA
Hiligaynon
To inform
G12

PAGBANTALA
SCHOOL-BASED RESEARCH CONGRESS

PAGBANTALA is the first event in the circuit. It is a local research congress where scholars present their studies to a panel of experts. The logo therefore features a caricature of the main scene in Pagbantala: a panel of three, sitting behind the table facing the scholars and their presentation – collectively represented by the incomplete frame. As the first event, Pagbantala is colored red, symbolizing the flames igniting the Research Circuit.

PAGBALANDRA
SCHOOL-BASED POSTER PRESENTATION

PAGBALANDRA is where scholars present their posters to an audience. The logo therefore features a caricature of an individual presenting his/her poster. Here, scholars prepare and showcase three materials: a technical poster for professionals, a community poster for elementary school students, and a headline poster to capture their audience's attention.

BALANDRA
Hiligaynon
To show
G12

hinunan-anon
Hiligaynon
To inquire
G11

PAGHINUN-ANON
GRADE 11 RESEARCH SEMINAR

PAGHINUN-ANON is an event for Grade 11 scholars. As in Pagbantala, the logo features the main scene in Paghinun-anon: the work unit, a group of scholars, and a three man panel sit face to face to discuss the research proposal, the panel guiding the scholars in their proposed study. The logo is yellow – a joyful color – as this is a time of celebration, the first step towards realizing a study in the research curriculum.

PAHISAYOD
RESEARCH WORKSHOPS & GIMICKS

PAHISAYOD is among the largest events in the circuit. Scholars teach skills they've acquired while performing their studies to a group of students from provincial high school, as well as present their study to elementary students through an interactive game. The logo therefore shows the caricature of two individuals: one representing the scholars, the other the students they're presenting to, the white matter being the knowledge shared in this event. The green marks a transition in energy, from school-based events we now move on towards the larger community.

HISAYOD
Akeanon
To announce
G12

Cont'd

Cont'd

WARAGWAG
Hiligaynon
To broadcast

G12

PAGWARAGWAG
COMMUNITY-BASED RESEARCH CONGRESS

PAGWARAGWAG is Pagbantala, Pagbalandra and Pahisayod combined, this time brought to a larger audience outside the school. Every year, Pagwaragwag is brought to a different province. This is represented in the logo where the caricature shows a group of individuals facing a group of three: the scholars. The incomplete frame that represented the scholars in Pagbantala are now complete researchers in Pagwaragwag with the ability to communicate science in an elementary and secondary level.

INDIS-INDIS
Hiligaynon
To compete

G12

PAINDIS-INDIS
JOURNAL COVER PAGE COMPETITION

PAINDIS-INDIS is an on-campus cover page competition. This is how the cover of Publiscience is decided. Hence, the logo shows multiple panels that showcase each submission, two individuals are shown holding similar panels, as if they were issuing a vote. Each of Batch 2020's work units submitted an entry, the number of which is reduced in every stage of voting with teachers issuing the final vote.

PABALHAG
Hiligaynon
To publish

G12

PAGPABALHAG
RESEARCH JOURNAL PUBLICATION

PAGPABALHAG is the event that formally launches this year's Publiscience issue. Through the journal, the audience of the scholar's studies are expanded, networking through various individuals or groups that possess a copy. This is represented in the logo by caricatures of individuals surrounding the journal, giving it the collective shape of an atom. This is reminiscent of the PSHS logo, a symbol of the institution which nurtured the scholars up to this point. The same atom which can diffuse through borders and catalyze the exchange of knowledge.

SUGUID
Hiligaynon
To report

G10

PAGSUGUIDADON
GRADE 10 RESEARCH CONGRESS

PAGSUGUIDADON is the culminating event for Grade 10 scholars. Work units composed of five scholars present their study to a panel. In the logo, the five scholars are shown, the descending white matter representing their initiation into the research process. The white-grey color represents a blank slate, scholars that are ready to be molded, brimming with unknown potential.

END OF SCHOOL YEAR

RESEARCH CONFERENCES

Title of Conference	Date	Studies Participated
Philippine Science High School System (PSHSS) Science Research Summit 2019	August 27-20, 2019	1, 2
2nd Japan Society for the Promotion of Science - JSPS Alumni Association of the Philippines - Department of Science and Technology (JSPS-JAAP-DOST) International Conference	December 4-7, 2019	3
Regional Invention Contest and Exhibition	October 21-23, 2019	4
Research Fair 2020	January 30 - February 1, 2020	1, 2, 3, 5, 6

STUDIES PARTICIPATED

1. Column adsorption of cadmium (II) and lead (II) using rice husks and mango peels *(Bandiola et al.)*

2. Larvicidal activity of *Citrofortunella microcarpa* (calamansi) peel essential oil against third and early fourth instar *Aedes aegypti*
(Carigaba et al.)

3. Microplastic occurence in the coastal sediments of selected barangays of Anilao, Iloilo, Philippines
(Colacion et al.)

4. Use of 1:7 rice bran wax to rice bran oil mixture as phase change material in increasing the efficiency of photovoltaic cells
(Barrera et al.)

5. The extraction and isolation of polyethylene-based plastic-degrading bacteria from Iloilo City Engineered Sanitary Landfill, Mandurriao, Iloilo City
(Canja et al.)

6. The effects of acetyl l-carnitine on the prevention of platelet storage lesions
(Alvarez and Oberio)

KEYWORD INDEX

Page numbers followed by f, t, and p indicate figures, tables, and plates, respectively.

INSTITUTIONAL PARTNERS

The authors of this volume would like to recognize the unequivocal contribution of the following institutions for opening its facilities to the researchers, and extending consultative and technical support in the conduct of their studies:

Department of Agriculture - Region VI (DA-VI)

Iloilo Research Outreach Station -Sta. Barbara (DA)

Department of Agriculture– Western Visayas Integrated Research Center (DA-WESVIARC)

Department of Environment and Natural Resources – Region VI (DENR-VI)

Department of Health – Region VI (DOH-VI)

Department of Science and Technology – Industrial Technology Development Institute (DOST-ITDI)

Advanced Device and Material Testing Laboratory (DOST-ITDI ADMATEL)

Department of Science and Technology – Regional Standards and Testing Laboratories Region VI (DOST-RSTL VI)

Iloilo Provincial Agricultural Office

Local Government Unit of Anilao

Philippine Red Cross – Iloilo Chapter

Southeast Asian Fisheries Development Center (SEAFDEC)

Aquatic Department (SEAFDEC/AQD)

University of the Philippines – Diliman, Marine Science Institute (UPD-MSI)

University of the Philippines – Visayas (UPV)

University of San Agustin

University of Tokyo – Okada Laboratory

ACKNOWLEDGMENT

The authors of the studies presented in this journal would like to extend their warmest appreciation, first and foremost, to the institution of Philippine Science High School - Western Visayas Campus for nurturing their scientific abilities and technical capabilities for the pursuit of the untarnished truth. The publication of these studies would not have been possible without the continuous support, patience, and guidance of the Research Committee of Philippine Science High School - Western Visayas Campus.

Finally, the authors would like to express their deep gratitude to the science research assistants (SRA), research teachers, research advisers, faculty and staff, and families and friends who have provided counsel, support, and inspiration in pursuing their aspirations as world-class Filipino scientists.